Machine Learning to Characterize Motor Patterns and Restore Walking after Neural Injury

by

Ashley N. Dalrymple

A thesis submitted in partial fulfillment of the requirements for the degree of

Doctor of Philosophy

Neuroscience
University of Alberta

Abstract

Walking is a locomotor task that integrates information from all over the nervous system. The lumbosacral spinal cord houses neural networks that contribute to locomotion. These networks dominate locomotor activity during development and may provide suitable targets for restoring function after injury.

Motor activity of the developing spinal cord under electrical or pharmacological activation has been extensively used to study locomotor networks, leading to various models of the central pattern generator. Spontaneous activity of the developing spinal cord, which represents the locomotor networks at rest, may also contribute to understanding of the development of these networks. In the postnatal rodent spinal cord, it is characterized by stochastic and complex patterns of activity, which correspond to kicking-like movements. Spontaneous activity has been challenging to characterize as there are no current analysis methods. I developed a software tool to characterize and classify episodes of spontaneous activity from developing spinal networks of the neonatal mouse using supervised machine learning. I tested the software's ability to detect changes in activity by increasing network excitability with KCl. Supervised machine learning-based classification revealed global and class-specific changes after increasing excitability. This software will add to the toolbox of methods used to study developing locomotor networks under varying conditions.

After a SCI, spinal neural networks and their connections to the leg muscles remain intact. An incomplete SCI causes partial paralysis. To restore walking after an incomplete SCI, residual function needs to be augmented. Intraspinal microstimulation (ISMS) entails implanting

electrodes into the ventral horn of the lumbosacral enlargement to activate the muscles of the legs. I used ISMS to restore walking in a model of hemisection SCI, which affects one hind-limb. Anaesthetized cats with an intact cord were implanted with ISMS unilaterally and the voluntary movements of one hind-limb were mimicked by a person moving that limb. Feedback from external sensors on the person-moved limb, representing residual function, was used to move the other limb to the opposite phase of the gait cycle using ISMS.

The first demonstration of augmenting remaining function was performed in cats on a split-belt treadmill. The belt ipsilateral to the ISMS-controlled limb remained stationary, while the other turned at varying speeds. Sensors measuring residual function of the person-moved limb were used to anticipate changes of the walking phases, and triggered ISMS to move the other limb to the opposite phase. At faster speeds of stepping, the feedback-initiated transitions were insufficient causing a loss of weight-bearing. Four different supervised machine learning methods were used to predict the step period of the person-moved limb. If the prediction indicated a faster step, the control strategy changed to feed-forward, using the predicted value to determine the time spent in each phase of the cycle. Three of the four prediction methods resulted in improved weight-bearing, and maintained alternation at varying speeds. This control strategy augmented remaining function, while allowing the user to step at a self-selected speed through automatic adaptation using supervised machine learning.

For more personalized control of walking, other machine learning methods were employed. Commercially available walking systems use the same open-loop control strategy for each user, forcing them to accommodate to the control system. Feedback from external sensors can improve

control strategies; however, with a large burden of tuning, as each person walks differently from others as well as among themselves. I propose that machine learning can reduce the burden of tuning and demonstrate this using ISMS in a feline model of hemisection SCI. Reinforcement learning generated predictions for sensors measuring residual function during walking. Thresholds on the predictions indicated phases of the walking cycle and produced fixed responses in the ISMS output to move the other limb to the opposite phase (Pavlovian control). Learning parameters were either initialized to zero or built upon learned predictions from previous walking trials. Predictions were quickly learned and initiated changes between the phases of the walking cycle to produce alternating over-ground walking. Learning was able to adapt to different people walking the limb and between different cats. Furthermore, learning was able to recover from mistakes made during walking. This work demonstrated that Pavlovian control using reinforcement learning can adapt to different subjects walking without the need for retuning. It allowed for personalized walking that augmented remaining function.

Preface

This thesis work is an original work by Ashley N. Dalrymple. The research projects, of which this thesis is part, received research ethics approval from the University of Alberta Research Ethics Board, Project Name "Neural Adaptations Following Lesions of the Central Nervous System", Protocol AUP00000301, Mar. 18, 2013, and the University of Calgary Health Sciences Animal Care Committee, Project Name "Spinal Control of Locomotion in the Neonatal Mouse", Protocol AC16-0182, Oct. 17, 2016.

Experiments for chapter 2 were done in Dr. Patrick Whelan's laboratory at the University of Calgary. This work was designed and drafted by Dr. Patrick Whelan, Simon Sharples, and Ashley Dalrymple. Simon Sharples collected the *in vivo* recordings. I performed the analysis and testing of the machine learning methods. I wrote and published the classification software. The studies for chapters 3 and 4 were conducted in Dr. Vivian Mushahwar's laboratory at the University of Alberta. I designed and programmed both controllers. The study for chapter 3 was conceived by Dr. Vivian Mushahwar and Ashley Dalrymple. Surgery and data collection were done by myself and Dr. Dirk Everaert. I analyzed the data with help from David Hu for motion tracking. I drafted the manuscript with feedback from the co-authors. The study for chapter 4 was conceived by Dr. Vivian Mushahwar, Dr. Richard Sutton, and Ashley Dalrymple. Surgery, data collection and analysis were done with David Roszko. I drafted the manuscript with feedback from the co-authors.

The literature review in chapter 1 was written by Ashley Dalrymple. Parts of this review were published in a book chapter in May 2017 in Neuroprosthetics: Theory and Practice by World Scientific, doi: 10.1142/9789813207158_0025. Chapter 2 has not been published except in abstract form. It is under revision with a peer-reviewed journal. Chapter 3 was published in Oct 2018 by the Journal of Neural Engineering, doi: 10.1088/1741-2552/aad872. Chapter 4 has not been published except in abstract form. It will be submitted to a peer-reviewed journal. Chapter 5 was the original work of Ashley Dalrymple.

Dedication

I would like to dedicate my work to my beautiful grandmother, Mary Schierling. She has always inspired my independence, determination, and resilience. To you, Gma!

"Science rules!"

-*Bill Nye the Science Guy*

"Take chances, make mistakes, and get messy!"

-*Miss Frizzle, The Magic School Bus*

"I'm going to show [them] what little girls are made of"

-*Miranda Lambert, Gunpowder and Lead*

Acknowledgements

Behind every student is a team cheering them on, supporting them, and pushing them to do better. Thank you to my team, for I could not have done it alone.

Throughout my PhD I have had an amazing support system that encouraged me to pursue my goals. The entire Mushahwar lab, past and present, challenged me to be a better student, peer, and mentor. I would especially like to thank Amirali Toossi for always being available to bounce ideas around, Rod Gramlich for technical assistance, and most of all, Dirk Everaert for all of the invaluable training and late night amusement during experiments. I would also like to thank my supervisor, Vivian Mushahwar, for guiding my projects into unexpected and fascinating areas. I could not have asked for more supportive supervisory committee members. Thank you, Dave Collins and Rich Sutton, for the encouragement and mentorship. I would also like to thank my team of Patricks: Pilarski and Whelan, for teaching me in areas foreign to me and for the support of my very interdisciplinary work. I would also like to thank the SRN group for the stimulating and curiosity-triggering conversations.

I've also had the continuous support of my friends and family, which are too numerous to mention everyone. They don't all fully understand what I do but they've accepted my nerdiness anyway! A special thanks to my Grandma Mary, for always taking the time to ask about my work and doing her best to understand what I do. To my best friend, Hope, thank you for the weekly lunches and always having an open ear. Good or bad I always had to share my news with you! To Roopa, for the late and sometimes tearful phone calls filled with encouragement and support. Thank you to my kitties, Tootsie and Ser Pounce, for always cuddling me after the late nights and over-night experiments. And finally, to my husband-to-be, John. Words cannot describe how supportive you've been throughout my journey. You are my rock, my shoulder to cry on, and are always full of excitement over my accomplishments, big or small. My scientific journey is not over, and I am so fortunate to have the love and support of so many wonderful people!

Table of Contents

List of Tables

List of Figures

List of Algorithms

List of Abbreviations and Notations

E	Embryonic
P	Post-natal
Ca	Calcium
K	Potassium
KCl	Potassium chloride
Pt-Ir	Platinum-Iridium
BBB	Blood-brain barrier
GABA	Gamma-Aminobutyric acid
KCC2	Potassium-Chloride co-transporter 2
NMDA	N-methyl-D-aspartate
AMPA	Alpha-amino-3-hydroxy-5-methyl-4-isoxazolepropionic acid
TNF-α	Tumor necrosis factor alpha
IL-1β	Interleukin 1 beta
GM-1	Monosialotetrahexosylganglioside
Ia	Primary muscle spindle afferents
Ib	Primary afferents from Golgi tendon organs
II	Secondary muscle spindle afferents
CSF	Cerebral spinal fluid
MLR	Mesencephalic locomotor region
T	Thoracic
L	Lumbar
CPG	Central pattern generator
DRG	Dorsal root ganglia
MTP	Metatarsal phalanges
SCI	Spinal cord injury
ASIA	American spinal injury association impairment scale
BWSTT	Body-weight supported treadmill training
FES	Functional electrical stimulation
EMG	Electromyography
EEG	Electroencephalography

SCS	Spinal cord stimulation
ISMS	Intraspinal microstimulation
IMS	Intramuscular stimulation
F	Flexion
E1	Extension 1
E2	Extension 2
E3	Extension 3
SCL	Stimulation-controlled limb
EML	Experimenter-moved limb
PML	Person-moved limb
FDA	Food and drug administration
AC	Alternating current
DC	Direct current
GUI	Graphical user interface
MLP	Multilayer perceptron
IL	Inductive learning
ALN	Adaptive logic network
ANN	Artificial neural network
TP	True positive
TN	True negative
FP	False positive
FN	False negative
MAE	Mean absolute error
S	Small
LnR	Large, not rhythmic
LR	Large, rhythmic
MnR	Multi-burst, not rhythmic
MR	Multi-burst, rhythmic
PID	Proportional-integral-derivative
PI	Proportional-integral
SMC	Sliding mode control

RL	Reinforcement learning
MDP	Markov decision process
TD	Temporal difference
TOTD	True online temporal difference
GVF	General value function
SKC	Selective Kanerva coding
S, s	Set of states, state
A, a	Set of actions, action
R	Set of rewards
G	Return
$\boldsymbol{e}$	Eligibility trace
Z	Cumulant
v	Value function
q	State-value function
$\mathbf{w}$	Weight vector
$\mathbf{x}$	Feature vector
π	Policy
α	Step size
ε	Probability of taking random action in an ε-greedy policy
δ	Temporal difference error
λ	Decay rate parameter
γ	Discount rate parameter
P	Prototypes
K	Number of prototypes
c	Parameter for closest prototypes
η	Ratio for determining c-closest prototypes
T	Time-step
US	Unconditioned stimulus
CS	Conditioned stimulus
UR	Unconditioned response
CR	Conditioned response

R	Response
ANOVA	Analysis of variance
cm	Centimeter
ms	Millisecond
m	Meter
km	Kilometer
Hz	Hertz
V	Volts
µA	Microamps
µs	Microseconds
s	Second

Chapter 1: Introduction

This thesis work demonstrates the utility of machine learning in solving neuroscience problems, specifically related to the characterization and restoration of locomotion at the spinal level. Interdisciplinary work brings ideas and concepts from multiple fields together. Machine learning itself is highly interdisciplinary. The concepts used in machine learning are derived from the knowledge of biological learning. It aims to mimic or replicate natural learning processes. This can be in the form of modeling neurons and how they form connections to each other, to emulating broader concepts in learning, such as reinforcement, demonstration, association, repetition, and memory. As machine learning is biologically-inspired, using machine learning to characterize complex locomotor signals or to control a neural prosthesis to restore walking is a step towards more biologically-relevant solutions.

Walking is a multifaceted locomotor task that integrates information from many regions in the nervous system. The basic goal of walking is to enable a being to travel from one place to another using their limbs. Although walking is a seemingly periodical task, especially when compared to the variety of movements performed by the upper limbs, there are intricate central mechanisms to consider. The spinal cord is part of the central nervous system and plays a critical role in walking. It houses tracts between the peripheral and autonomic nervous systems to the cortex, cerebellum, and brainstem (Kandel 2013). These tracts enable balance and voluntary movement, and relay pain and sensory information. Additionally, the spinal cord houses neurons that integrate information from descending tracts, afferent inputs from the periphery, and inputs from propriospinal neurons. Injuries to these tracts and neurons results in motor and sensory deficits, as well as autonomic dysfunction. A spinal cord injury (SCI) results in drastic lifestyle changes including loss of independence. The degree of paralysis and dysfunction depends on the level and extent of damage to the spinal cord. Injuries can be complete or incomplete according to the extent of the deficits. The level of the injury defines whether a person is tetraplegic (cervical level) or paraplegic (thoracic, lumbar, or sacral level).

One common method used to study the developing spinal cord is fictive locomotion. Fictive locomotion entails inducing alternating, locomotor-like activity in an *in vitro* spinal cord using electrical or pharmacological activation (Kiehn and Dougherty 2013). Through manipulating and

modeling activity produced during fictive locomotion, much of the structure and outputs of the spinal central pattern generator (CPG) have been uncovered (McCrea and Rybak 2008). However, there is still much to learn regarding the structure and function of the CPG, especially in larger mammals and during development.

Motoneurons and spinal networks can be activated after a SCI using electrical stimulation, enabling the restoration of walking. Stimulation of the peripheral nerves can produce direct motor outputs as well as motor responses through reflex activity (Pierrot-Deseilligny and Mazevet 2000; Lou et al. 2017). Spinal networks can be more directly targeted using epidural electrical stimulation (Angeli et al. 2018; Wagner et al. 2018), transcutaneous electrical stimulation (Hofstoetter et al. 2015; Inanici et al. 2018), or intraspinal microstimulation (Saigal et al. 2004; Holinski et al. 2016) to assist with or to restore walking. However, control methods for these electrical stimulation techniques are needed in order to provide a more integrated and personalized neural prosthesis. Commercially available systems using peripheral electrical stimulation such as the Parastep initiate open loop, or pre-timed, walking movements using manual push buttons on a walker (Chaplin 1996). Exoskeletons also employ an open loop control strategy initiated by tilt sensors (Chang et al. 2015; Ekelem and Goldfarb 2018). These systems force the users to adapt their walking to the control strategy of the device. One approach to improving the control methods includes adding feedback. For example, feedback from sensors can be used to interrupt the open loop timing, detect the intent of the user to step, or to track joint movements (Popović 1993; Guevremont et al. 2007; Dutta et al. 2008; Nekoukar and Erfanian 2012; Holinski et al. 2016).

Machine learning may also be a viable option for improving control strategies. Machine learning methods are capable of analyzing complex data, are suitable for noisy or missing data, and are fast, automatic, and powerful. Examples of uses for machine learning methods span from labelling emails as spam (Cormack 2008) to self-driving cars (Bojarski et al. 2016) to medical diagnoses including skin cancer classification (Esteva et al. 2017). Machine learning methods have also been used to study walking, including to analyze electromyography (EMG) signals recording during walking (Miller et al. 2013), to diagnose gait deficits in Parkinson's disease (Zeng et al. 2016), for joint tracking (Abbas and Triolo 1997), or to predict the phases of the gait

cycle (Kirkwood et al. 1989). Machine learning methods have also been used to detect the intention to step (Kirkwood and Andrews 1989; Kostov et al. 1992, 1995; Tong and Granat 1999; Sepulveda et al. 1997), control joint angles (Chen et al. 2004), for finite state control (Popović 1993), to switch between gait types such as sitting to standing to walking (Graupe and Kordylewski 1995), and even to produce walking in robots (Endo et al. 2008; Li et al. 2013).

This work details the use of machine learning to characterize spontaneous motor activity recorded from the developing spinal cord. Spontaneous activity differs from fictive locomotion as it is the activity produced by the spinal cord in its more natural state. The activity produced during different stages of development is unique and may provide additional information about the developing spinal locomotor networks. This work also demonstrates different methods of machine learning to control walking by targeting the spinal cord. The control strategies aim to augment remaining function in a model of incomplete SCI, as well as adapt the walking through speed-adaptability and automatic personalization using learned predictions. Together this work strives to demonstrate how the spinal cord and machine learning can be used to understand locomotion and to restore locomotion.

1.1 Spinal Cord Development

1.1.1 Spontaneous Activity

Spontaneous activity is a common feature of developing neural networks throughout the central nervous system. It is present during development in several regions of the nervous system including the spinal cord (O'Donovan and Landmesser 1987; Jiang et al. 1999; Whelan et al. 2000), retina (Galli and Maffei 1988; Torborg and Feller 2005), hippocampus (de la Prida et al. 1996; Garaschuk et al. 1998; Sipilä et al. 2006), cerebellum (Watt et al. 2009), and thalamus (Pangratz-Fuehrer et al. 2016; Mooney et al. 1996). It plays an important role in network development and consolidation. Specifically, spontaneous activity has been shown to guide axons (Hanson and Landmesser 2004; Cang et al. 2005) and refine synaptic transmission (Yu et al. 2004).

In the spinal cord, spontaneous activity can be recorded in the absence of pharmacological or electrical activation. Spontaneous activity in the spinal cord leads to the emergence of

locomotor-like movements during development, including kicking *in utero* and postnatally, which eventually develops into locomotion (Hernandez et al. 1991; Whelan et al. 2000). Studying spontaneous activity throughout development can facilitate the understanding of how the movements develop as the central nervous system matures.

Much of the work has been performed in chick, mouse, and rat models (Fellippa-Marques et al. 2000; Hanson and Landmesser 2003; Landmesser and O'Donovan 1984; O'Donovan 1999; Ren and Greer 2003; Whelan et al. 2000); however, specific time points described throughout refer to mouse development. The chick model is most often used to study embryonic development as the fetus is encapsulated in an egg outside of the mother's body, allowing *in ovo* (Landmesser and O'Donovan 1984) or *in vitro* (Nishimaru et al. 1996) access to the fetus. The rat and mouse models have been used to record prenatal (Nakayama et al. 1999; Hanson and Landmesser 2003) and postnatal (Smith and Feldman 1987) activity. The neonatal mouse spinal cord preparation is advantageous as it is smaller, allowing for study *in vitro* at later time points as the tissue can remain viable for longer (Jiang et al. 1999). Furthermore, genetic manipulations can be applied to mice to further investigate the development of spinal locomotor networks (Cazalets et al. 2000; Smith et al. 1993). These animals all have very small spinal cords, allowing for *in vitro* preparations to be used. *In vitro* preparations allow for neurophysiological measurements directly on the spinal cord and roots, as well as the application of drugs without the need to cross the blood-brain barrier (BBB).

Recordings of spinal cord spontaneous activity are typically obtained through extracellular suction electrodes placed at the proximal stump of the ventral roots (Nishimaru et al. 1996). The raw neurograms include subthreshold network activity as well as suprathreshold spiking activity (Figure 1.1).

Recording spontaneous activity perinatally has facilitated the understanding of the development of spinal motor networks. However, spontaneous activity is complex, making it difficult to study in detail. Much of the analysis of spontaneous activity generated by spinal circuits have used high-pass filtered or AC-coupled recordings as they provide a simpler presentation of the activity.

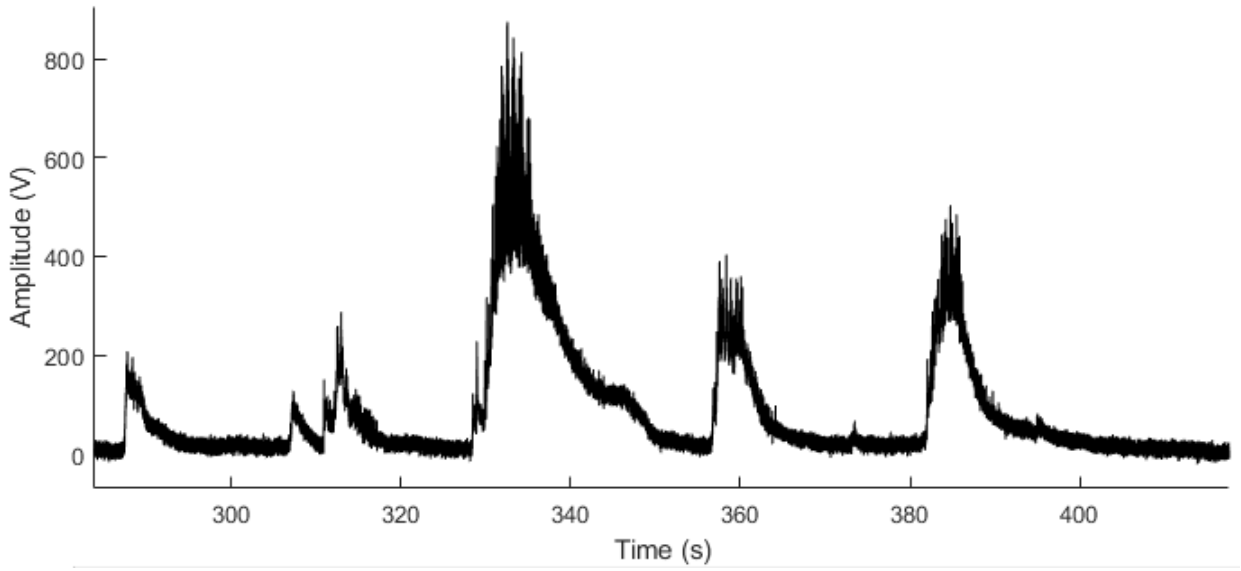

Figure 1.1. Example of spontaneous activity recorded from the left L2 ventral root from a neonatal mouse (P0-P3).

1.1.2 Embryonic Development

In the spinal cord, spontaneous activity first appears before supraspinal and afferent inputs reach the lumbar spinal cord (Kudo et al. 1993; Kudo and Yamada 1987). The earliest spontaneous motor activity embryonically is comprised of infrequent and brief bursts of action potentials (O'Donovan and Landmesser 1987) that increase in frequency and regularity (embryonic day (E) 12-18) (Nakayama et al. 1999; Yvert et al. 2004). At this stage (E12.5), the genesis of spontaneous activity is dependent on electrical transmission through gap junctions (Hanson and Landmesser 2003; Whelan 2003), as well as by glycine and GABA, which are functionally excitatory at this stage in development (Nishimaru et al. 1996). Glycine and GABA are excitatory early in development due to higher concentrations of chloride in the motor neurons. As a result, chloride moves out of the cell upon activation of glycine and GABA receptors, leading to depolarization of the post-synaptic membrane. Around E18.5, spontaneous activity transitions from glycine to glutamate-dependent mechanisms (Nishimaru et al. 1996). This is due to the increased expression of the potassium-chloride-co-transporter 2 (KCC2) (Delpy et al. 2008) which results in chloride-dependent synaptic transmission becoming functionally inhibitory. There is also a loss of GABAergic interneurons in the ventral horn (Antal et al. 1994). In addition to changes in intrinsic network function, there are also changes in the efferent pathways. Some descending pathways from the brainstem to the spinal cord begin to emerge,

including reticulospinal, vestibulospinal, serotonergic, and noradrenergic pathways (Clarac et al. 1998; Kudo et al. 1993; Ballion et al. 2002). As a consequence, spontaneous activity becomes more complex and variable (O'Donovan and Landmesser 1987; O'Donovan et al. 1998; Branchereau et al. 2002).

1.1.3 Post-Natal Activity

In the presence of olfactory or cutaneous stimulation, neonatal rodents are capable of generating stepping movements as soon as a few hours after birth; however, the gait is ataxic and weight-bearing is largely absent (Fady et al. 1998; Jamon and Clarac 1998; Hernandez et al. 1991). During the first few days of life, the majority of movements occur spontaneously and can be recorded *in vitro.* During this time, episodes of spontaneous activity are highly irregular and are often accompanied with superimposed rhythms that are synchronous or alternating across different ventral roots (Whelan et al. 2000). This is attributed to incomplete propriospinal and corticospinal innervations and immature synapses, even at post-natal day (P) 4 (Hernandez et al. 1991; Stelzner et al. 1986).

Posture and locomotion develops rostro-caudally, with the forelimbs making locomotor movements before the hind-limbs (Nakayama et al. 1999; Clarac et al. 1998). At about one week old rodents begin to bear weight and present postural-related reflexes, coinciding with the corticospinal pathways reaching the lumbar levels (Clarac et al. 1998; Whelan 2003). Mice at this stage are considered functionally motor mature as weight-bearing occurs in the presence of sensory stimulation (Jiang et al. 1999). From P10-13 the eyes begin to open and the mice can achieve weight-bearing, albeit slow, quadrupedal locomotion (Clarac et al. 1998; Westerga and Gramsbergen 1990). Serotonergic pathways continue to develop during the first two weeks after birth. Walking subsequently becomes faster and more complex behaviours emerge, including rearing and sitting, corresponding to the maturation of sensory afferent pathways (Clarac et al. 1998). Between two and three weeks, descending innervation is fully developed (Westerga and Gramsbergen 1990).

The early post-natal activity has been described as either alternating, unilateral, or synchronous across ventral roots (Whelan et al. 2000) However, these descriptions refer to AC-coupled or

high-pass filtered recordings of spontaneous activity. The low-pass filtered or DC-coupled recordings retain the fine details of the episodes of activity. Although the activity is often synchronous between roots, the intra-episode activity is different between roots, each with varying rhythmicity and patterns. These intra-episode patterns have not been studied as the details have been difficult to characterize. However, these patterns may reveal important components of neural activity that are necessary for the development of rhythmic movements such as locomotion.

1.2 Walking

1.2.1 Early Walking in Humans

Humans are unable to walk at birth; however, infants display stepping behaviour independent of volitional control (Forssberg 1985). Because the motor tracts and cortex are immature at birth with undeveloped myelin (Altman and Bayer 2001), this locomotion behaviour in infants is thought to be of spinal origin up to one year of age (Yang et al. 2004). Furthermore, sensory input can initiate stepping in infants. When held to stand on a flat surface and tilted forward, infants will take a couple of steps. When held over a treadmill belt, infants could step with some weight-bearing, with better stepping ability correlated with more weight-support. As the treadmill belt speed increased, the infants continued to alternate their legs (Vasudevan et al. 2016).

When infants step, they make contact with the forefoot instead of the heel (Forssberg 1985). The initiation of stepping in infants requires weight-support as well as rapid extension of the hip (Pang and Yang 2000). In infants younger than a year, flexion and extension movements occur together in the hip, knee and ankle joints, with foot drag frequently occurring at the beginning of the swing phase (Yang et al. 2004). The foot drag may be due to the immaturity of the central and peripheral nervous systems.

Studies in developing nervous systems, such as those of prenatal and neonatal animals, as well as infants, provide understanding and evidence for the organization of the spinal networks that contribute to locomotion. These networks may be taken advantage of after the loss of voluntary movements, such as with a SCI, by targeting them with therapies or stimulation.

1.2.2 The Gait Cycle

Generally, walking consists of the legs alternating between swing and stance phases, with periods of double-limb support to transition the body weight from one leg to the other. The gait cycle of one leg can be divided into 4 phases indicating flexion and extension movements: F, E1, E2, and E3 (Goslow et al. 1973; Engberg and Lundberg 1969). These correspond to toe-off to early swing, late swing to heel strike, heel strike to mid-stance, and mid-stance to toe-off, respectively. The swing phase includes F and E1 and correspond to the acceleration (flexion) and deceleration (extension 1) of the leg as it swings forward; the stance phase includes E2 and E3, which correspond to weight-bearing and propulsive extension movements, respectively. Typically, 60% of the gait cycle is spent in stance. As the speed of walking increases, the proportion of time spent in stance decreases (Liu et al. 2014; Hebenstreit et al. 2015). The alternation of the swing and stance phase is mediated by networks in the spinal cord: the central pattern generator.

1.2.3 Spinal Central Pattern Generator

A locomotion central pattern generator (CPG) is defined as a neural network that is capable of producing coordinated and rhythmic alternation of flexor and extensor motoneurons in the absence of descending drive or afferent input (Guertin 2009; McCrea and Rybak 2008). It resides in the spinal cord and has been shown to exist in invertebrates such as crayfish (Stein 1971) and leeches (Kristan and Weeks 1983), and in vertebrates including lamprey (Wallén and Williams 1984; Messina et al. 2017) and cats (Brown 1911; Jankowska et al. 1967; Pearson and Rossignol 1991). There is evidence that the CPG may also exist in humans (Calancie et al. 1994; Bussel et al. 1996; Dimitrijevic et al. 1998; Yang et al. 2004; Minassian et al. 2007). The CPG produces the basic motor commands for walking: coordinated flexion and extension within a limb as well as left-right alternation. Over the past century, various models of the CPG network have been theorized, stemming from experiments performed frequently in cats.

1.2.3.1 Half-Center Model

The half-center model was proposed by T. Graham Brown in the early 1900s. He demonstrated that basic stepping movements could be produced by the spinal cord in the absence of descending motor control and afferent feedback in spinalized, decerebrate cats (Brown 1911).

The half-center model is the most basic description of flexion-extension alternation. In this model, interneurons directly activate either flexion or extension motoneurons, and through inhibitory interneurons, suppress the motoneurons of the opposite function through reciprocal inhibition (Brown 1914).

During activation of extensors for the stance phase in the gait cycle, reciprocal inhibition is accomplished through two mechanisms: first by inhibiting the flexor motoneuron pools directly, and second, by inhibiting the neurons that directly activate flexor motoneuron pools. Switching from extension to flexion was thought to occur through a fatigue mechanism (Brown 1914), whereby the drive from the extension neurons would slowly decrease, or fatigue. Once below a threshold, the inhibition of the flexors would cease and the flexors would now be active, and inhibit the extensors. The exact mechanism of alternation has been debated (Miller and Scott 1977; Guertin 2009), and still remains to be determined. One theory is that there is calcium-mediated adaptation of the excitatory interneurons that releases the reciprocal inhibition to allow the other function to take over (Kiehn and Dougherty 2013).

There is also alternation between the two hind-limbs through similar reciprocal inhibition via inhibitory commissural interneurons. Reciprocal inhibition for left-right alternation occurs through two main groups of commissural interneurons: inhibitory commissural interneurons that act on motoneurons and excitatory commissural interneurons that act on premotor inhibitory interneurons. These dual actions may have a role in regulating left-right alternation at different speeds of locomotion (Talpalar et al. 2013).

1.2.3.2 Unit Burst Generators

The concepts behind unit burst generators builds upon the half-center model. It was developed in an effort to explain why some motoneuronal pools are active during both flexion and extension phases of the gait cycle (Rossignol et al. 1996). Unit burst generators are separate modules made of oscillators (half-centers) that control subsets of motoneurons, and the modules are coupled together to produce more complex patterns (Grillner 1981). In this scheme, each joint has its own module, and the modules communicate through excitatory and inhibitory synapses. However, the unit burst generator still failed to explain the multitude of patterns that can occur during

locomotion. For example, the unpredictable phenomenon of deletions, in which a silencing of motoneurons for one function (for example, extension) is accompanied by continued rhythmic activation of the flexor motoneurons, with the rhythm of the extensor motoneurons resuming after the deletion (Guertin 2009; Lafreniere-Roula and McCrea 2005). The continuation of rhythmic activity following a deletion implies that there is a separate mechanism for generating the basic rhythmic output.

1.2.3.3 Two-Layer Model

Various two-layer models have been proposed by numerous research groups (Orsal et al. 1990; Rybak et al. 2006a; Rybak et al. 2006b; McCrea and Rybak 2007, 2008; Koshland and Smith 1989; Kriellaars et al. 1994). In each case, the top layer is the rhythm generator network. A rhythm generator behaves much like a clock timer function, and is responsible for the alternation between flexion and extension. The second layer is the pattern formation network, which is responsible for the selection of the motoneuron populations that produce muscle contractions.

McCrea and Rybak (2008) proposed a hierarchical two-layer model. The rhythm generator and pattern formation networks receive inputs from peripheral afferents (Ia and Ib sensory fibers), as well as descending drive from the mesencephalic locomotor region (MLR) in the brainstem and other cortical areas. These inputs can modify the timing and/or the pattern of walking, such as changing the speed of locomotion or when walking on difficult terrain. The pattern formation network makes connections with a motoneuron level, including flexor and extensor motoneurons. This local neural network also has afferent feedback mechanisms, including Ia inhibitory interneurons and Renshaw cells, and is involved in reciprocal and non-reciprocal interactions between antagonistic muscles.

1.2.4 Descending Inputs

The initiation of gait and skilled locomotion originate supraspinally. Stimulation of the MLR in the brainstem can elicit locomotion (Whelan 1996) and even modify the cadence according to stimulation intensity (Shik et al. 1966). The MLR projects to other brainstem nuclei that then project to interneurons in the spinal cord (Noga et al. 1988; Steeves and Jordan 1984). Other regions, such as the subthalamic locomotor region, medullary reticular formation and the

pontomedullary locomotor strip can initiate locomotion as well (Armstrong 1988; Nga et al. 1988; Mori et al. 1977). These brainstem regions receive inputs from the basal ganglia and the forebrain to modulate locomotor patterns.

Descending inputs also play a large role in the execution of skilled locomotion, such as over uneven terrain or around obstacles. Volitional control originates in the motor cortex. The primary motor cortex primarily projects directly to the spinal cord via the corticospinal tract (Takakusaki 2013). Other cortical regions including the premotor area and supplementary motor area project to the primary motor cortex, but also have corticoreticular projections to the brainstem. The cortex integrates sensory signals including vision and proprioception to perform skilled, volitional walking (Drew 1988). The cerebellum contributes to walking by recalibrating the gait pattern using predictions of the motor outcomes. It makes corrections to the output if there are discrepancies between the efferent copy from the motor cortex and the afferent copy from the spinocerebellar tract (Pisotta and Molinari 2014; Takakusaki 2013; Shadmehr et al. 2010). The corrections made by the cerebellum are anticipatory (Morton and Bastian 2006).

1.2.5 Afferent Inputs

Sherrington proposed that spinal reflexes were responsible for producing gait (Sherrington 1910). He suggested that proprioceptive stimuli were responsible for an alternating reflex composed of flexion and extension, and that alternation was achieved through a refractory period of the responses. He believed that the flexion phase was equivalent to the nociceptive-induced flexor withdrawal response and the contralateral limb's extension phase equivalent to the crossed-extension part of the reflex. However, stronger evidence supporting the existence of inherent spinal circuitry for locomotion led to the pursuit of the CPG (Brown 1911; Lundberg 1965; Jankowska et al. 1965; Grillner and Wallen 1985).

Although the CPG can produce alternation in the absence of afferent input, there is evidence for afferent inputs playing important roles during locomotion. Afferent inputs facilitate loading and posture during certain states, influence state transitions, and provide a corrective response to perturbations during locomotion. Specifically, the stretch reflex, which is triggered by Ia afferents in the muscle spindle, has been shown to provide load compensation during the stance

phase of gait in cats (Akazawa et al. 1982) and humans (Capaday and Stein 1986). Ib afferents from Golgi tendon organs carry muscle tension information and have been shown to reverse their role of inhibition to excitation during locomotion in the cat (Pearson and Collins 1993; Pearson 1995) and humans (Stephens and Yang 1996). These data suggest that Ia and Ib afferents largely contribute to weight support and postural responses during stance (Zehr and Stein 1999). Afferent input is also believed to gate the excitation of motoneurons according to the phase of the walking cycle (McCrea and Rybak 2008). Additionally, afferent input can influence the timing of the transitions between the phases of the walking cycle. For example, to transition from swing to stance, two sensory-based conditions must occur: hip flexion and unloading of ankle extensors (Duysens and Pearson, 1980; Ekeberg and Pearson, 2005; Grillner and Rossignol, 1978). If the ankle extensors are loaded during stance, their Ib afferents inhibit flexor burst activity (Duysens and Pearson 1980). Electrical stimulation of the Ib afferents has a similar effect, prolonging the stance phase (Whelan and Pearson 1997; Whelan et al. 1995) and inhibiting flexor activity (Conway et al. 1987; Guertin et al. 1995). Flexion can be initiated by stretching hip flexor muscles, activating Ia and II muscle spindle afferents (Grillner and Rossignol 1978; Hiebert et al. 1995; Kriellaars et al. 1994). The importance of these two sensory signals was demonstrated in cats (McVea et al. 2005) and in a computer simulation (Ekeberg and Pearson 2005; Prochazka and Yakovenko 2007). The conditions prescribed by these sensory signals can be utilized in control systems for restoring walking (Prochazka 1993; Guevremont et al. 2007; Holinski et al. 2011; Mazurek et al. 2012; Prochazka 2011).

Afferent input can be used to make corrections during walking. Forssberg (1979) was the first to assess the functional role of cutaneous reflexes during locomotion by combining kinematics and neural responses. He electrically and mechanically stimulated the dorsum of a cat's paw during the swing phase of locomotion, and observed a stumbling corrective response, where the perturbed limb continued past the obstacle in order to maintain stability. It was later demonstrated that the origin of the response is the cutaneous afferents (Prochazka et al. 1978; Wand et al. 1980). This response was also elicited in people by stimulating the superficial peroneal nerve, which innervates the dorsum of the foot (Van Wezel et al. 1997; Zehr et al. 1997).

Further investigations into the role of cutaneous reflexes on locomotion used electrical stimulation of various nerves in order to activate cutaneous afferents of the foot in humans (Zehr et al. 1997; Zehr et al. 1998). During the stance to swing transition, tibial nerve (innervating the plantar surface of the foot) stimulation elicited a withdrawal response, which allowed for the continuance of the intended swing phase. However, during late swing, the same stimulus generated a placing response, ensuring stability during the weight-transfer. During early swing, stimulation of the superficial peroneal nerve generated a stumble corrective response characterized by knee flexion, as if the limb was clearing an obstacle that made contact with the dorsum of the foot. Stimulation of the sural nerve has different effects for the swing and stance phases of gait (Duysens et al. 1992). During swing, a withdrawal of the foot occurs through knee flexion and ankle dorsiflexion for an avoidance movement, whereas during stance the withdrawal is characterized by hip and knee flexion and ankle dorsiflexion, transferring the body weight to the unperturbed limb. The absence of cutaneous input can be detrimental to gait, particularly during skilled walking (Bouyer and Rossignol 2003a, 2003b). However, the deficits can largely be compensated for, even after spinalization.

1.3 Spinal Cord Injury

1.3.1 Epidemiology and Costs

According to the Rick Hansen Foundation, there are 86,000 people in Canada living with a SCI, with 4,300 new cases per year (Noonan et al. 2012; Farry 2011). Over half of all SCIs occur in young adults between 16 and 30 years of age, 81% of them being males ("Spinal Cord Injury (SCI) 2017 Facts and Figures at a Glance" 2017; Farry 2011). With a vast portion of the population incurring the injury in their prime working years, there is a large financial burden on society due to medical costs and lost earnings, totaling $2.7 billion per year for newly injured Canadians (Farry 2011).

The most common causes for traumatic SCIs are motor vehicle collisions and falls ("Spinal Cord Injury (SCI) 2017 Facts and Figures at a Glance" 2017; Noonan et al. 2012). The most frequent type of SCI is incomplete, affecting more than 60% of the SCI population. The survey conducted by Andersen et al. 2004) revealed that people with paraplegia prioritize regaining walking movements, ranking it first or second nearly 40% of the time, to improve their quality of life.

Additionally, people with SCI experience numerous secondary complications, largely spawning from limited mobility. Secondary complications from a SCI include spasticity (Rekand et al. 2012), bone density loss (Dolbow et al. 2011), muscle atrophy (Moore et al. 2015), pressure ulcers (DeJong et al. 2014), infections (Garcia-Arguello et al. 2017), diabetes (Lai et al. 2014), autonomic dysreflexia (Cowan 2015), chronic pain (Saulino 2014), and cardiovascular dysfunction (Hagen et al. 2012).

1.3.2 Stages of Injury

SCI can be separated into two stages of injury: primary and secondary (Kim et al. 2017). The primary injury consists of the initial mechanical insult to the spinal cord. This results in axonal damage and compromises the BBB. The secondary injury exacerbates the injury through acute and chronic immune responses. The secondary injury can be divided into three sub-phases according to their time of onset and duration.

The acute phase of the secondary injury lasts up to 48 hours after the initial injury (Tator and Fehlings 1991; Kwon et al. 2004). Vascular disruption causes both hemorrhage and ischemia throughout the spinal cord. Damage to the BBB results in increased permeability of inflammatory factors such as TNF-α and IL-1β (Pineau and Lacroix 2007). Inflammatory reactions from incoming macrophages and T-cells and resident astrocytes and microglia are initiated to clear the damaged tissue. Damage to cell membranes causes cell lysis and dysfunction of organelles, as well as the production of reactive oxygen species (Donnelly and Popovich 2008). There is an increased activation of excitatory neurotransmitters which act on receptors on intact cell membranes. These cells become over-excited, causing high levels of Ca^{2+} to enter the cell and activate enzymes that cause damage to the cell structure. This process is known as excitotoxicity (Li and Stys 2000). Excitotoxicity leads to apoptosis of neurons and glial cells; oligodendrocytes, responsible for neuron myelination, are especially susceptible to excitotoxicity (Park et al. 2004). Demyelination peaks at 24 hours after the injury in rats (Totoiu and Keirstead 2005).

The sub-acute phase occurs between 2 days and up to 2 weeks after the initial injury and is also called the phagocytic phase (Kim et al. 2017). Astrocytes proliferate to begin to form the glial

scar around the injury, which also creates a barrier for axonal regeneration (Faulkner et al. 2004). There is a reduction in edema and the infiltration of immune cells is limited as the integrity of the BBB is being re-established (Herrmann et al. 2008). There are also growth factors produced, which aim to facilitate oligodendrocyte-precursor cell migration, proliferation, and differentiation. The chronic phase of the secondary injury lasts more than 6 months after the initial injury. In this stage the lesion matures, with the glial scar present. Finally, the syrinx develops, which is a fluid-filled cavity within the lesion (Kim et al. 2017).

1.3.3 Impairments in Walking

Muscle paralysis can lead to complete lack of function or muscle weakness, resulting in reduced stride length and joint range of motion, lack of coordination, and abnormal muscle activity (Pépin et al. 2003; Awai and Curt 2014; Dietz et al. 1995; van der Salm et al. 2005; Grasso et al. 2004). Also contributing to impaired walking is compromised balance control (Scivoletto et al. 2008). Often, people with an incomplete SCI rely on assistive devices and compensatory strategies to ambulate, including limping and leaning (Arazpour et al. 2016; Behrman et al. 2012). Individuals with hemiparalysis, which affects one side more than the other, depend on the stronger leg for support, reducing the stance time of the affected leg (Balasubramanian et al. 2007).

Spasticity can also interfere with walking performance after a SCI as it causes involuntary and abnormal muscle activity (Adams and Hicks 2005). Clonus can make gait unstable as it causes phasic flexion/extension movements at the affected joint (Gross et al. 2012). Co-contraction of muscles can reduce joint mobility, restricting the generation of walking movements (Ekelem and Goldfarb 2018). Furthermore, spasticity reduces the velocity of the knee and ankle joints, limiting their range of motion during walking (Krawetz and Nance 1996). However, moderate spasticity can be beneficial with respect to performing transfers, reducing muscle atrophy, and preventing thromboses (Adams and Hicks 2005; Ekelem and Goldfarb 2018).

1.3.4 Treatments after Spinal Cord Injury

As there is no cure for a SCI, there are three primary streams of research aiming to improve function after SCI: neuroprotection, regeneration, and rehabilitation. These streams target the

different phases of the secondary injury: neuroprotection targets the acute phase, whereas regeneration and rehabilitation target the sub-acute to chronic phases.

1.3.4.1 Neuroprotection

The goal of neuroprotection is to reduce the size of the secondary injury by preventing any further damage from occurring near the lesion in the acute phase of a SCI (Kwon et al. 2004). Decompression surgery shortly after injury has been shown to improve motor recovery and reduce the length of stay in hospital (Dvorak et al. 2015). Another common, but controversial, neuroprotective approach is administering a high dose of methylprednisolone, an anti-inflammatory corticosteroid (Kwon et al. 2004). This treatment is accompanied by severe side effects such as gastrointestinal hemorrhage, pulmonary embolism, pneumonia and death, and has not been shown to have any neurological improvements in clinical trials. It is not recommended by the Congress of Neurological Surgeons (Kim et al. 2017; Hurlbert et al. 2015).

Other therapies that have been shown to be neuroprotective and led to improved motor function include GM-1 and minocycline (Geisler et al. 2001; Casha et al. 2012). Other neuroprotective approaches include administering erythropoietin (Boran et al. 2005), or by targeting excitotoxicity through NMDA or AMPA antagonists (Feldblum et al. 2000; Wrathall et al. 1997), blocking Ca^{2+} channels (Fehlings et al. 1989), or by restoring the conductance of action potentials by blocking K^{+} channels exposed from demyelination (Cardenas et al. 2007). Hypothermia has also been explored as a neuroprotective treatment (Dididze et al. 2013; Ahmad et al. 2014; Ok et al. 2012). However, many of these approaches are plagued by conflicting evidence, adverse effects, or a lack of subsequent clinical studies.

1.3.4.2 Regeneration

The ultimate treatment is regeneration of damaged axons. Several techniques investigated for neuroregeneration include replacement or remyelination therapies using stem cells (Assinck et al. 2017; Nistor et al. 2005; Biernaskie et al. 2007; Ramer et al. 2004), bridging the lesion site with a physical scaffold (Jian et al. 2015), introducing growth factors to facilitate a supportive growth environment (Fortun et al. 2009; Vavrek et al. 2006; Romero et al. 2000), or inhibiting or eliminating anti-growth factors near the injury site (Bradbury et al. 2002; Zörner and Schwab

2010). Although tremendous advances have been made in spinal cord regeneration research (Murray and Fischer 2001, Raisman 2001, Davies et al 1997, Novikova et al 2017), human trials to date have failed to produce functional benefits (Hulseboch et al 2000, Kim et al 2017). An important aspect of regeneration is ensuring that the regenerated axons innervate functionally relevant targets. If misguided growth occurs and the axons synapse on inappropriate targets, complications including spasticity, chronic pain, and autonomic dysreflexia may arise (Romero et al. 2000; Finnerup 2013; D'Amico et al. 2014). Rehabilitation combined with regenerative methods may help regenerating axons reach relevant targets, improving function and reducing undesired consequences (Ying et al. 2008; Lu et al. 2012).

1.3.4.3 Rehabilitation

Traditional rehabilitative strategies aim to develop and improve compensatory skills required to perform tasks of daily living utilizing remaining function. Such approaches include strength training, acquiring new motor strategies, and using assistive devices such as wheelchairs and braces (Behrman et al. 2012; Harkema et al. 2012). A relatively newer approach to rehabilitation focuses on training to promote plasticity and recover function. An example of this is gait training, which involves large repetitions of stepping movements (Behrman et al. 2012; Harkema et al. 2012). Body-weight supported treadmill training (BWSTT) is a very common gait training paradigm that allows for a large number of step repetitions even before patients can bear weight (Wessels et al. 2010; Barbeau 2003; Gardner et al. 1998; Dietz et al. 1994). It entails suspending a person using a harness over a moving treadmill belt. Often assistance is required to properly step and place the foot during training by a physical therapist. There are also systems that use robots for assisting the stepping over the treadmill belt (Lam et al. 2015; Alcobendas-Maestro et al. 2012). As the stepping improves, the support of the body-weight is gradually reduced. BWSTT has been shown to improve balance and walking in people with a chronic incomplete SCI (Dietz et al. 1994; Wessels et al. 2010; Harkema et al. 2012). Over-ground and skilled walking training has also been implemented, aiming to enhance function through more conscious effort by the individual to perform the task. Skilled walking training has been shown to improve walking function, however; to a lesser extent than BWSTT, possibly due to a fewer number of steps taken during training (Yang et al. 2014). BWSTT with and without robotic assistance can

also be combined with functional electrical stimulation (FES) to assist with leg movements and prevent muscle atrophy (Laursen et al. 2016; Field-Fote 2001).

1.4 Functional Electrical Stimulation

FES is a broad term for a technique that uses electrical stimulation to produce or restore a function. Peripheral FES refers to peripheral activation of motor units, either through surface or implanted electrodes. After a SCI, the spinal networks below the lesion and their connections to muscles remain intact (Hunter and Ashby 1984). This is the basis for many rehabilitative interventions that activate the remaining motor units using peripheral FES. The motor units are activated extracellularly by the stimulating current, causing the nerve fibers to depolarize and activate the muscles (Merrill et al. 2005; Gater et al. 2011). The activation of motor units has been characterized as disorderly and synchronous with limited spatial-activation favouring fast fatigable motor units (Gregory and Bickel 2005; Bickel et al. 2011; Maffiuletti 2010). Larger motor units have a lower impedance and are therefore easier to depolarize with externally-applied currents (Gregory and Bickel 2005; Henneman et al. 1965). These units are more fatigable than smaller, more fatigue-resistant motor units. However, the larger fibered fast fatigable and fast fatigue-resistant motor units produce a larger force than slow fatigue-resistant fibers. The large force production by peripheral FES has been utilized in many applications for exercise and rehabilitation after SCI; however, the use of peripheral FES systems is limited by the rapid fatigue caused by the reversed recruitment order (Peckham and Knutson 2005; Maffiuletti 2010; Triolo et al. 2012). Nonetheless, peripheral FES has been used for a variety of rehabilitative applications including improving bone and muscle health (Bélanger et al. 2000), reduce spasticity (Braun et al. 1985; Stefanovska et al. 1988, 1989; Mirbagheri et al. 2002), increase circulatory function (Rangappa et al. 2010), and restore functions including respiration (Talonen et al. 1983), bladder evacuation (Brindley 1977; Tanagho et al. 1989), grasping (Gan et al. 2012; Ajiboye et al. 2017), standing (Bajd et al. 1981; Vette et al. 2009; Triolo et al. 2012), and even walking (Strojnik et al. 1987; Kobetic et al. 1999; Guiraud et al. 2006).

1.4.1 FES Uses in Walking

The first use of peripheral FES to restore function during walking was in the early ‘60s to correct foot drop by stimulating the peroneal nerve during the swing phase (Liberson et al. 1961).

Similar systems have been developed and commercialized (O'Dell et al. 2014; Everaert et al. 2013).

An example of a surface peripheral FES system is the Parastep (Sigmedics, Inc., Northfield, IL, USA) (Chaplin 1996), which is the only FDA approved walking peripheral FES system. The Parastep activates knee and hip extensors for the stance phase, and peroneal nerves to induce the flexor withdrawal reflex for the swing phase. With adequate training, walking distances achieved ranged from 30 feet to 1 mile (Graupe and Kohn 1998). In a study with 16 Parastep users, an average of 120m of walking was achieved after 11 weeks of training (Klose et al. 1997). Large metabolic costs were reported, limiting this system to an exercise tool rather than a solution for walking (Spadone et al. 2003).

Peripheral FES systems that use implanted electrodes were developed for use in people with both complete (Kobetic et al. 1999; R. Davis et al. 1999; Johnston et al. 2005; Guiraud et al. 2006) and incomplete (Hardin et al. 2007; Dutta et al. 2008) SCIs. Implanted electrodes have the benefit of reaching deeper muscles and do not require daily placement of electrodes. Each system used between 8 and 22 channels, distributed throughout the legs and trunk muscles for stability. Results demonstrated standing times from 3 minutes to over 60 minutes (R. Davis et al. 1999; J. Davis et al. 2001) and walking up to 100 m (Guiraud et al. 2006) and 300 m (Hardin et al. 2007) for complete and incomplete SCI, respectively. Dutta and colleagues (2008) added surface electromyographic (EMG) recordings as feedback signals to trigger the stimulation to restore walking. However, a study done by Triolo and colleagues (2012) involving 15 participants found that their system was used primarily for exercise. Despite the tremendous outcomes of peripheral FES systems, people who use them experience rapid fatigue of their muscles and plateaus in strength (Peckham and Knutson 2005); thus limiting the use of these systems for accomplishing daily activities. However, modifying stimulation parameters (Zheng and Hu 2018; Lou et al. 2017) and targeting reflexive activation of muscles (Bergquist et al. 2014) have been shown to reduce muscle fatigue and may increase the longevity of peripheral FES use.

1.5 Spinal Cord Stimulation

Spinal cord stimulation is a type of FES, and can be achieved through several different modalities, varying in their targets and location with respect to the spinal cord. Specifically, spinal cord stimulation can be achieved by placing surface electrodes over the spinal cord, implanting electrodes epidurally or intraspinally, or recently, using magnetic stimulation over the lower back.

1.5.1 Magnetic Spinal Cord Stimulation

Recently, a non-invasive approach to stimulating the spinal cord to produce leg movements has emerged. Magnetic stimulation over the lumbar vertebrae, in combination with surface electrical stimulation of the sural nerve, has been shown to produce walking movements in healthy participants in a lateral recumbent position (Sasada et al. 2014). At 47% body weight support, the participants moved forward using walking-like movements. EMG activity recorded from either the posterior deltoid during arm swing or the first dorsal interosseous during hand grip were used to control the frequency of the magnetic pulses delivered to the spinal cord as well as the frequency and amplitude of the sural nerve. The participants showed variation in the optimal stimulation site over the vertebrae: T12-L1, L1-L2, or over L2-L3. The reason for individual differences is unknown at this time and is of interest since these participants had an intact nervous system. The authors speculate that it may be due to differences in the participants' posture or gait strategy.

The mechanism of magnetic spinal cord stimulation has yet to be elucidated; however, the authors propose that it likely activates spinal circuits in addition to non-selective activation of afferents in the dorsal roots through the eddy currents produced by the coil. Specifically, they believe that large diameter propriospinal and cutaneous afferents are activated and drive the locomotor CPG. Stimulating the sural nerve activates the flexor-crossed extension reflex to enhance the walking movements.

1.5.2 Transcutaneous Electrical Stimulation

Transcutaneous electrical stimulation entails activation of spinal networks via tonic (30 Hz) stimulation through surface electrodes applied over the lumbar spine (Hofstoetter et al. 2015;

Minassian et al. 2016) or cervical spine (Inanici et al. 2018). In participants with an incomplete SCI, the stimulation produced a tingling sensation in the lower limbs, but was not strong enough for eliciting muscle reflexes (Hofstoetter et al. 2015). It was proposed that transcutaneous electrical stimulation provided a general increase in spinal excitability through activation of the dorsal roots (Minassian et al. 2016). When combined with BWSTT in participants with an incomplete SCI, transcutaneous stimulation augmented stepping, especially facilitating hip flexion during swing (Hofstoetter et al. 2015). In complete SCI participants, in combination with BWSTT and robotic-assistance, the number of rhythmically active muscles was increased (Minassian et al. 2016). Transcutaneous stimulation may augment rehabilitation training through reflexive activation of the spinal cord in a non-invasive manner.

1.5.3 Epidural Spinal Cord Stimulation

Epidural spinal cord stimulation (SCS) entails delivering electrical pulses to the dorsal surface of the spinal cord through electrodes that are implanted exterior to the dura mater. It was originally developed for the treatment of chronic pain (Shealy et al. 1967), and is now a widely used clinical neuromodulation tool to treat pain (Raslan et al. 2007; Tator et al. 2012). It has also been explored as a possible treatment for spasticity (Richardson and McLone 1978; Barolat et al. 1988; Pinter et al. 2000; Dekopov et al. 2015).

1.5.3.1 Mechanism of Epidural Spinal Cord Stimulation

Many theories on the mechanism of epidural SCS have been proposed, primarily based on the concept that the stimulation increases the excitability of the spinal cord, similar to the mechanism proposed for transcutaneous spinal cord stimulation (Hofstoetter et al. 2015). Several studies proposed that epidural SCS could be activating intrinsic spinal networks, such as a CPG for locomotion (Iwahara et al. 1992; Dimitrijevic et al. 1998; Gerasimenko et al. 2002; Gerasimenko et al. 2003; Huang et al. 2006; Minassian et al. 2007; Courtine et al. 2009) or for standing (Rejc et al. 2015). It has also been proposed that the stimulation enhances the response of spinal networks to sensory input associated with weight-bearing (Ichiyama et al. 2005), especially proprioceptive feedback (Minassian et al. 2007; Musienko et al. 2012) to control stepping-like patterns. Lavrov (2006) suggested that after an acute SCI, epidural SCS assisted with the return of spinal reflexes, and only then could stepping be initiated. It is also possible that

the increased spinal excitability in combination with training reactivates spared neural networks and enhances plasticity (Herman et al. 2002; Harkema et al. 2011; Capogrosso et al. 2016). In fact, remodeling of corticospinal projections and the formation of intraspinal and supraspinal relays that detoured an injury were identified after a dual hemisection SCI and volitional effort-based training (van den Brand et al. 2012). However, a recent modelling study corroborated with *in vivo* experiments suggests that epidural SCS indirectly activates motoneurons and interneurons through the recruitment of Group I and II afferents (Capogrosso et al. 2013), supporting a previous modelling study (Holsheimer 1998). This was supported by a study comparing the neural activation of epidural and transcutaneous SCS, concluding that both stimulation methods activate the spinal cord via afferent fibers (Hofstoetter et al. 2018).

1.5.3.2 Use in Rehabilitation of Walking

A study by Iwahara and colleagues (1992) demonstrated that epidural SCS in the decerebrate cat could elicit locomotion over a moving treadmill. Specifically, stimulation over the cervical enlargement elicited stepping in all four limbs, and stimulation of the lumbosacral enlargement elicited stepping in the hind-limbs only. Locomotor activity over a moving treadmill in the chronically spinalized cat was demonstrated using epidural SCS between the L4 and L5 spinal segments (Gerasimenko et al. 2002; Gerasimenko et al. 2003). In spinalized rats, rhythmic activity could be elicited, but typically only in a single limb for a short duration of time (<10 s) and required at least 5% of body weight support (Ichiyama et al. 2005). After an acute SCI, only weak rhythmic movements that were not weight-bearing were generated in cats (Musienko et al. 2007). Similar results were seen in the acute spinalized rat, where stepping could only be achieved 3 weeks after the injury, and improved up to 6 weeks post-injury (Lavrov et al. 2006). Epidural SCS in hemiparetic monkeys was able to restore weight-bearing treadmill and over-ground locomotion within 6 days post-injury (Capogrosso et al. 2016).

Epidural SCS over the lumbar enlargement could generate rhythmic flexion and extension muscle activity in individuals with a chronic SCI in the supine position (Calancie et al. 1994; Dimitrijevic et al. 1998; Gerasimenko et al. 2002; Minassian et al. 2007; Danner et al. 2015). Enhanced muscle activity and walking function resulted from epidural SCS in combination with

BWSTT in chronic incomplete SCI participants (Herman et al. 2002; Carhart et al. 2004; Huang et al. 2006).

Studies in human participants with SCI have shown remarkable results where, after training with epidural SCS, some voluntary function returns. A subject with an injury classified as ASIA-B (motor complete, sensory incomplete) underwent 7 months of stand training in combination with epidural SCS (Harkema et al. 2011). At the end of the 7-month period, the subject was able to stand with minimal assistance for at least 4 minutes, and had recovered the ability to perform some toe extension, and ankle and hip flexion. This led to follow-up studies with additional participants (1 ASIA B, 2 ASIA A) (Angeli et al. 2014; Rejc et al. 2015). All participants underwent at least 80 locomotor training sessions before receiving an implant, then underwent standing followed by step training with epidural SCS after receiving the implant (Angeli et al. 2014). By the end of training, 3 out of 4 participants were able to oscillate their leg between flexion and extension, and modulate the force produced during leg movement (one individual could not perform these tasks due to severe clonus). All participants achieved full weight-bearing with minimal assistance (Rejc et al. 2015). Interestingly, the ASIA A (motor and sensory complete) participants required less assistance for standing than the ASIA B participants (holding onto horizontal bars for balance versus elastic bands attached to a frame for assistance with hip extension).

Earlier this year, 3 studies reported the restoration of over-ground walking in people with a SCI using epidural SCS with an extensive rehabilitation program. One study described an ASIA A subject who, after 43 weeks of multi-modal training, was able to walk over-ground with epidural SCS and assistance from a trainer for hip support (Gill et al. 2018). This person was able to walk at 0.2 m/s, with a step period of 4 s, and a maximum distance of 102 m. One study included ASIA A and B participants (Angeli et al. 2018). The ASIA A participants were only able to achieve treadmill locomotion with body-weight support. However, the ASIA B participants were able to accomplish over-ground walking with an assistive device or by holding onto poles held by trainers. This study reported a maximum walking speed of 0.19 m/s and 90.5 m of continuous walking. The most recent study used targeted epidural SCS, which activated the motoneuron pools by selecting the appropriate dorsal roots (Wagner et al. 2018). After 5 months of locomotor

training using targeted epidural SCS, an ASIA C (motor and sensory incomplete) and an ASIA D (less severe motor and sensory incomplete) participants were able to walk over-ground with 35% body-weight support at the hips. A different ASIA C participant required only a walker to locomote over-ground. The over-ground distances and walking speeds were not reported. All participants were able make 1200 steps over a treadmill with 15% body-weight support in 1 hour, corresponding to a distance of 1 km and step period of 3 s.

1.5.3.3 Combined with Pharmacological Activation

Recent studies in completely spinalized rats have demonstrated that training combined with epidural SCS and amine agonists can restore weight-bearing stepping over a treadmill in the presence of stimulation (Courtine et al. 2009; Musienko et al. 2012). Rats with staggered hemisection SCIs that were trained using a transition from treadmill stepping to intentional over-ground stepping in addition to the electrical and chemical stimulation regained full weight-bearing bipedal locomotion after 5 to 6 weeks (van den Brand et al. 2012). Furthermore, an additional 2 to 3 weeks of training, the rats were able to avoid obstacles and climb stairs in the presence of stimulation.

By increasing the excitability of spinal networks through afferent activation, epidural SCS has improved walking function after incomplete and complete SCI. It presents as a powerful rehabilitative tool for rehabilitation after severe SCI. However, specificity of activation in the spinal cord is limited as much of the current spreads in the cerebrospinal fluid (Holsheimer 1998).

1.5.4 Intraspinal microstimulation

Intraspinal microstimulation (ISMS) entails implanting fine microwires into the grey matter of the spinal cord (Figure 1.2). It originated as a research tool to study spinal networks. Renshaw (1940) stimulated in the spinal cord to measure the synaptic delay in reflex pathways. Later, mapping experiments were performed to investigate the connections between interneurons mediating reciprocal inhibition (Jankowska and Roberts 1972). ISMS in cats showed that motoneurons can be activated directly if the tip of the electrode was adjacent to the initial segment of the motoneuron axon, or the soma itself (Gustafsson and Jankowska 1976). ISMS

was used to study the organization of spinal circuitry in the intermediate grey matter of bull frogs (Bizzi et al. 1991; Giszter et al. 1993). More recently, ISMS in the ventral horn of the spinal cord grey matter has been explored as a possible intervention to restore walking after injury or disease. ISMS has been tested in various animal models including rats, cats, pigs, and monkeys. The majority of work investigating the use of ISMS to produce walking has been tested in cat and rat models.

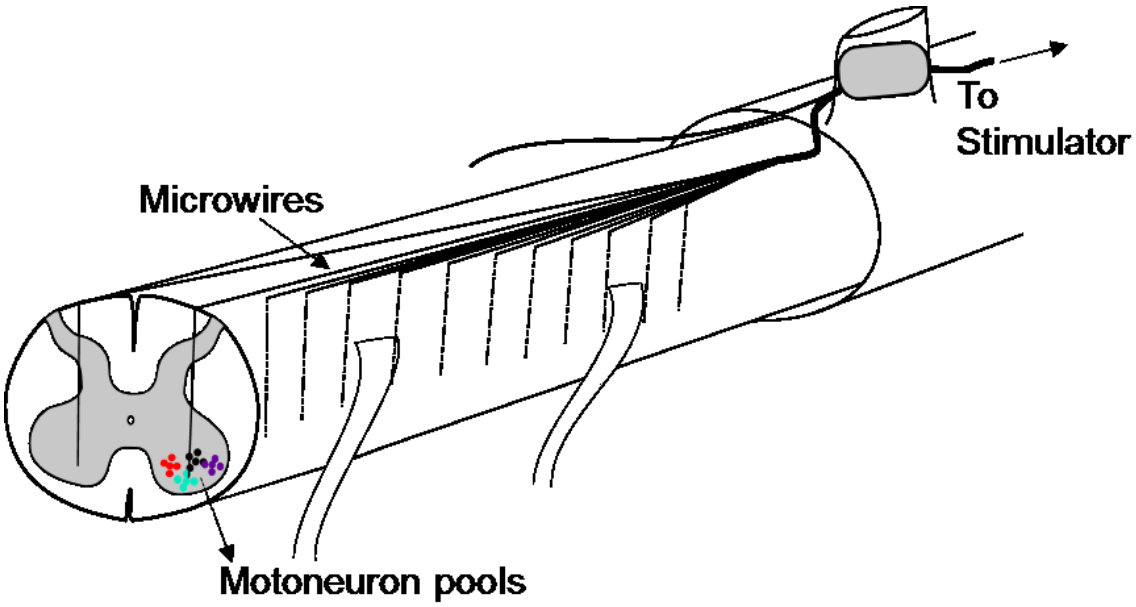

Figure 1.2. ISMS implant. Microwires are implanted into the ventral horn of the lumbosacral enlargement.

1.5.4.1 Mechanism of Intraspinal Microstimulation

ISMS can selectively generate movements in muscles of the hind-limbs as well as produce multi-joint synergies necessary for walking (Mushahwar and Horch 2000) using very low currents (on the order of μA) through a single electrode (Mushahwar and Horch 1998; Saigal et al. 2004; Holinski et al. 2011). Selective activation of muscle groups is possible because the electrodes are implanted into lamina IX of the ventral horn of the lumbosacral enlargement in the spinal cord (Vanderhorst and Holstege 1997; Mushahwar and Horch 2000). This region contains the motoneuron pools for the lower limb muscles. Despite the close proximity to the motoneuron pools, ISMS likely activates them indirectly through networks of afferent projections, propriospinal, and other interneuronal pathways (Mushahwar et al. 2003; Bamford et al. 2005; Gaunt et al. 2006; Bhumbra and Beato 2018).

1.5.4.2 Advantages of Intraspinal Microstimulation

There are three main advantages of ISMS: The ISMS implant is distant from moving muscles; the ISMS implant is small and contained within a localized region; and ISMS preferentially recruits fatigue-resistant muscle fibers.

Peripheral FES systems activate peripheral nerve axons by stimulating through surface or implanted electrodes. Surface peripheral FES systems require much effort donning and doffing the electrodes, while implanted systems are susceptible to lead breakage and dislodgement or shifting from the implant site due to the contractions of the muscles surrounding them (Kilgore et al. 2003). However, an intraspinal implant, which is contained within the spinal cord, may be less susceptible to dislodgement or lead breakage because it is distant from contracting muscles and moving joints (Mushahwar et al. 2000). There is the possibility of some shifting of the electrode locations due to extreme trunk movements and the relative motion between the spinal cord and the fixation point on the vertebral body; however, this possibility can be avoided by using strain-relief mechanisms such as coiling of the lead wires (Toossi et al. 2017).

The lumbar enlargement, which is the implant region, is only 3 cm long in cats and 5 cm long in humans. The number of implanted electrodes required to produce walking movements can be as few as 4 (Saigal et al. 2004); however, it is advantageous to implant more electrodes to achieve redundancy in responses, higher selectivity (Holinski et al. 2011), and to deliver the stimulation in an interleaved manner (Mushahwar and Horch 1997; Lau et al. 2007; Bamford et al. 2011). Interleaved stimulation entails stimulating through two electrodes targeting the same function at half of the desired frequency such that the combined frequency will be the desired frequency. This has the advantage of recruiting motor units at a lower frequency, thereby reducing fatigue of the muscles.

The entire ISMS system is implantable. Specifically, implantable wireless stimulators have been developed that can be fixed onto the same spinous process that the electrode lead wires are adhered to (Troyk et al. 2012; Grahn et al. 2014). They communicate and receive power via radio frequency to an external coil that lies on the surface of the skin over the implant area.

Additionally, ISMS control strategies have been successfully implemented on an implantable microchip (Mazurek et al. 2010) that was used *in vivo* to produce walking (Mazurek et al. 2016).

ISMS preferentially recruits fatigue-resistant muscle fibers. ISMS has been shown to activate motor units in a near-normal recruitment order (Bamford et al. 2005) to produce graded responses after a complete SCI (Saigal et al. 2004). This may be due to the implant's location in the central nervous system facilitating trans-synaptic activation of motor units (Gaunt et al. 2006; Mushahwar et al. 2003).

1.5.4.3 Disadvantages of Intraspinal Microstimulation

The implant procedure is invasive, especially compared to the other FES methods described. It requires a laminectomy over two spinal segments to expose the lumbar enlargement (Bamford et al. 2016). Furthermore, in humans, the dura mater will need to be opened in order to access the spinal cord for implanting the electrodes. However, with the increase in invasiveness, ISMS offers higher selectivity in the responses that are evoked (Mushahwar and Horch 1998; Guevremont et al. 2006). Furthermore, laminectomies are not uncommon procedures (Tohidi et al. 2018). Further development of the implant array may allow for a faster procedure with smaller and fewer components. Additionally, collaborations with neurosurgeons may assist with developing methods that are more suitable for clinical implementation.

ISMS for standing and walking has yet to be tested in humans. Although the development of the technology and surgical techniques is underway, this limits the comparisons of the results of ISMS with other FES techniques. For example, a recent study demonstrated that anaesthetized cats were able to walk between 609 and 835 m using ISMS (Holinski et al. 2016). These are long distances; however, similar distances have been reported in humans using peripheral FES (Graupe and Kohn 1998). It is difficult to compare these distances as cats and humans have different step periods and stride lengths.

Furthermore, little work has been done using ISMS to restore walking after a chronic SCI. One study demonstrated that stepping over a stationary treadmill belt could be achieved using ISMS 2 to 4 weeks after a complete SCI (Saigal et al. 2004). However, follow-up studies demonstrating

over-ground walking using ISMS after a chronic SCI are needed. Additionally, further demonstration of the efficacy of chronic ISMS implants is needed. Chronic ISMS implants from 2 to 24 weeks in intact cats have shown that the responses remained consistent in 67% of the electrodes (Mushahwar et al. 2000). More studies are needed to repeat these results as well as to extend the testing period to further assess the longevity of ISMS implants.

1.5.4.4 Restoring Other Functions

1.5.4.4.1 Reaching and Grasping

ISMS is also being investigated in the cervical enlargement to restore reaching and grasping after a SCI in both rat (Kasten et al. 2013; Sunshine et al. 2013) and non-human primate models (Moritz et al. 2007; Zimmermann et al. 2011; Zimmermann and Jackson 2014). Zimmerman and Jackson (2014) induced hand paralysis by injecting a temporary paralytic muscimol in the primary motor cortex, and used signals from an implant located in the ventral pre-motor area to control the rate of stimulation delivered to the spinal cord to achieve a grasping task. In some cases, the muscimol did not fully paralyze the hand muscles, mimicking an incomplete SCI. In those cases, residual voluntary muscle activity was used to control the stimulation. Cervical ISMS has also been shown to improved motor function, with benefits lasting beyond the stimulation trial (Kasten et al. 2013). Cervical ISMS after incomplete SCI may promote long-term recovery of function, possibly attributed to axonal growth and elongation regulated by neural activity, synaptogenesis, and dendrite stability (Mondello et al. 2014).

1.5.4.4.2 Respiration

Recently, ISMS implants in the cervical and high thoracic spinal cord has been shown to activate the diaphragm and intercostal muscles in intact (Sunshine et al. 2018) and hemisected (Mercier et al. 2017) rats. It was found that intact medullary drive modulated the muscle activation differently during inspiration and expiration (Sunshine et al. 2018). Furthermore, tongue muscle activity during inspiration was used to trigger ISMS targeting the phrenic motor pool, demonstrating a possible closed loop method for restoring breathing (Mercier et al. 2017).

1.5.4.4.3 Micturition

The sacral spinal cord contains motoneurons innervating the external urethral sphincter and the detrusor muscle (Gaunt and Prochazka 2006). For successful micturition, the detrusor muscle contracts the bladder and the external urethral sphincter is relaxed. Intraspinal electrodes implanted in the intermediolateral grey matter of the sacral spinal cord was able to increase bladder pressure and cause bladder voiding in approximately half of implanted animals (Friedman et al. 1972; Nashold et al. 1971). Based on the results from these studies, 27 people were implanted with penetrating electrodes in the sacral spinal cord (Nashold et al. 1972; Nashold et al. 1981). Adequate voiding was achieved in 10 of the 13 females but only in 5 of the 14 males. The males often experienced a spastic urethral sphincter during stimulation (Nashold et al. 1981) which was sometimes resolved with a partial transurethral sphincterotomy. Overall, the sacral implants had about a 60% success rate for bladder voiding. This may be due to the difficulty in targeting in the small sacral cord, as well as current spread (Gaunt and Prochazka 2006). Later work utilized smaller electrodes, limiting bladder and sphincter co-contractions (Carter et al. 1995; Grill et al. 1999). However, possible interneuron activation may have prevented voiding due to contraction of the external urethral sphincter (Buss and Shefchyk 2003; Gaunt and Prochazka 2006). As smaller electrode arrays and stimulation protocols are developed, intraspinal solutions for restoring micturition may have better results in the future.

By targeting the motor regions of the spinal cord, various functions may be restored after neural injury or disease. However, activation of these regions must be coordinated to successfully restore more natural function. Many control methods have been developed to restore walking in SCI models using various forms of FES, targeting the periphery and the spinal cord. Some of the control methods include a machine learning approach.

1.6 Machine Learning

Machine learning techniques learn from data to make predictions or find trends. There are several fields within machine learning, each modelled after different aspects of biological learning. Machine learning can be applied to large and noisy data sets, with both offline and online capabilities. It may a valuable tool to study spinal locomotor networks and to restore function after a SCI.

1.6.1 Supervised Machine Learning

Supervised machine learning uses pre-labelled data to obtain generalizations between paired inputs and outputs. The inputs are features or attributes that describe or represent the data, and the outputs can be classification or numerical values (Witten et al. 2016). The biological equivalent is concept learning, which entails using previous experiences to form associations or recognize resemblances to categorize objects or respond to stimuli (Zentall et al. 2014). Learning is achieved by providing examples which are used to form a new concept from the generalizations made about the examples. For example, suppose you are presented with examples of fruits such as an apple, orange, banana, and pineapple as well as examples of vegetables including carrots, broccoli, asparagus, and potatoes. Then you are presented a beet, of which you have never seen before, and are asked to classify it as a fruit or a vegetable. You would likely approach this task by visually comparing it to the fruits and vegetables that you have seen before. You may also consider other attributes, such as taste, smell, or colour to come to a conclusion. In supervised machine learning, the attributes are used as inputs, and the output is the classification of fruit or vegetable. A generalization of the attributes to either a fruit or vegetable has been learned by experiencing different fruits and vegetables. Using those generalizations, an estimate of which class the new piece of produce belongs to can be made.

The stage of presenting an algorithm with known examples to obtain a generalization is referred to as training. Once an algorithm has been sufficiently trained, new input data is presented. The predicted output can be compared to the known output to determine the testing accuracy. This demonstrates how well the algorithm generalized the training data to make effective predictions on unseen data. Ideally, the generalizations are broad enough to perform well at classifying new data, and does not over-fit to the training data.

1.6.1.1 Typical Procedures

General terminology: inputs are referred to as features or attributes. Each example, or instance, can have a set (or vector) of attributes to each output. The output can be either a class value or a numeric value.

A large set of pre-labelled data is split into two sets: the training data set and the testing data set. Often, 80-90% of the data are assigned to the training data set, with the remainder in the testing data set (Witten et al. 2016). The sets of data should comprise of randomly assigned and proportional distributions of the defined classes.

During the training process, to avoid over-fitting to the training data, it is recommended to perform cross-validation. Often, 10-fold cross-validation is performed during training. Each fold consists of partitioning the training data into two sets: 90% into the validation-training set and 10% into the validation set. The function is trained using the validation-training set and the validation set is used to test the performance of the generalization. This process is repeated ten times (equal to the number of folds) with different partitions of the data. The final generalization consists of an average of the results over the multiple folds. The process of cross-validation is similar to the standard partitioning of the entire data set into training and testing sets, but allows for the validation sets to be used repeatedly throughout training. It rigorously tests for generalizability and performance, as the training accuracy can be calculated for each fold, while utilizing the available data maximally for training.

Following training, the inputs for each instance in the testing data set, of which the algorithm has never seen before, is presented. The output from the algorithm for each instance is compared to the actual output in order to determine the testing accuracy. To generalize appropriately, the algorithm must be presented with many examples with variability similar to the data it is designed to predict. Sufficient generalizability is acquired when there is a high training and testing accuracy, meaning that the algorithm did not over-fit to the training data. What is considered to be high accuracy is problem-dependent and must be determined by the problem designer.

There are dozens of different supervised machine learning algorithms, each with their own strengths and weaknesses. Choosing the algorithm that is appropriate for the problem may not be straightforward. Software such as Weka (Frank et al. 2016) enables users to try various algorithms to determine which is most suitable for solving their problem.

1.6.1.2 Relevant Algorithms

1.6.1.2.1 Multilayer Perceptron

A multilayer perceptron (MLP) is type of feed-forward artificial neural network (ANN). Its structure is modeled after biological neural networks (Minsky et al. 2017). An MLP consists of three layers of nodes, or neurons, which are linked through weighted connections (Figure 1.3). These layers are in the input, hidden, and output layers. The number of nodes in the input and output layers are defined by the number of features and classes, respectively. The input and hidden layers contain a bias unit of 1 that connects to the nodes in the following layer.

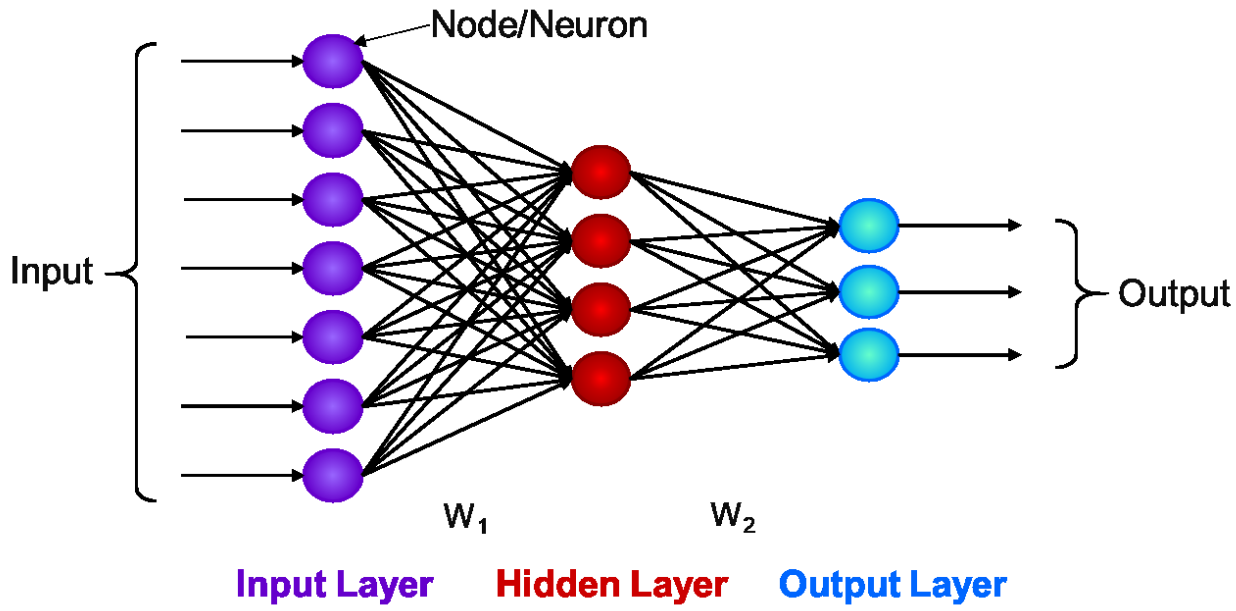

Figure 1.3. Example of multilayer perceptron (MLP). It consists of three layers connected by weights.

The weights connecting the nodes of the input layer to hidden layer, and hidden layer to output layer, are learned through back-propagation during training. The MLP was popularized by the addition of backpropagation, which uses gradient descent to update the weights by minimizing errors, enabling the MLP to separate non-linear data (Rumelhart et al. 1986). Although gradient descent only finds the local minimum, MLPs trained using backpropagation are powerful and have been widely used. How quickly gradient descent converges depends on the learning rate, or step size (Witten et al. 2016). If the learning rate is too large, it may overshoot and fail to converge; if the learning rate is too small, convergence is very time-consuming. The learning process can be accelerated by adding a momentum term while updating the weights. The

momentum adds a portion of the update value from the previous update to the new weight. These are parameters that should be tuned when training an MLP.

During testing, the input layer receives normalized values of the inputs, or features, which are relayed to the hidden layer by multiplying them by their corresponding weights. The activation of the hidden layer is done using a sigmoid function, a mathematically-convenient substitution for a step function.

$$y = \frac{1}{(1+ e^{-x})} \tag{1.1}$$

This enables the MLP to separate non-linear data. Activation of the output layer is also done using a sigmoid function, taking in the outputs from the hidden layer multiplied by their weights. Classification is finalized at the output layer; the output node with the greatest activation corresponds to the class to which the instance of data belongs.

MLPs are capable of representing complex expressions. The weights can be updated online, meaning that the network can continue training as new data become available. Albeit, this process may be time-consuming and computationally expensive. A disadvantage of MLPs is the structure is difficult to interpret; the impact of the values of the weights is often unclear because of the hidden layer (Witten et al. 2016). Additionally, MLPs are susceptible to over-fitting to the training data, especially if the network is too large. Methods to reduce over-fitting include early stopping, weight decay, or 10-fold cross-validation. An advantage of MLPs includes being able to form generalizations to perform both numeric and class prediction. The predictions can be made on non-linear data and complex systems, making them applicable to real-world problems. MLPs are not restricted to the types of inputs; they can still generalize with noisy or missing values. Additionally, MLPs are simple to implement as they require only simple linear algebra for the inputs and weights, and use a sigmoid function for node activation.

1.6.1.2.2 Linear Regression

Linear regression can be used for numeric prediction using numeric attributes (Witten et al. 2016). The prediction is formed by linearly combining the input attributes with weights, which are learned during training:

$$x = w_0 + w_1 a_1 + w_2 a_2 + \cdots + w_n a_n \quad (1.2)$$

The weights are calculated by minimizing the sum of squares of the differences between the actual and predicted values of the output (cost function):

$$J_n = \frac{1}{n}\sum_{i=1}^{n}(y_i - \boldsymbol{w}^T \boldsymbol{x}_i)^2 \quad (1.3)$$

Minimization is often done using gradient descent (Ng 2012). The result of linear regression is a linear approximation of the data, often referred to as the line of best fit. This technique is very simple and commonly used, but is limited by its linearity.

1.6.1.2.3 Model Tree

A model tree is a combination of a decision tree with a linear model to obtain a numeric prediction (Witten et al. 2016; Quinlan 1992). To build the tree, during training, attributes are tested to determine which one best maximized the expected error reduction (Witten et al. 2016). That attribute is chosen to form the splitting criterion at that particular node of the tree. Additional nodes are added to the tree until the error reduction is very small or there are very few instances remaining. The final leaf of the decision tree contains the linear model, which is found using linear regression. During testing, attribute values are compared to the splitting criterion at the nodes to by routed down a branch of the tree towards a leaf with a linear regression model.

Model trees can grow substantially during training and over-fit to the training data. Over-fitting can be reduced through pruning the tree. Starting from the leaf, the expected error at each node is calculated. If the expected error is reduced, then the tree is pruned to that node. This process continues until the expected error is no longer decreasing. An advantage of model trees is that they have clear and interpretable rules for partitioning the data and indicating which attributes are important for classification. They can handle continuous, discrete, noisy, or missing data. They are not limited to linear data as is regression. Additionally, they are easy to implement as the calculations at each node and leaf are simple comparisons.

1.6.1.3 Uses and Limitations

Supervised machine learning can be a powerful tool in interpreting large volumes of data and learning relationships between variables. It can also find and use trends or patterns in the data that are not obvious to the human users. Supervised machine learning algorithms are limited to the data they train on. For example, if a new class arises that was previously unknown, then it will be misclassified to one of the classes identified during training. For training an algorithm, intimate knowledge of the data is necessary for accurate labelling of examples. The training process often requires a lot of computation time, so it is usually done offline. However, compared to unsupervised machine learning methods, which do not use pre-labelled data to find relationships in data, supervised methods have a higher accuracy and are more reliable.

Supervised methods also have the advantage when interpreting results and accuracy, as unsupervised methods require no prior knowledge and have no answers to compare the results to. Supervised machine learning allows experts to teach an algorithm by providing it with many examples to create a model or function relating the data. In tasks where the outputs are known but manual labelling is time-consuming, supervised methods can be employed to automatically perform tasks quickly and reliably. Supervised machine learning is also useful for prediction problems, where an output needs to be calculated from available information in order to make a decision. Other machine learning algorithms are capable of learning without the need for pre-labelled data, which is beneficial if pre-labelled examples do not exist or are difficult to accurately acquire.

1.6.2 Reinforcement Learning

Reinforcement learning (RL) is an area of machine learning concerned with achieving a goal by maximizing future reward (Sutton and Barto 2018). Traditional RL is analogous to operant conditioning (Skinner 1963; Staddon and Cerutti 2003). The consequences of a behaviour lead to a reinforcing stimulus, either to reward or punish the behaviour. The dopaminergic reward system in the nucleus accumbens, which is the region of the brain concerned with pleasure-seeking (du Hoffmann and Nicola 2014), provides a biological model for many RL algorithms (Sutton and Barto 2018).

1.6.2.1 RL Framework

The RL framework is formalized as a Markov decision process (MDP): a learning agent interacts with its environment by taking certain actions (A) defined by a policy (π) (Figure 1.4; Sutton and Barto 2018). The environment supplies the agent with information regarding the agent's state in the environment (S) and the value of the reward corresponding to the state (R). The goal of the agent is to maximize the reward over the long-term. The return, G_t, is defined as the discounted sum of future rewards:

$$G_t = \sum_{k=0}^{\infty} \gamma^k R_{t+k+1} \tag{1.4}$$

where γ is the discounting factor, and ranges from (0, 1]. Future rewards are discounted because they represent the present value of the future rewards. Upon each iteration, the agent selects an action according to a distribution from its policy, and receives the new state and reward from the environment. The reward is used by the agent to compute or estimate the value of the current state (state value function, v_π) or of the action taken from that state (action value function, q_π).

$$v_\pi(s) \stackrel{\text{def}}{=} \sum_a \pi(a|s) \sum_{s'r} p(s', r|s, a) \left[r(s') + \gamma v_\pi(s')\right] \tag{1.5}$$

$$v_\pi(s) = \mathbb{E}_\pi[G_t|S_t = s] = \mathbb{E}_\pi[R_{t+1} + \gamma G_{t+1}|S_t = s] \tag{1.6}$$

Equation 1.5 is the Bellman equation for the state value function, which defines that the value of a state is the discounted value of the next state and the reward expected at that next state following a policy π. This is the recursive relationship between the value of a state s and the value of the next state s'. Equation 1.6 denotes the expected return when starting in state s and following a policy π. The estimate of the value function is updated, or learned, through interaction with the environment:

$$NewEstimate \leftarrow OldEstimate + \alpha(Target - OldEstimate) \tag{1.7}$$

where α is the step size, or learning rate. The return, G_t, is the target; the difference between the return and the old estimate for the value function is the error in the estimate.

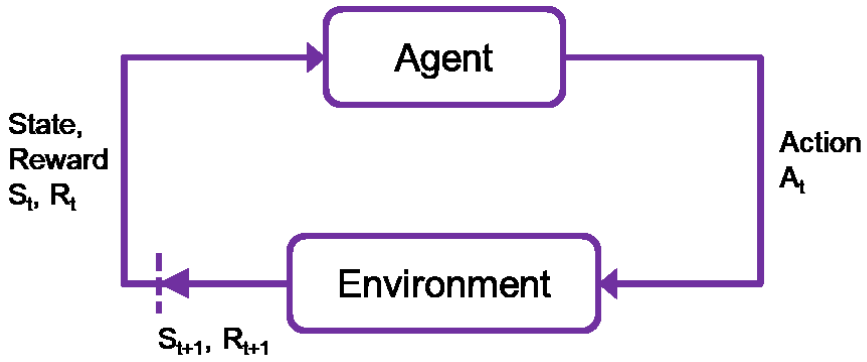

Figure 1.4. Reinforcement learning framework as a Markov decision process. The agent interacts with its environment and receive state and reward information.

The policy defines the probability of an action being selected given a current state. The policy is updated by the agent based on experience. There are two main types of policies: greedy and ε-greedy. Greedy refers to the agent always taking the action that leads to the state with the highest estimated value function. This maximizes the immediate reward by exploiting the current knowledge. ε-greedy refers to a greedy policy where the greedy action is taken $(1 - \varepsilon) \times 100$ percent of the time, and a different action the other times. An ε-greedy policy promotes exploration, which may lead the agent to discovering more optimal actions to states with greater value, maximizing the long-term reward. The learning task is solved by interacting with the environment to obtain the optimal policy (π_*), which is the policy with the largest expected return for all states. Policies can be updated using policy gradient, which uses gradient descent to update the policy in the direction of optimality.

1.6.2.2 Temporal Difference Learning

Temporal difference (TD) learning is a method for estimating the value function using previously obtained estimates (Sutton 1988; van Seijen et al. 2015; Sutton and Barto 2018). This is known as bootstrapping. TD does not require a model of the environment as it learns only from interactions with the environment. By bootstrapping on previous estimates, TD methods update the current estimate of the value function on the following time step:

$$V(S_t) \leftarrow V(S_t) + \alpha(R_{t+1} + \gamma V(S_{t+1}) - V(S_t)) \tag{1.8}$$

From the previous update equation (1.7), the target of the return, G_t, is replaced by $R_{t+1} + \gamma V(S_{t+1})$, which denotes the current reward and the discounted estimate of the future value function. The term comprising of the target compared to the old estimate of the value function is referred to as the temporal difference error (δ_t), as it uses successive estimates in the update:

$$\delta_t = R_{t+1} + \gamma V(S_{t+1}) - V(S_t) \tag{1.9}$$

By updating the value function using other estimates, TD learning can learn faster than other methods (van Seijen et al. 2015). The updates presented so far occur over one time step, as they use an estimate from only the successive time step.

1.6.2.3 Natural Temporal Difference Learning

Reinforcement learning has many properties in common with the dopaminergic reward system. One region where dopamine is produced is by neurons in the ventral tegmental area (Glimcher 2011). These neurons project to other brain regions related to learning, decision making, and motivation. The dopaminergic reward system in the nucleus accumbens uses predictions of a cue or event to alter the excitation of neurons (McGinty et al. 2013; Nicola et al. 2004; Roitman et al. 2005). The neural activity in the nucleus accumbens is stronger when a reward is more available and is in closer proximity (McGinty et al. 2013). This results in reward-seeking behaviour and is pivotal for survival.

The reinforcement signal for TD learning is the TD error (δ), which is the discrepancy between the current and earlier expectations of reward over the long term (Sutton and Barto 2018). The *reward prediction error hypothesis of dopamine neuron activity* postulates that the phasic activity of dopaminergic neurons deliver an error between the old and new estimates of expected future reward (Montague et al. 1996; Schultz et al. 1997). In early learning, upon receiving an unexpected reward, a TD error occurs, reinforcing the events that lead to receiving that reward. If a task is repeated and a reward is repeatedly given upon task completion, then the TD error decreases as there is now an expectation for reward. Experiments in monkeys have demonstrated that there is a shift in neuronal firing from receiving the reward (TD error) to the predictive stimuli of the reward (expectation) during training (Ljungberg et al. 1992). If the monkey pressed

the wrong lever, resulting in no reward being delivered, there was a decrease in the firing rate of the neurons (TD error). Furthermore, neurons related to movement initiation increased their firing rate upon the expectation of food reward, rather than the movements to retrieve the food or to the sensory stimuli upon retrieving the food (Romo and Schultz 1987). Natural and computational approaches to RL and TD learning continue to inform the other (Ludvig et al. 2008, 2012).

1.6.2.4 State Representation

Sensor signals inform the agent about the state of the environment. They are complex with a wide range of possible values. It is computationally useful to represent the state space of sensor signals such that the value function can be approximated. Linear function approximation of the state value function is executed by multiplying a weight vector, **w**, by a feature vector, **x**:

$$v = \boldsymbol{w}^{\mathrm{T}}\boldsymbol{x}(s) \tag{1.10}$$

The feature vector is a binary representation of the state space. The weight vector is updated and learned. The linear combination of the learned weight vector and the state-dependent feature vector results in the estimation of the value function. The following sections will describe a common form of state representation, as well as the state representation method used in this work.

1.6.2.4.1 Tile Coding

Tile coding entails partitioning the state space into grid-like tilings. Each block element is called a tile. If the current sensor values fall within a tile, that tile is active, set to one; all other tiles in this tiling are zero. The size of the tiling, number of tiles, and layering of many tilings can be customized for both coarse and fine representation of the state space. For example, there may be sensor values in the state space that are very unlikely to be active, so there are large, coarse tiles in that region of the state space. On the contrary, there may be a region where fine discrimination of the state space is necessary for learning, in which case there may be smaller tiles or overlapping tilings in that region. Overlapping tilings are common as they provide both coarse

and fine representation. The size of the binary feature vector is the number of tiles in all the tilings; however, many of the values are equal to zero at one time.

1.6.2.4.2 Selective Kanerva Coding

This method of state representation builds off of the work of Pentti Kanerva (Kanerva 1988). Kanerva formulated a model of sparse distributed memory, which is conceptually similar to long-term memory in humans. It postulates that a high-dimensional binary state space can be represented by a set number of randomly placed points, referred to as prototypes. Kanerva coding finds the number of prototypes within a set radius from the current state and activates those prototypes. All other prototypes are set to zero, resulting in a binary feature vector. The number of features in the feature vector does not increase with the addition of sensors; therefore, this method is not susceptible to the dimensionality issues that plague tile coding. An analogy for Kanerva coding is if our galaxy were the state space (3-dimensional for the purpose of this example) and the prototypes were the stars. If the Earth indicates our current location in the state space, then Kanerva coding would define our location by the stars with a set radius, say 20 light-years. Depending on where we are in the state space, a different number of stars will fall within that radius, resulting in a different number of ones in the feature vector, possibly leading to uneven learning according to the locations.

Selective Kanerva coding (SKC) activates the *c* closest prototypes to the current state according to their Euclidean distance, rather than using the activation radius. This ensures that the same number of features are active for every timestep, which is an advantage in common with tile coding. Furthermore, SKC is not affected by the distribution of the prototypes, which can largely affect the performance using traditional Kanerva coding (Travnik and Pilarski 2017). This is analogous to using the, for example, 10 closest stars to our current state, to define the feature vector.

1.6.2.5 Eligibility Traces

Eligibility traces allow for TD learning to occur using estimates of value functions for more than one time step. An eligibility trace (e) is a temporary record of which states were recently visited by the agent. Recency is determined by the factor $\gamma\lambda$, where γ is the discounting factor and λ is

the trace decay parameter (Sutton and Barto 2018). When a temporal difference error occurs, only the recently visited states are eligible for undergoing learning. The most recently visited states are assigned the highest credit for the TD error. The presence of an eligibility trace in TD learning is referred to as TD(λ) and can make learning more efficient. The update equation for the weight vector using an eligibility trace is:

$$\boldsymbol{w}_{t+1} \leftarrow \boldsymbol{w}_t + \alpha\delta_t\boldsymbol{e}_t \tag{1.11}$$

where

$$\boldsymbol{e}_t \leftarrow \gamma\lambda\boldsymbol{e}_{t-1} + \boldsymbol{x}(s_t) \tag{1.12}$$

This is one example of an eligibility trace, referred to as an accumulating trace, as it accumulates credit each time a state is visited.

1.6.2.6 General Value Functions

Up to now I have discussed primarily state value functions, which describe 'how good it is' to be in a particular state. The 'goodness' of a state is continually learned and updated from interacting with the environment and estimating the future value of that state. The same RL methods can be used to learn the future values other signals of interest (Sutton et al. 2011). The goal is no longer to maximize future rewards, but to predict future values of arbitrary signals. An arbitrary signal of interest is referred to as a cumulant (Z), and is predicted using a general value function (GVF). GVFs of a cumulant signal can be learned using methods such as TD learning. The goal is no longer to maximize the future value of the signal of interest, rather the target accumulates and therefore summarizes future values of the cumulant signal. The equation for the target, which was previously denoted the return (G_t) is now:

$$G_t = \sum_{k=0}^{\infty} \gamma^k Z_{t+k+1} \tag{1.13}$$

where γ is now referred to as the termination signal (White 2015). The termination signal can be used to define events of interest in the cumulant signal that are desirable to predict within a particular time-frame:

$$\gamma = 1 - \frac{1}{T} \tag{1.14}$$

where T is the number of timesteps. As the GVF is the discounted sum of the future values of the cumulant, the prediction does not exactly follow the same shape of the cumulant signal. Instead, it is the convolution of the cumulant with a decaying exponential due to γ. Putting these concepts together: using TD learning and an eligibility trace to obtain a GVF for a cumulant signal, represented using linear function approximation:

Algorithm 1.1 TD(λ) with GVFs

Input α, λ, γ

Initialize **w**, **e**, s, **x**

Repeat every timestep:

Obtain s' and cumulant z'	from environment
get $\boldsymbol{x}'$	from state representation method
$V \leftarrow \boldsymbol{w}^T \boldsymbol{x}$	old general value function
$V' \leftarrow \boldsymbol{w}^T \boldsymbol{x}'$	new general value function
$\delta \leftarrow Z + \gamma V' - V$	TD error
$\boldsymbol{e} \leftarrow \gamma\lambda \boldsymbol{e} + \boldsymbol{x}$	accumulating eligibility trace
$\boldsymbol{w} \leftarrow \boldsymbol{w} + \alpha\delta \boldsymbol{e}$	update/learn weight vector
$\boldsymbol{x} \leftarrow \boldsymbol{x}'$	replace feature vector

1.6.3 Pavlovian Control

Pavlovian control refers to the use of concepts from classical conditioning to produce a control output.

1.6.3.1 Classical Conditioning

Classical conditioning, also referred to as Pavlovian conditioning, is a type of learning where a learned prediction of a stimulus is paired with a fixed response (Modayil and Sutton 2014). Unlike reinforcement learning, there is no reward signal. An example of classical conditioning includes the work of the well-known Ivan Pavlov in the late 1800s. In his experiments, Pavlov noticed that when dogs were presented with food, they would salivate (Pavlov 1883; Rehman and Rehman 2018). Later, the dogs salivated slightly before they were presented with food. He realized that the dogs were associating noises that preceded the food arrival with the food

arriving. To formally test his theory, he performed experiments where he rang a bell prior to presenting the dogs with food. At first, the dogs only salivated when the food arrived; however, later the dogs began to salivate when the bell rang. In formal classical conditioning terms, the unconditioned stimulus (US) is the food, which leads to the unconditioned response (UR) of salivating. The UR automatically responds to the US and is not under control of the dogs. A conditioned stimulus (CS), in this case the ringing of the bell, is a stimulus that the dogs learn to associate with the conditioned response (CR) of salivating. Since the UR and CR are often the same, the term response (R) will be used to refer to them.

The learned association of the CS with the R requires that the CS arrive before the US. In other words, the bell must ring before the food arrives for the dog to associate the bell with the arrival of food and begin salivating. Animals learn to predict the onset of a stimulus and respond accordingly. The interval between the onset of the CS and the onset of the CR is very important. The optimal interval between the stimuli varies according to the scenario and the delay between the onset of the CS and the onset of the response. For example, rabbits learn to predict a puff of air directed at the eye (US) from a tone (CS) and blink (R) within tens of milliseconds before the arrival of the US. In this case, the optimal interval between the US and the CS was 250 ms (Kehoe and Macrae 2002). However, conditioning over a longer interval has been demonstrated in taste aversion learning (Garcia et al. 1966; Schafe et al. 1995). The CS was flavoured water and the US was a nausea-inducing agent and were separated by hours, but still produced a strong aversion to the flavoured water.

The cerebellum is responsible for the learning of the timing relationships between the CS, US, and R (Jirenhed and Hesslow 2011). Normally, climbing fibers carry afferent sensory information from the spinal cord and brainstem, which is used by the Purkinje cells to generate a motor response (Xu et al. 2006). Climbing fibers synapse directly onto Purkinje cells. Mossy fibers indirectly relay sensory information to the Purkinje cells through connections with the parallel fibers and therefore have a longer latency and smaller effect on Purkinje cells. The role of the cerebellum in classical conditioning is well known for the eye-blink conditioning reflex (McCormick and Thompson 1984; Christian and Thompson 2003; Thompson and Steinmetz 2009). Specifically, the Purkinje cells in the eye-blink controlling area fired (R) to electrical

stimulation of the mossy fibers (CS) and the climbing fibers (US). Most often the Purkinje cells developed a conditioned R with an interval of 200 ms between the CS and US (Jirenhed and Hesslow 2011).

1.6.3.2 Machine Learning in Pavlovian Control

Biologically, classical conditioning relates a predicted sensory stimulus to a particular motor response. This concept can be translated into control problems. In particular, predictions can be formulated from available sensor data, and used to trigger a pre-defined output, or response. The control output is defined to specify the desired behaviour or movement. The predictions can be learned through machine learning methods such as GVFs and TD learning, as detailed in the previous section on RL. TD is an appropriate algorithm to generate predictions for Pavlovian control as it is inherently structured to do so. Specifically, the TD model infers that the CS is used to predict the US through temporally-successive prediction errors (Ludvig et al. 2012). The prediction error strengthens or weakens the association between the CS to the US.

Using machine learning-derived predictions to produce a fixed control output is a relatively new concept in the field. There are two streams of using predictions for control purposes: prosthetic arms and a mobile robot. GFVs can be used to predict switching events of a prosthetic arm controlled by EMG signals, which determine which joint of the arm to control (Pilarski et al. 2012; Pilarski et al. 2013a, 2013b). The prediction of switching events was tested in a robot arm controlled by able-bodied participants (Edwards et al. 2013) and amputees (Edwards et al. 2016). Adaptive control using the learned predictions significantly decreased the number of switch events and switching time compared to a set order of switching. Although not explicitly stated, in these studies the switching events were the US, the new joint to actuate is the R, and the CS is the prediction of switching event determined by the GVFs of the servo motors for each joint.

Work in a mobile robot formalized the concept of nexting: the ability to continually predict the immediate future (Modayil et al. 2014). To next requires knowledge of the environment, which can be learned and predicted. Large scale predictions of on-board sensor signals at multiple time-scales has been demonstrated using TD learning of GVFs (Modayil et al. 2012; Modayil et al. 2014) and used to trigger fixed responses in the robots (Modayil and Sutton 2014). A GVF of the

over-current signal of the motor was used to predict motor stalls (US). If the prediction reached a pre-defined threshold (CS), indicating a high probability of an impending motor stall, the motors were shut off (R). Pavlovian control reduced the number of over-current events, which were potentially damaging to the robot. This work also explored the prediction of human-provided commands to steer a robot (Modayil and Sutton 2014). Specifically, the position of the left elbow joint (US) was predicted (CS) to initiate the robot to spin left (R). All of the described work used tile coding for function approximation of the state space.

The association of the environment with a fixed response can be formed through repetitive behaviour, and is the foundation for habit learning (Renaudo et al. 2014). Although this work did not learn predictions to trigger the fixed response, as in Pavlovian control, they demonstrated that more accurate selection of actions in a habitual simulated robot. However, habit learning struggled with adapting to changes in the environment. Therefore, the combination of online learned predictions with a fixed response is needed to produce adaptive behaviour.

Pavlovian control allows the integration of expert knowledge through the design of the CS leading to the desired R. It outperformed reactive control of prosthetic arms (Edwards et al. 2016) and mobile robots (Modayil and Sutton 2014) by more efficiently selecting the joint to actuate and predicting dangerous events and control commands, respectively. As walking is a repetitive task that requires precise control for safety purposes, Pavlovian control may be an appropriate approach to achieve adaptive control of walking in a SCI model.

1.7 Control of Walking

To restore walking using electrical stimulation, either targeting the periphery or the spinal cord, control strategies need coordinate the activation of the muscles and movements. For more seamless and natural-like control, the strategies should aim to replicate how the nervous system naturally controls locomotion. However, this is not a straightforward task as motor control is very complex and the mechanisms are still being investigated. Therefore, the control strategies that have been developed range from simple and limited control to strategies that attempt to incorporate concepts from natural motor control.

1.7.1 Feed-Forward Control

Feed-forward control, or open-loop control, entails delivering stimulation in a pre-timed pattern with pre-set amplitudes to produce the desired movements. This is much like the concept of the CPG without sensory feedback, where there is an inherent timing mechanism that drives activation of muscles to move the limbs. Feed-forward control can dictate the timing and grouping of muscle activations with phases of walking or control the trajectory of the limb.

The simplest way to implement feed-forward control is to alternate between flexion and extension movements, which act as the swing and stance phases, respectively. This has been accomplished by placing surface electrodes over the quadriceps, for knee extension, and the peroneal nerve, to produce a flexor-withdrawal response (Bajd et al. 1985). This is also the same strategy used by the Parastep and Praxis systems, in which users press buttons on a walker to initiate each step (Chaplin 1996; Johnston et al. 2005). Some Parastep units also include extra channels on the glutei and/or paraspinal muscles for hip and lower back extension. However, habituation of the common peroneal nerve stimulation has shown to attenuate movements such as hip flexion (Granat et al. 1993). The alternation between flexion and extension has been accomplished using IMS in cats (Guevremont et al. 2007) as well as using ISMS with as little as 2 electrodes per side of the spinal cord in intact cats (Mushahwar et al. 2002) and 4 electrodes per side in spinalized cats (Saigal et al. 2004).

A different method of producing walking is to replicate the timing of the muscle activation as closely as possible to natural walking (Popović et al. 2003). Coarse movements using 6 intramuscular electrodes were produced in cats through open-loop stimulation of hip, knee, and ankle flexor and extensor muscles (Guevremont et al. 2007). For finer control of individual muscles, a combination of up to 16 implanted and surface electrodes has produced walking in people with complete (Kobetic et al. 1997; Guiraud et al. 2006) and incomplete (Hardin et al. 2007) SCI. The systems used by humans are initiated by push buttons by the users (Chaplin 1996; Kobetic et al. 1997; Johnston et al. 2005; Guiraud et al. 2006; Hardin et al. 2007), which can become quite cumbersome (Braz et al. 2009).

Another method of feed-forward control involves dividing the walking cycle for cats into 4 phases: F, E1, E2, and E3 (Engberg and Lundberg 1969; Goslow et al. 1973), which correspond to lift off to early swing, late swing to touch down, touch down to mid-stance, and mid-stance to push-off and constitute 20%, 20%, 20%, and 40% of the step cycle, respectively. Partitioning the gait cycle in this way is similar to the two-level CPG model, where there is still an inherent timing mechanism but the pattern of movements is separately produced. Each phase of the gait cycle can be produced separately by stimulating through a combination of ISMS electrodes, depending on their function. Once each phase is constructed, they can be concatenated in a cyclical manner to produce a gait cycle (Holinski et al. 2011; Mazurek et al. 2012). However, hyperextension during the push-off phase was noted in these studies, causing loss of weight-bearing. Since this was a feed-forward controller, it was not possible adapt the stimulation output to make corrections to the walking produced.

1.7.2 Feedback Control

Feed-forward control systems lack the ability to adapt their output to disturbances or alterations in terrain or muscle activation. Since FES is prone to produce muscle fatigue, instances such as knee buckling during walking have contributed to the development of feedback, or closed-loop, control systems (Mulder et al. 1990; Braz et al. 2009). Feedback from sensors allows for modifications to the stimulation output. The sensors used for feedback range from measuring biological signals such as EMG or EEG activity, to artificial signals from force-sensitive resistors, force plates, goniometers, gyroscopes, and accelerometers measuring force or joint angles and positions. A simple use of a sensor signal to detect the subject's intention to step can be utilized to initiate open-loop stimulation of a step cycle (Dutta et al. 2008; Sweeney et al. 2000). This replaces the need for users to press a button for each step they wish to take.

Aside from feedback used to indicate user intent, feedback can also be used to initiate transitions between the phases of the walking cycle using finite state control (Popović 1993). Sensor feedback is used to transition between states. The states can be different modes, such as sitting, standing, or stepping (Braz et al. 2009), or they may be the different states of the gait cycle (Andrews et al. 1988; Sweeney et al. 2000; Guevremont et al. 2007). Phase transitions can be

accomplished using IF-THEN rules to using information from force plates and accelerometers (Guevremont et al. 2007).

State transitions using similar rules have also been implemented for IMS on a neuromorphic silicon chip was developed to mimic the function of the half-center CPG (Vogelstein et al. 2008). Sensory inputs conveying information about the cats' hip angle and limb loading were relayed to the CPG network and used to initiate transitions between the swing and stance states. In both studies, pure feedback control was not very successful as the thresholds used to initiate state transitions were highly sensitive. Reasons for failure included slips and misses that resulted in the paw losing traction with the walkway, double-unloaded stance where both limbs were fully extended behind the animal, standing, stepping in place (no forward progression), and poor limb movements (Guevremont, et al. 2007). Control using the neuromorphic chip produced walking that differed from normal (Vogelstein et al. 2008). Specifically, the swing-stance ratio was much smaller than in normal walking, and because there were only flexion and extension states, the timing of the onset of different muscles was different from normal walking. Nonetheless, the stimulation was still able to propel the animal across the walkway. Within a state, feedback may be used to make modifications to ensure safety. For example, if knee buckling occurs, as measured by goniometers, then the stimulation amplitude must be increased through the channel delivering current to the quadriceps (Davis et al. 1999).

1.7.3 Combined Feed-Forward and Feedback Control

Mammals are constantly processing sensory information to accommodate their gait. Moreover, the CPG, which by itself is a feed-forward system, integrates sensory information from proprioceptive and cutaneous afferents, as well as descending information from visual centers and the cerebellum, to adjust the timing and pattern of walking. Therefore, it is logical to replicate physiological control mechanisms to control walking using ISMS. Guevremont and colleagues (2007) proposed and tested this concept initially using IMS, and it was further developed and tested in simulation (Mazurek et al. 2010) as well as using both IMS (Mazurek et al. 2012) and ISMS (Holinski et al. 2011; Holinski et al. 2013, 2016) in cats. Each controller implemented a feed-forward control by generating intrinsically-timed walking. Feedback signals from force plates, gyroscopes, and accelerometers were then used to monitor the walking using

various IF-THEN rules that interrupt and modify the feed-forward control. In one study, feedback from recordings from an implant in the dorsal root ganglia (DRG) at the L6 and L7 spinal levels were used to adapt ISMS-controlled unilateral stepping. The interrupt rules adjusted the transition times between the phases of the step cycle, as well as adapt the stimulation output to ensure sufficient weight-bearing.

1.7.4 Joint Tracking

More traditional control methods, such as proportional-integral-derivative (PID) controllers have also been implemented. These types of controllers modify the stimulation output in order to track a target, which could be a joint angle or limb trajectory (Quintern et al. 1997; Kurosawa et al. 2005). Non-linear control methods have also been implemented for joint tracking. Non-linear control methods are more robust and accurate than linear methods, which may be advantageous for control.

1.7.4.1 Fuzzy Logic Control

Fuzzy logic is a method of using values ranging between 0 and 1 as logical probabilities, depicting the inexact way of the world, making it closer to human thinking. In the context of control, fuzzy logic can incorporate expert knowledge (Lee 1990; Kovacic and Bogdan 2005). There are four main components to fuzzy logic control: fuzzification, fuzzy rules, implication, and defuzzification (Roshani and Erfanian 2013b). Fuzzification entails modifying the inputs by converting them from a numerical value into a linguistic value by association with a membership function so that they can be interpreted in the rule base. The fuzzy rules are a set of IF-THEN rules, and this is where the prior knowledge is stored. Fuzzy implication uses an inference engine to decide which rules are currently relevant and what the input should be. Defuzzification converts the fuzzy decisions to control actions.

Fuzzy logic control has been used to control the ankle joint using ISMS in a rat model, with separate fuzzy controllers for dorsiflexion and plantarflexion (Roshani and Erfanian 2013a, 2013b) aimed to track a target trajectory. Each controller controlled two electrodes, for a total of four electrodes controlling ankle movements measured by a motion tracking system. The authors noted a 200 ms time delay in the neuromusculoskeletal response to the stimulation in the spinal

cord. To improve the transient response of the controller, a lag compensator was incorporated into the fuzzy logic control system (Roshani and Erfanian 2013b). A different study used fuzzy logic to trigger the onset of the flexion phase of the gait cycle using ISMS (Saigal et al. 2004).

1.7.4.2 Sliding Mode Control

Sliding mode control (SMC) is a non-linear control method known for its accuracy, robustness to uncertainty, perturbation rejection, and simple implementation (Utkin 2009). The goal of the control system is to track a desired trajectory or target by driving the system states onto a surface in the state space, known as the sliding surface (Vecchio 2008). Once the states reach the sliding surface, SMC forces the states to stay within a boundary along the sliding surface.

Initial control strategies utilizing SMC were tested using surface electrical stimulation over leg muscles at the level of a single joint (Ajoudani and Erfanian 2007; Kobravi and Erfanian 2009; Nekoukar and Erfanian 2010), for standing (Kobravi and Erfanian 2012) and to produce walking (Nekoukar and Erfanian 2012). Only later was it tested using ISMS (Asadi and Erfanian 2012; Asadi 2014) and epidural SCS (Khazaei and Erfanian 2016).

The SMC controller developed by Kobravi and Erfanian (2009) was used to control ankle joint movement in paraplegic participants during quiet standing using surface FES (Kobravi and Erfanian 2012). The goal of this work was to replicate the ankle strategy used to maintain posture in intact individuals, thereby eliminating the need for the paraplegic participants to hold on to an assistive device and freeing their arms for other tasks. The participants were suspended in a harness system for safety and placed in a body brace to lock the joints above the ankles. The body's inclination angle was measured by placing a motion tracking sensor over the 3rd lumbar vertebrae and was used as a feedback signal for the controller. Center of pressure was also measured and used as for stability analysis. During independent quiet standing, the controller rapidly switched stimulation between ankle flexors and extensors to correct for body sway, maintaining a safe center of pressure. After a few trials, participants were able to stand for about 10 minutes before falling.

As seen with approaches such as the Parastep (Chaplin 1996) and IMS walking systems (Triolo et al. 2012) discussed above, users rely on their upper body for support and fatigue quickly. This motivated the development of new closed-loop control strategies for controlling the legs during walker-assisted FES (Nekoukar and Erfanian 2012), whereby the walking pattern followed a target trajectory to minimize the effort exerted on the upper body. A walking reference for trunk, hip, knee, and ankle trajectories were obtained from a healthy male subject that walked slowly with the walker. The controllers were tested in complete SCI participants. Surface electrodes were placed over the quadriceps, gluteus maximus/minimus, soleus and gastrocnemius, and iliacus muscles as well as over the common peroneal nerve. Feedback measurements included trunk, hip, knee, and ankle joint angles, ground reaction force, and handle reaction force for a single hand. Trajectory matching was aimed to be within one standard deviation of the reference joint angles. During swing there was ample foot clearance. The participants only exerted an average of 12.05% of their body weight on the walker for stability, and could walk at approximately 0.55 m/s (the target speed).

Control of knee and ankle joints using ISMS in rats was realized using SMC (Asadi and Erfanian 2012). Trajectory tracking for each joint resulted in trials lasting 7 minutes, demonstrating robustness of the tracking to fatigue by adjusting the stimulation amplitudes accordingly. This SMC controller was further tested using ISMS in the intermediate spinal cord of the rat to target movement primitives (Asadi 2014; Giszter 2015). The tracking was not as accurate as with ISMS in the ventral horn of the grey matter. SMC using ISMS electrodes implanted in both the ventral and intermediate spinal cord to track joint angles produced air and treadmill stepping in anaesthetized cats (Rouhani and Erfanian 2018). SMC was also used to control epidural SCS for multi-joint tracking to create extension and flexion movements in cats, with separate controllers for each function (Khazaei and Erfanian 2016).

SMC-based controllers have been shown to be accurate in tracking joint trajectories using surface stimulation, ISMS, and epidural SCS. They are also robust to external disturbances as well as to muscle fatigue. However, this control method requires that a target trajectory to be known and available. To acquire a target requires much knowledge of the system or an example of a desired limb trajectory, for example, from an intact individual. This could be difficult to

implement clinically since each individual would need a reference from a person that is of similar height and weight. This requires much trial and error for tuning (Matjacić et al. 2003). Additionally, the users would need to have goniometers and possibly other sensors placed on their legs to provide feedback to the controllers.

1.7.5 Machine Learning Control of FES

There has been much work, primarily in the 1990's, investigating machine learning methods to control FES to restore walking. Various supervised machine learning methods were implemented in computer simulation and in participants with a SCI.

Three main algorithms have been used in various capacities to control FES: inductive learning, artificial neural networks, and adaptive logic networks. Briefly, inductive learning (IL) produces a decision tree, which consists of sequential decision rules to partition the input data to obtain the desired output (Kirkwood et al. 1989). An adaptive logic network (ALN) is a type of artificial neural network (ANN) (Kostov et al. 1995). A common ANN is an MLP, which is feed-forward, as opposed to recurrent ANNS in which nodes have successively and recurrent connections. Conversely, ALNs encode continuous values into Boolean vectors (containing 0s and 1s only) and uses logical operators (AND, OR, LEFT, or RIGHT) to connect the layers (Kostov et al. 1992, 1995; Supynuk and Armstrong 1992). Computationally ALNs are simpler and faster to execute (Kostov et al. 1995). These three algorithms have been implemented repeatedly to control FES in various ways.

Just as traditional control methods may be used to control FES to track joint angles, machine learning methods have also been tested for this purpose. An ANN was used to track the knee torque during an FES-induced isometric contraction of the quadriceps muscles in people with a SCI (Abbas and Triolo 1997). The knee joint angle and muscle activity of knee flexor muscles was predicted in a simulation of FES-walking in SCI participants (Popović et al. 1999) using two types of ANNs and IL (Jonić et al. 1999). These methods may be useful for controlling the knee torque during stand-sit transfers or during standing or walking. Control of the ankle joint during walking is also very important. ANNs were used to control the ankle joint by tracking a desired trajectory in computer-simulated cats (Qi et al. 1999) and people with stroke (Chen et al. 2004).

One way to reduce the burden on an FES user is to replace the use of hand-switches controlling a step initiation with an automated method. For example, all 3 of the aforementioned machine learning algorithms have been used to predict the participant's intention to take a step and trigger stimulation for the flexor-withdrawal reflex for the swing phase in participants with a SCI (Kirkwood and Andrews 1989; Kostov et al. 1992, 1995; Tong and Granat 1999; Sepulveda et al. 1997). A study comparing the performance of IL versus an ALN found that IL was faster, but the ALN had a smaller test error. One study used machine learning to control the hip and knee joints during walking in a subject with complete SCI using a combination of inductive learning and an ANN (Fisekovic and Popovic 2001). They reported faster walking with less effort with automatic control compared to hand-control of FES. Similarly, ANNs have been used to trigger the onset of FES in a foot-drop device in people with a stroke (Shimada et al. 2005; Hansen et al. 2004).

Different states of the gait cycle have been predicted using IL (Kirkwood and Andrews 1989) and an ALN (Williamson and Andrews 2000) in able-bodied participants; however, the utility of the predictions were not tested using FES. Heller et al. (1993) compared IL with an ANN in reconstructing muscle activation during walking in able-bodied participants, with no clear superior method and was not utilized in an FES system. A type of ANN was used for finite state control of FES walking in intact participants with restrictive braces and a participant with a complete SCI (Popović 1993).

Switching between gait types such as standing, sitting, and stepping using the Parastep system in people with a SCI was accomplished using a type of ANN (Graupe and Kordylewski 1995). A similar approach to predicting gait types attempted to use EMG activity from an intact subject to train an ANN to control FES in participants with cerebral palsy (Sepulveda and Cliquet Júnior 1995). This study demonstrated the importance of training the algorithms with data from the intended population. Numerous networks were tested and struggled to produce the desired EMG output in the cerebral palsy population because they were trained in intact individuals.

1.7.6 Reinforcement Learning Methods for Walking

Much of the research employing RL methods to produce walking occurs in simulated environments or in robots. One RL method that has been tested in Nao humanoid robots is actor-

critic (Endo et al. 2008; Li et al. 2013). Actor-critic is a TD method that separates the action selection (by the actor based on a policy) and the estimation of value functions and policy updates (performed by the critic using TD learning). In these studies, the actor controlled the output to a central pattern generator CPG model to either control joint trajectories. The critic used sensor values and reward signals to evaluate the walking and update the policy using gradient descent. Reward signals included falling, distance moved forward (Li et al. 2013), the height of the pelvis, and forward velocity (Endo et al. 2008). Both approaches reduced the state space to include only relevant sensor signals, rather than using function approximation. Stable walking was achieved in 200 trials (Endo et al. 2008) and 10 trials (Li et al. 2013), even after starting from learned parameters in simulation (Endo et al. 2008).

Starting from a simulation is common as it can more quickly learn without damaging robot hardware. Even so, learning a map for limb trajectory from a simulator to a bipedal robot with no ankle joint still needed 100 trials of 30 steps to walk successfully (Morimoto and Atkeson 2007). A different study controlled only the hip joint of a robot and took 20 minutes of continuous learning to walk, after 15 hours of simulation (Schuitema et al. 2005). This study rewarded the agent for taking steps, resulting in shuffling, asymmetrical stepping, and marching in early learning trials.

More skilled walking was also achieved using RL methods. Fast walking was achieved in a robot using policy gradient to select the next walking motion within 10 trials (Li et al. 2011). This robot lacked a knee joint and was very unstable. By shaping the reward to favour stability over velocity, fewer falls occurred but required more trials for learning. A robot without knee joints and a single hip joint walked up a 5º incline within 20 episodes using a greedy policy to select the joint movements (Salatian et al. 1997). The joint trajectories were executed by a proportional-integral (PI) controller.

Reinforcement learning performs well in stochastic, non-stationary walking, making it a reasonable choice for a control algorithm to produce walking. Applying various RL methods to produce walking in robots has been successful; however, there are many limitations and assumptions to consider. Many of the robots used did not have hip, knee, and ankle joints

(Salatian et al. 1997; Schuitema et al. 2005; Morimoto and Atkeson 2007; Li et al. 2011). While this makes the problem simpler, it is not realistic for applications in rehabilitation. Many studies assumed symmetry of the limbs to decrease computation time and simplify the control problem (Endo et al. 2008; Schuitema et al. 2005; Salatian et al. 1997). However, this may not be a feasible approach in rehabilitation applications, as the injuries that are being compensated for may not be symmetrical. Finally, many of these methods demonstrated slow learning, even after hours of simulations. This can be affected by the computations needed to execute joint trajectories (Endo et al. 2008) or because the reward signal must prioritize stability over speed (Li et al. 2011). It could also be due to the chosen RL method and how often learning occurred. RL can be slow because learning requires trying many options in a large state space (exploration). Restricting the state space to relevant regions is one method to try and speed up learning (Endo et al. 2008; Li et al. 2013).

There are several methods that have been investigated to restore walking after a SCI. The studies collectively demonstrate the importance of sensor feedback to make corrections to the output. All the control strategy development to date has focused on restoring walking in a model of complete SCI. This means that the control strategy and stimulation were entirely responsible for the walking produced. However, approximately half of all SCIs are incomplete, with varying degrees of residual function. For a neuroprosthesis to be truly effective in a SCI population, augmentation of residual function needs to occur. Furthermore, the aim of control strategies should be to adapt to the individual as stimulation requirements may change over time. Reinforcement learning and Pavlovian control may offer the needed adaptability for restoring walking after an incomplete SCI.

1.8 Thesis Outline

There were three primary aims of my thesis work. My first aim was to characterize motor activity from the developing spinal cord. Next, I tapped into spinal networks in order to augment remaining function in a model of incomplete SCI. Specifically, I adapted the control of walking to walking speed. Finally, I developed a personalized control strategy that automatically adapted to given subjects. These aims contributed to the overall goal of this work which was to characterize motor activity and restore function after neural injury.

The work outlined in chapters 2 and 3 demonstrate the utility of supervised machine learning in real-world, neuroscience problems. The work in chapter 2 poses a classification task, where experts label examples of episodes of spontaneous activity recorded from the developing spinal cord to train MLPs. Manual classification of the episodes is extremely time-consuming. Three experts transfer their combined knowledge and expertise to the MLPs for fast and automatic classification of episodes of activity. The software encompassing the feature detection and classification for spontaneous activity enables the investigation of DC-coupled recordings, revealing the fine details of neural network activity during development.

The work in chapter 3 details how numeric prediction of the stepping speed using regressions and model trees can be used to select the control strategy for ISMS in a hemisection SCI model. These algorithms were trained to predict the step period of a person-moved limb using timing information from a portion of the step taken. The predicted step period value was then used to select a control strategy appropriate for the walking speed, and was also used to calculate the stimulation times for the other limb for faster steps. This presents the first control strategies aimed at augmenting remaining function to produce stepping in a model of incomplete SCI. Both bodies of work demonstrate the power of supervised machine learning methods to learn and perform tasks.

Supervised methods are not appropriate for all problems. The work in chapter 4 demonstrates how predictions learned using RL can be used for Pavlovian control of over-ground walking. Prediction-initiated transitions between the phases of the walking cycle had fewer errors than reaction-based control. Furthermore, RL was able to acclimate to different people walking the limb and to different cats, eliminating the need for tuning of individual parameters within and between experiments. Pavlovian control allows personalized control that augments remaining function in a model of incomplete SCI by quickly and automatically adapting to different individuals.

Chapter 2: A Supervised Machine Learning Approach to Characterize Spinal Network Function[1]

2.1 Introduction

For decades, isolated embryonic or neonatal spinal cord preparations have been used to study sensorimotor integration (Kudo and Yamada 1987; O'Donovan and Landmesser 1987; Smith and Feldman 1987; Clemens and Hochman 2004; Mentis et al. 2011) and to examine patterns of movement-related network activity (Smith and Feldman 1987; Cowley and Schmidt 1997; Whelan et al. 2000). Neonatal mice generate stepping movements when exposed to olfactory or cutaneous stimulation (Fady et al. 1998; Jamon and Clarac 1998) and patterns of locomotor-like activity can be generated *in vitro* by inducing a high excitability state in the network through electrical, optical, or neurochemical stimulation (Gordon and Whelan 2006; Gordon et al. 2008; Hägglund et al. 2010; Kiehn 2016). However, the vast majority of hind-limb movements produced by neonatal rodents are sporadic ataxic episodes of uncoordinated rhythmic action (Jamon and Clarac 1998). A fictive correlate of these movements is recognizable *in vitro* as spontaneous activity, which represents the motor output of the developing spinal networks in a more natural activity state. Spontaneous activity plays a critical role in the development of motor networks, in synaptic and receptor plasticity, and in guiding the innervation of descending motor and ascending sensory afferents, both of which are sparse at birth.

The qualitative complexity and stochastic nature of spontaneous activity patterns make them challenging to study. Previous work investigating spontaneous network behaviour has primarily focused on quantifying AC-coupled or high-pass filtered activity (for examples, see Fellippa-Marques et al. 2000; Hanson and Landmesser 2003), which can detect activity peaks but may miss finer details such as intra-episode spiking and rhythmicity. In contrast, DC-coupled recordings detect extraordinarily rich and detailed sub-threshold information (O'Donovan 1987; Whelan et al. 2000; Figure 2.1), which provides important clues about network dynamics that could be used as biomarkers for developmental disorders, such as cerebral palsy.

Dalrymple, A.N.[1], Sharples, S.A.[2,3], Osachoff, N.[4], and Whelan, P.J.[2,3,4]
[1] Neuroscience and Mental Health Institute, University of Alberta, Edmonton, AB, Canada; [2] Hotchkiss Brain Institute, University of Calgary, Calgary, AB, Canada; [3] Graduate Program in Neuroscience, University of Calgary, Calgary, AB, Canada; [4] Department of Comparative Biology and Experimental Medicine, University of Calgary, Calgary, AB, Canada.

To enable the examination of such activity including the sub-threshold components, we created a software tool which uses machine learning to classify episodes of spontaneous patterns of motor activity recorded from isolated mouse neonatal spinal cords *in vitro*. Using Matlab (MathWorks Inc., Natick, MA, USA), we developed the software in a graphical user interface (GUI) that allows users to detect, visualize, and characterize episodes of spontaneous motor activity. This tool, called SpontaneousClassification, quickly and automatically extracted features and classified episodes using supervised machine learning. This approach is substantially faster and easier than manual classification. In addition, it detected changes in stochastic spontaneous network activity after an induced increase in spinal network excitability.

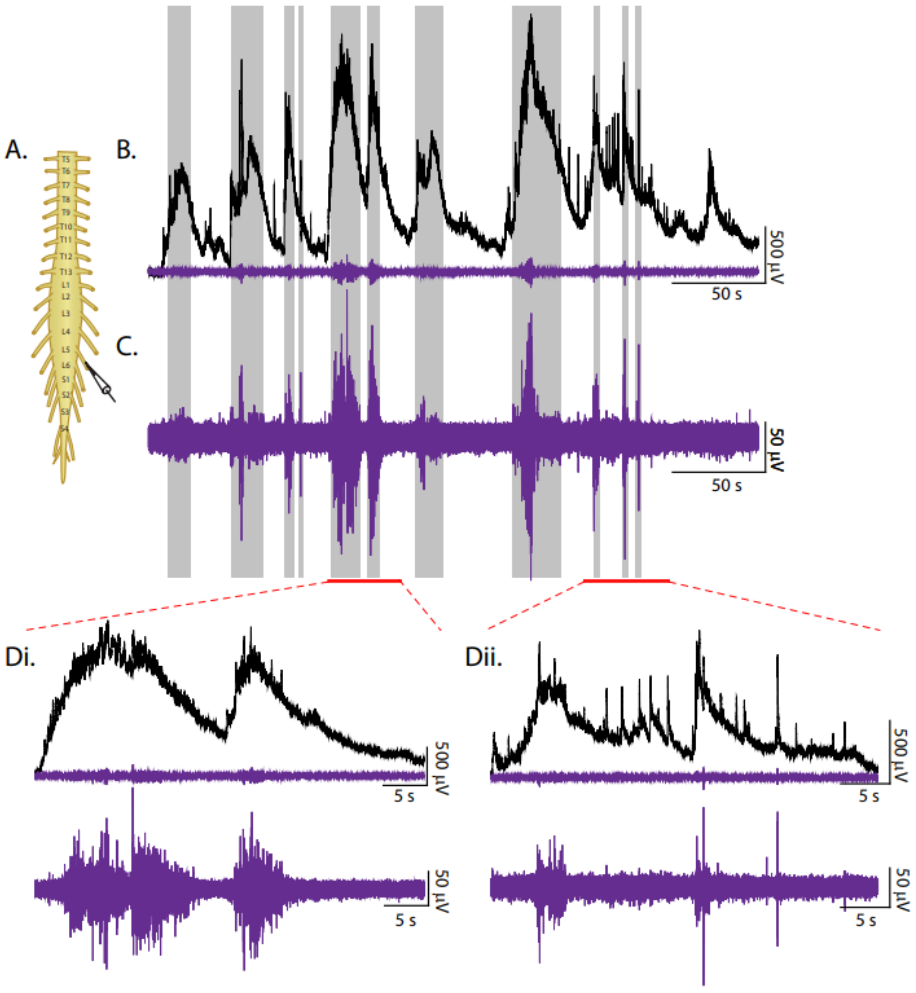

Figure 2.1. Spontaneous network activity recorded from the lumbar spinal cord. A) Experimental setup: suction electrodes recorded activity from the L2 and L5 ventral roots of neonatal mice (P0–P3). B) DC-coupled neurogram; grey bars highlight episodes detected in AC-coupled neurogram. C) High-pass filtered (100 Hz) neurogram; grey bars highlight episodes detected in AC-coupled neurogram. Da and Db) Enlarged regions: Top traces depict DC-coupled neurograms, bottom traces depict AC-coupled neurograms.

SpontaneousClassification may facilitate investigations of spinal network function in a different manner than currently available techniques, expanding the toolbox of methods used to investigate spinal neural networks.

2.2 Methods

2.2.1 Tissue Preparation

Experiments were performed in neonatal C57BL/6 mice (P0–P3; n = 16) obtained from timed-pregnant females housed in the animal care facility at the University of Calgary until they gave birth. Neonates were anaesthetized by cooling, then decapitated and eviscerated to expose the vertebral column. The remaining tissue was placed ventral side up in a dissection chamber filled with room-temperature carbogenated (95% O_2, 5% CO_2) artificial cerebrospinal fluid (aCSF) (128 mM NaCl, 4 mM KCl, 1.5 mM $CaCl_2$, 1 mM $MgSO_4$, 0.5 mM Na_2HPO_4, 21 mM $NaHCO_3$, 30 mM D-glucose). A ventral laminectomy exposed the spinal cord. We cut the dorsal and ventral roots, removed and transferred the spinal cord to a recording chamber, ventral side up, with recirculating carbogenated aCSF at a flow rate of 20 mL/min, and gradually heated them from room temperature to 27ºC. This temperature is closer to the physiological neonatal core temperature (32ºC, (Goodrich, 1977)), is above room temperature, which tends to fluctuate, and is known to produce more reliable activity in our experience.

2.2.2 Electrophysiological Recordings

Using Clampex software (Molecular Devices, Sunnyvale, CA), we acquired DC-coupled neurograms from the isolated spinal cords (i.e., spontaneous motor activity) by drawing the ventral roots from the bilateral second and fifth lumbar segments (L2, L5) into tight-fitting suction electrodes filled with aCSF (Figure 2.1A). Neurograms were amplified 1000 times, digitized using a 2.5 kHz sampling frequency (Digidata 1440, Molecular Devices), and analyzed with our custom-designed Matlab program SpontaneousClassification on a laboratory computer. The recordings from each root were treated independently for analysis.

2.2.3 Classification Software

SpontaneousClassification has three modules: visualization, data preparation and feature extraction, and classification. The classification module includes two supervised machine

learning classifiers trained on spontaneous motor activity episodes recorded from the isolated spinal cords. A user manual and video describing SpontaneousClassification is available as supplementary files.

2.2.4 Visualization Module

This module displays a trace from the loaded neurogram file in the GUI where users can access multiple zooming, shifting, and sliding options that operate along the x- and y-axes. Traces can also be split into multiple files for further analysis. See the user manual in the supplementary documents for further details.

2.2.5 Data Preparation and Feature Extraction Module

This module prepares the data for further stages of analysis and extracts features of interest from the episodes.

2.2.5.1 Episode Detection

Episode detection first requires the trace to be detrended to remove the drift acquired during the recording. After detrending the trace, thresholds must be selected for each trace to separate the episodes. Episode threshold was determined by first sorting all data points from each trial into bins of ascending amplitude. Figure 2.2B depicts the highest amplitude data points, which likely represent bursting activity, on the right side of the x-axis, and a flat region to their left, with lower amplitude, non-bursting activity. The flat region's limits can be determined by viewing the bins, and will likely need to be tuned for each different trace, based on variation in recording quality (i.e., signal to noise) and amplitude range, which depends on the amount of spontaneous activity. To determine the episode threshold, we added a multiple of the standard deviation of non-bursting baseline data points to the mean of the data points within a selected region of the non-bursting baseline. We found that a multiple of four times the standard deviation optimized results. We then used the episode threshold to determine temporal criteria for episode onset and offset boundaries (time required above threshold and time required below episode threshold, respectively). In our experiments, we defined episode onset as the recording spending 0.25 s above threshold and episode offset as the recording spending 0.25 s below threshold. For some

traces, the automatic separation of episodes did not correctly capture all the episodes; therefore, some episodes were separated manually.

SpontaneousClassification allows for both automatic and manual episode separation. Displaying the detected episodes in the SpontaneousClassification GUI can be helpful when tuning detection parameters (Figure 2.2C).

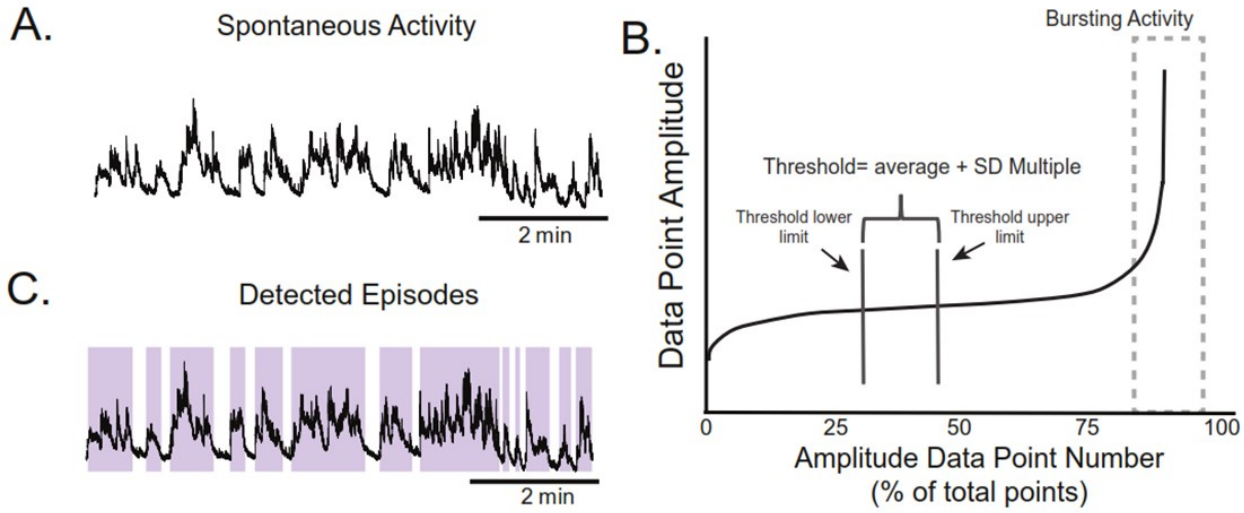

Figure 2.2. Detecting episodes of spontaneous activity. A) DC-coupled neurogram. B) Amplitude of data points from (A) sorted in ascending order. Threshold reflects user-defined upper and lower limit values of the sorted amplitudes within the flat region. The average amplitude of the data points plus a user-defined standard deviation of the data points within this region is then set as the episode detection threshold. C) Boundaries of detected episodes are highlighted in grey.

2.2.5.2 Feature extraction

SpontaneousClassification identified 902 episodes of spontaneous activity in 40 traces recorded from the 17 spinal cords. Twelve episodes from one animal were excluded from analysis due to aberrant multi-spike activity that was extremely low frequency and long in duration. The remaining 890 episodes were categorized into one of five classes.

From each episode, SpontaneousClassification extracted four time-, two amplitude-, and three frequency-related features (Figure 2.3Aa). Time-related features for a given episode *e* include (1) the start and end times for the episode, (2) the time from the previous episode's offset to *e*'s

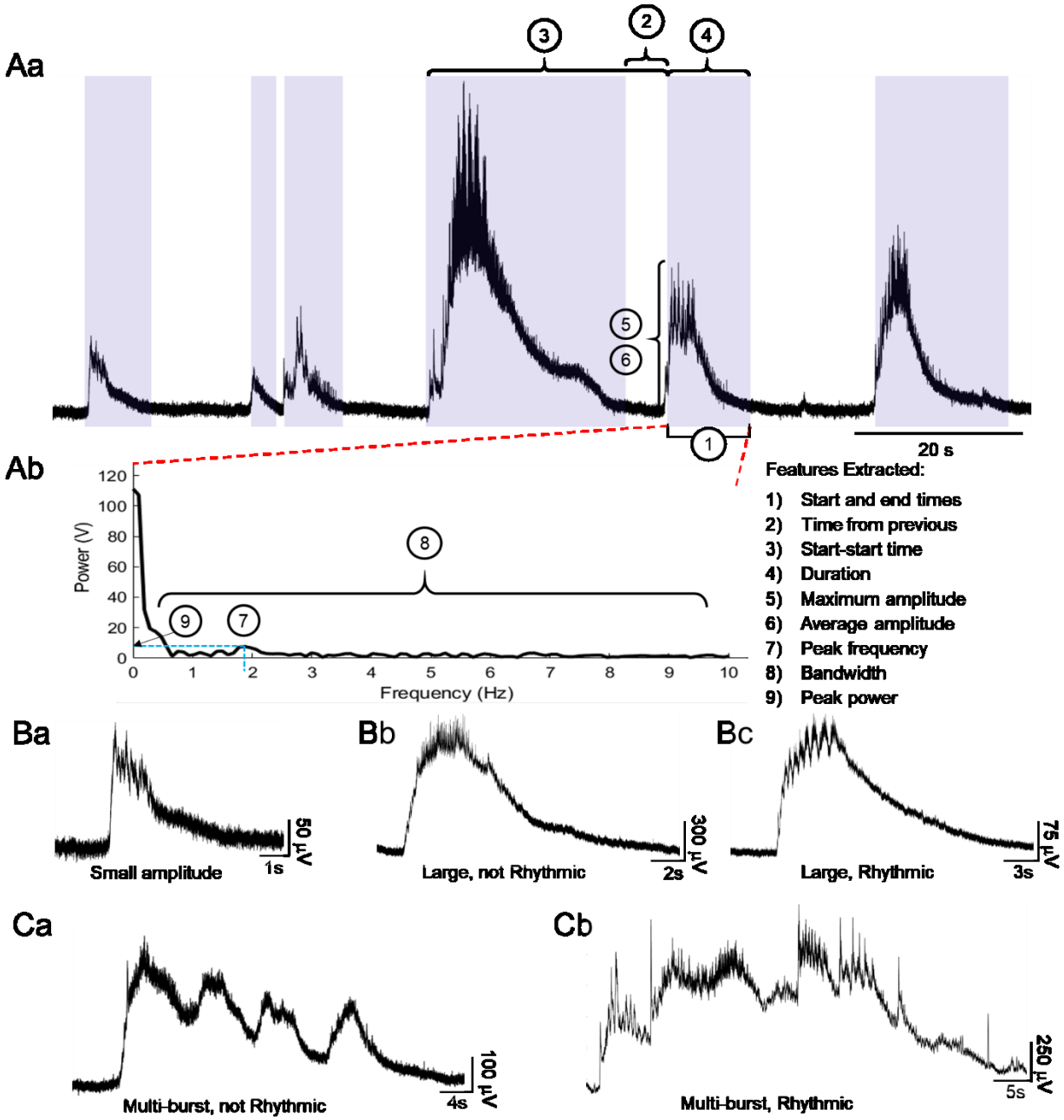

Figure 2.3. Features extracted from each episode of spontaneous activity. Aa) Time- and amplitude-based features extracted from each episode: (1) start and end times (2) time from the previous episode, (3) start-start time, (4) duration, (5) maximum amplitude and (6) average amplitude; both amplitudes expressed as raw voltage and percentage of largest amplitude in the trace. Ab) Fourier transform of the episode to extract frequency-related features; (7) largest non-zero frequency component; (8) bandwidth of peak components, excluding zero and frequency components larger than 10 Hz; and (9) power at most prominent non-zero frequency component. B, C) Examples of classes of spontaneous activity: Ba) Small, Bb) Large, not rhythmic, Bc) Large, rhythmic, Ca) Multi-burst, not rhythmic, and Cb) Multi-burst, rhythmic.

onset (time from previous), (3) the time from the previous episode's onset to *e*'s onset (start-start time), and (4) the duration of *e*. Amplitude-related features included the maximum and the average amplitude, expressed as both raw voltage and as a percentage of the absolute maximum in a trace. The frequency-related features (Figure 2.3Ab), obtained using a discrete Fourier transform, include the largest frequency component (peak frequency), the bandwidth, and the power at the largest frequency component (peak power). To focus on features related to activities of interest, such as locomotion or scratching, we limited the frequency components to those below 10 Hz. We defined bandwidth as the highest frequency component (limited to 10 Hz) minus the lowest (non-zero) frequency component.

2.2.6 Classification module

After automatically extracting features from each episode of spontaneous motor activity, the classification module uses those features to classify episodes according to generalizations obtained from a trained supervised machine learning algorithm programmed into SpontaneousClassification. SpontaneousClassification comes with pre-trained machine learning classifiers. The following sections describe how we trained and tested them.

2.2.6.1 Supervised machine learning

Supervised machine learning entails using pre-labelled data to derive generalizations about the relationship between inputs and outputs. Features that describe or quantify the data serve as inputs, and the outputs may be classification or numerical values (also referred to as supervisory signals; Witten *et al.*, 2016). The inferred function from training with pre-labelled examples is then presented with new, unlabelled data, and tested for how well it can generalize on novel data. To determine the accuracy of the generalization on a testing data set, predicted outputs are compared to actual outputs. Ideally, the generalizations are broad enough to properly classify new data without over-fitting the inference function to the training data.

2.2.6.2 Supervised classification procedure

The episodes in the training dataset were classified by the experts in two batches; batch one contained 576 episodes and batch two contained 253 episodes. Three individuals classified each episode of activity as either rhythmic, not rhythmic, multi-burst and rhythmic, or multi-burst and

not rhythmic. The final classes also indicated whether an episode's amplitude was larger or smaller than 50% of the maximum amplitude of a single trace. Therefore, five classes were derived based on the following descriptors: small amplitude; large amplitude, not rhythmic; large amplitude, rhythmic; multi-burst, not rhythmic; and multi-burst, rhythmic (Figure 2.3Ba-c, Ca-b). Further segregation of small amplitude classes was not necessary as they were non-rhythmic and not multi-burst.

For the first batch, each expert classified the episodes independently. Any episodes that did not have 100% agreement were reclassified by all three experts as a group. We added the second batch of episodes to increase the representation in each class; those episodes were classified by the same individuals as a group. After classification, the episodes were divided into a training set, consisting of 90% of the episodes (n = 735), and a testing set, consisting of the remaining 10% of the episodes (n = 82). The episodes in the testing set were selected proportionally according to class. We used a random number generator to assign episodes within each class to the training or testing set. A third batch (73 episodes) was used as an additional independent test set. The classes assigned by the experts were considered to be true and used to train and compare supervised machine learning algorithms.

2.2.6.3 Training procedure

To train the machine learning algorithms, we matched the eight automatically extracted features related to time, amplitude, and frequency (inputs) to the class labelled by experts (output) for each episode in the training data set (735 episodes). Using the data mining platform Weka 3.8.0 (Frank *et al.*, 2016) and the training data set from the first batch of episodes we swept through numerous supervised machine learning algorithms, using varied parameters. The second batch of episodes were added after this initial sweep through the algorithms. Each run of the training data set through an algorithm and parameter setting was 10-fold cross-validated. We tested 13 classifying algorithms: Bayesian network, naïve Bayes, multilayer perceptron (MLP), simple logistic model, k-nearest neighbour, sequential minimal optimization (SMO; for training a support vector classifier), instance-based learning (K*), J48 (a decision tree), reduced error pruning (REP) tree, decision stump, Hoeffding tree, logistic model tree, and random tree. We

selected the best algorithms, and parameters within algorithms, for further testing, based on the cross-validated classification accuracy results.

Across all classification methods tested, we executed a total of 2,947 sweeps through algorithms and parameters. Initially, classification to one of the five classes was performed by a single algorithm; the best training accuracy achieved was 56.5% using an MLP. An MLP is a type of feed-forward artificial neural network modelled after biological neural networks (Minsky et al. 2017). The neurons, or nodes, in an MLP are connected by weights, forming a network capable of representing complex expressions. Additional hidden layers, such as those in deep neural networks, can further increase the complexity of the representations (see Figure 2.4). This technique has been applied to face recognition (Sun et al. 2015; Parkhi et al. 2015), speech recognition (Hinton et al. 2012; Amodei et al. 2015), and medical diagnostics (Lu et al. 2018; Burt et al. 2018; Song et al. 2018).

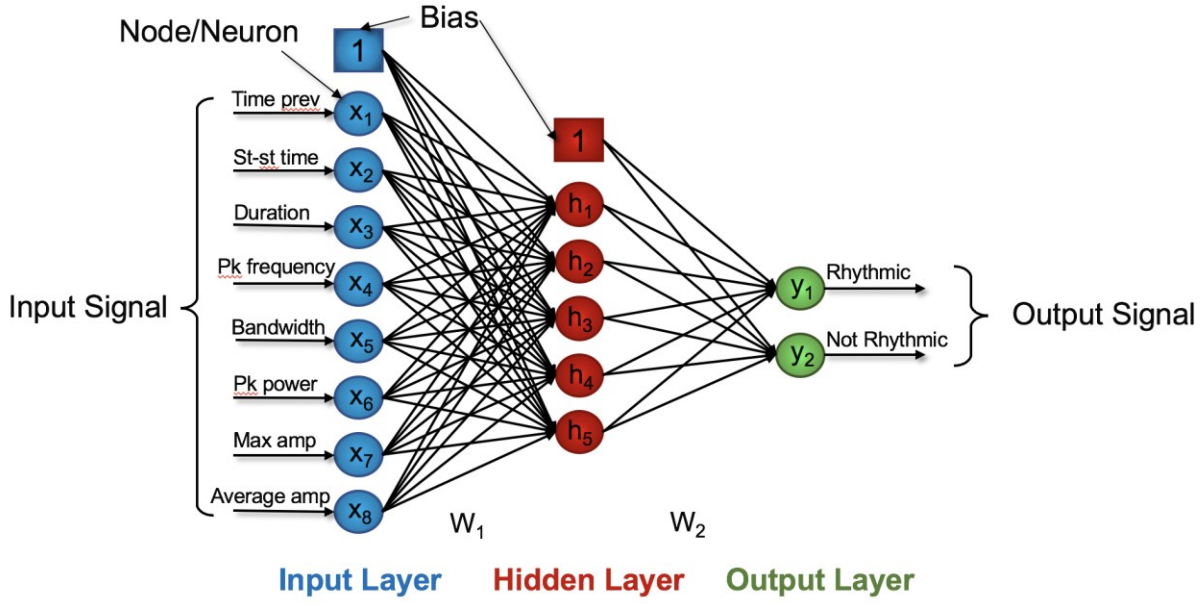

Figure 2.4. Structure of multilayer perceptron (MLP) used for classifying episodes as rhythmic or not. The input layer (x, blue) receives normalized values of the features extracted from each episode. The weights between the input layer and the hidden layer (h, red), and the hidden layer and the output layer (y, green) were determined during training. The output layer consists of two binary nodes: 0 = not rhythmic, 1 = rhythmic. The hidden layer and output layer nodes are activated using the sigmoid function. The MLP for classifying episodes as multi-burst or not has a similar structure, with a different number of nodes in the hidden layer and different learning parameters (learning rate and momentum) used during training to obtain the weight values.

Since the episodes could be separated by their descriptors, two binary classifiers were found to have the best overall classification performance. One binary classifier determined if episodes were rhythmic or not, and the other determined if episodes were multi-burst or not. The normalized maximum amplitude determined the size of each episode. According to classification performance, the top contenders for binary classification during training for rhythmicity were an MLP and a Bayesian network; an MLP was the top choice for determining if an episode was multi-burst or not.

2.2.6.4 Testing procedure

After determining the final classifying algorithms, we used the testing data sets to evaluate performance of the trained algorithms on new data. The first testing data set included the 10% hold-out set from the initial two batches of episodes (n = 82 episodes). A third, independent batch of episodes was also included to test the performance of the MLPs (n = 73 episodes). Performance metrics for training and testing were used to compare algorithms for the binary classifications.

Accuracy describes the number of episodes for which class was correctly predicted by the algorithm:

$$Accuracy = \left(\frac{TP+TN}{TP+TN+FP+FN}\right) \times 100 \quad (2.1)$$

where TP = the number of true positive classifications, TN = the number of true negative classifications, FP = the number of false positive classifications, and FN = the number of false negative classifications. For example, for the rhythmicity classifier, positive refers to a rhythmic episode, while negative refers to a non-rhythmic episode.

Specificity indicates the number of correctly predicted negative episodes, calculated as follows:

$$Specificity = \left(\frac{TN}{TN+FP}\right) \times 100 \quad (2.2)$$

Sensitivity measures the number of positive class episodes correctly identified:

$$Sensitivity = \left(\frac{TP}{TP+FN}\right) \times 100 \quad (2.3)$$

Finally, precision measures the number of positive episodes correctly classified:

$$Precision = \left(\frac{TP}{TP+FP}\right) \times 100 \quad (2.4)$$

We selected the supervised machine learning algorithms implemented in SpontaneousClassification based on a balance between training performance and testing performance. The same performance metrics were used to assess agreement between the experts who initially classified the episodes.

During testing of the final algorithms, the MLP had a higher accuracy, specificity, and precision than the Bayesian network for training and testing rhythmicity (see Table 2.1) and thus, we implemented the MLP in SpontaneousClassification. The MLP during testing had a relatively smaller sensitivity to rhythmicity due to higher false negative classifications, but had a moderate precision and very high accuracy and specificity due to a large number of true negative and satisfactory true positive identifications.

Rhythmic	**Expert A**	**Expert B**	**Expert C**	**MLP Train**	**MLP Test**	**Bayes Train**	**Bayes Test**
Accuracy (%)	94	87	83	84	78	78	71
Specificity (%)	91	77	97	91	91	80	76
Sensitivity (%)	98	98	69	39	44	70	42
Precision (%)	91	79	95	43	66	37	23
Multi-burst							
Accuracy (%)	97	93	90	86	83		
Specificity (%)	97	100	89	92	89		
Sensitivity (%)	98	78	92	74	73		
Precision (%)	92	98	78	83	82		

Table 2.1. Classification performance for each expert who labelled episodes for training and for the final supervised machine learning algorithms chosen for testing. Classification included labelling episodes as rhythmic or not and multi-burst or not.

2.2.6.5 Multilayer perceptrons (MLP)

As mentioned earlier, an MLP, such as those we chose to implement in SpontaneousClassification, is a feed-forward artificial neural network with an input layer, a hidden layer, and an output layer, each with nodes that represent neurons. Figure 2.4 depicts a schematic of an MLP for rhythmic binary classification.

For our MLPs, the number of nodes in the input and output layers was defined by the number of features and classes, respectively. Therefore, each MLP has eight input nodes, one for each normalized feature, and two output nodes, 0 (false, or non-rhythmic) and 1 (true, or rhythmic). The number of nodes in the hidden layer was based on performance during training. The MLP trained for classifying rhythmic and non-rhythmic episodes has five nodes in the hidden layer (Figure 2.4). The MLP for classifying whether or not episodes are multi-burst has 10 nodes in the hidden layer. The input and hidden layers also contain a bias unit of 1 that connect to the nodes in the following layer.

The weights connecting the nodes of the input layer to the hidden layer, and the hidden layer to the output layer, were learned through back-propagation during training in Weka (ver. 3.8.0; Frank et al. 2016). Back-propagation uses gradient descent to update the weights by minimizing errors (Witten et al. 2016). The step size for gradient descent and learning momentum were determined based on training performance. We obtained the best results using a learning rate equal to 0.7 and a momentum equal to 0.5 for the rhythmic or not MLP, and a learning rate of 0.1 and momentum of 0.4 for the multi-burst or not MLP. The hidden and output layers are activated using a sigmoid function. The binary classification is finalized at the output layer, where the node with the greatest activation determines an episode's class.

2.2.7 GUI Capability Summary

Figure 2.5 depicts the final classification procedure implemented in the GUI. It includes the two MLPs (one to classify episodes for rhythmicity and the other for whether it is multi-burst or not) that use weights and parameters obtained through training, features extracted from the data preparation and feature extraction module, the output of the MLPs, and the normalized maximum amplitude to automatically classify each episode into one of the five classes (c.f.

Figure 2.3B). The entire process of episode detection, feature extraction, and classification takes a matter of minutes to perform. The automated classification process is completed in seconds or less, significantly reducing the analysis process from manual classification, and conveniently compiling everything into a spreadsheet.

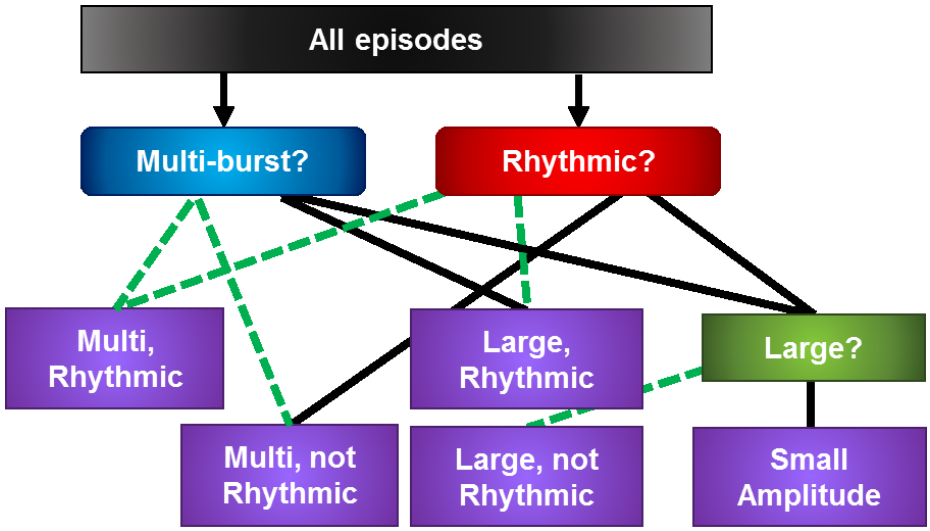

Figure 2.5. Final classification procedure. Two multilayer perceptrons were used to classify episodes, one as rhythmic or not, and the other as multi-burst or not. The results from these two binary classifiers combine to label episodes into classes: large rhythmic, multi-burst not rhythmic, multi-burst rhythmic. Amplitude information serves to further classify episodes as large non-rhythmic and small amplitude.

2.2.8 Statistics

We used $\mathbf{X}^2$ tests to compare performance measures from three expert (human) classifiers, with cross tabulations generated for all pairwise combinations. We compared episode features, before and after inducing excitation with KCl, via paired *t* tests. We used Wilcoxon (*W*) signed-rank tests whenever data failed tests of normality or equal variance. The proportion of episodes within each class between the two excitability states were compared using the $\mathbf{X}^2$ test, with cross-tabulations generated all pairwise combinations. $P \leq 0.05$ was used to indicate significance for all tests.

2.3 Results

Values for each feature extracted from the episodes of activity are listed in Table 2.2. On average, episodes were 18.2 s (SD = 17.6) long, had the largest frequency component near 1 Hz

(0.9 Hz, SD = 1.4), and had a wide range of amplitudes, averaging 654.1 μV (SD = 414.3). The remarkable diversity with respect to the qualitative nature of the recorded episodes was well-suited to inform supervised machine learning approaches to classify the different types of episodes we observed.

Class	Total (#, %)	Train-ing (#)	Test-ing (#)	Time from Prev (s)	St-st Time (s)	Dur-ation (s)	Peak Freq. (Hz)	Band-width (Hz)	Peak Power (V)	Max. Amp. (μV)	Avg. Amp. (μV)
S	367 (44.9%)	330	48	15.4 (19.2)	34.9 (27.5)	7.5 (7.2)	1.6 (1.7)	8.7 (1.3)	23.6 (30.9)	371.9 (180.2)	156.2 (76.5)
LnR	124 (15.2%)	112	24	20.2 (26.2)	36.6 (30.9)	16.5 (13.8)	0.8 (1.0)	9.3 (0.7)	79.1 (169.1)	807.5 (428.2)	282.5 (154.6)
LR	42 (5.1%)	38	19	14.3 (15.8)	28.1 (23.9)	20.2 (12.8)	0.8 (0.9)	9.6 (0.3)	78.3 (142.5)	876.4 (367.9)	312.1 (129.4)
MnR	77 (9.4%)	69	27	15.9 (24.3)	30.1 (29.5)	33.6 (18.1)	0.2 (0.4)	9.8 (0.2)	90.1 (82.2)	944.6 (416.4)	324.0 (142.5)
MR	207 (25.3%)	186	37	15.8 (25.0)	33.1 (31.5)	30.3 (20.3)	0.3 (0.5)	9.7 (0.4)	87.3 (82.4)	856.9 (414.5)	304.3 (142.5)
Over-all	890	735	155	16.2 (22.3)	33.8 (29.1)	18.2 (17.6)	0.9 (1.4)	9.2 (1.0)	58.7 (96.8)	654.1 (414.3)	240.7 (140.7)

Table 2.2. The number and proportion of episodes within each class and overall, along with the average (± standard deviation) value for each feature. Episodes were classified as small (S), large nonrhythmic (LnR), large rhythmic (LR), multi-burst not rhythmic (MnR) or multi-burst rhythmic (MR).

The expert individuals who classified the first batch of episodes reached majority consensus for 95.3% of the episodes (55.4% [319/576] unanimous agreement, 39.9% [230/576] two of three agreed; 4.7% [27/576] no agreement). Of the episodes where two of three experts agreed, experts A and B agreed 53.0% of the time, experts B and C agreed 10.9% of the time, and experts A and C agreed 36.1% of the time. Table 2.1 presents a more detailed assessment of the experts'

agreement and human error, evaluated using the metrics described above. Each individual was compared to the consensus of the other two experts to demonstrate the consistency among the experts as they were considered to be the gold standard for the algorithms. Overall, all experts had high accuracy. Expert A performed well at labelling episodes as rhythmic and multi-burst. Expert B had high specificity for labelling episodes as multi-burst or not ($P \leq 0.001$; $\mathbf{X}^2$), but not rhythmic or not ($P < 0.0001$; $\mathbf{X}^2$). Expert C was not very sensitive to labelling episodes as rhythmic or not ($P < 0.0001$; $\mathbf{X}^2$) but was for multi-burst or not ($P < 0.0001$; $\mathbf{X}^2$). Expert B was less precise at labelling episodes as rhythmic or not ($P \leq 0.001$; $\mathbf{X}^2$), while expert C was less precise at labelling episodes as multi-burst or not ($P < 0.0001$; $\mathbf{X}^2$). Since the second and third batches was classified as a group or pair, these metrics could not be calculated for classifying those episodes.

We first determined the accuracy of episode classification by the algorithms (for an overview of classes see Figure 2.3B, C), as that information was required to form the training set for the machine learning aspect of the software and to reveal the value of classifying spontaneous activity. As can be seen in Table 2.2, the data are rich with detail. We found that a majority of the episodes were small in amplitude and duration (44.9%). While large episodes were most often not rhythmic (15.2%), multi-burst episodes were most often rhythmic (25.3%). Multi-burst, non-rhythmic episodes had the largest maximum and average amplitudes, suggesting that larger amplitudes may not correlate with the probability of rhythmic activity. The duration of multi-burst non-rhythmic episodes was longer than all other classes. Notably, frequency-related features extracted from each episode and analyzed using traditional approaches, such as peak frequency, bandwidth, and peak power, were similar for rhythmic and non-rhythmic episodes. This implies that rhythmicity within an episode cannot be detected simply using extracted features and thresholds. Therefore, the data were used to train and test two multilayer perceptrons to classify episodes as rhythmic or not, and multi-burst or not. SpontaneousClassification also used the normalized amplitude to classify episodes into one of five classes (see methods and Figs. 2.3 and 2.5). The ability to discriminate between rhythmic episodes using a combination of all of the features demonstrates the power of machine learning methods to make inferences and predictions using data beyond simple time- and frequency-domain based analyses.

We next tested the ability of SpontaneousClassification to detect changes in spontaneous network activity following an increase in excitability. This allowed us to compare normal network features with features of a perturbed network. Increasing the extracellular concentration of KCl from 4 mM to 8 mM (for n = 8 spinal cord preparations) resulted in a robust depolarization of the DC potential in the ventral roots of the lumbar spinal cord (ΔVoltage = 2100 [SD = 2183] μV). An overall increase in the number of episodes (baseline: 271 episodes, KCl: 387 episodes; $t_{(7)} = 4.1$; P = 0.005) accompanied the depolarization, but the increase was not uniform across classes; only small amplitude (baseline: 137 episodes, KCl: 203 episodes; $t_{(7)} = 2.3$; P = 0.05) and multi-burst, rhythmic (baseline: 89 episodes, KCl: 132 episodes; $t_{(7)} = 3.1$; P = 0.02) episodes increased significantly in number (Figure 2.6 Ca.). Of note, while the number of episodes changed, the relative proportion of each episode class when normalized to the total number of episodes remained unchanged compared to baseline (P = 0.429, $\mathbf{X}^2$).

In some cases, global episode features changed, due to changes in their assigned episode classes. For example, globally, episodes were shorter (duration, baseline: 24.0 s (SD = 3.5), KCl: 19.0 s (SD = 3.4) ; $t_{(7)} = 3.40$; P = 0.01; Figure 2.6 Da) and had smaller mean and maximum amplitudes (mean amplitude, baseline: 252.2 μV (SD = 156.7), KCl: 112.3 μV (SD = 79.7); $t_{(7)} = 6.7$; P = 0.0003; maximum amplitude, baseline: 819.4 μV (SD = 546.3), KCl: 547.3 μV (SD = 334.4); $t_{(7)} = 5.8$; P = 0.00065; see Figure 2.6 Db, Dc). A reduction in duration was only significant in the small amplitude episode class (baseline: 9.9 s (SD=3.4), KCl: 6.6 s (1.8); $t_{(7)} = 2.9$; P = 0.02) and a reduction in amplitude only in the small amplitude (maximum amplitude, baseline: 451.3 μV (SD=112.8), KCl: 340.7 μV (SD=86.1); $t_{(7)} = 4.4$, P = 0.003; average amplitude, baseline: 150.3 μV (SD=38.7), KCl: 67.6 μV(SD=22.5); $t_{(7)} = 7.3$, P = 0.0002) and multi-burst rhythmic classes (maximum amplitude, baseline: 1167 μV (SD=422), KCl: 736 μV (SD=268); Wilcoxon signed-rank test (W) = −36, $T^+ = 0.00$; $T^- = -36$, P = 0.008; average amplitude, baseline: 353 μV (SD=126), KCl: 155 μV (SD=53); $t_{(7)} = 4.7$, P = 0.003).

In other instances, we observed no change in global episode features, but did find changes for some features within a specific episode class. For example, global peak frequency (Figure 2.6 Ea; $t_{(7)} = 0.5$, P = 0.6) and bandwidth (Figure 2.6 Ec; $W = -10$, $T^+ = 13$, $T^- = -23$; P = 0.5) were comparable before and after exciting the network; however, for the multi-burst rhythmic episode

class, the peak frequency increased ($t_{(7)} = 3.3$, P = 0.01) and its mean bandwidth decreased ($t_{(7)} = 2.7$, P = 0.03). Our approach, therefore, affords the capacity to account for changes in global episode features in specific episode classes, and to tease out more subtle changes in episode features within a class that might be missed when considering the population of all episodes.

2.4 Discussion

In vitro preparation of neonatal rodent spinal cords are a powerful tool for understanding how spinal networks generate the rhythmic activity that enables mammals to walk (Gordon and Whelan 2006; Gordon et al. 2008; Hägglund et al. 2010). In the past, investigations involved evoking *in vitro* patterns of fictive locomotor-like rhythmicity consistent with walking. Although newborn rodents can air-step at birth (Jamon and Clarac 1998), the vast majority of movements observed in neonates are sporadic and ataxic. *In vitro* recordings of neuronal activity underlying those sporadic, ataxic movements reveal spontaneous activity, which is critical for maturation of spinal network function (Yu et al. 2004; Hanson and Landmesser 2004; Cang et al. 2005). However, the qualitatively rich and diverse nature of the spontaneous activity makes it challenging to study. We developed SpontaneousClassification, a software tool to detect episodes of spontaneous activity and use supervised machine learning to identify five distinct episode classes based on quantitative and qualitative features of neuronal recordings.

SpontaneousClassification enables evaluation of subtle components of DC-coupled traces by detrending without the use of high-pass filters. Furthermore, SpontaneousClassification automatically characterizes episodes of spontaneous activity based on their features and then groups them into one of five classes of episodes. This automated classification process is extremely fast, enabling large volumes of data to be analyzed quickly. Analyzing DC-coupled neurograms through machine learning classification enables researchers to investigate the nature and development of spontaneous activity in finer detail and with a new outlook than previously available techniques.

2.4.1 When Should this Tool be Used?

SpontaneousClassification was designed to discriminate subtleties in stochastic, DC-coupled neurograms recorded from neonatal mouse spinal cords. Because its classifiers were trained on

episodes of this specific type of recording, they are only appropriate for similarly acquired and structured data. SpontaneousClassification should not be used on AC-coupled or high-pass filtered neurograms, nor on very high-frequency episodes (i.e., > 10 Hz). However, the feature extraction methods employed in SpontaneousClassification may be of interest for analyzing AC-coupled data. After the features are extracted, they can help determine if the classifiers are appropriate for the data and if the classification is working correctly. All investigators should have intimate knowledge of their data. If the class distributions seem odd considering the appearance of the data, researchers should re-check the feature extraction and consider other methods.

2.4.2 Classification of Other Biological Signals

A similar machine learning approach could be applied to other types of activity. Supervised machine learning has been used to detect abnormalities in the electrocardiogram characteristic waveforms to automatically diagnose arrhythmias (Gao et al. 2004; Khazaee and Ebrahimzadeh 2010; Li et al. 2014), ischaemic events (Papadimitriou et al. 2001; Papaloukas et al. 2003; Choi et al. 2017), and acute coronary syndromes (Harrison and Kennedy 2005; Myers et al. 2005). It can also predict brain disorders such as epilepsy (Diambra 2002; Subasi and Ismail Gursoy 2010) and schizophrenia (Sabeti et al. 2007) from electroencephalography (EEG) signals. MLPs are often used to classify electrical activity recorded from muscles (electromyography; EMG) for the control of myoelectric prostheses (Kelly et al. 1990; Hiraiwa et al. 1992; Hargrove et al. 2007; Karlık 2014).

These methods differ from spike sorting (Lewicki 1998), which uses clustering methods to separate, or sort, waveforms. Clustering in this manner is unsupervised learning; features of the waveform are compared to values defining individual clusters, sorting the waveforms into one of the clusters. Clustering methods have been used to classify AC-coupled potentials recorded from the dorsum of the lumbosacral spinal cord (Martin et al. 2015); episodes were detected based on their peak and selected a set time surrounding the peak, but this selection method is useful only when episode duration varies little. This method replaced template matching, which was previously used by the same group (Chávez et al. 2012), but they noted that it was time-consuming and required constant supervision.

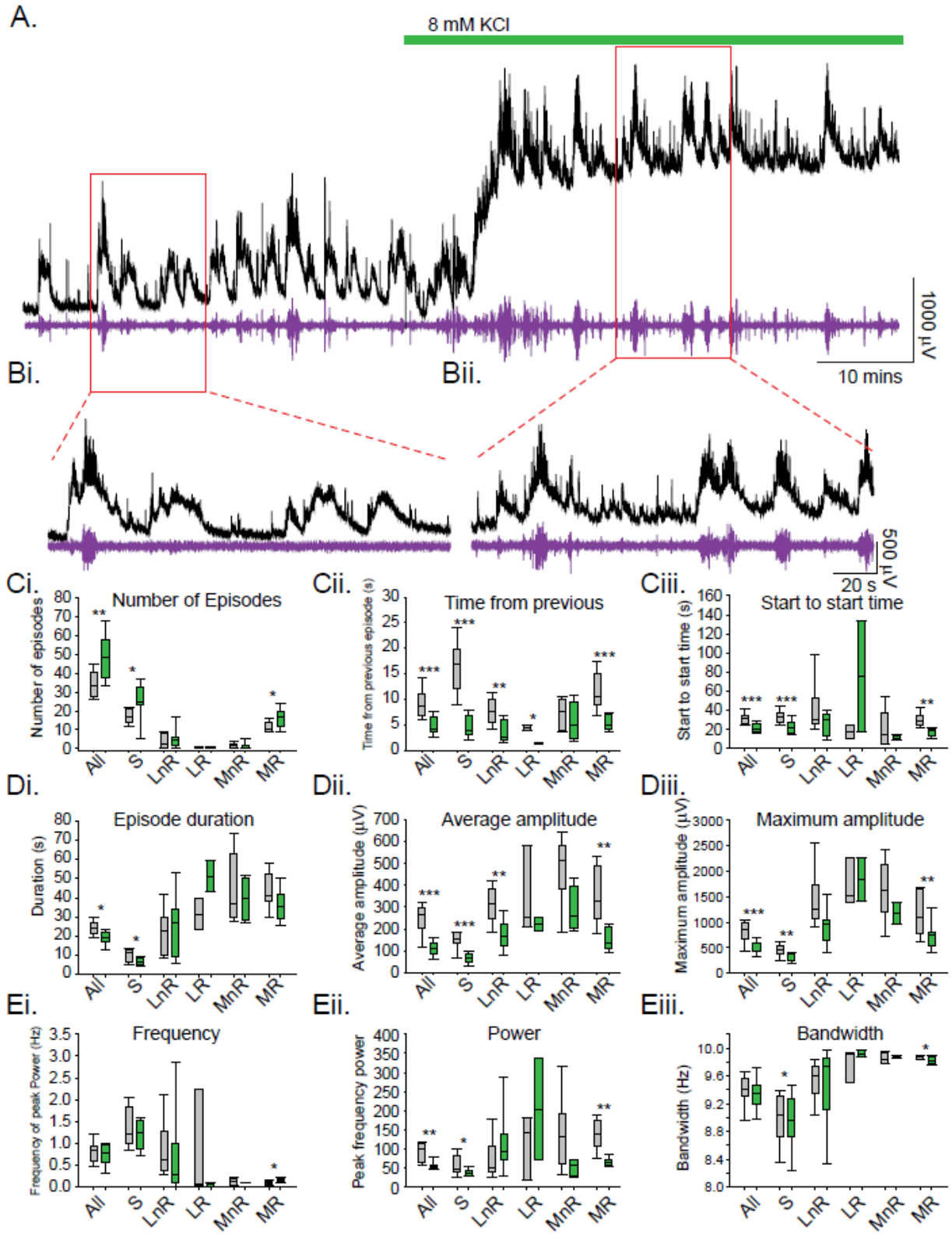

Figure 2.6. Alterations in spontaneous episode class activity under conditions of enhanced excitability by increased KCl concentration. A) DC-coupled neurogram recorded from lumbar ventral roots at baseline and after increasing the concentration of KCl from 4 mM to 8 mM (green bar). The traditionally analyzed high-pass filtered (100 Hz)

neurogram is below the DC-coupled recording (purple). B) Enlargement of regions at baseline (Ba) and at the higher concentration of KCl (Bb). The addition of KCl increased the excitation of network activity, depolarizing the DC potential, and altered several features extracted from each episode (C–E). Episode features were compared overall and for each of the five episode classes (small [S], large non-rhythmic [LnR], large rhythmic [LR], multi-burst not rhythmic [MnR] or multi-burst rhythmic [MR]). Box-and-whisker plots display interquartile range (boxes), median (horizontal black lines), maximum and minimum values in data range (whiskers). Means were compared using paired *t* tests. Asterisks denote significant differences before and after increasing KCl *P < 0.05, **P < 0.01, ***P < 0.001.

In the present study, episodes of activity recorded from the ventral root were too variable in shape and duration to apply template matching. Furthermore, we attempted several clustering methods and they failed to produce the classes previously defined (results not shown). Therefore, visual identification of classes and training with supervised machine learning prevailed as the most viable option for classifying episodes of spontaneous activity.

2.4.3 Limitations

Detrending each trace is unique to the DC-drift in the recording and must be customized by the user. Selecting thresholds for episode detection is also a subjective process. After choosing threshold values to detect episodes, users can view them to ensure they were detected correctly. There may be some variability in settings between traces, especially if background excitability or noise show large fluctuations. Future work may explore a more automated detection process.

Supervised machine learning is guided by the experts classifying the data. It allows experts to relay their knowledge to an algorithm to perform tasks more quickly and automatically. Therefore, the algorithm is limited by the class labels it trains on. To reduce subjectivity as much as possible, we had three expert individuals classify episodes of activity and used those data to train the algorithm. Initial classification of the first batch of episodes resulted in 95.3% agreement between at least two of three experts. Despite this high percentage, initial training accuracy was low. This prompted the experts to refine their criteria for rhythmicity. Revising the visual criteria for rhythmicity increased the experts' confidence in labelling the episodes as rhythmic or not, as well as their classification performance. Although this introduced some subjectivity to the class labels, it was a necessary step that clarified what was considered to be rhythmic. The classification accuracy achieved with the revised criteria confirmed that the

individuals and the program classified episodes similarly. This was further corroborated by the high accuracy obtained during classification of novel episodes during the testing phase, which presented the algorithms with fresh data. This demonstrated that the individuals were able to relay their expertise to the program for fast, automatic, and accurate classification.

Increasing the number of episodes in the training dataset would increase the representation of each class and may help the algorithm generalize more effectively. However, the process of manual classification is time-consuming and there is no universal criterion for the number of instances of data that are needed. A balance between data availability and training accuracy must be attained.

2.5 Conclusions

This work provides and demonstrates a software tool (SpontaneousClassification) for characterizing and classifying episodes of spontaneous activity from the lumbar spinal cord. Supervised machine learning classification of episodes allowed for the analysis of DC-coupled neurograms. We demonstrated the utility of SpontaneousClassification by comparing the features and class distributions between episodes of two different activity states. The data reconfirmed that the addition of KCl non-specifically excites spinal motor networks, resulting in a similar proportion of episodes in each class, even with an increase in overall number. This is an interesting result in of itself as it points to the fact that although the rhythm may appear stochastic, the overall composition is quite robust and resistant to perturbations. While it is difficult to speculate, this may be accomplished by a decrease in calcium-activated potassium conductances, or other voltage-gated potassium conductances. SpontaneousClassification is easy to use and enables fast and automatic characterization of spontaneous activity. Furthermore, no knowledge of machine learning is needed to use SpontaneousClassification. Future applications for SpontaneousClassification may include characterization of spontaneous activity from other regions of the spinal cord, such as the cervical and thoracic regions, throughout different timepoints in development, or with the addition of neuromodulators, as we can now investigate and analyze features of spontaneous activity quickly and automatically. This analysis may be used to further reveal the cellular components and network structure of the spinal cord during development, complimenting other methods of studying spinal motor activity.

Chapter 3: A Speed-Adaptive Intraspinal Microstimulation Controller to Restore Weight-Bearing Stepping in a Spinal Cord Hemisection Model[2]

3.1 Introduction

A spinal cord injury (SCI) results in severe motor and sensory paralysis, as well as autonomic dysfunction. Incomplete injuries account for two-thirds of all SCIs ("Spinal Cord Injury (SCI) 2017 Facts and Figures at a Glance" 2017). Regaining the ability to walk is a high priority for people with paraplegia (Brown-Triolo et al. 2002; Anderson 2004). Although tremendous advances have been made in spinal cord regeneration (Murray and Fischer 2001; Raisman 2001; Davies et al. 1997; Novikova et al. 2017), human trials to date have failed to produce functional benefits (Hulsebosch et al. 2000; Kim et al. 2017). If regeneration succeeds in the future, it will likely require additional rehabilitation interventions.

To date, several interventions using functional electrical stimulation (FES) have been developed to restore walking after SCI (Chaplin 1996; Kobetic et al. 1999; Hardin et al. 2007; Guiraud et al. 2006). FES of peripheral nerves and muscles produces large forces that enable multiple tasks (e.g., standing, walking, reaching, grasping). However, this technique is limited by rapid fatigue (Peckham and Knutson 2005), thus restricting its use to short distances of walking (< 100m (Thrasher and Popovic 2008)). An alternative approach is to target the spinal cord to activate the muscles of the legs. Epidural stimulation of the dorsal surface of the spinal cord has been shown to aid in the generation of voluntary leg movements (Angeli et al. 2014; Barolat et al. 1986). Alongside body-weight-supported treadmill training (BWSTT), epidural stimulation could achieve standing with minimal assistance in participants with a chronic motor complete SCI (Rejc et al. 2015). Epidural stimulation applied with BWSTT in people with incomplete SCI improved over-ground walking capacity (Carhart et al. 2004). In animal models of SCI, epidural stimulation in combination with intensive BWSTT and pharmacological activation has been shown to restore locomotion (Courtine et al. 2009; Musienko et al. 2012; van den Brand et al.

---

[2] Ashley N Dalrymple[1,3], Dirk G Everaert[2,3], David S Hu[2,3], Vivian K Mushahwar[1,2,3]
[1]Neuroscience and Mental Health Institute, University of Alberta, Edmonton, AB, Canada
[2]Division of Physical Medicine and Rehabilitation, Department of Medicine, Faculty of Medicine and Dentistry, University of Alberta, Edmonton, AB, Canada
[3]Sensory Motor Adaptive Rehabilitation Technology (SMART) Network, University of Alberta, Edmonton, AB, Canada

2012; Capogrosso et al. 2016). Epidural stimulation may have assisted with endogenously occurring spinal cord plasticity by increasing the basal activity of neurons, as has also been demonstrated through transcutaneous spinal cord stimulation in individuals with SCI (Hofstoetter et al. 2015; Inanici et al. 2018; Minassian et al. 2016). However, it is unclear if the epidural stimulation alone is able to produce functional, weight-bearing over-ground walking. Intraspinal microstimulation (ISMS) produces large forces in the leg muscles that are fatigue resistant (Bamford et al. 2005; Saigal et al. 2004; Mushahwar and Horch 1997). By implanting fine microwires (30 to 50 μm diameter) into the ventral horn of the lumbosacral enlargement, ISMS activates individual muscles as well as produce multi-joint synergies (Mushahwar and Horch 1998, 2000; Saigal et al. 2004; Holinski et al. 2011). ISMS has been used to restore standing (Lau et al. 2007) and walking in anaesthetized cats (Holinski et al. 2013, 2016), as well as cats with a complete SCI (Saigal et al. 2004). In a recent study, ISMS produced nearly 1 km of over-ground, weight-bearing walking in anaesthetized cats (Holinski et al. 2016).

ISMS has also been used to produce reaching and grasping movements by implanting electrodes in the cervical enlargement in rats with a contusion SCI (Kasten et al. 2013; Sunshine et al. 2013) as well as monkeys (Moritz et al. 2007; Zimmermann et al. 2011; Zimmermann and Jackson 2014). Recently, ISMS in the cervical and high thoracic spinal cord has been shown to activate the diaphragm and intercostal muscles in intact (Sunshine et al. 2018) and hemisected (Mercier et al. 2017) rats. Taken together, studies in both the lumbar and cervical enlargements demonstrate that ISMS can activate muscles and muscle synergies to restore function in a fatigue-resistant manner in models of complete and incomplete SCI.

A number of control strategies have been implemented for ISMS to restore walking (Dalrymple and Mushahwar, 2017). To date, these control strategies focused on models with complete SCI. Open loop stimulation patterns were initially developed to achieve alternation of swing and stance (Mushahwar et al. 2002) but lacked the ability to adapt the stepping to changes in terrain or fatigue. Conversely, a purely feedback-driven approach utilizing sensor information to transition the limbs between swing and stance phases has been tested in cats (Guevremont et al. 2007; Vogelstein et al. 2008). Later studies combined feed-forward and feedback control to produce functional walking. Specifically, feed-forward, intrinsically-timed transitions between

states of the gait cycle were implemented. Feedback from external sensors (Guevremont et al. 2007; Mazurek et al. 2012; Holinski et al. 2016) or from recordings from the dorsal root ganglia (Holinski et al. 2013) interrupted the intrinsic timing using pre-defined rules to improve over-ground walking and ensure safe stepping. Other studies have explored the use of fuzzy logic or sliding mode control to produce single joint movements using ISMS (Roshani and Erfanian 2013a, 2013b; Asadi and Erfanian 2012) or to trigger the onset of the flexion phase of the gait cycle (Saigal et al. 2004).

Earlier work in the field of FES and locomotion has explored numerous machine learning algorithms to control various aspects of the step cycle. Supervised machine learning uses previously obtained data to train an algorithm, which develops a generalization between inputs and outputs. The accuracy of the generalization is then tested using new data, where the real outputs are compared to the outputs predicted by the algorithm. Often, machine learning algorithms were used to predict the subject's intention to take a step and trigger stimulation of the flexor-withdrawal reflex to initiate the swing phase (Kirkwood et al. 1989; Kostov et al. 1992; Tong and Granat 1999; Sepulveda et al. 1997). These algorithms were used to produce stepping in an open-loop manner (Graupe and Kordylewski 1995) and for triggering IF-THEN control rules (Popović 1993). Adapting the stimulation output to muscle fatigue has also been explored (Graupe and Kordylewski 1995; Abbas and Triolo 1997).

In this study, we developed control strategies to produce weight-bearing stepping using ISMS in a hemisection SCI model. This presents the first application of supervised machine learning to control stimulation in the spinal cord. The control strategy used information from external sensors regarding the movements of the "unaffected" hind-limb to control the "affected" hind-limb. Moreover, supervised machine learning was employed to ensure weight-bearing at different stepping speeds. Specifically, multiple machine learning algorithms were trained to predict the stepping speed using data from external sensors from previous ISMS experiments and tested in later ISMS experiments in the study. This resulted in a unique combination of supervised machine learning and FES, since the learned predictions were used to select a control strategy based on the stepping speed, and within that strategy, the predicted value was used to control the stimulation output.

3.2 Methods

3.2.1 ISMS Implant Procedure and Stimulation Protocol

Six adult male cats (4.5 to 6.9 kg) were used in acute, non-recovery experiments. All experimental procedures were approved by the University of Alberta Animal Care and Use Committee. The surgery and experiments were conducted under sodium pentobarbital anesthesia. A laminectomy was performed to remove the L4 to L6 vertebrae to expose the lumbosacral enlargement.

A custom-made electrode array comprised of 12 micro-wires was implanted unilaterally throughout the lumbosacral enlargement. The wires were 50 µm in diameter, 80/20 % Pt-Ir, and insulated with 4 µm polyimide except for the tip, which had approximately 400 µm of exposure. The implant was performed according to established procedures (Mushahwar et al. 2000; Saigal et al. 2004; Holinski et al. 2016; Bamford et al. 2016), targeting lamina IX in the ventral horn based on maps of motoneuronal pools (Vanderhorst and Holstege 1997; Mushahwar and Horch 1998, 2000). In addition to the motoneuronal pools, this region contains neural networks that produce single joint and coordinated multi-joint synergistic movements of the leg when stimulated (Kiehn 2006; Bhumbra and Beato 2018). The stimuli comprised of asymmetric, biphasic, charge-balanced pulses 290 µs in duration delivered at a rate of 50 Hz. Stimulation was delivered using a current-controlled stimulator and was controlled through a custom graphical user interface designed in MATLAB (MathWorks Inc., Natick, MA, USA). Stimulation amplitudes typically ranged from threshold (<20 µA) to levels that produced weight-bearing movements (60 to 80 µA). Stimulation amplitudes did not exceed 110 µA through any electrode. Trains of stimuli were delivered as a trapezoidal waveform; the ramping occurred over 3 time-steps, with a time-step occurring every 40 ms. The movements achieved by stimulation through single electrodes were hip flexion, knee extension, ankle dorsiflexion, ankle plantarflexion, and a backward extensor synergy. Simultaneous stimulation through electrodes with desired evoked movements was used to construct synergies corresponding to the phases of the step cycle. Of the twelve electrodes implanted, only six to eight were needed to generate the desired stepping movements and included some redundancy in the functional targets.

3.2.2 Experimental Setup

After implantation of the ISMS array, the cats were transferred to a custom-built split-belt treadmill (Figure 3.1a). The cats were partially suspended in a sling and remained anaesthetized for the duration of the experiment. The sling supported the head, forelimbs, and trunk, allowing the hind-limbs to move freely. Reflective motion-tracking markers were placed on the iliac crest, hip, knee, ankle, and metatarsophalangeal (MTP) joints of both hind-limbs. Bilateral kinematics were recorded using two cameras (120fps, JVC Americas Corp., Wayne, NJ, USA), with the lens positioned parallel to the hind-limbs and 1.8 m away from the center of the treadmill. Marker positions were digitized using custom MATLAB software (MotionTracker2D) written by Dr. Douglas Weber (University of Pittsburgh, Pittsburgh, PA, USA). Gyroscopes were placed on the tarsals of each hind-limb to measure angular velocity. Vertical ground reaction forces were measured for each hind-limb by force transducers mounted underneath each of the treadmill belts. The sensor signals were filtered using a hardware second-order Butterworth filter (f_C = 3 Hz) and digitized at 1 kHz using the Grapevine Neural Interface Processor (Ripple, Salt Lake City, UT, USA) and streamed into MATLAB.

3.2.3 Control Strategy

The functional consequences of a hemisection SCI were simulated in the anaesthetized cats by an experimenter manually moving one hind-limb through the stepping cycle (Figure 3.1a). This injury model is similar to Brown-Sequard syndrome in humans, where one limb is paralyzed and the other remains motor-intact (Hayes et al. 2000; Bosch et al. 1971; Gil-Agudo et al. 2013). Three different experimenters took turns to move the limb through the gait cycle. Each experimenter moved the hind-limb over a moving treadmill belt and was given a target for downward force production. This limb represented the limb on the intact side of the spinal cord, and the experimenter simulated voluntary control of the limb. The other limb, ipsilateral to the ISMS implant, moved only through ISMS and represented the limb that would be paralyzed by a hemisection SCI. This stimulation-controlled limb (SCL) moved over a stationary treadmill belt; therefore, all movements of that limb were entirely produced by the stimulation in the spinal cord. Because the cat was anaesthetized, no reflexive responses were produced either by the moving treadmill belt ipsilateral to the EML nor by the movements produced by ISMS of the SCL.

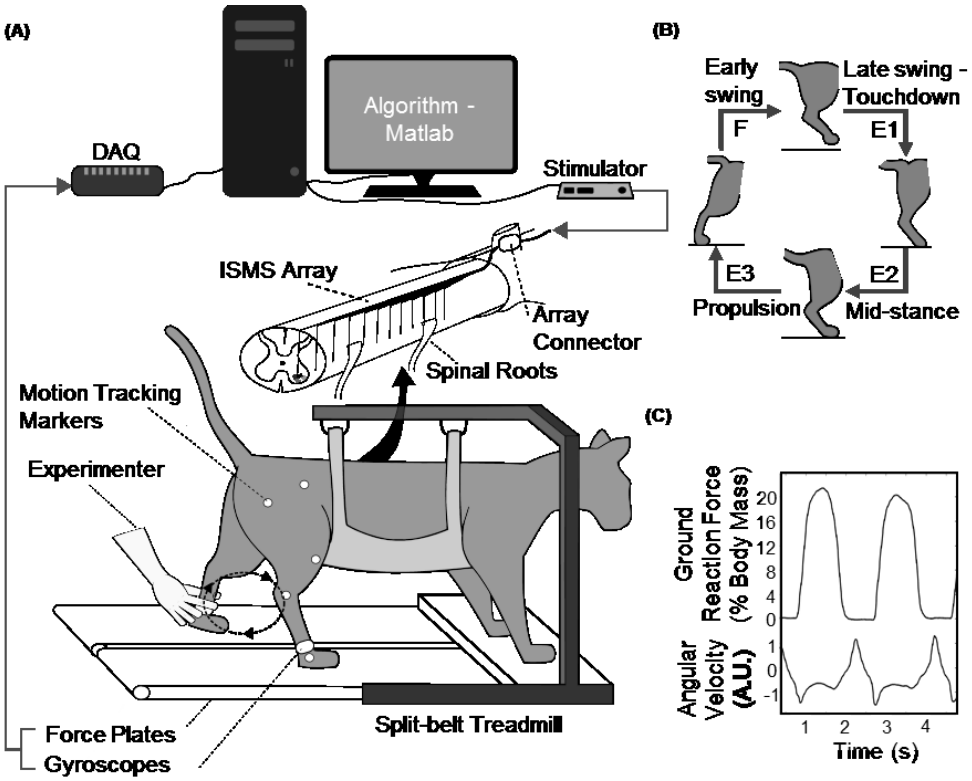

Figure 3.1. Experimental setup. **(A)** An experimenter moved one hind-limb through the gait cycle over the ipsilateral moving belt of a split-belt treadmill. Sensor signals from force plates under the treadmill belt and a gyroscope on the tarsals were converted to digital signals and used by a custom algorithm to control the stimulation to the spinal cord such that the other limb was in the opposite state of the gait cycle over a stationary treadmill belt. **(B)** States of the gait cycle. **(C)** Sample data from the force plates (ground reaction force) and gyroscopes (angular velocity) from the EML (experimenter-moved limb).

The stepping cycle was divided into 4 states indicating flexion and extension movements: F, E1, E2, and E3 (Goslow et al. 1973; Engberg and Lundberg 1969). These corresponded to toe-off to early swing, late swing to paw-touch, paw-touch to mid-stance, and mid-stance to propulsion, respectively (Figure 3.1b). The goal of the controller was for the legs to step reciprocally; the state of the experimenter-moved limb (EML) was used to control the stimulation to the spinal cord such that the SCL was in the opposite state (Figure 3.2a). The states of the gait cycle were discriminated using ground reaction force and angular velocity of the foot (Figure 3.2b).

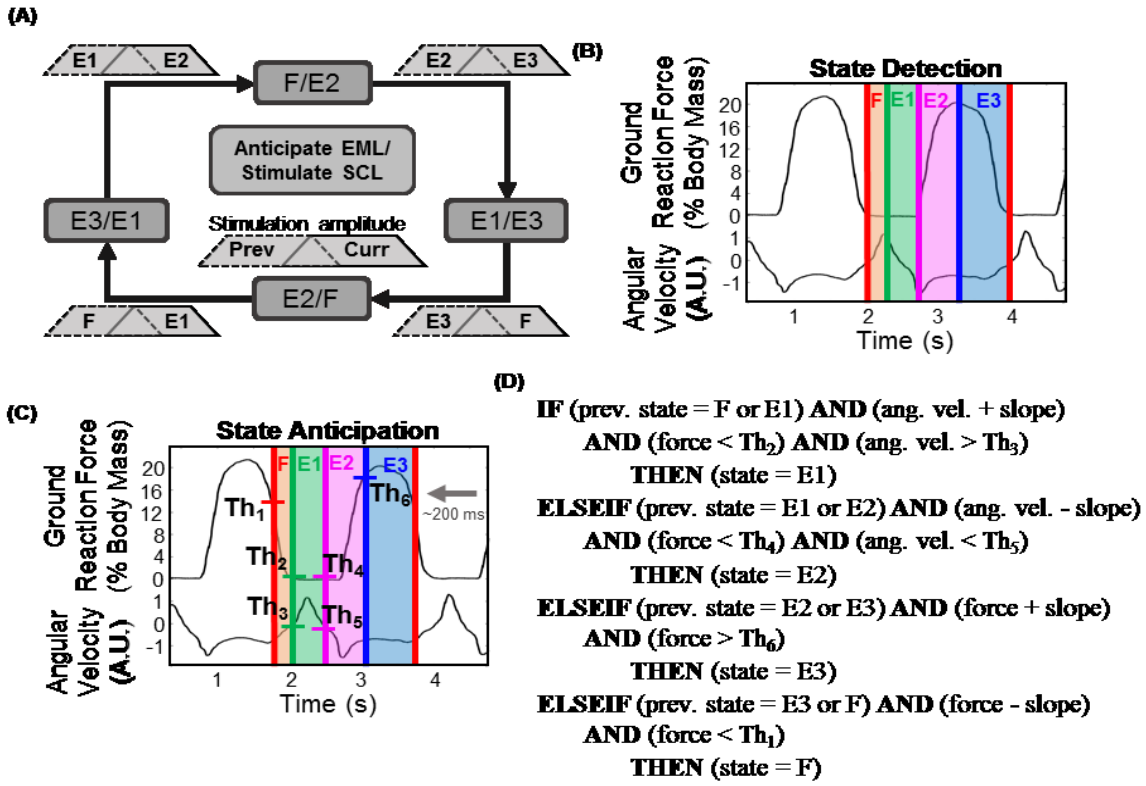

Figure 3.2. Control strategy. EML = experimenter-moved limb; SCL = stimulation-controlled limb. (A) Transitions between states of the gait cycle for the SCL, opposite to the state of the gait cycle of the EML. Transitions between states for the SCL were done by ramping down stimulus amplitude through the channels for the previous state, and ramping up the amplitude for the current state, indicated by the trapezoids. (B) Time when states of the gait cycle occurred relative to the ground reaction force and angular velocity of the EML. F = early swing, E1 = late swing to paw touch-down, E2 = mid-stance, and E3 = propulsion. (C) Anticipation of states to account for an electromechanical delay of 200ms. Thresholds were used to define the voltage values to which the signals were compared. (D) Algorithm used to anticipate states of the gait cycle using thresholds from C.

Specifically, the ground reaction force was used to detect E2 (onset of loading to peak force production), E3 (peak force to unloading), and F (unloading of limb). Angular velocity measured by a gyroscope at the tarsals was used to detect the onset of E1 (peak angular velocity). By using only 2 sensors per limb, all four states of the stepping cycle were detected. However, the stimulation needed to be delivered prior to the onset of a state to account for electromechanical delay between the stimulation delivered to the spinal cord to the time that a forceful movement was produced, which was up to 200 ms across all cats. It was comprised of the filter delay (~16 ms), computational delay (40 ms), and the delay from the stimulation command to the production of a movement in the limb (~120 ms). A 200 ms neuromusculoskeletal delay to produce a

movement around the ankle joint using ISMS has been previously reported (Roshani and Erfanian 2013a). Therefore, states were anticipated using pre-defined thresholds for the force and angular velocity signals that were approximately 200 ms before the onset of a given state (Figure 3.2c). The threshold-based control rules for anticipating each state of the gait cycle are described in Figure 3.2d.

The previous state information was used to ensure that the anticipated state was the current or next state in the gait cycle, forcing a forward trajectory through the gait cycle. The direction of the slope for each signal was used in combination with the voltage value to define threshold. The thresholds were tuned and remained constant throughout all experiments.

An additional control rule was implemented to ensure weight-bearing as needed. Since E3 is proportionally a longer phase of the gait cycle compared to E1, when the EML was in E3 and the SCL in E1 the SCL would spend a proportionally long time in E1. This caused the SCL to remain in the final position of E1, extended towards paw touch-down and partially loaded. This was followed by an increase in loading when the SCL transitioned into E2, but often the transition would result in a loss of over-all weight-bearing. This was ameliorated by the swing-to-stance rule (Mazurek et al. 2012): if the SCL was in E1 and the limb achieved partial weight-bearing, then transition the SCL to E2. This improved overall weight-bearing. The pseudo-code for this rule was as follows:

IF force > threshold,

THEN transition from E1 to E2

3.2.3.1 Speed Adaptability

The speed of the treadmill belt was varied within a single stepping trial (treadmill belt speed: 0.09 to 0.42 m/s). A stepping trial consisted of 10 to 24 steps. Although these are relatively slow speeds of stepping, they correspond to treadmill belt speeds at which cats with a complete spinal transection were able to step at in the early stages to full recovery (Bélanger et al. 1996). During the speed-varying stepping trials, it was noted that at faster speeds (defined by step period of EML < 1.95s), there was a loss of weight-bearing at the onset of loading for the SCL. This was due to the states themselves having a shorter duration than the electromechanical delay.

Therefore, further adaptations needed to be made to the stimulation output for the faster steps. A step-by-step feed-forward method was implemented to adapt the stimulation output for faster steps based on the step period. The step period of the EML, the measurable analogue of speed, was defined as the onset of limb loading to the onset of limb loading of the next step in the EML. Feed-forward refers to open-loop transitions between states of the step cycle in the SCL. The amount of time spent in each state was calculated from the predicted value of the step period for the EML using a variation of an equation derived from (Kirtley, Whittle, and Jefferson 1985) (3.1). The time spent in stance was split evenly between E2 and E3 (stance phases), and the remaining time was split evenly between F and E1 (swing phases).

$$T_{stance} = -0.073 \times \left(\frac{60}{StepPeriod}\right) + 67 \tag{3.1}$$

This allowed for a realistic adaptation of the amount of time spent in each state according to the step period. This process was repeated for each fast step. If the step period prediction indicated a slower step, then the state transitions were controlled individually according to the state-anticipation method.

The feed-forward stimulation to control the SCL started in E1. This state was chosen since it is the state just prior to primary limb loading, E2, and the goal was to increase the number of weight-bearing steps at faster speeds. Therefore, the step period of the EML had to be predicted prior to the anticipation of E3 (opposite to E1 in the SCL) in order to calculate the feed-forward times for the step.

3.2.3.2 Step Period Prediction

To adapt the stimulation output using the step-by-step feed-forward control strategy for the faster steps only, the speed was indirectly predicted and measured using the step period of the EML. Supervised machine learning methods were used to predict the step period. A total of 1721 steps from the first two cats were used for the training data set. All training steps were from one experimenter moving the hind-limb. The features used by the prediction algorithms were:

time spent in F; is time spent in E1; time spent in E2; time spent in F and E1; time spent in E1 and E2; time spent in F and E2; time spent in F, E1, and E2; angular acceleration shortly after the onset of E1; angular acceleration shortly after the onset of E2; and the slope of force shortly after the onset of E2.

Using the data mining platform Weka 3.8.0 (Witten et al. 2016), 66 combinations of these features were tested using linear regression to narrow down the set. Many of the combinations produced identical or near identical correlation coefficients and mean absolute errors; therefore, the parameter combinations that were chosen for further testing were selected based on their reliability and ease of measurement. The final three parameter combinations were the *(i)* time spent in F, time spent in E1, time spent in E2, and slope of force as individual parameters; *(ii)* time spent in F, time spent in E1, time spent in E2 as individual parameters; and *(iii)* time spent in F, E1, and E2 as a single parameter. Using these combinations, various supervised machine learning algorithms were tested using Weka to provide a numeric prediction of the step period.

The supervised machine learning algorithms we tested included simple linear regression, multivariate linear regression, least mean squares linear regression, model tree, k-nearest neighbor, artificial neural network, and support vector machine. In total, 397 combinations of features and algorithm parameters were tested. Results from 10-fold cross-validation were used to compare algorithms. Based on the mean absolute error and ease of implementation, simple linear regression, multivariate linear regression, and two different model trees were employed to predict the step period during stepping trials.

Simple (univariate) linear regression used the sum of the times spent in F, E1, and E2 as a single parameter to predict the step period. During training, the prediction was formed by linearly combining the features (in this case the sum of the state times) with weights, which were calculated from the training data, and minimizing the sum of squares of the differences between the predicted and actual values over all training instances (Witten et al. 2016). The resulting relationship from training the univariate linear regression model to predict the step period was:

$$StepPeriod = 1.642(T_F + T_{E1} + T_{E2}) - 0.0185 \quad (3.2)$$

Multivariate linear regression used the times spent in F, E1, and E2 as individual parameters. The algorithm training procedure was identical to that described for simple linear regression. The resulting equation from the multivariate linear regression was:

$$StepPeriod = 1.314 \times T_F + 2.3647 \times T_{E1} + 2.4025 \times T_{E2} - 0.3605 \quad (3.3)$$

Finally, two different model trees were implemented. A model tree is a combination of a decision tree and a linear model, where the linear relationship is the final leaf in the tree. The splitting criterion at each node was formed by testing each feature and determining the one that best maximized the expected reduction in error (Witten et al. 2016). The first model tree used only the time spent in F as a predictor to both make the routing decision (Figure 3.3a) and in the linear models 1 to 3 (3.4-3.6). The second model tree used each of the time spent in F for the routing decision (Figure 3.3b), and all three state times (time in F, E1, and E2) as individual parameters in linear models 4 and 5 (3.7-3.8). The linear models for each tree were:

Linear Model 1:

$$StepPeriod = 2.9401 \times T_F + 0.6944 \quad (3.4)$$

Linear Model 2:

$$StepPeriod = 3.3862 \times T_F + 0.5214 \quad (3.5)$$

Linear Model 3:

$$StepPeriod = 0.9397 \times T_F + 2.1271 \quad (3.6)$$

Linear Model 4:

$$StepPeriod = 1.9605 \times T_F + 2.0345 \times T_{E1} + 1.1872 \times T_{E2} - 0.1384 \quad (3.7)$$

Linear Model 5:

$$StepPeriod = 0.9547 \times T_F + 2.549 \times T_{E1} + 2.6454 \times T_{E2} - 0.158 \quad (3.8)$$

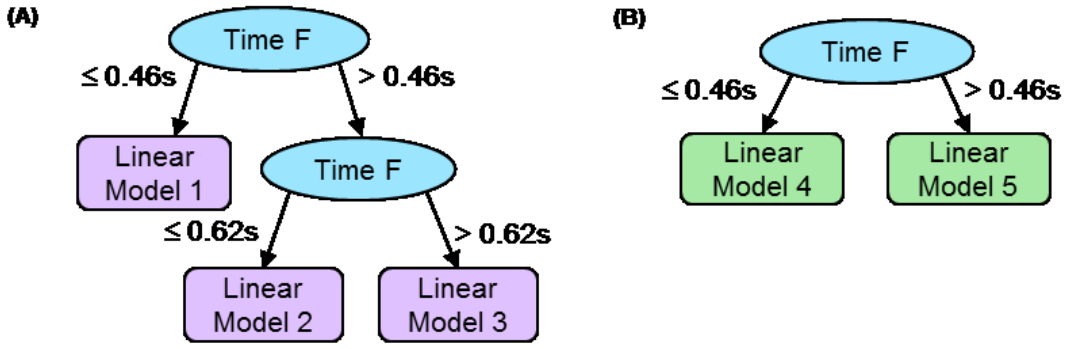

Figure 3.3. Trained model trees for numeric prediction. (A) Univariate model tree used the time spent in F to make routing decisions leading to one of three linear models. Linear models 1 – 3 used only the time spent in F as a variable. (B) Multivariate model tree used the time spent in F to make a routing decision to one of two linear models. Each of the linear models utilized three state times (time spent in F, E1, and E2).

3.2.4 Outcome Measures

Since the primary goal was to achieve alternating, weight-bearing stepping in the hind-limbs, several measures were developed to determine if the goal was met. All measures were calculated on a step-by-step basis.

Alternation was defined using two different measures. First, the ground reaction forces produced by each limb were used to verify if the limbs were 180º out of phase with each other. Specifically, the time each limb spent in loading was measured and converted into degrees of a circle, such that the onset of loading for the EML was equal to 0º, and the onset of loading of the EML for the next step was equal to 360º (Figure 3.4a). The half-way points of loading were calculated for each limb ($T_{E1/2}$, $T_{S1/2}$), converted to degrees, and the difference calculated. For perfect alternation, a phase difference of 180º would be seen between the forces from the limbs. The second measure of alternation was determined based on limb angle obtained from motion-capture. The limb angle was the angle between the vertical axis at the hip and the segment between the hip and the MTP joint. The limb angle was positive when the endpoint (MTP joint) was in front of the hip, and negative when it was behind the hip (Figure 3.4b). For each step, the point in time when the EML was at the largest positive limb angle (T_E), and the time when the SCL was at the largest negative limb angle (T_S) were determined. The time difference ($\Delta T = T_E - T_S$) was normalized by dividing by the step period of the EML. During perfect alternation, these two times would be equal resulting in an alternation measure of zero.

Ideally, the time spent in swing and stance would be equal for the two hind-limbs in a single step cycle. The time spent in swing and stance for each limb was calculated and normalized to the step period of the EML (Figure 3.4c). The stance symmetry and swing symmetry were calculated by taking the ratio of the normalized times in stance (3.9) and swing (3.10), respectively. A ratio of 1 for both measures would indicate that the both limbs spent the same amount of time in stance and swing.

$$Stance\ Symmetry = \frac{T_{St_{EML}}}{T_{St_{SCL}}} \tag{3.9}$$

$$Swing\ Symmetry = \frac{T_{Sw_{EML}}}{T_{Sw_{SCL}}} \tag{3.10}$$

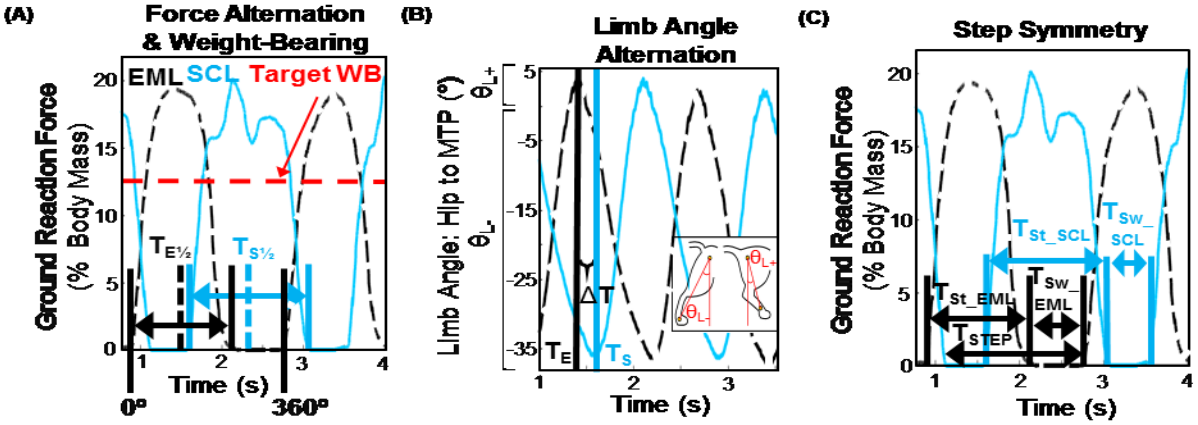

Figure 3.4. Outcome measures. EML = experimenter-moved limb; SCL = stimulation-controlled limb. (A) Force alternation and weight-bearing. The force produced by the EML was scaled down to match the SCL. Each limb exceeded the target force of 12.5% of body-weight, indicated by the horizontal dashed line. One step cycle of the EML was converted into the degrees of a circle (0° - 360°), indicated by the black vertical lines with the degree markers. The midway point of loading is indicated by the dashed vertical lines and marked by $T_{E½}$, $T_{S½}$ for the EML and SCL, respectively. These time-points were converted to degrees, and the difference between them was the phase difference of the two hind-limbs (ideally = 180°). (B) Limb angle alternation. The limb angle was measured as the angle between the vertical line from the hip and the segment between the hip and the MTP (metatarsophalangeal) joint, as demonstrated by the inset of the cat hind-limbs. Limb angle was negative when the foot was behind the hip, and positive when the foot was in front of the hip. Alternation of limb movements was measured by taking the time difference between when the foot of the EML was at the furthest point in front of the hip, and the foot of the SCL was furthest behind the limb ($\Delta T = T_E - T_S$), normalized by the step period of the EML. (C) Step symmetry. The time spent in stance and swing for the EML and SCL were labelled as T_{St_EML}, T_{Sw_EML}, T_{St_SCL}, T_{Sw_SCL}, respectively. The stance symmetry was calculated by taking the ratio of the stance times, normalized by the step period of the EML; the swing symmetry used the ratio of the normalized swing times. Dashed trace: EML; Solid trace: SCL.

To determine if the stepping was weight-bearing, the forces produced by each hind-limb were summated and compared to a threshold that defines body-weight support in the setup (12.5% of body weight for each limb (Lau et al. 2007)) (Figure 3.4a). The force produced by the EML was scaled down by the maximal value of force achieved in a stepping trial to avoid possible bias from the experimenter. The force produced by the SCL was not scaled since it demonstrates the true output of the stimulation in the spinal cord.

The accuracy of the step period predictions by the supervised machine learning algorithms was determined by comparing the predicted step period with the actual, measured step period for each step. From these, the mean absolute error for each prediction method was calculated. Even though the step period was only used to adapt to the faster steps, the prediction accuracy was calculated for all speeds.

3.2.5 Experimental Protocol

Trials were conducted with the EML moved through the gait cycle over a moving belt of a split-belt treadmill at a constant speed (treadmill belt speed: 0.17 to 0.2 m/s). The belt on the side of the SCL remained off throughout the experimental protocol. To test the limits of the controller, and to be more realistic of a SCI rehabilitation scenario, trials were conducted where the speed of the treadmill belt on the EML side was varied within a single stepping trial (0.09 to 0.42 m/s). The experimenter moving the EML adjusted their cadence to match the speed of the treadmill belt. The speed was limited by the abilities of the experimenters moving the EML. For the speed-varying trials, the experimenter was blinded to the type of step period prediction method (or lack thereof) tested. Stepping trials were between 30 and 60 s in duration.

The steps from the speed-varying trials were divided into two groups for analysis: slower (step period $\geq$1.95 s) and faster (step period < 1.95 s) steps. The slower steps did not require adaptation and were all grouped together. This allowed the measures from the faster steps without adaptation to be compared to the faster steps that used the step period prediction measures for the feed-forward adaptation.

3.2.6 Statistics

One-way analysis of variance (ANOVA) was used to test the difference between population means for each of the trial types for force alternation, limb angle alternation, stance and swing symmetry ratio, and step period prediction accuracy. Homogeneity of variance was tested using the Levene's test, and normality was tested using the Kolmogorov-Smirnov statistic. Tamhane T2 corrected post-hoc tests were reported if the Levene's test was significant. A p-value ≤ 0.05 was used to indicate significance. The $\mathbf{X}^2$ test was used to compare the success of weight-bearing between trial types. Cross-tabulations were generated for all pair-wise combinations. $\mathbf{X}^2$ with continuity correction was reported for 2x2 contingency tables, and the α-level was adjusted using the modified Bonferroni correction for multiple comparisons.

3.3 Results

A total of 6177 steps from 429 trials in 6 cats were recorded. Some steps were excluded from analysis if not all outcome measures could be calculated for a particular step, such as the first or final step in a trial (n = 209). Therefore, 5968 steps were used to calculate all outcome measures.

3.3.1 Stepping at a Constant Speed with No Speed Adaptation

The EML was moved at a constant speed (treadmill belt speed: 0.17 to 0.2 m/s; step period of EML: 2.03 ± 0.28 s) for 852 steps in 66 trials. The mean phase difference in forces between the EML and SCL in these steps was 177° (± 5.6°), and the mean absolute deviation from 180° was 4.37° (± 4.35°). This deviation from 180° was small, amounting to < 20 ms of shifting to the left or right. An example of the ground reaction forces produced by the hind-limbs is shown in Figure 5a, and a histogram of the alternating phase differences is shown in Figure 3.5c.

Raw data for limb angle alternation are shown in Figure 3.5b. The average time difference between when the EML was furthest in front of the hip and when the SCL was furthest behind the hip normalized to the step period for all steps was -0.03 ± 0.06. The negative value indicates that the SCL reached its furthest extension before the EML was at its furthest point in front of the hip (SCL leads the EML). The normalized time difference for all steps had a large variation. Even though the average normalized time difference was negative, for 272 (33.5%) steps the difference was positive (Figure 3.5d).

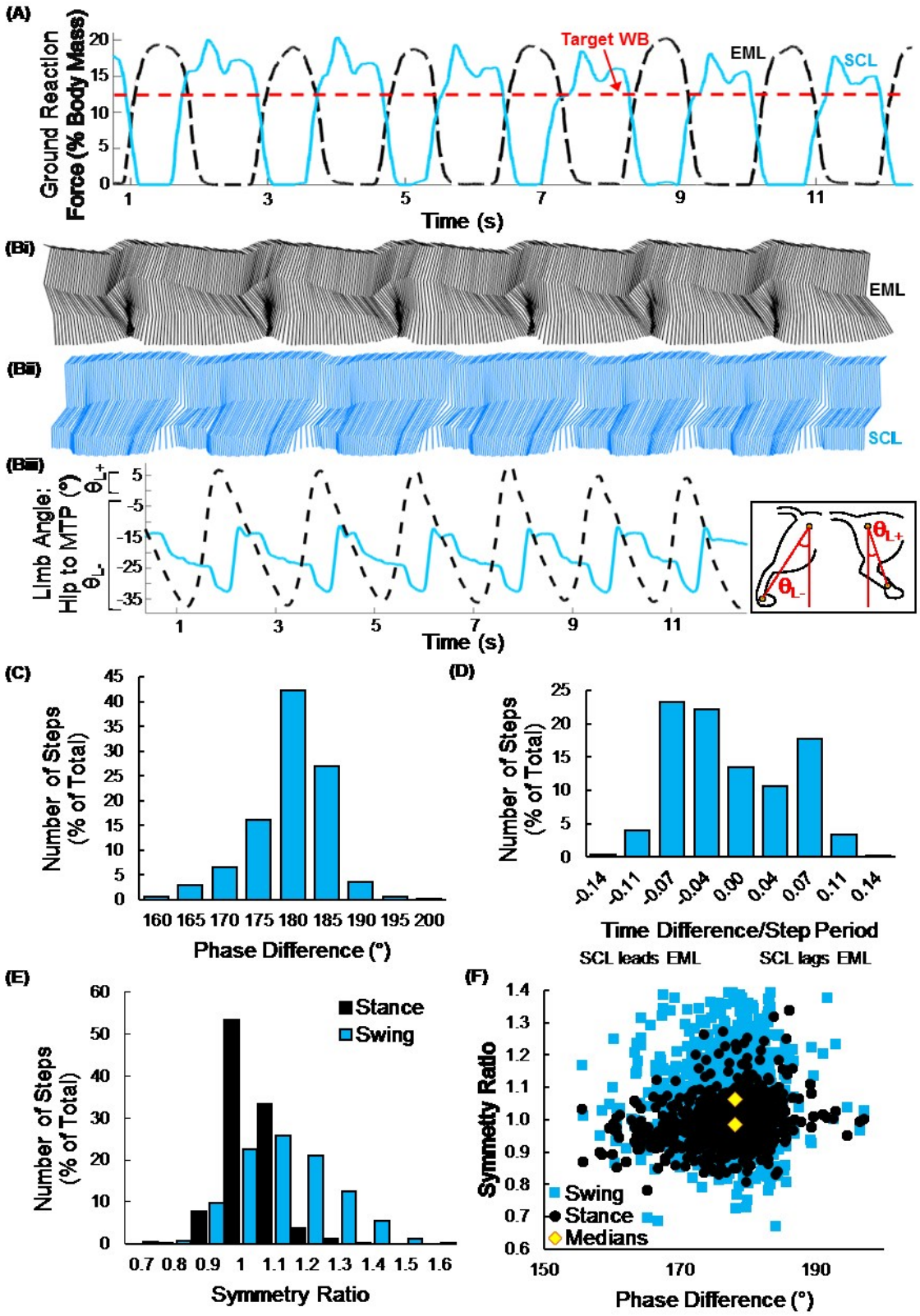

Figure 3.5. Results for stepping at a single speed (n = 852 steps). EML = experimenter-moved limb; SCL = stimulation-controlled limb. (A) Raw ground reaction forces. The force produced by the EML was scaled down to

match the SCL. Each limb exceeded the target force of 12.5% of body-weight, indicated by the horizontal dashed line. Dashed trace: EML; Solid trace: SCL. (B) Motion tracking of hind-limbs. (i) stick figure of EML. (ii) stick figure of SCL. (iii) Limb angle alternation. The movements produced by the experimenter were often larger than normal stepping and were scaled down for this figure. (C) Distribution of phase differences from force alternation. (D) Distribution of the normalized time differences obtained for the limb angle alternation. (E) Distribution of the stance symmetry ratio and swing symmetry ratio. (F) Phase difference of force alternation versus stance (circles) and swing (squares) symmetry. The diamonds indicate the medians for the phase difference and symmetry measures (upper = swing, lower = stance).

The stance and swing ratios for the steps in these trials were 0.99 ± 0.09 and 1.07 ± 0.15, respectively, indicating that the hind-limbs spent similar amounts of time in stance, but the EML on average spent more time in swing than the SCL. The swing ratio had a large variability compared to the stance ratio (Figure 3.5e). Figure 3.5f demonstrates that the steps had median values for the alternation phase difference and symmetry ratios close to their ideal values, with the stance ratio being closer to 1 than the swing ratio.

All 852 steps were weight-bearing. This meant that there were no steps where the sum of the forces produced by the two hind-limbs was below the weight-bearing threshold (12.5% of body weight for each limb).

3.3.2 Stepping at Varying Speed with No Speed Adaptability

Stepping metrics produced by the basic control algorithm were also obtained for varying stepping speeds of the EML. In these trials, the speed of the treadmill belt on the EML side was initially set between 0.09 and 0.15 m/s and increased twice during the trials to values between 0.19 and 0.42 m/s, with the EML moved at a matching speed.

In 363 trials, 1506 steps were at a slower speed (treadmill belt speed: approximately 0.09 to 0.25 m/s; step period of EML: 2.70 ± 0.44 s) and 1845 steps were at a faster speed (treadmill belt speed: approximately 0.26 to 0.42 m/s; step period of EML: 1.51 ± 0.25 s). On average, the phase for the slower steps had a significantly larger deviation from 180° than the faster steps (slower: 19.9° ± 11.9°; faster: 5.24° ± 5.83°; $p < 0.001$). The slower steps had a phase difference of 161° ± 12.9° which was significantly lower than that in the trials at the single speed (177° ±

5.6°; $p < 0.001$; Figure 3.6a). This meant that the force produced by the SCL was shifted earlier compared to the center of the forces produced by the EML. This was due to the swing-to-stance rule, which triggered an early transition into E2 if the limb stayed in E1 long enough to reach its endpoint, partially loaded. The faster steps had a phase difference of 181° ± 7.8°, which was significantly higher and closer to 180° than in the trials at a single speed ($p < 0.001$; Figure 3.6a). The time difference of the limb angle alternation for the slower steps was -0.016 ± 0.05, which is significantly closer to zero than steps at a single speed ($p < 0.001$). The time difference for the faster steps were also closer to zero (-0.004 ± 0.07, $p < 0.001$) than the steps at a single speed. For both speed ranges, the SCL reached its maximal backwards extension before the EML reached its maximal forward extension, the same as in the steps at a single speed.

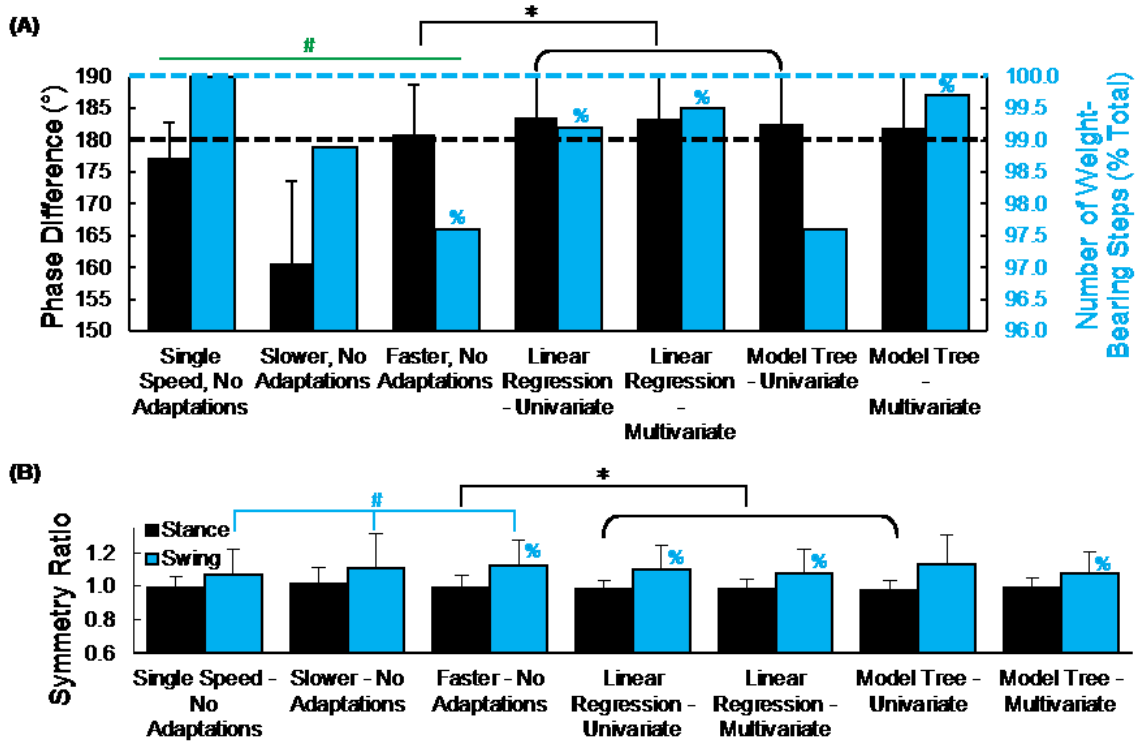

Figure 3.6. Outcome measures for all trial types. Steps with no feed-forward adaptations used only state-anticipation to control the SCL (stimulation-controlled limb). (A) The phase difference from the force alternation of the two hind-limbs (left y-axis) and the number of weight-bearing steps as a percent of the total steps in a trial (right y- axis). The horizontal dashed lines indicate the target for their corresponding outcome measure. The bars indicated by the supervised machine learning methods represent faster steps only. * $p < 0.05$, phase difference; # $p \leq 0.002$, both measures; % $p < 0.04$, weight-bearing, fast no adaptation versus others. (B) Stance and swing symmetry ratios for all trial types. * $p < 0.04$, stance symmetry; # $p < 0.001$, swing symmetry; % $p < 0.005$, swing symmetry, fast no adaptation versus others.

Slower steps had a stance ratio of 1.02 ± 0.10, which was significantly higher than steps at a constant speed (stance ratio = 0.99 ± 0.09; $p < 0.001$; Figure 6b) and steps at a faster speed (stance ratio = 0.99 ± 0.07), although this difference is unlikely be meaningful. Faster steps did not have a significantly different stance ratio than steps at a constant speed ($p = 0.97$). However, the swing ratio for both slower steps (1.11 ± 0.20) and faster steps (1.13 ± 0.15) were both significantly higher than that at a constant speed (1.07 ± 0.15; $p < 0.001$), indicating that at varying speeds the SCL spent less time in swing than at a constant speed.

Even though the faster steps had a phase difference closer to 180°, they were more likely to lose weight-bearing than slower steps (slower: 14/1506 steps, faster: 44/1845 steps, $p = 0.002$). The reasons for the loss of ground reaction force produced by the SCL were investigated and summarized in four categories (Figure 3.7): *(i)* the onset of force production was too late; *(ii)* the profile of the ground reaction force at loading was uneven; *(iii)* slipping during propulsion; and *(iv)* initiating the stimulation for swing too early. A breakdown of how often these occurred is presented in Table 3.1.

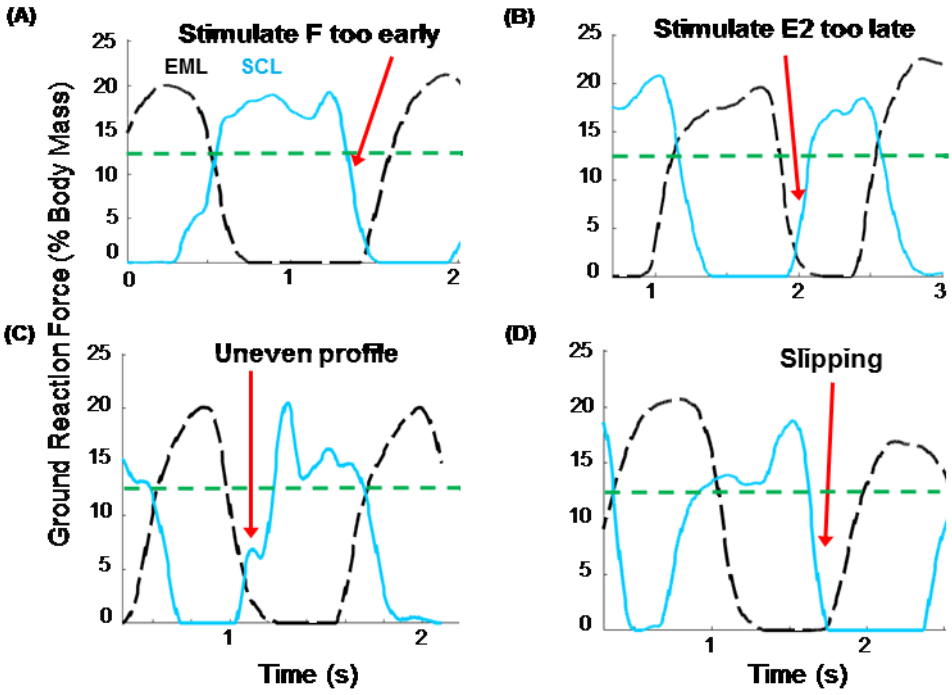

Figure 3.7. Examples of unloading. EML = experimenter-moved limb; SCL = stimulation-controlled limb. **(A)** Stimulation for F (early swing) started too early, prematurely lifting the SCL into swing. This occurred if the predicted step period was less than the actual step period of the EML, terminating E3 (propulsion) too soon in the SCL, or if during the anticipation of E2 (mid-stance), the timing of when the angular velocity signal crossed the

threshold was too early. **(B)** Stimulation for E2 started too late, resulting in a phase difference > 180°. **(C)** Loading started but with an uneven profile, possibly due to friction over the stationary treadmill belt. **(D)** Slipping during the propulsion phase of the SCL. This occurred if the movement was strong enough to propel the cat, but the body was unable to move because it was held in the sling and the ipsilateral treadmill belt was stationary, resulting in a phase difference < 180°.

Loss of Weight-Bearing									
	Occurrences by Trial Type						By Cat		
	S - NA	F - NA	LR - Uni	LR - Multi	MT - Uni	MT - Multi	Steps:	#	%
Loading of SCL							Cat 1	8	1.31
Too late	2	28	1	0	0	0	Cat 2	27	2.91
Slip, irregular	0	8	0	0	1	0	Cat 3	9	2.15
Unloading of SCL							Cat 4	12	1.01
Slipping	5	5	4	0	0	0	Cat 5	18	1.30
Swing too early	7	3	0	2	8	1	Cat 6	1	0.07
Number of steps (loss WB/total)	14/ 1506	44/ 1845	5/ 618	2/ 673	9/ 372	1/ 399			
Number of steps (percent)	0.93	2.38	0.81	0.53	2.42	0.25			
Duration (ms): M (± SD)	127.8 (75.1)	72.0 (45.3)	33.0 (21.4)	124.0 (162.6)	120.7 (47.8)	9.0			
Loss of force (%BW): M (± SD)	8.03 (4.90)	3.30 (2.56)	4.15 (5.66)	14.26 (8.82)	6.59 (3.46)	10.29			

Table 3.1. Breakdown of occurrences of unloading by trial type and by cat. The causes of the loss of weight-bearing (WB) are listed on the left, along with the incidence, the duration, and extent of unloading. SCL = stimulation-controlled limb; BW = body-weight; S-NA = slow - no adaptation; F-NA = fast - no adaptation; LR-Uni = linear regression - univariate; LR-Multi = linear regression - multivariate; MT-Uni = model tree - univariate; MT-Multi = model tree - multivariate.

For the slower steps, half of the instances of loss of weight-bearing were due to initiating the stimulation for F too early (Figure 3.7a). The stimulation for F occurs when E2 was anticipated in the EML, which depended largely on the angular velocity of that limb (Figure 3.2c). When the experimenter moving the EML caused a change in the slope of the angular velocity early in the swing phase, this caused the SCL to transition into early swing, leading to double-unloading. This led to a loss in force production (8.0 ± 4.9% BW loss) for a relatively long time (128 ± 75 ms). The faster steps were more prone to insufficient force production at the onset of loading

(Figure 3.7b), which caused a large deviation from 180° in some instances by up to 45.9°. The insufficient force was at times due to abnormal, uneven force production (Figure 3.7c), likely due to the paw of the SCL slipping over the stationary surface of the treadmill belt while pushing down. However, when the faster steps lost weight-bearing, it was often for a short duration (72 ± 45 ms), and for a lower amplitude relative to body weight (3.3 ± 2.6% loss) than in the slower steps. Because in most of the faster steps with a loss of weight-bearing the loss was due to the timing of the states and the onset of loading, a step-by-step feed-forward method was implemented for the faster steps.

3.3.3 Stepping at Varying Speeds with Speed Adaptability

Since the faster steps had significantly more steps that were below the weight-bearing threshold compared to steps at single and slower speeds ($p = 0.002$), the step-by-step feed-forward adaptation was implemented. Table 3.2 denotes the correlation coefficient and mean absolute error from training the linear regression and model tree algorithms. Using multiple features resulted in slightly higher performance than using a single feature for prediction during training.

Training of supervised machine learning algorithms Features	Performance measure	Linear Regression	Model Tree
T_F, T_{E1}, T_{E2} (multivariate)	Correlation coefficient Mean absolute error	0.901 0.206	0.911 0.195
$T_{F, E1, E2}$ (univariate)	Correlation coefficient Mean absolute error	0.894 0.208	0.910 0.196

Table 3.2. Training of supervised machine learning algorithms to predict the step period. The features used to train the algorithms were combinations of the time spent in F (T_F), time spent in E1 (T_{E1}), time spent in E2 (T_{E2}). $T_{F, E1, E2}$ is a single term comprised of the sum of the state times.

A comparison of the predicted step period with the actual step period for each of the four methods is shown in Figure 3.8a-d. The accuracy of prediction for all methods was higher for the smaller step periods (faster steps). The univariate linear regression and multivariate model tree methods had significantly lower prediction error than the multivariate linear regression and univariate model tree methods ($p < 0.001$; Figure 3.8e). On average, all four methods predicted a larger step period.

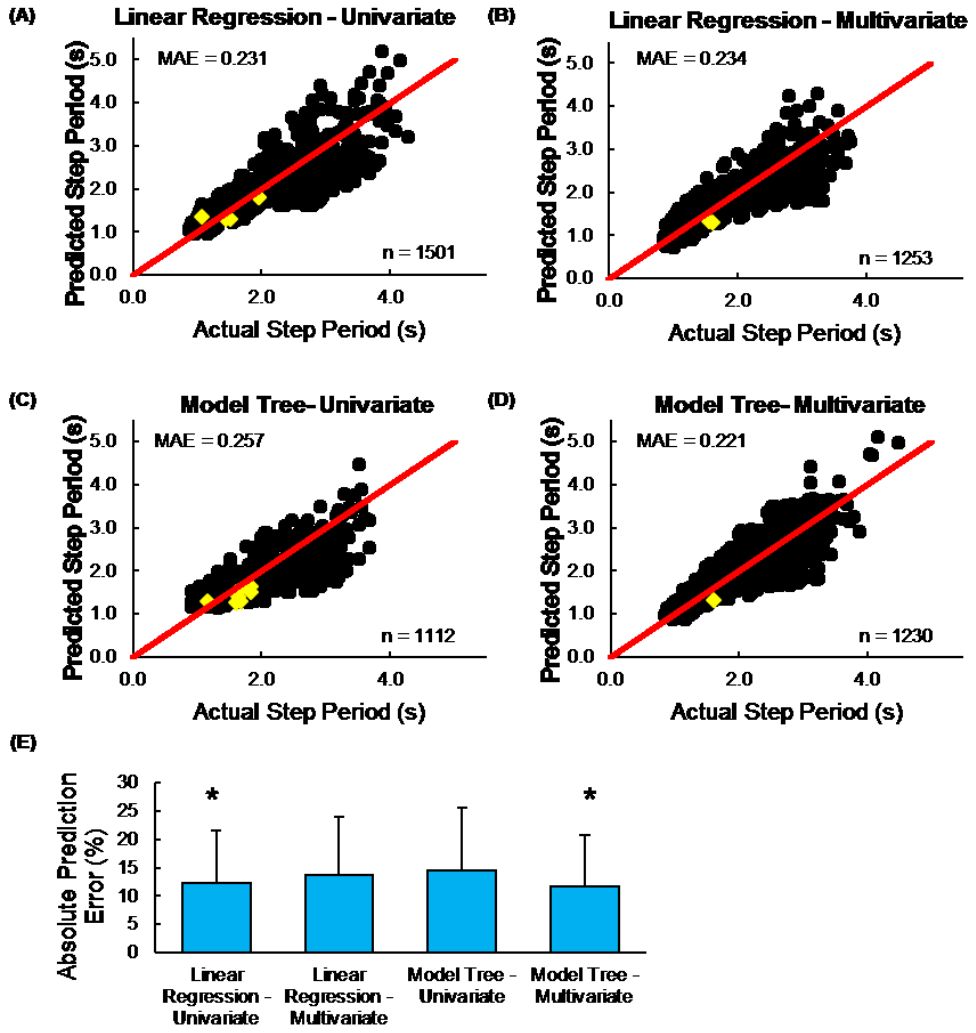

Figure 3.8. Accuracy of step period prediction. Comparing the step period predicted by the trained machine learning algorithm to the actual step period of the EML (experimenter-moved limb). Circles represent the data points from the stepping trials; the line indicates prediction unity; and the diamonds indicate when unloading occurred. (A) Univariate linear regression model predicting the step period. (B) Multivariate linear regression. (C) Univariate model tree. (D) Multivariate linear regression. (E) Comparison of the accuracy of each prediction method. MAE: mean absolute error of the prediction accuracy for steps at all speeds. *$p \leq 0.001$.

Examples of the ground reaction forces for the speed-varying stepping trials with no adaptation and trials from each of the four prediction methods are displayed in Figure 3.9. The relationship between the phase difference of the hind-limbs and the number of weight-bearing steps for all trials is demonstrated in Figure 3.6a. Of the four prediction methods, the multivariate model tree was the only one without a significantly different phase difference ($p = 0.602$) from the faster steps without adaptation. This is good since the faster steps without adaption had an average

phase difference very close to 180° (181° ± 7.8°). The justification for switching to speed-adaptive control was to increase the number of weight-bearing steps, as many faster steps without adaptation had insufficient weight-bearing. However, maintaining alternation close to 180° is also important, and the multivariate model tree method achieved that.

The univariate linear regression had a similar limb angle alternation time difference as the faster steps without adaptation (-0.003 ± 0.103; p = 1.00). The other three methods all had a significantly higher time difference than the faster steps without adaptation ($p < 0.001$), with the EML moving forward now leading the SCL moving backward.

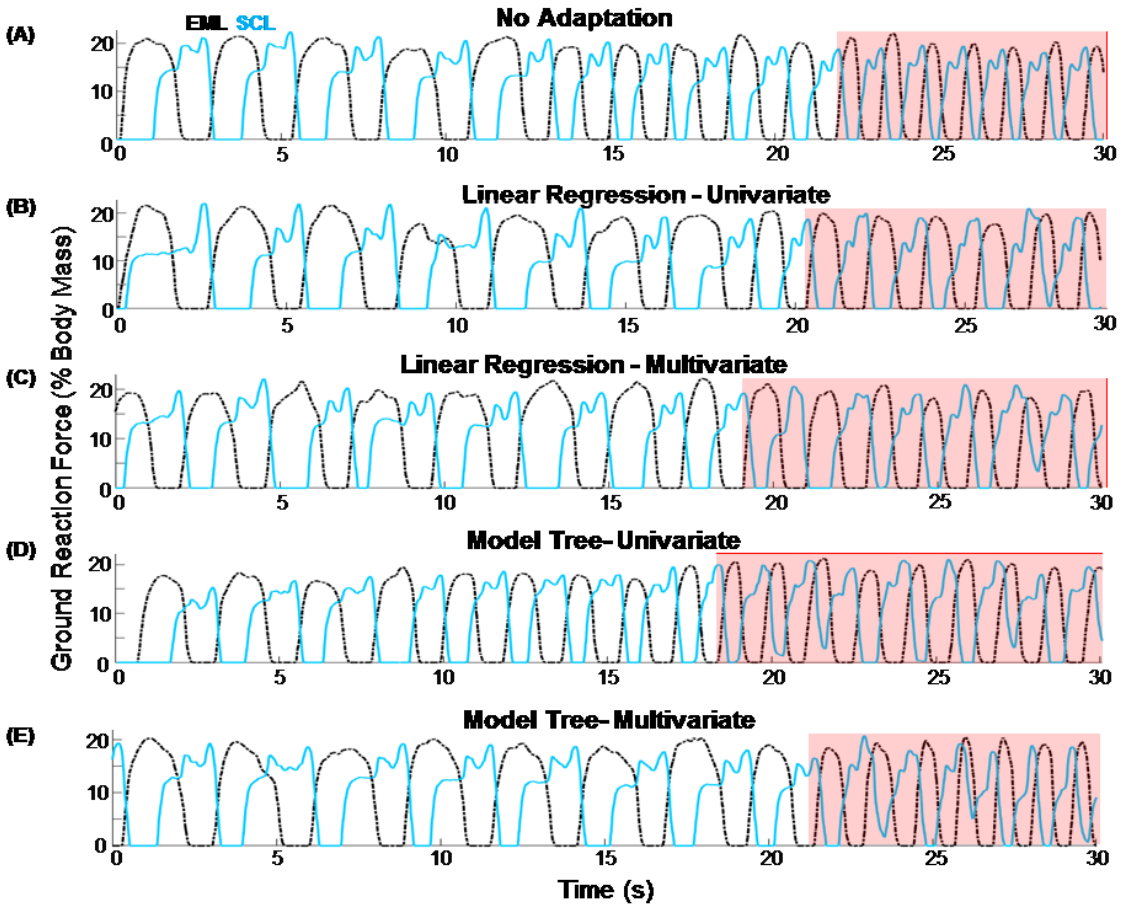

Figure 3.9. Ground reaction forces at varying speeds.EML = experimenter-moved limb; SCL = stimulation-controlled limb. Raw ground reaction forces for the EML (dashed) and SCL (solid) for an entire trial transitioning from very slow to faster speeds. The faster steps (step period < 1.95) are highlighted at the end of each trace. (A) No adaptation. (B) Adaptation with univariate linear regression numeric prediction of the step period for step-by-step feed-forward control strategy for faster steps. (C) Adaptation with multivariate linear regression. (D) Adaptation with univariate model tree. (E) Adaptation with multivariate model tree.

The stance ratio for both univariate and multivariate linear regression, as well as the univariate model tree were all significantly lower than the stance ratio for the faster steps without adaptation (stance ratio, faster = 0.99 ± 0.07; univariate and multivariate linear regression, univariate model tree = 0.98 ± 0.06; $p < 0.04$; Figure 3.6b). The stance ratio for the multivariate model tree (0.99 ± 0.06) was not significantly different from the stance ratio of the faster steps without adaptation ($p = 1.00$), which is a positive outcome because both values were very close to the ideal value of 1. However, the swing ratio for all methods except the univariate model tree (univariate linear regression = 1.10 ± 0.14; multivariate linear regression = 1.07 ± 0.15; univariate model tree = 1.13 ± 0.18; multivariate model tree = 1.08 ± 0.13) was significantly lower than that for faster steps without adaptation (1.13 ± 0.15; $p < 0.005$), bringing the swing ratio closer to 1. This improvement in the swing ratio means that three of the four adaptation methods elongated the swing phase of the SCL to be proportionally closer to the duration of the swing phase of the EML. The multivariate model tree method was the only method to both maintain the stance ratio very close to 1 and bring the swing ratio closer to 1, followed by multivariate linear regression.

The univariate model tree was the only prediction method that was unable to achieve a significantly higher number of weight-bearing steps relative to no adaptation ($p = 1.00$). In fact, it had the same percentage of steps that did not achieve weight-bearing as the no adaptation method (97.6%). Using feed-forward control for faster steps resulted in a total of 17/1765 steps with a loss of weight-bearing, with the majority (9/17) occurring when using the univariate model tree prediction method.

Incorrect step period prediction was the cause for loss in weight-bearing in 9 of the 17 fast feed-forward steps, and was seen to some extent in all methods. In one of those instances, the predicted step period was much larger than the actual step period (error = 26.6%, univariate linear regression), resulting in the stimulation for E1 lasting too long, and a delayed start to the stimulation for E2 (Figure 3.7b). This resulted in a phase difference of 224°. When the predicted step period was lower than the actual step period, the E3 phase terminated too early, triggering an earlier transition into F, which caused unloading (Figure 3.7a). This often resulted in a phase difference as low as 143° and was prevalent in steps using both model trees and the multivariate

linear regression method. In 7 of the 17 instances of decreased weight-bearing the cause was slipping of the SCL at the end of the step (Figure 3.7d, univariate linear regression and model tree). This occurred because the setup with the cat suspended in a sling over a treadmill allowed only in-place stepping on the stationary belt for the SCL. These instances saw a reduction in the phase difference by up to 137°. One of the 17 instances was due to an abnormal, uneven loading profile (Figure 3.7c, univariate model tree) and may be due to slipping during loading. The faster steps with insufficient weight-bearing caused by erroneous step period predictions had error values from 11.0 % to 26.6%. These were large prediction errors relative to the small step periods of the faster steps. If the predicted value of the step period for the faster steps was more than 200 ms from the actual step period, the result was incorrectly timed state transitions and unloading during feed-forward control. Table I also lists the instances of insufficient weight-bearing by individual cats. Cat 2 had the most instances, whereas cat 6 only had 1 instance. Two-thirds of the instances from cat 2 were from faster steps with no adaptation, caused by a late transition into E2.

In summary, the multivariate model tree method outperformed the other three prediction methods tested. It resulted in significantly less loss of weight-bearing, a stance symmetry remaining close to the ideal value of 1, a swing symmetry closer to 1, and maintained alternation near 180°.

3.4 Discussion

The goal of this study was to produce, for the first time, bilateral alternating, weight-bearing stepping of the hind-limbs in a model of incomplete SCI using ISMS. We developed control strategies to take advantage of residual function in a model of hemisection SCI to restore weight-bearing stepping in anaesthetized cats over a split-belt treadmill. We also employed adaptive control strategies to ensure weight-bearing at different speeds of stepping. The speed of stepping was predicted based on generalizations obtained through supervised machine learning relating external sensor information to the step period. The predicted step period was then used to adapt the control strategy to step-by-step feed-forward control for fast steps. Through the adaptive control strategies, we were able to restore weight-bearing and maintain alternation and step symmetry in three of the four supervised machine learning numeric prediction methods. The best

method according to alternation, weight-bearing, and step symmetry was a multivariate model tree algorithm.

3.4.1 Comparison to Natural Walking

During normal walking, the movements of the legs are controlled by integrating input from various sources. The brain contributes initiation commands and coordinates complex walking tasks, such as avoiding expected obstacles and walking on difficult terrain (Takakusaki et al. 2008; Cinelli and Patla 2008; Marigold and Patla 2005). Brainstem regions, such as the mesencephalic locomotor region (MLR), generate excitatory drive to the spinal cord and affect the rate and pattern of hind-limb movements (Grillner and Shik 1973; Orlovskiĭ et al. 1966; Ryczko and Dubuc 2013; Mori et al. 1992; Shik et al. 1966). The cerebellum makes anticipatory corrections to the gait pattern if the limb movements differ from the intended movements (Morton and Bastian 2006). In the lumbar spinal cord, the central pattern generator (CPG) is a neural network that can produce alternating movements of the hind-limbs in the absence of phasic sensory afferent information (Grillner and Wallen 1985; Guertin 2009). However, afferent feedback does play a critical role in controlling the transition from stance to swing (Duysens and Pearson 1980; Ekeberg and Pearson 2005; Grillner and Rossignol 1978) and reacting to perturbations (Forssberg 1979; Hiebert et al. 1995).

The CPG has been shown to exist in invertebrates such as crayfish (Stein 1971) and leeches (Kristan and Weeks 1983) and vertebrates including lamprey (Wallén and Williams 1984; Messina et al. 2017) and cats (Brown 1911; Jankowska et al. 1967; Pearson and Rossignol 1991). There is evidence that the CPG may also exist in humans (Dimitrijevic et al. 1998; Calancie et al. 1994; Minassian et al. 2007; Bussel et al. 1996). A prominent model of the CPG proposes that movements are generated by a two-layer network for rhythm generation and pattern formation (McCrea and Rybak 2008); each limb has its own CPG that mutually inhibits the other. The rhythm generating network is responsible for alternation of flexion and extension; the pattern formation network is responsible for coordinating limb movements. Sensory afferents from the limbs can modulate both the timing and pattern of the CPG to adjust walking. The CPG receives inputs from the brain, brainstem, and sensory afferents. Together, these afferents, efferents, and intraspinal networks interact to produce walking (Guertin 2012).

After a spinal cord injury, the spinal cord no longer receives descending drive from the brain and brainstem. In chronically injured cats locomotor stepping on the moving belt of a treadmill can be restored by activation of the CPG through sensory afferents (Pearson and Rossignol 1991). Tonic excitation of the lumbar spinal cord, such as with epidural stimulation or transcutaneous spinal cord stimulation, can produce flexion-extension alternation of the legs in the supine position (Dimitrijevic et al. 1998; Calancie et al. 1994) or in combination with BWSTT (Angeli et al. 2014; Carhart et al. 2004; Dietz et al. 1994; Harkema et al. 2011; Hofstoetter et al. 2015). Additionally, epidural stimulation in supine humans with complete SCI has produced other rhythmic motor patterns including synchronized and reciprocal activation of muscles (Danner et al. 2015), suggesting a flexible organization of the pattern formation network.

The current control strategy anticipated the state of the EML and activated the SCL to be in an opposite state, resulting in a feedback-driven mutual inhibition of flexion and extension between the two limbs. All anticipations of state transition utilized limb loading information. Limb loading information provided by Golgi tendon organs is critical for biological walking as well, particularly for the transition from stance to swing. To initiate the swing phase, unloading of ankle extensor muscles must occur along with hip extension (Duysens and Pearson 1980; Ekeberg and Pearson 2005). A gyroscope, which provided angular velocity, and its slope (i.e. angular acceleration), does not have a direct biological equivalent. However, information such as muscle length and velocity are measured by Ia and II muscle spindle afferents (Boyd 1980), and indicate hip extension during the stretching of the hip muscles, assisting the aforementioned transition from stance to swing (Grillner and Rossignol 1978).

The change in control strategy from reactive to predictive feed-forward control is comparable to the role of the cerebellum in walking. Sensor information was used to predict the speed of walking as well as adjust the time spent in each state during feed-forward control. The cerebellum contributes to walking by recalibrating the gait pattern using predictions of the motor outcomes. It makes corrections to the output if there are discrepancies between the efferent copy from the motor cortex and the afferent input from the spinocerebellar tract (Pisotta and Molinari 2014; Shadmehr et al. 2010; Takakusaki 2013).

3.4.2 Comparison to other Control Strategies

Control strategies developed for ISMS to restore walking in a complete SCI model were CPG-inspired (Vogelstein et al. 2008; Saigal et al. 2004; Guevremont et al. 2007; Mazurek et al. 2012; Holinski et al. 2013, 2016). More traditional control approaches have also been used to control ISMS. Fuzzy logic control to generate ankle movements aimed to track a desired trajectory (Roshani and Erfanian 2013a, 2013b). Trajectory tracking of knee and ankle movements was also performed using sliding mode control of ISMS (Asadi and Erfanian 2012). However, trajectory tracking may prove difficult as each individual has different joint targets to match, along with numerous body-worn sensors for a feedback system to ensure accurate tracking.

Control strategies for peripheral FES often include the detection of the user's intention to step, initiating an open-loop control strategy. Walking can be produced by stimulating the peroneal nerve to trigger the flexor-withdrawal reflex (Kirkwood and Andrews 1989; Kostov et al. 1992; Tong and Granat 1999) and the quadriceps muscles for knee extension (Bajd et al. 1985; Andrews et al. 1988; Chaplin 1996) through surface electrodes. It can also be produced by stimulating flexor and extensor muscles through implanted epimysial or intramuscular electrodes (Popović 1993; Kobetic et al. 1999; Hardin et al. 2007; Guiraud et al. 2006; Dutta et al. 2008). The initiation of movements can be triggered by a hand-switch (Kobetic et al. 1999; Hardin et al. 2007; Guiraud et al. 2006) or triggered by the user's intention to step as determined from EMG activity (Dutta et al. 2008) or ground reaction forces (Kostov et al. 1992).

Using sensory information from an intact limb to control the movements of an affected limb was used in this study; it is similar to control strategies developed for restoring walking in stroke patients using an exoskeleton (Murray et al. 2014). This may also be a viable approach to lower limb prosthetic control for people with amputations in the future.

3.4.3 Signals for Control Strategies of ISMS

Feedback of sensory information is necessary for control strategies to adapt to their surroundings. This study employed external sensors as feedback signals for the controller, as they are easy and reliable to use for proof-of-concept testing of control strategies. The gyroscopes were small devices place on the tarsals. The force plates were mounted underneath

the treadmill belts, but there are commercially available force sensitive resistors that can be placed on the insoles of shoes and have been used as feedback sensors in other work (Kirkwood et al. 1989; Kostov et al. 1992; Lovse et al. 2012). Previous studies also used accelerometers in combination with gyroscopes to represent limb angle (Lovse et al. 2012; Mazurek et al. 2012; Holinski et al. 2016). Conversely, neural recordings could also be used as feedback signals for control. Extracellular recordings from the dorsal root ganglia have been used as a feedback signal to control ISMS in a model of complete SCI (Holinski et al. 2013); however, the reliability of the recordings degrade over times as the implants are encapsulated by glial tissue (Weber et al. 2007).

Neural recordings could also be obtained from the pre-motor or motor cortex and used as an input to ISMS. Using cortical recordings from the cortex to control ISMS enables communication between the brain and spinal cord, restoring voluntary control of paralyzed muscles (Mushahwar et al. 2006; Shahdoost et al. 2014). Cortical recordings have been used to control cervical ISMS in monkeys to control grasping (Zimmermann and Jackson 2014). They have also been used to control flexor and extensor activations in the hind-limb during treadmill stepping with epidural stimulation in monkeys (Capogrosso et al. 2016), and control prosthetic arms in humans (Collinger et al. 2013; Hotson et al. 2016; Fetz 1999; Wang et al. 2013). EEG (electroencephalography) signals have been used to control movements of an upper-limb prosthesis (Bright et al. 2016; Müller-Putz et al. 2010) and an upper-limb exoskeleton (Sullivan et al. 2017).

For restoring walking after an incomplete SCI electromyography (EMG) activity may be a useful control signal as it can be used to detect the intentions of the user to step, and also informs the controller about residual muscle activity. EMG has been used to control implanted intramuscular stimulation systems for walking (Dutta et al. 2008) as well as to control the rate of stimulation in the spinal cord during cervical ISMS to control grasp (Zimmermann and Jackson 2014). Adaptive control of walking would likely require a variety of sensor signals to indicate intention, limb position, force production, muscle activity, and the presence of obstacles, just as the brain and spinal cord receive input and feedback from a variety of sensory streams.

3.4.4 ISMS and Incomplete SCI

For restoring walking after a complete SCI, all limb movements were produced by electrical stimulation. After an incomplete SCI, some descending voluntary control remains, and varies depending on the severity and level of the injury. The best approach for a neural prosthesis after an incomplete SCI is to augment the remaining function by providing stimulation only to compensate for the deficits from the injury. Residual voluntary activity must therefore be measured and used as input to the controller. In the current study, residual voluntary function was simulated by an experimenter manually moving one hind-limb. To control the affected limb, information regarding the movements of the unaffected limb were utilized.

After an incomplete SCI, it is possible to achieve functional improvements with training and exercise (Field-Fote 2001; Barbeau and Rossignol 1987; Thrasher et al. 2006), or through the activation of spinal networks using electrical stimulation (Angeli et al. 2014; Barolat et al. 1986; Capogrosso et al. 2016; Carhart et al. 2004; Mondello et al. 2014). A recent study in non-human primates with a unilateral corticospinal tract lesion, similar to the hemisection model described here, demonstrated that treadmill and over-ground walking could be restored in as early as 6 days post-injury using epidural stimulation (Capogrosso et al. 2016). More longitudinal stimulation with rehabilitation in a staggered hemisection model showed extensive intraspinal remodeling and restoration of over-ground walking in the presence of the stimulation (van den Brand et al. 2012).

Chronic ISMS may amplify spinal cord plasticity through at least 3 mechanisms: 1) stimulation in the ventral horn could strengthen nearby locomotor networks, specifically, interneurons that synapse on motoneuronal pools, 2) limb movements could strengthen sensory afferents to the spinal cord, and reinforce motor networks through natural feedback mechanisms, and 3) descending connections could be strengthened by volitional control during walking (Mondello et al. 2014). Cervical ISMS after a contusion SCI showed improved forelimb function that lasted beyond the stimulation trial, suggesting it may be a viable method for enhancing spinal plasticity (Kasten et al. 2013).

3.4.5 Experimental Limitations

A limitation of the experimental setup is that it required an experimenter to move one hind-limb (EML) through the gait cycle. Nonetheless, this study demonstrated a proof-of-concept testing of the controller. Furthermore, the speeds of the treadmill used in the experiments (0.09 to 0.42 m/s) represent relatively slow speeds and corresponded to treadmill belt speeds at which cats with a complete SCI were able to step at in the early to late stages of recovery on a treadmill (Bélanger et al. 1996). Interestingly, by adapting to different walking speeds, the controller was indifferent to which experimenter moved the limb through the gait cycle, even though the supervised machine learning algorithms used to predict step period were trained using data from only one of the three experimenters. This suggests that the algorithms sufficiently generalized to the training data.

Since the cat was suspended in a sling over the split-belt treadmill, it was unable to propel itself forward and displace its position, resulting in in-place stepping as opposed to walking. During the propulsive phase (E3), the cat was physically prevented from moving forward. This created a large resistance between the stationary treadmill belt and the paw of the SCL during E3. To avoid kicking movements as the SCL overcame static friction, stimulation amplitudes through the channels comprising E3 were decreased, but were still high enough to lift the cat out of the sling. This led to a decreased range of motion during extension of the SCL. Full weight-bearing and range of motion of the SCL was achieved by turning the treadmill belt on. These trials were not included in the analysis since we wanted to ensure all movements were due to ISMS and not external forces. Future experiments will be performed on a walkway such that the cat is able to displace its position (Holinski et al. 2016, 2013; Mazurek et al. 2012; Guevremont et al. 2007).

With the experimental setup, it was difficult to conclude if the instances of decreased weight-bearing would be detrimental to walking since the cat's body was supported by the sling, especially those instances of short duration and small amounts of decreased weight-bearing. Realistically, if a person were to have an ISMS implant, they would require a walking-aid such as crutches or a walker to help with balance and trunk control. Small amounts of insufficient weight-bearing could be alleviated through partial upper-body support on the walking-aid. However, other studies using peripheral FES to restore walking with assistance from a walking-

aid have reported rapid fatigue of the arms and a large sense of effort if the legs were not producing stable and sufficient forces (Kobetic et al. 1999; Triolo et al. 2012). Relying on the arms for partial weight-bearing prohibits the users from reaching for objects while standing. Therefore, we aim for reliable and continuous body-weight support using ISMS. ISMS is more resistant to muscle fatigue (Bamford et al. 2005; Lau et al. 2007), and weight-bearing can be achieved for very long durations and distances compared to peripheral FES systems (Holinski et al. 2016).

The feed-forward steps that had instances of insufficient weight-bearing were largely affected by incorrect predictions of the step period. Generally, the accuracy of the step period prediction increased as speed increased. Most often the unloaded steps resulted from the predicted step period being too small, which resulted in early unloading. Although the ability of the controller to detect the states of the gait cycle was unaffected by which experimenter was moving the EML, subtle timing differences of when the states were detected occurred. State anticipation thresholds were held constant throughout all trials; therefore, even the step-by-step feed-forward control strategy was prone to errors stemming from variation in stepping patterns, since it used the state times to predict the step period. Adaptive thresholds for the state detections may provide further accuracy of step period predictions and increase the number of weight-bearing steps.

3.4.6 Future Considerations

Further speed adaptation for the slower steps using similar speed-prediction methods may improve alternation at those speeds. Specifically, the swing-to-stance rule may be disabled for the slower steps, correcting the early onset of force production by the SCL.

Expanding the application of ISMS to bilateral contusion SCIs, which leaves varying levels of residual voluntary drive, necessitates a control strategy that can adapt to the variability of deficits seen from these injuries. One approach could be to use machine learning to predict the state changes and learn the predictions over many steps. Since the predictions would be continuously learned and updated, the controller would be adaptable during walking. This may perform better than using rigid thresholds since walking patterns vary within and between people. Pavlovian control (Modayil et al. 2014; Modayil and Sutton 2014) may be a viable option for adaptable and

safe control of walking. Pavlovian control could use reinforcement learning to learn predictions about the gait cycle, and use those predictions to elicit a fixed stimulation response to produce consistent walking. EMG activity may be a useful input for Pavlovian control of ISMS as it can indicate movement intentions and residual muscle function.

Chapter 4: Pavlovian Control of Intraspinal Microstimulation to Produce Walking[3]

4.1 Introduction

After a spinal cord injury (SCI), people experience motor and sensory paralysis to varying degrees, depending on the severity and level of the injury. Two-thirds of all SCIs in the USA are incomplete ("Spinal Cord Injury (SCI) 2017 Facts and Figures at a Glance" 2017). For people with paraplegia, regaining the ability to walk is a high priority, ranking first or second nearly 40% of the time (Anderson 2004). Currently, SCI has no cure; therefore, regaining the ability to walk has been pursued through other means such as rehabilitation (Musselman et al. 2009; Lam et al. 2015; Morrison et al. 2018), neural interfaces (Kobetic et al. 1997; Hardin et al. 2007; Holinski et al. 2016), or a combinatorial approach (Angeli et al. 2018b; Gill et al. 2018; Carhart et al. 2004).

Current commercially available devices for restoring walking after SCI, such as the Parastep, Praxis, and various exoskeletons, have limited control options. The Parastep and Praxis systems use surface and implanted functional electrical stimulation (FES) electrodes, respectively (Chaplin 1996; Johnston et al. 2005). Walking is accomplished using open loop alternation between stimulation of the quadriceps muscles and the peroneal nerve, with each step initiated using push-buttons on a walker. Powered exoskeletons initiate open-loop walking initiated by the user leaning forward (Chang et al. 2015; Ekelem and Goldfarb 2018). The users are expected to adapt their walking to accommodate the control strategy of the device.

Substantial work has been dedicated to improving the control strategies for walking such as incorporating feedback from sensors. Walking using finite state control can be described as a set of IF-THEN rules (Popović 1993; Prochazka 1996). Finite state controllers designed to transition

[3] Ashley N Dalrymple[1,4], David A Roszko[1,4], Richard S Sutton[2,4], Vivian K Mushahwar[1,3,4]
[1]Neuroscience and Mental Health Institute, University of Alberta, Edmonton, AB, Canada
[2]Department of Computing Science, Faculty of Science, University of Alberta, Edmonton, AB, Canada
[3]Division of Physical Medicine and Rehabilitation, Department of Medicine, Faculty of Medicine and Dentistry, University of Alberta, Edmonton, AB, Canada
[4]Sensory Motor Adaptive Rehabilitation Technology (SMART) Network, University of Alberta, Edmonton, AB, Canada

the legs through the phases of the walking cycle used feedback signals including ground reaction force and hip angle (Andrews et al. 1988; Guevremont et al. 2007), which represent important physiological signals in defining phase transitions (Grillner and Rossignol 1978; McVea et al. 2005; Figueiredo et al. 2018). Proportional-integral-derivative (PID) controllers have been implemented to track joint or limb trajectory during FES walking (Quintern et al. 1997; Kurosawa et al. 2005). Non-linear methods such as sliding mode control have also been used to track joint angles (Nekoukar and Erfanian 2012). New control strategies for exoskeletons include joint tracking (Quintero et al. 2012) and supplementing movements and torques during open loop control through gravity compensation and impedance-based assistance (Murray et al. 2014; Marchal-Crespo and Reinkensmeyer 2009). However, tracking joint targets requires extensive knowledge of the system and often involves trial and error for tuning the control parameters (Matjacić et al. 2003).

This study focused on developing a predictive control strategy for restoring walking using intraspinal microstimulation (ISMS). ISMS entails implanting fine microwires in the ventral horn of the lumbosacral enlargement. Stimulation in this region produces graded single joint movements as well as coordinated multi-joint synergies (Mushahwar and Horch 1998, 2000; Saigal et al. 2004; Holinski et al. 2011). ISMS has been used to restore walking in anaesthetized (Holinski et al. 2013, 2016) and spinalized cats (Saigal et al. 2004).

Controllers developed for ISMS have primarily focused on restoring walking in complete SCI models (Dalrymple and Mushahwar 2017). Open loop control was used to alternate between flexion and extension movements (Mushahwar et al. 2002; Saigal et al. 2004). Feedback, such as ground reaction forces, hip angle, or activity of neurons from the dorsal root ganglia, was introduced to modify the inherent timing of the transitions between the phases of the gait cycle (Saigal et al. 2004; Holinski et al. 2011; Holinski et al. 2013, 2016).

To restore walking after incomplete SCI, the control strategy needs to utilize residual function and deliver stimulation to compensate for the deficits. A recent paper depicted the first control strategies developed for ISMS in a model of incomplete SCI (Dalrymple et al. 2018). There, supervised machine learning was used to adapt the control strategy for different speeds of

walking. However, as people with SCI experience varying levels of paralysis, each person would require their own custom stimulation settings to restore walking. Manual tuning of settings could be burdensome, especially if the settings require frequent tuning. Ideally, stimulation settings would be tuned once during the initial set-up for each person, and thereafter automatically adjust to any daily gait changes. Control strategies utilizing machine learning may be needed for automatic adaptation of stimulation settings to restore walking.

Supervised machine learning has been used to control surface FES systems in people with SCI to track joint angles (Abbas and Triolo 1997; Popović et al. 1999; Qi et al. 1999), initiate the swing phase (Kirkwood and Andrews 1989; Kostov et al. 1992, 1995; Tong and Granat 1999; Sepulveda et al. 1997), control FES over multiple joints (Fisekovic and Popovic 2001), predict different phases of the gait cycle in able-bodied participants (Kirkwood and Andrews 1989; Williamson and Andrews 2000), and in finite control of FES walking after complete SCI (Popović 1993). However, supervised learning requires manual labelling of data and is limited by the data set used for training. Many examples with sufficient variability are needed in the training data set to obtain an accurate generalization yet avoid overfitting to the training data. Furthermore, it is often difficult and computationally expensive to learn online.

The present study proposes using reinforcement learning (RL) to learn predictions during walking to control electrical stimulation. Similar to operant conditioning, RL is an area of machine learning that accomplishes a goal by maximizing future reward (Skinner 1963; Staddon and Cerutti 2003; Sutton and Barto 2018). RL can also estimate, or predict, the future values of signals other than reward. General value functions (GVFs) can be learned to predict arbitrary signals of interest, called cumulants (Z) (White 2015). Many GVFs can be learned simultaneously to produce predictions of many cumulants. The GVF is formulated using the discounted sum of future values of the cumulant, using a discounting factor γ. The result is a prediction signal that is larger in amplitude than the cumulant and follows the shape of the cumulant convoluted with a decaying exponential. Temporal difference (TD) learning is a method that can be used to estimate the GVFs using previously obtained estimates, called bootstrapping (Sutton 1988; van Seijen et al. 2015; Sutton and Barto 2018). Learning speed

improves further with the addition of eligibility traces, which are a temporary record of recently visited states, as in TD(λ) (Sutton and Barto 2018).

Work using RL to produce walking has been primarily performed in simulations and robots. RL has been used to control joint trajectories in Nao humanoid robots to produce stable walking in 10 (Li et al. 2013) to 200 (Endo et al. 2008) trials. Mapping a limb trajectory from a simulation to a bipedal robot required 100 trials consisting of 30 steps each to walk successfully (Morimoto and Atkeson 2007). Another study that controlled the hip joint of a robot required 15 hours of simulation and 20 minutes of continuous learning to walk (Schuitema et al. 2005). RL performs well in non-stationary, stochastic environments, which includes walking. However, learning is often slow and requires many iterations to find the optimal (or near-optimal) control solution. Nevertheless, RL is a powerful tool that can be employed in many ways, such as providing predictions online that can then be used to produce control decisions.

Predictions from RL can be used for Pavlovian control. Pavlovian control refers to using learned predictions to trigger fixed or pre-defined outputs, such as a stimulation output (Modayil and Sutton 2014). These concepts are inspired by classical, or Pavlovian, conditioning and the well-known work of Ivan Pavlov. When Pavlov presented his dogs with food (unconditioned stimulus; US) they would salivate (response; R) (Pavlov 1883; Rehman and Rehman 2018). If a bell preceded the presentation of food, over time, the dogs salivated at the sound of the bell (conditioned stimulus; CS), as they associated the bell with the expectation of food. The R is a fixed, automatic response to the US and was not under the dogs' volition. These concepts can be applied to control problems including robotics and rehabilitation. GVFs from TD-learning predicted joint switching events of an upper-limb myoelectric prosthesis (Pilarski et al. 2012; Pilarski et al. 2013a; 2013b) and were successfully tested in able-bodied participants (Edwards et al. 2013) and persons with amputation (Edwards et al. 2016). In a mobile robot, large-scale online predictions over multiple time-scales using GVFs from TD learning were feasible (Modayil et al. 2012; Modayil et al. 2014). Learned predictions of the robot's motor stalling and human-delivered commands were used to trigger fixed responses including shutting off the motor and spinning left, respectively. Pavlovian control combines expert knowledge of a control problem with the flexibility and adaptability provided by RL.

In this study, we compared more traditional control methods with Pavlovian control to produce over-ground, alternating walking in a model of hemisection SCI. Specifically, we assessed the need for manual tuning of control settings between reaction-based control and Pavlovian control over several cat experiments and with different people participating to move one limb through the walking cycle and after perturbations. This presents the first application of Pavlovian control to produce walking. It is also the first known application of RL techniques in a spinal neural interface. By learning predictions using RL and using those predictions for Pavlovian control, we demonstrate that alternating over-ground walking can be achieved quickly, and that the thresholds for Pavlovian control do not require re-tuning across different conditions.

4.2 Methods

4.2.1 Implant Procedure and Stimulation Protocol

All experimental procedures were approved by the University of Alberta Animal Care and Use Committee. Acute, non-recovery experiments were performed in eight adult male cats (3.96 to 5.22 kg). Surgical procedures and data collections were performed under sodium pentobarbital anesthesia. A laminectomy removing the L4 at L5 vertebrae was performed to expose the lumbosacral enlargement.

A custom 12 electrode array was made from Pt-Ir (80/20) wires 50 µm in diameter, insulated with 4 µm polyimide except for approximately 400 µm exposure at the tip. The wires were implanted unilaterally throughout the lumbosacral enlargement according to established procedures (Mushahwar et al. 2000; Bamford et al. 2016), targeting lamina IX in the ventral horn based on functional maps of the motoneuron pools (Vanderhorst and Holstege 1997; Mushahwar and Horch 1998, 2000). This region also contains neural networks that, when stimulated, produce movements around a single joint as well as coordinated multi-joint synergistic movements of the leg (Kiehn 2006; Bhumbra and Beato 2018). Trains of stimuli were delivered using a current-controlled stimulator and consisted of a trapezoidal waveform that ramped from threshold to chosen amplitude over 3 time-steps (time-step = 40 ms). The stimulus pulses in the trains were 290 µs in duration, biphasic, charge-balanced and delivered at a rate of 50 Hz. Stimulation amplitudes ranged from threshold (<20 µA) to amplitudes that produced weight-bearing movements (60 to 80 µA) and did not exceed 130 µA through any electrode.

The movements elicited by stimulation through single electrodes were hip flexion, hip extension, knee extension, ankle dorsiflexion, ankle plantarflexion, and a backward extensor synergy, which were combined to construct a full walking cycle. Of the twelve electrodes implanted unilaterally, between 5 and 9 were needed to produce the desired walking movements and included redundancy in the functional targets. A combination of stimulation channels with particular functions were used to construct the four phases of the walking cycle: F (early swing), E1 (late swing to paw-touch), E2 (mid-stance), and E3 (propulsion) (Engberg and Lundberg 1969; Goslow et al. 1973).

4.2.2 Experimental Setup

Following the implantation of the ISMS array, the cats were partially suspended in a sling, supporting the weight of the head, forelimbs, and trunk, allowing the hind-limbs to move freely over a custom-built walkway (Figure4.1). The cats remained anaesthetized for the duration of the experiment. The sling was fixed on a cart that moved with the cat over the walkway. The cart was partially unloaded to offset the weight of the recording and stimulating equipment.

Reflective markers were placed on the iliac crest, hip, knee, ankle, and metatarsophalangeal (MTP) joints of the right hind-limb. Kinematics of this limb were recorded using a camera (120fps, JVC Americas Corp., Wayne, NJ, USA) positioned 4.5 m away from the center of the walkway. Marker positions were tracked using MotionTracker2D, custom Matlab software (MathWorks, Inc., Natick, MA, USA) written by Dr. Douglas Weber (University of Pittsburgh, Pittsburgh, PA, USA).

Gyroscopes were placed on the tarsals of each hind-limb to measure angular velocity. Three-dimensional force plates were mounted underneath the walkway and used to measure vertical ground reaction forces of each limb. The sensor signals were filtered using a hardware Butterworth filter (f_C = 3 Hz, 2nd order) and digitized at 1 kHz using the Grapevine Neural Interface Processor (Ripple, Salt Lake City, UT, USA) and streamed into Matlab during walking.

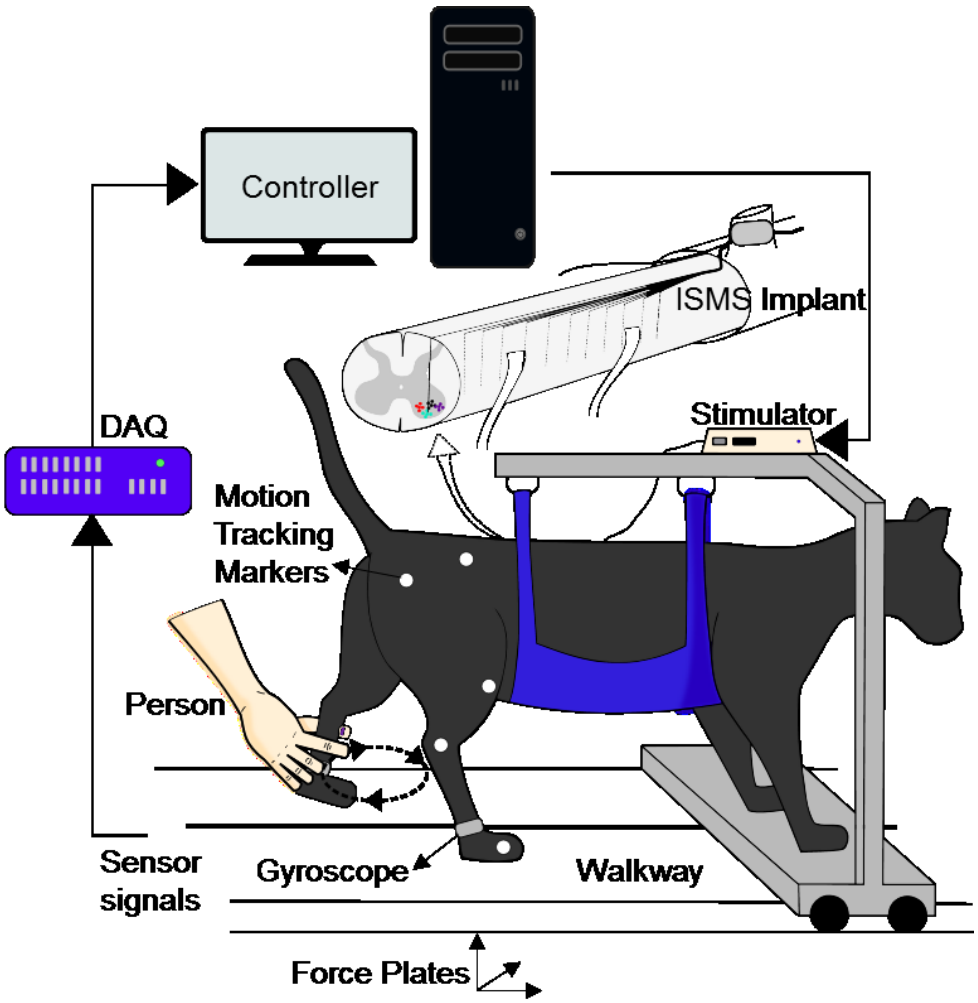

Figure 4.1. Experimental setup for over-ground walking. A person moved one hind-limb through the walking cycle. Sensor signals from force plates under the walkway and a gyroscope on the tarsals from both hind-limbs were converted to digital signals by the DAQ and streamed into Matlab. In Matlab, a custom control algorithm was used to control the stimulation to the spinal cord to move the other hind-limb to the opposite phase of the walking cycle.

4.2.3 Control Strategies

A hemisection SCI was modeled in the anaesthetized cats with an intact spinal cord. A person manually moved one hind-limb through the walking cycle (person-moved limb (PML); to represents the intact leg), while the other limb was moved using ISMS (stimulation-controlled limb (SCL); and represented the paralyzed leg; Figure 4.1). This hemisection SCI model is similar to Brown-Sequard syndrome in humans, where one leg is paralyzed and the other is motor-intact (Kunam et al. 2018).

The walking cycle was divided into 4 phases for finite state control: F, E1, E2, and E3, which corresponded to toe-off to early swing, late swing to paw-touch, paw-touch to mid-stance, and mid-stance to propulsion, respectively (Engberg and Lundberg 1969; Goslow et al. 1973); Figure 4.2a). The goal of the control strategies were to transition the SCL through the walking cycle such that the phase of the SCL was opposite to the phase of the PML. Each control strategy determined when the SCL transitioned from one phase to the next based on sensor information from the PML.

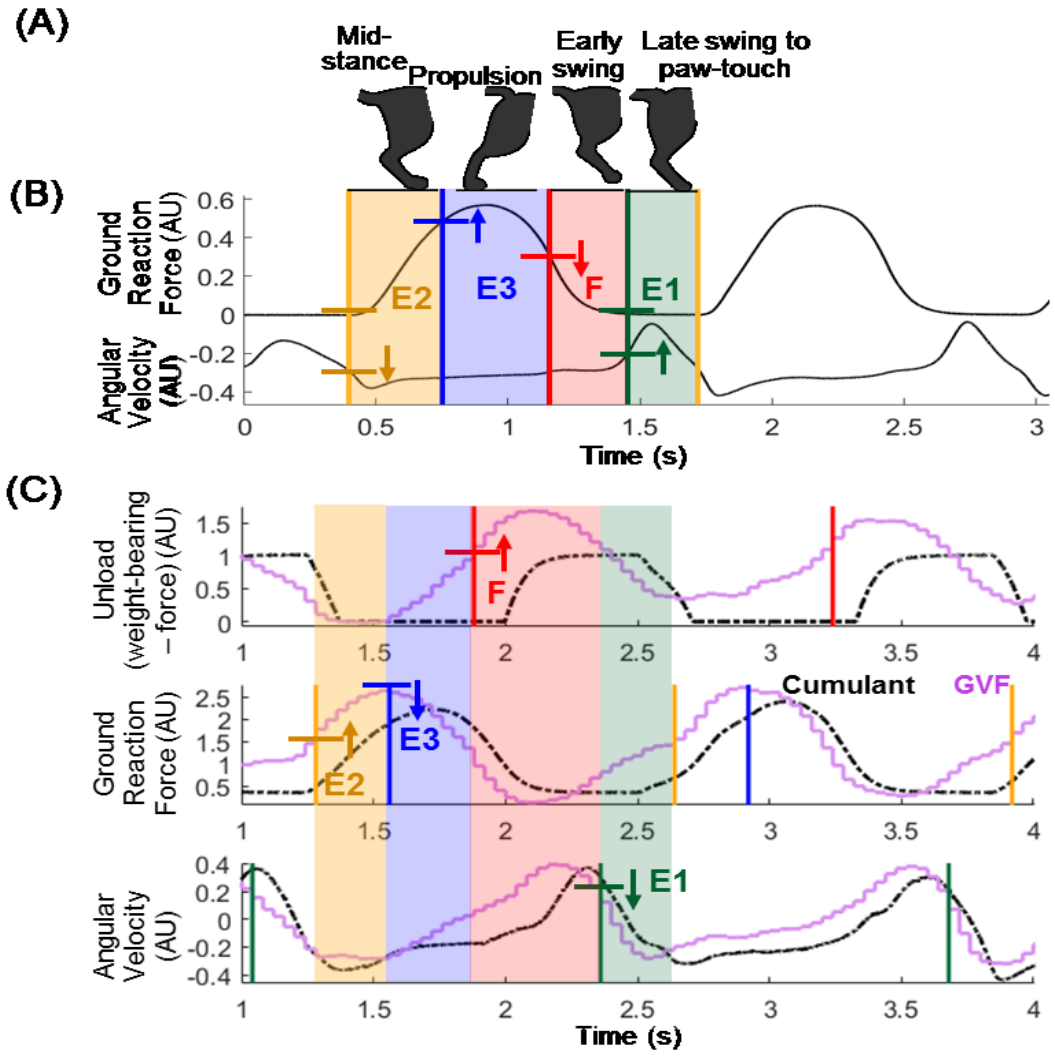

Figure 4.2. Controller decisions. (A) Phases of the walking cycle, lined up with phases marked in (B). (B) Threshold settings for person A on raw data from the PML (person-moved limb). (C) Thresholds on predictions of sensor signals from the PML. AU = arbitrary units. Shaded regions indicate the phase of the walking cycle detected on the PML. Horizontal lines mark the threshold values for corresponding phase. Arrows indicate the direction of the slope of the signal required by the algorithm.

4.2.3.1 Reaction-Based Control Strategy

Reaction-based control entailed placing thresholds on the sensor signals recorded from the PML during walking to trigger transitions between the phases of the walking cycle in the SCL. The transitions were controlled by rules involving: the current phase in the walking cycle, comparing the sensor values with threshold values, and the direction of the slope of the sensor values. The sensor signals used for defining the transitions between phases of the walking cycle were ground reaction force and angular velocity of the PML (Figure 4.2b). The thresholds were placed on the sensor signals such that they anticipated when the transitions would normally occur to account for the electromechanical delay of approximately 200 ms (Dalrymple et al. 2018).

4.2.3.2 Pavlovian Control Strategy

Pavlovian control also used thresholds to transition the SCL from one phase of the walking cycle to the next; however, the thresholds were placed on the output of the GVFs, or learned predictions, of walking-relevant signals of the PML, rather than the raw signal values (Figure 4.2c). The signals of interest were the ground reaction force, angular velocity, and unloading of the PML. Unloading was defined as the weight-bearing threshold (equal to 12.5% of the cat's body weight in this setup (Lau et al. 2007)) minus the ground reaction force. Unloading differs from ground reaction force as it informs when the PML is below or above a weight-bearing threshold. The GVFs were generated using RL and the phase transitions were triggered by the learned predictions crossing a threshold value, initiating a fixed output (i.e. Pavlovian control).

4.2.3.3 State Representation of Sensor Signals

Sensor signals are complex with a wide range of possible values. Learning requires a combination of sensor values to be visited multiple times. With highly sampled, broad ranges of values for multiple sensors, exact duplicates of overlapping sensor values are unlikely to occur, making learning slow. Therefore, it is necessary to generalize the state space of sensor signals by function approximation. This process converts the complex high-dimensional sensor data into a binary vector representation of the state space, named the feature vector, $\mathbf{x}$.

Six sensors were used to form the state space: left ground reaction force, right ground reaction force, the sum of left and right ground reaction forces, left angular velocity, right angular

velocity, and the exponential moving average of the left ground reaction force. The exponential moving average gives a history of the force signal. The values of the sensor signals were first normalized from their usable range to values between 0 and 1. Selective Kanerva coding (Travnik and Pilarski 2017) was used in this work to represent the normalized sensor values as a binary vector.

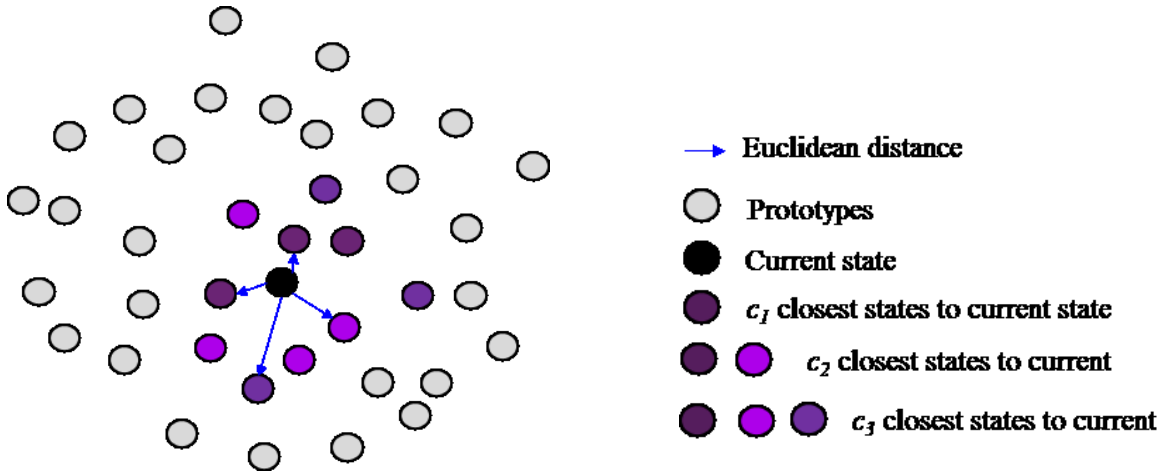

Figure 4.3. A depiction of selective Kanerva coding (SKC). Prototypes closest to the current state within the state space are activated.

Over the entire normalized, 6-dimensional state space (n = 6 sensors), K = 5000 specific states, called prototypes, were randomly distributed and held constant for all experiments (Figure 4.3). Hoare's quickselect was used to find the c closest prototypes to the current state according to their Euclidean distance. Three values of c were used, determined by choosing small ratios, η, such that $c = K\eta$. The c values used were 500, 125, and 25, corresponding to η values of 0.1, 0.025, and 0.005, respectively. Using multiple c values is similar to the use of overlapping tilings in tile coding (Sutton and Barto 2018); it allows for coarse and fine representation of the state in the feature vector. When a combination of sensors values occurred, defining the current state in the state space, the c-closest features were activated (set equal to one) in the feature vector, while the rest were equal to zero. The total number of features was $3K$, of which 650 ($c_1 + c_2 + c_3$) were active at each time. The pseudocode for selective Kanerva coding as used in this work is given in Algorithm 4.1. Bolded variables refer to vectors or matrices. Italicized variables refer to constants with values that pertain to this work.

Algorithm 4.1 Selective Kanerva Coding

Parameters provided: K, n, c_1, c_2, c_3

Initialize prototypes **P** randomly once ever

Input new state **S**

Reset **D** = zeros(K,1)

For i = 1 to K

For j = 1 to n

$\mathbf{D}_i \leftarrow d(\mathbf{P}_{i,j}, \mathbf{S}_j)$ d = Euclidean distance

I ← Quickselect(**D**) indices of sorted distances

For m = 1 to 3

$\mathbf{ind}_m \leftarrow \mathbf{I}(1 \text{ to } c_m)$

$\mathbf{x}_{indm} \leftarrow 1$ offset by (m-1) x K

Output **x**

4.2.3.4 True Online Temporal Difference Learning

In the theoretical forward view of TD(λ), at each time-step the estimate is moved toward a target, called the λ-return (van Seijen and Sutton 2014; Sutton and Barto 2018). The λ-return requires the subsequent cumulant values and expected return. These can only be known at the end of an episode and can only be approximated during online learning. True online temporal difference (TOTD) learning matches the forward view online exactly by adding terms to the eligibility trace and weight update equations (van Seijen and Sutton 2014; van Seijen et al. 2015).

During walking, TOTD was used to estimate future values of three signals recorded from the PML: unloading, ground reaction force, and angular velocity. Specifically, the returns of the cumulants were estimated online by the inner product of the weight vector (updated during TOTD) and the feature vector from function approximation, to produce the GVF for that cumulant (Algorithm 4.2). The learning step-size (α), which constrains the speed of learning by controlling the magnitude of the update was set to 0.001 as determined empirically during bench testing. The bootstrapping parameter for the eligibility trace (λ) was set to 0.9 as is often standard. Different termination signals (γ) for each cumulant were determined empirically, and

were set to 0.9 for unloading, 0.71 for ground reaction force, and 0.75 for the angular velocity. As $\gamma = 1 - \frac{1}{T}$, where T = 40 ms (one time step), these values correspond to timescales of 400 ms, 138 ms, and 160 ms, respectively.

Algorithm 4.2 True Online TD(λ)

initialize $\mathbf{w}$, $\mathbf{e}$, V_{old}, S, $\mathbf{x}$

Repeat every timestep:

Generate next state S' and cumulant Z'

$\mathbf{x}' \leftarrow SKC(S')$

$V \leftarrow \mathbf{w}^T \mathbf{x}$

$V' \leftarrow \mathbf{w}^T \mathbf{x}'$

$\delta \leftarrow Z + \gamma V' - V$

$\mathbf{e} \leftarrow \gamma\lambda\mathbf{e} + \mathbf{x} - \alpha\gamma\lambda(\mathbf{e}^T\mathbf{x})\mathbf{x}$ dutch trace

$\mathbf{w} \leftarrow \mathbf{w} + \alpha(\delta + V - V_{old})\mathbf{e} - \alpha(V - V_{old})\mathbf{x}$

$V_{old} \leftarrow V'$, $\mathbf{x} \leftarrow \mathbf{x}'$

Thresholds that were placed on the GVFs, the direction of the slope of the GVF, and the current phase of the walking cycle of the PML, triggered transitions between the phases of the walking cycle of the SCL to be in the opposite state of the PML (Figure 4.2c). These thresholds were chosen based on the past experience of the designer to mark the best transition points to achieve alternation. The prediction of a sensor value produced a fixed stimulation response (as the stimulation parameters did not vary during walking), thus utilizing Pavlovian control to produce over-ground walking. The phase transitions were triggered by the raw sensor values crossing a threshold (US) if the predicted value (CS) did not elicit a response. These are referred to as back-up reactions. The thresholds for the back-up reactions were held constant throughout all walking trials.

4.2.4 Experimental Protocol

A walking trial consisted of one trip across the walkway (~ 3 m). An experimenter manually moved the PML through the walking cycle and the SCL pushed the cat and cart across the

walkway. Up to four different people moved the limb through the walking cycle in each experiment. The control method (reaction-based or Pavlovian) used for each walking trial was determined randomly by a different person than the one walking the PML, or by a random number generator. The person moving the limb was blinded to the control method driving ISMS for each trial. For some trials, experimenters were told to purposefully make a mistake during walking. A mistake was never defined and was left to the discretion of the person. Mistakes that were purposefully made included elongating the stance or the swing phases, shaking the limb in the air, or slipping forward or backward.

4.2.4.1 Reaction-Based Control Trials

Phase transition thresholds were acquired for each individual based on sensor values they produced during 2 consecutive walking trials. The person-specific thresholds remained constant throughout all cat experiments. Each person performed walking trials using the customized thresholds from the three other people in addition to trials with their own thresholds.

4.2.4.2 Pavlovian Control Trials

Several different trial types were run to investigate early learning, continued learning, and how the learning adapted or recovered after changes in cat experiments and people walking the PML. Early learning was evaluated by initializing the learning weights, eligibility trace, and GVFs to zero at the beginning of a walking trial. In these trials, learning began anew with no prior knowledge. These early learning trials were repeated in every cat experiment with different people walking the PML. Learning was also continued across several walking trials in each cat experiment. Throughout these trials within the experiment, multiple people took turns to walk the PML through the walking cycle. Furthermore, the carry-over of learning from one cat experiment to the next was tested over 5 cats. Repeating these carry-over trials in a new cat experiment allowed repeated investigation of the transfer of learning between experiments with different cats and people walking the PML. There was also a set of trials where learning continued throughout all 5 cat experiments, where multiple people took turns to walk the PML within each experiment. These trials investigated the long-term learning and the adaptation to changes in cats and people walking the PML.

4.2.5 Statistics

A one-sample t-test was used to compare the alternation phase differences with the target of 180°. A p-value $\leqslant 0.05$ was used to indicate significance. Cohen's d was used to determine the effect size.

A $\mathbf{X}^2$ test was used to compare the proportion of GVF-triggered phase transitions between different Pavlovian control walking trial types (early, within one cat, carry-over, and continued), as well as for comparing the proportion of missed steps across control methods. Cross-tabulations were generated for all pair-wise combinations. $\mathbf{X}^2$ with the continuity correction was reported for 2 × 2 contingency tables, with the α-level adjusted using the modified Bonferroni correction for multiple comparisons.

4.3 Results

A total of 7943 steps from 770 trials were recorded from 8 cats. On average, the step period was 1.32 s (SD = 0.26 s) and ranged from 0.44 s to 2.82 s.

4.3.1 Walking with Reaction-Based Control

Reaction-based control was tested in all eight cats, resulting in 264 walking trials. Figure 4.4a shows an example of the variation in force production and angular velocity across the 4 people during a walking trial. Because thresholds on these 2 sensor signals were used to transition the SCL through the walking cycle, the dissimilarity in these sensor values during walking necessitated individualized thresholds. Each individual's thresholds were used during walking trials for all other individuals to test the translatability of the thresholds. Table 4.1 outlines the percentage of steps that failed to transition due to inappropriate thresholds for each combination of threshold settings and person walking the PML. For each threshold setting more than 40% of the steps failed when another person walked the PML. In total, 18.7% (680/3645) of the total number of steps in all walking trials under rule-based control were missed due to the inability of the sensor values to cross thresholds.

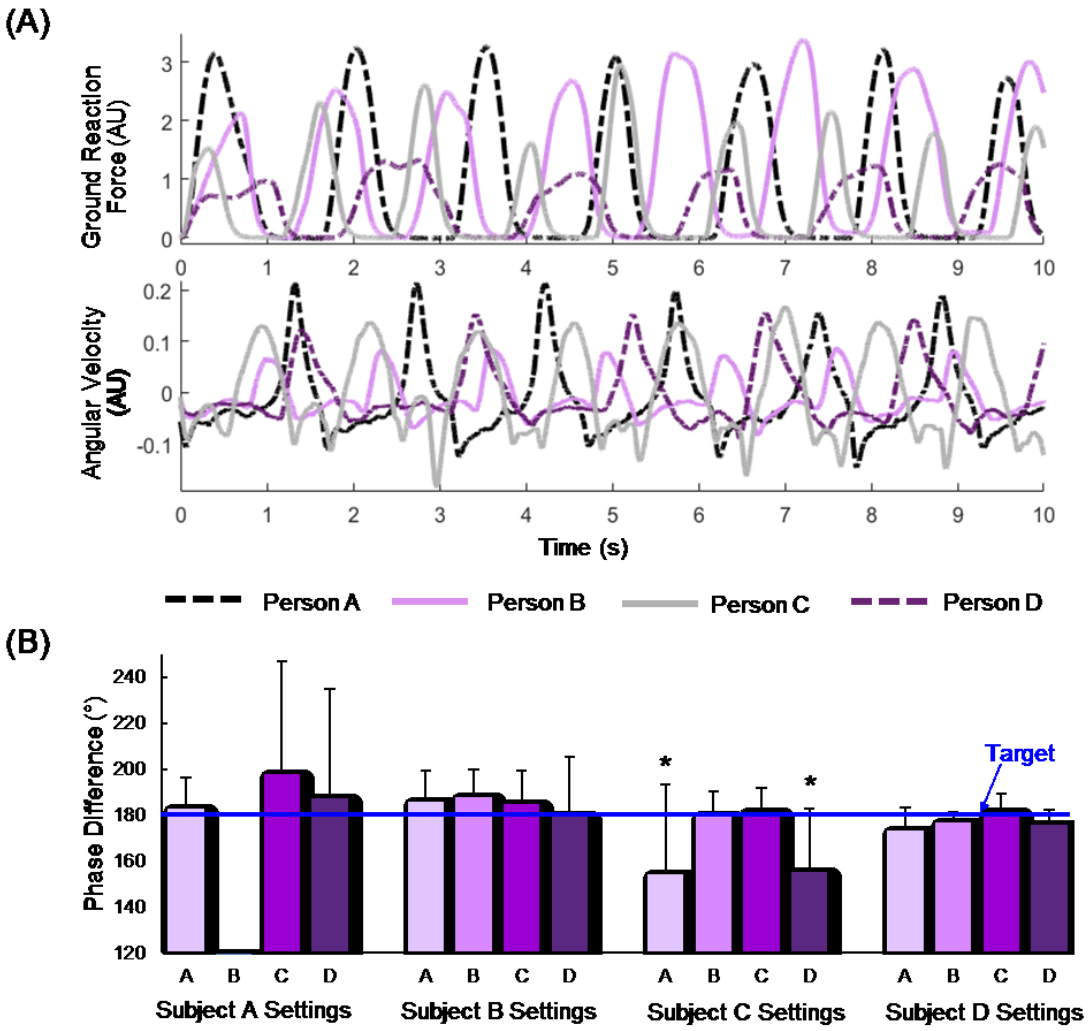

Figure 4.4. Walking using reaction-based control (n = 264 trials). (A) Ground reaction forces and angular velocities produced by each of the 4 people walking the PML (person-moved limb). (B) Alternation phase differences of the hind-limbs for each person walking the PML with threshold settings tuned for each person. * $p < 0.0001$.

The phase difference between the PML and SCL was calculated based on previously defined methods (Dalrymple et al 2018). Briefly, the time spent loading in the two limbs was converted to a circle for each step in which alternation results in a phase difference of 180°. Figure 4.4b displays the phase differences for each combination of threshold settings and person walking the PML. Most trials had sufficient alternation despite missing many steps. Interestingly, for trials with settings for person C where persons A and D walked the PML had the fewest percentage of missed steps, walking had the worst alternation. This is because A and D made larger movements with larger sensor values than required for the settings tuned for person C, triggering

phase transitions between the phases of the gait cycle earlier than required to produce alternating walking. This produced a phase difference significantly less than 180° with very large effect sizes (phase difference for A = 155.0°; phase difference for D = 155.9°; $p < 0.0001$; df = 173, 46; one-sample t-test; Cohen's d = 0.64, 1.97).

Missed Steps (%)

Settings	Walking Limb A	Walking Limb B	Walking Limb C	Walking Limb D
A	11.0%	100%	94.0%	54.8%
B	7.1%	10.4%	46.6%	12.5%
C	5.9%	44.1%	12.0%	6.0%
D	12.4%	12.8%	42.0%	11.5%

Table 4.1. Proportion of missed steps for combinations of people walking the PML using customized threshold settings for each person.

4.3.2 Walking with Pavlovian Control

Of the eight cat experiments conducted in this study, the first 3 had one set of thresholds on the GVFs, while the remaining 5 had a different set of thresholds. The learning parameters and methods remained constant throughout the study.

4.3.2.1 Thresholds on predictions are important for Pavlovian control

The initial thresholds for Pavlovian control were chosen based on testing on previously collected data from treadmill stepping (Dalrymple et al 2018) and bench testing on the walkway without a cat. These thresholds were tested in the first three cat experiments, resulting in 1384 steps from 184 trials. Pavlovian control trials in these experiments included early learning where the weights, eligibility trace, and GVFs were initialized to zero, as well as trials that had learning continue throughout each individual cat. The phase difference achieved with these thresholds was 186.3° (SD = 18.5°). In early learning trials, 50.4% of the steps included at least one back-up reaction for a phase transition, with 16 steps (2.3%) failing to walk. In trials where learning continued within each cat experiment, 60.6% of steps included a back-up reaction for a phase

transition and 11 steps failed to walk (1.6%). Of the steps with phase transitions initiated by a back-up reaction, 83.8% were for the phase E2, or mid-stance. Therefore, for the following experiments the thresholds for E2 were placed on the ground reaction force, rather than on the prediction of limb unloading. Additionally, the thresholds for phases F and E1 were shifted to occur earlier on the GVFs for unloading and angular velocity, respectively. These revised thresholds remained constant throughout the following 5 experiments. The back-up reaction thresholds were unchanged.

4.3.2.2 Learning to predict sensor signals occurs quickly to produce over-ground walking

Early learning trials with the improved thresholds, where the weights, eligibility trace, and GVFs were initialized to zero at the beginning of the trial, were repeated for 5 cat experiments with all 4 people moving the PML to produce over-ground walking via Pavlovian control. Figure 4.5a-c displays the cumulants and the GVFs during walking, along with the alternating ground reaction forces and movements produced by the SCL. Early learning trials had an average phase difference of 181.9° which was significantly different from 180° but with a very small effect size (SD = 7.8°; $p = 0.027$; $df = 87$; one-sample t-test; Cohen's $d = 0.24$; Figure 4.5d). Back-up reactions for phase transitions most commonly occurred within the first step compared to later steps (Table 4.2), indicating that learning the predicted signals occurred quickly to initiate phase transitions. Within a maximum of 4 steps, predictions became the only signals that initiated phase transitions. Throughout all 1036 steps in the early learning trials, 3 failed to transition through the walking cycle. In 87.2% of the steps taken, the phase transitions were initiated by the GVFs crossing the thresholds (Figure 4.5e). Person B had the highest proportion of GVF-triggered transitions (92.0%), whereas person D had the lowest proportion of GVF-triggered transitions (72.5%).

For each early learning trial, the ideal return, which is the actual discounted sum of future values of the cumulant, was calculated post-hoc. The estimated return (GVF), computed online, was compared to the ideal return by calculating the mean squared error for each of the three signals of interest (Figure 4.6a-c). This figure depicts the average mean squared error over all 88 early learning trials. The fluctuation in the first 2 seconds is due to the person walking the PML starting in swing for some trials and starting in stance for others. Figure 4.6d shows an example

of the raw signals along with the ideal and estimated returns. The ideal and estimated returns overlapped quite well during walking, and improved over time, as demonstrated by the reduction in the mean squared error over time.

	Reactions in Early Learning Trials			
	1 Step	2 Steps	3 Steps	More
A	92.3%	3.8%	3.8%	0.0%
B	97.1%	2.9%	0.0%	0.0%
C	69.6%	8.7%	17.4%	4.3%
D	20.0%	0.0%	40.0%	40.0%
All	84.1%	4.5%	8.0%	3.4%

Table 4.2. Back-up reactions in early learning trials. Within how many steps at the beginning of a walking trials was a back-up reaction triggered broken down by person walking the PML.

4.3.2.3 Learning that continued within a cat experiment produced better Pavlovian control

The number of walking trials in which learning continued within a single cat experiment ranged from 7 (cat 7) to 40 (cat 4) trials, for a total of 99 trials and 1180 steps across 5 cats. The raw and predicted cumulants are shown in figure 4.7a. The GVFs became smoother and more regular with time, showing a rising and falling prior to the rising and falling of the raw signal. Indeed, the proportion of steps with phase transitions triggered by only GVFs crossing thresholds was significantly higher than the proportion of steps that transitioned due to a back-up reaction when compared to early learning trials (percent of GVF-triggered steps = 94.6%; $p < 0.0001$, $\mathbf{X}^2$ test). Person B had the highest proportion of GVF-triggered transitions (98.3%); while person D had the lowest proportion (89.4%). No steps were missed during these walking trials. The phase difference achieved in these trials was 181.1° and was not significantly different from the target of 180° (SD = 5.9°; $p = 0.077$; df = 98; one-sample t-test; Figure 4.7d).

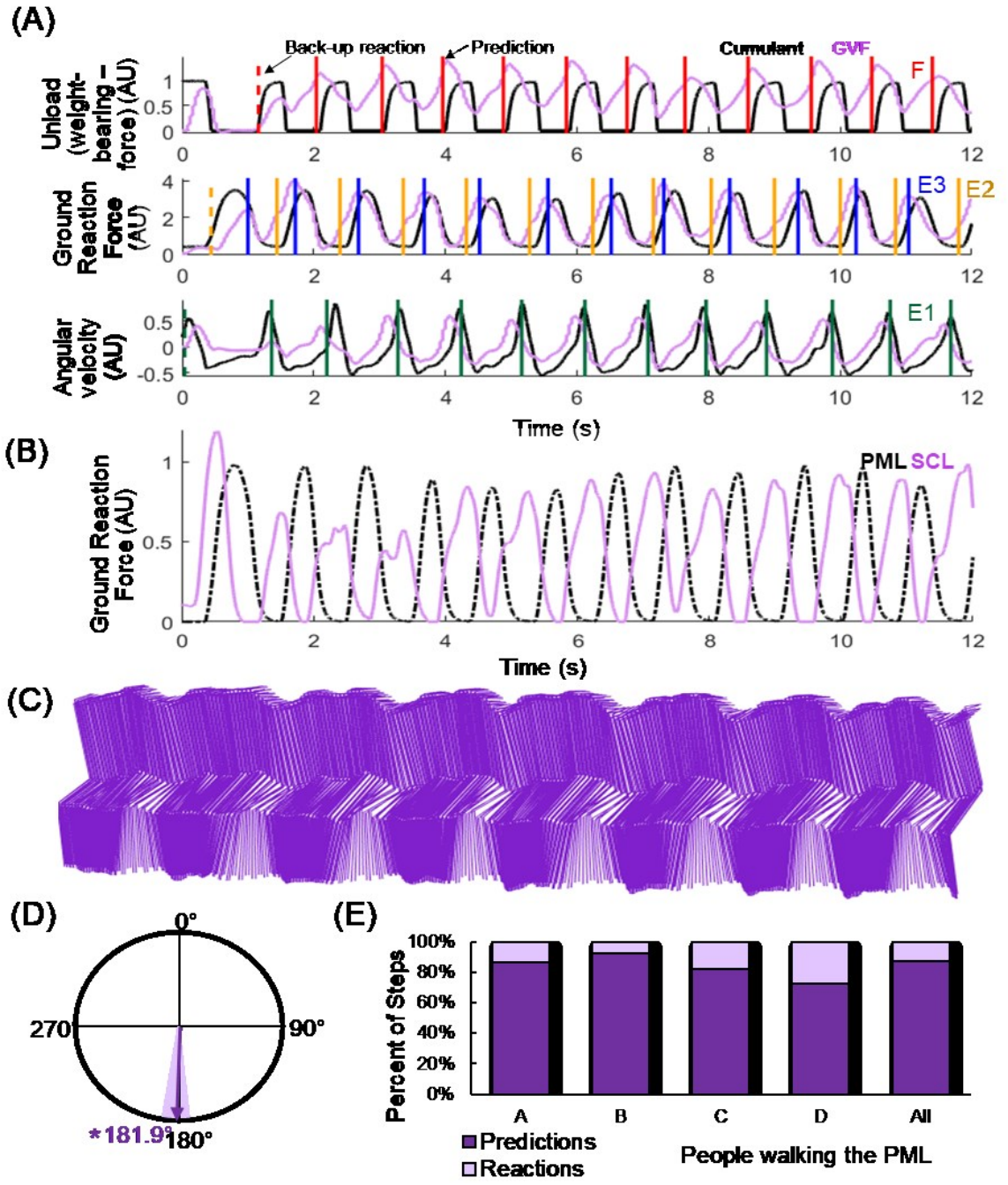

Figure 4.5. Walking during early learning using Pavlovian control (n = 88 trials). (A) Cumulants for unloading, ground reaction force, and angular velocity of the PML (person-moved limb) and their corresponding GVFs (general value functions, predicted using reinforcement learning). Back-up reactions indicated by vertical dashed lines; prediction-initiated transitions indicated by solid vertical lines. (B) Ground reaction forces produced by the PML (dashed trace) and SCL (stimulation-controlled limb; solid trace). (C) Stick figure of SCL. (D) Proportion of steps with phase transitions initiated by the predicted GVFs crossing the threshold or by the back-up reaction for all people walking the PML. (E) Average (arrow) and standard deviation (shaded) of the alternation phase difference of the hind-limbs. * $p = 0.027$.

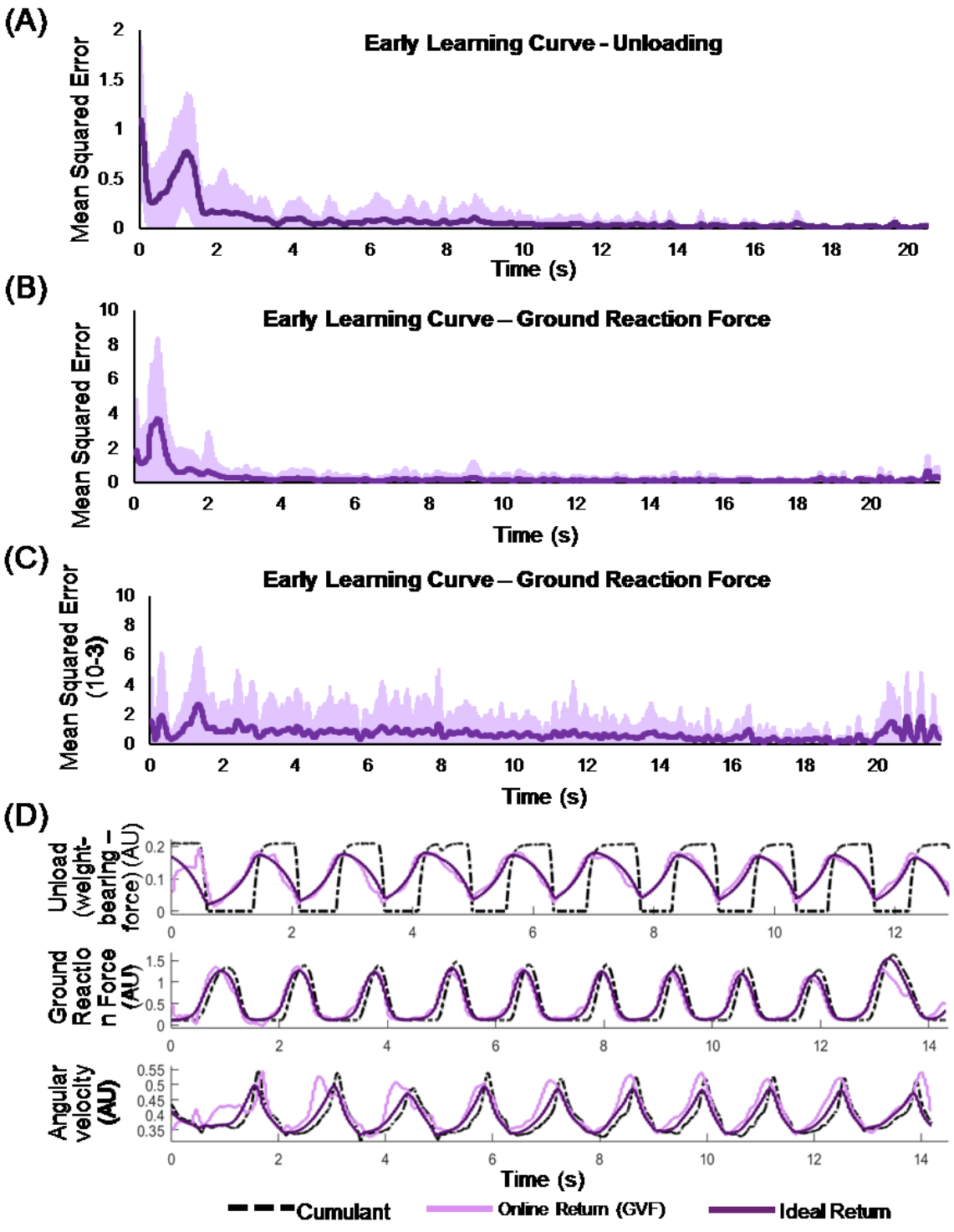

Figure 4.6. Characterizing speed of early learning (n = 88 trials). (A) Learning curve depicting the average (solid line) and standard deviation (shaded region) of the mean squared error of the unloading signal over time. (B) Learning curve for ground reaction force. (C) Learning curve for angular velocity. (D) Example of the actual cumulant signals, online estimated return (GVF), and the ideal return (actual discounted sum of future values of the cumulant).

4.3.2.4 Learning continued to initiate prediction-based Pavlovian control at the transition between cat experiments

For cat experiments 4 through 8, the carry-over of learning from one experiment to the next was repeated, resulting in 61 walking trials and 758 steps. Upon the transition between cat experiments, 83.3% of trials did not have a back-up reaction, and 10.0% of trials had a back-up reaction in the first step. This demonstrates fast adaptation to the new environment and was repeated several times for each carry-over between experiments as well as between different people walking the PML. Across all people who walked the PML, more than 91% of the steps were carried-over using the GVFs for all cats, with no missed steps. The steps in these walking trials were alternating, with an average phase difference of 179.1°, which was significantly different from 180° but with a small effect size (SD = 3.2°; $p = 0.026$; $df = 60$; one-sample t-test; Cohen's $d = 0.29$; Figure 4.8). Moreover, the phase difference did not significantly differ from 180° in each carry-over according to the cat ($p = 0.075$; one-sample t-test).

4.3.2.5 Learning continued across several cats and people to produce over-ground walking

One stream of trials continued to learn throughout cat experiments 4 through 8, with all 4 people taking turns walking the PML throughout. The stream of continued learning included 1394 steps in 115 walking trials. On average, these continuing walking trials had a phase difference of 180.8°, which was not significantly different from the target of 180° (SD = 5.5°; $p = 0.113$; $df = 114$; one-sample t-test; Figure 4.9b). The learned GVFs triggered phase transitions in more than 91% of the steps taken for all people walking the PML, with up to 98.7% of steps for person B (Figure 4.9c).

4.3.2.6 Pavlovian control recovered from mistakes

Varying types of mistakes were made by the people walking the PML throughout various stages of learning in the final 5 cat experiments. An example of the cumulants and GVFs during a trial with a mistake are shown in figure 4.10, as well as the ground reaction forces of the limbs. The GVFs displayed adaptation to the new and unexpected values of the cumulants when the repeated movements of walking ceased. Furthermore, the GVFs for all cumulants changed when the person picked up the limb, causing a change in the angular velocity, which occurred at

around 7 seconds in the trial. Following a mistake, 94.4% (51/54) of the steps that followed had phase transitions triggered by the predicted return (Figure 4.10c).

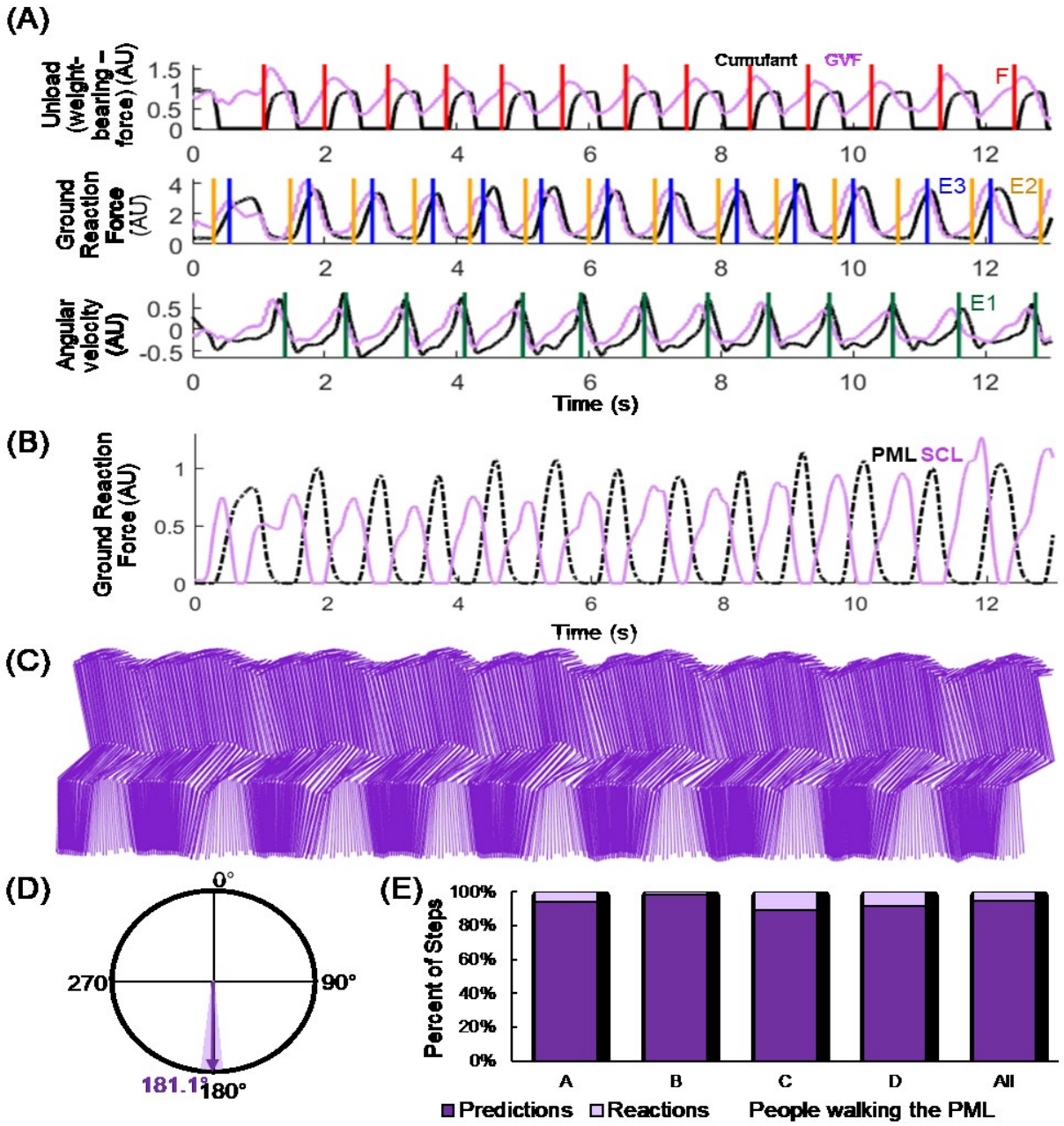

Figure 4.7. Walking with continued learning within a cat (n = 99 trials). (A) Cumulants for unloading, ground reaction force, and angular velocity of the PML (person-moved limb) and their corresponding GVFs (general value functions, predicted using reinforcement learning). Prediction-initiated transitions are indicated by solid vertical lines. (B) Ground reaction forces produced by the PML (dashed trace) and SCL (stimulation-controlled limb; solid trace). (C) Stick figure of SCL. (D) Proportion of steps with phase transitions initiated by the predicted GVFs crossing the threshold or by the back-up reaction for all people walking the PML. (E) Average (arrow) and standard deviation (shaded) of the alternation phase difference of the hind-limbs.

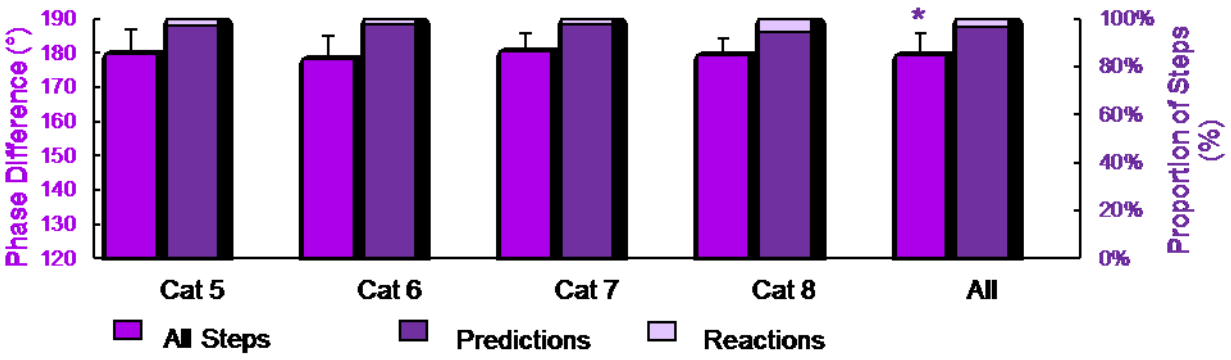

Figure 4.8. Walking produced by Pavlovian control using carry-over learning between cats (n = 61 trials). The phase difference of the hind-limbs is indicated by the left axis. The proportion of steps with phase transitions initiated by the predicted GVFs crossing the threshold or by the back-up reaction for each cat and overall. * p = 0.026.

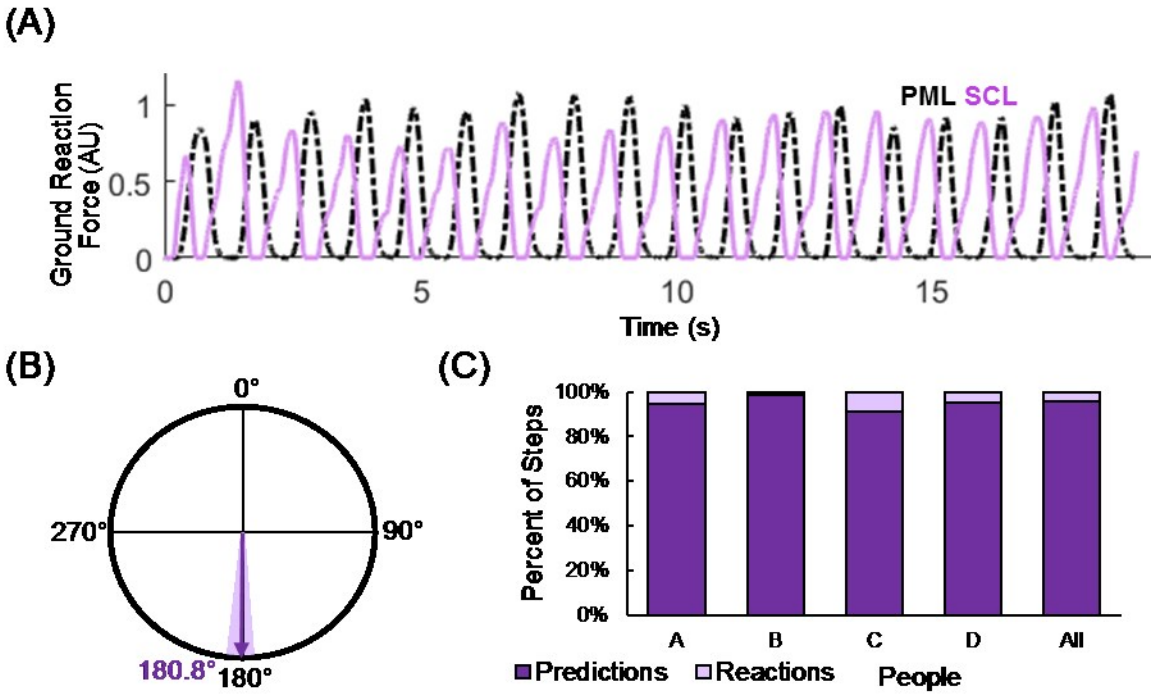

Figure 4.9. Summary of walking produced by Pavlovian control across 5 cat experiments and 4 people walking the PML (person-moved limb) (n = 115 trials). (A) Ground reaction forces produced by the PML (dashed trace) and SCL (stimulation-controlled limb; solid trace). (B) Proportion of steps with phase transitions initiated by the predicted GVFs (general value functions, predicted using reinforcement learning) crossing the threshold or by the back-up reaction for all people walking the PML. (C) Average (arrow) and standard deviation (shaded) of the alternation phase difference of the hind-limbs.

4.3.2.7 Pavlovian control successfully produced alternating, over-ground walking that acclimated to different people walking

Pavlovian control produced alternating, over-ground walking with very few errors. Three steps were missed during Pavlovian control with the optimized thresholds, all of which were limited to early learning trials. This is a significant reduction from trials using Pavlovian control with the initial thresholds ($p < 0.0001$; $\mathbf{X}^2$ test) and trials with reaction-based control ($p < 0.0001$; $\mathbf{X}^2$ test; Figure 4.11a). Furthermore, these trials were alternating, with a phase difference of the limbs equal to 180.4° (SD = 5.7°; $p = 0.272$; one-sample t-test; Figure 4.11a). As learning continued throughout the walking trials, the proportion of prediction-triggered transitions between the phases of the gait cycle significantly increased from the early learning trials ($p < 0.0001$; $\mathbf{X}^2$ test; Figure 4.11b).

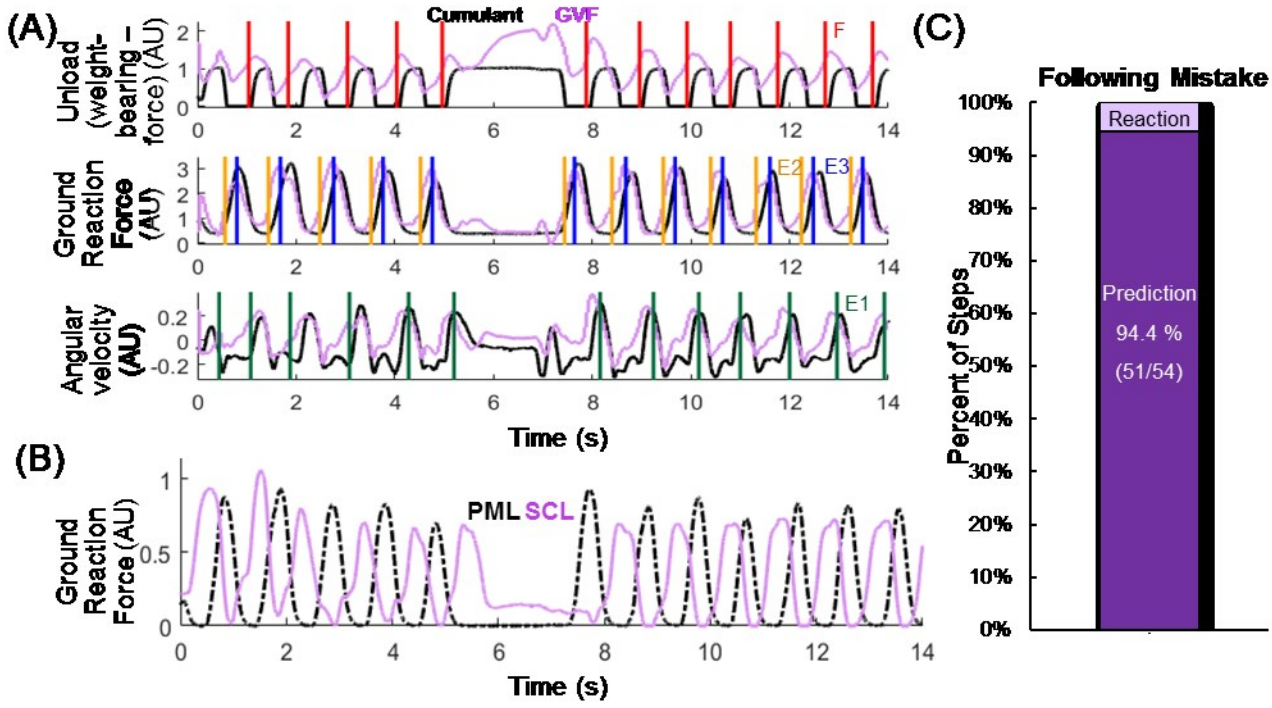

Figure 4.10. Example of a purposeful mistake (n = 54 steps). (A) Cumulants for unloading, ground reaction force, and angular velocity of the PML (person-moved limb) and their corresponding GVFs (general value functions, predicted using reinforcement learning). Prediction-initiated transitions are indicated by solid vertical lines. The mistake begins at approximately 5 s and ends near 7.5 s. (B) Ground reaction forces produced by the PML (dashed trace) and SCL (stimulation-controlled limb; solid trace). (C) Proportion of steps with phase transitions initiated by the predicted GVFs crossing the threshold or by the back-up reaction following a mistake.

As different people took turns to move the PML through the walking cycle (Figure 4.11c), TOTD quickly acclimated to the new person and their preferred style of walking. Of the 84 transition points between people, 64 of them did not require a back-up reaction to transition the SCL through the walking cycle. Only 5 trials required more than 1 step to adjust to the new person walking the PML until only GVF-triggered transitions occurred (Figure 4.11d).

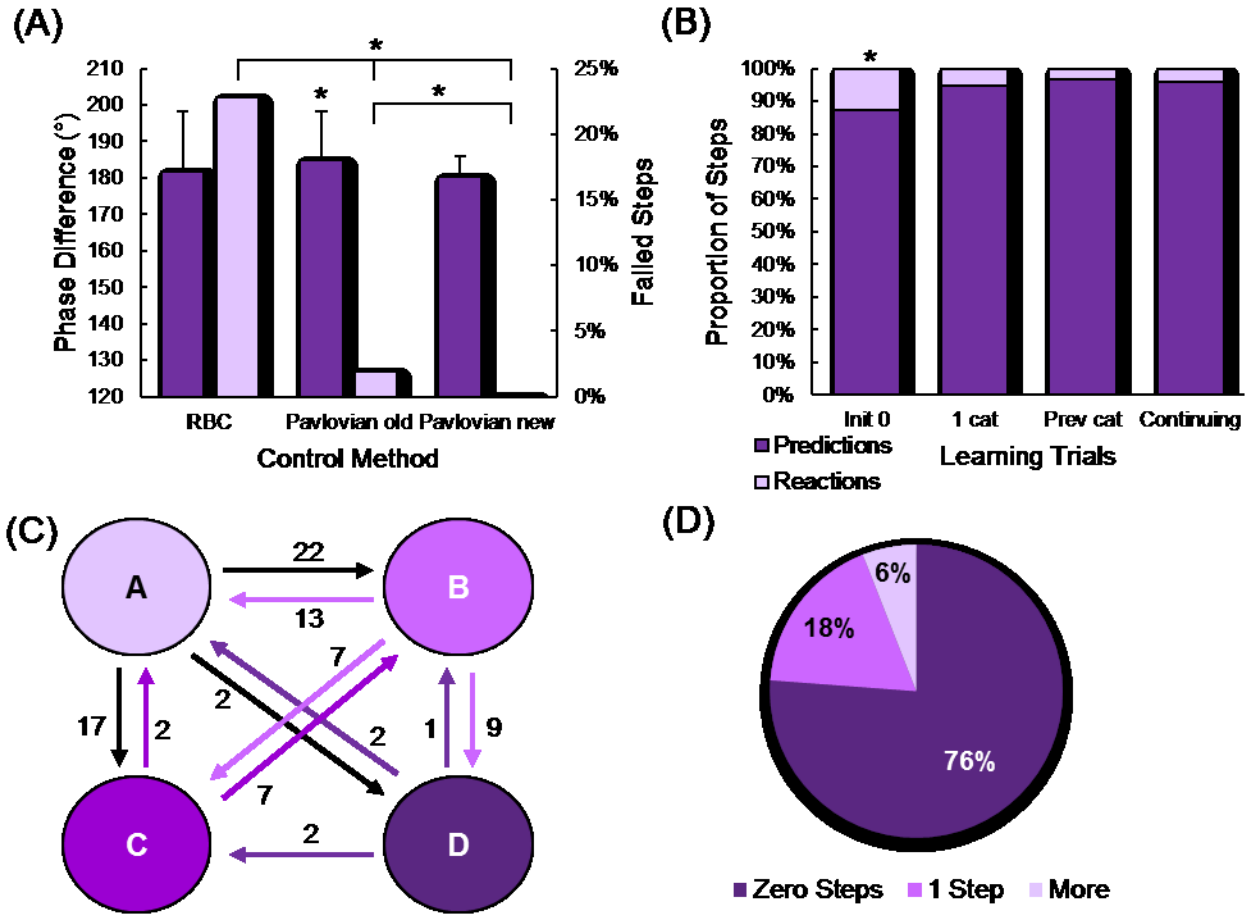

Figure 4.11. Comparison of outcomes using reaction-based and Pavlovian control strategies. (A) Phase difference of the hind-limbs and the number of failed steps for each control method: reaction-based control (RBC), Pavlovian control with the initial thresholds (cats 1-3), and Pavlovian control with the improved threshold selection (cats 4-8). (B) Proportion of steps with phase transitions initiated by the predicted GVFs (general value functions, predicted using reinforcement learning) crossing the threshold or by the back-up reaction at various stages of learning. (C) Direction and number of transitions between each of the 4 people walking the PML (person-moved limb). (D) Number of steps with a back-up reaction following a transition to a new person walking the PML. * $p < 0.0001$.

4.4 Discussion

The goal of this study was to produce, for the first time, predictive, versatile, alternating, over-ground walking in a model of hemisection SCI using ISMS. We used machine learning to take advantage of "residual function" and restore over-ground walking in anaesthetized cats. Reinforcement learning was used to learn predictions of walking-relevant sensor values, and Pavlovian control used the predicted sensor values. Threshold crossings on these predictions were used to control ISMS such that the "affected limb" is moved to the opposite phase of the walking cycle as the "unaffected limb" in the walking cycle. We demonstrated that Pavlovian control can be used across different people walking the "unaffected limb" and throughout different cat experiments without requiring adjustments to the threshold settings. Learning occurred very quickly and consistently produced prediction-driven transitions between the phases of the gait cycle. Pavlovian control was able to recover from intentional mistakes imposed during walking of the "unaffected limb", continuing with prediction-driven transitions between the phases of the gait cycle following the mistake. Personalized walking was possible for the first time because reinforcement learning acclimated to different people moving the "unaffected limb" and different and cats. This comes in contrast to other approaches where the pattern of walking by the user is dictated by the control algorithm.

4.4.1 Learning Methods

This study used TOTD to learn GVFs for three cumulants during walking that were used for Pavlovian control. When a GVF crossed a pre-defined threshold, a stimulation response was delivered to move the SCL to the opposite phase of the walking cycle as the PML. The selective Kanerva function approximation method, predictions using GVFs, learning through TOTD, and Pavlovian control are relatively recent advancements made in the field of computing science (Travnik and Pilarski 2017; Sutton et al. 2011; van Seijen et al. 2015; Modayil and Sutton 2014). Selective Kanerva coding was chosen as it has proven to perform well online with a large number of sensors (Travnik and Pilarski 2017). It is also simple to implement and conceptualize. GVFs have proven to be a valuable tool in RL. GVFs allow the prediction of arbitrary signals, which makes RL more powerful and applicable to more problems. In the field of rehabilitation, TD(λ) has been used to produce GVFs for upper-limb prostheses (Pilarski et al. 2012; Pilarski et al. 2013a; 2013b; Sherstan and Pilarski 2014; Edwards et al. 2016). TOTD offers an equivalence

to the theoretical forward view of TD learning with negligible increase in computational cost (van Seijen et al. 2015) and has been used to predict the shoulder angle of an upper-limb prosthesis (Travnik and Pilarski 2017). Pavlovian control has successively been used to control switching events of an upper-limb prosthesis in able-bodied study participants (Edwards et al. 2013) and participants with an amputations (Edwards et al. 2016). It has also been used to control the turning off and spinning of a mobile robot (Modayil and Sutton 2014).

Pavlovian control is an appropriate approach to restoring walking in a SCI model because learning the GVFs can occur very rapidly. Since the control strategy only requires the prediction to cross a threshold, online control can be initiated quickly. The learned predictions do not fluctuate nor are largely affected by sudden changes in the raw data, making them more reliable for placing thresholds on for control than the raw signals. Additionally, Pavlovian control does not require exploration of the state space, which is necessary in traditional RL control methods. This is beneficial during walking because exploration of the state space could pose a danger to the user. For example, exploration may produce unsafe movement combinations such as double limb unloading. The state space could be restricted to avoid these dangerous situations, but this would limit the capacity of RL and negate its usefulness. Therefore, Pavlovian control, which uses predictions to drive a fixed stimulation response, is suitable for a repetitive task such as walking.

Pavlovian control also allows for the knowledge of the expert designer to be incorporated into the rules that define the uses of the predictions and the output. This study, for the first time, combined all of these methods and used them to control a neural interface to produce over-ground walking *in vivo*.

4.4.2 Biological Parallels

Making predictions during a functional task is very useful and is commonly done naturally. For example, during walking, the central nervous system is continuously integrating sensory input from cutaneous receptors on the feet, stretch and loading sensors in the muscles and tendons, as well as visual and vestibular information to maneuver through the environment effectively and safely (Zehr et al. 1997; Zehr and Stein 1999; Donelan and Pearson 2004; Marigold 2008;

Mathews et al. 2017). These sensory streams can be used to form short-term predictions that can be used in turn to adapt the gait pattern. Unexpected sensory stimuli result in reflexive changes, and with repetition, adaptation to the sensory stimuli occurs. For example, if an obstacle is placed in front of a cat's hindlimb during the swing phase causing activation of cutaneous receptors on the dorsum of the paw, the knee will flex further to clear the obstacle (McVea and Pearson 2007). This is a reflexive, or automatic response to the sensory stimulus, which is mediated by the spinal cord. If the obstacle is present for 20 stimuli, the foot will lift higher during swing in anticipation of the obstacle. These effects last over 24 hours in some cases. This long-term adaptation of the gait pattern may be mediated by the cerebellum (Xu et al. 2006). Although this is not exactly an example of Pavlovian control, it demonstrates the usefulness of predictions and how they can be utilized by the nervous system.

Pavlovian control is modelled after classical conditioning. An earlier example described Pavlov's experiments in dogs where the dogs would salivate when a bell is rung because the ringing became associated with the presentation of food (Pavlov 1883). Another example of classical conditioning is the eye-blink reflex, which has been characterized extensively in rabbits (Kehoe and Macrae 2002; Lepora et al. 2007). In response to a noxious stimulus, such as a puff of air (US), the eye blinks (R). If the puff of air is preceded by a tone (CS), the rabbit blinks just prior to the arrival of the air, protecting the eye. This work is somewhat different from these examples of Pavlovian control because natural movements of one limb do not always dictate the movements of the other limb. However, this concept has similarities to the half-center concept from central pattern generators (Brown 1914). The half-center model of the central pattern generator proposed that the left and right limbs mutually inhibit each other such that when one limb is in flexion, the other must be in extension, and vice versa. The current work incorporated concepts from classical conditioning by also utilizing the sensor information for back-up reactions in the event that the prediction did not reach the threshold in time.

4.4.3 Relation to Other Control Strategies

Once the thresholds for Pavlovian control were modified after the initial cat experiments, they did not require further modification. Pavlovian control performed significantly better than

reaction-based control, providing fewer missed steps and requiring no tuning between transitions different people walking the PML or different cats.

Both the Pavlovian and reaction-based controllers were finite state controllers, which is a concept that has been used previously to produce walking in models of SCI. Finite state control has the advantage of incorporating expert knowledge in a straight-forward manner to define the rules for walking (Popović 1993; Sweeney et al. 2000). Finite state control of surface (Andrews et al. 1988) and intramuscular (Guevremont et al. 2007) FES of the leg muscles used information from ground reaction forces and hip angle to control the transition between the phases of the gait cycle. Previous controllers for ISMS in a model of complete SCI used ground reaction forces and hip angle (Saigal et al. 2004; Holinski et al. 2011; Holinski et al. 2016) or recordings from the dorsal root ganglia (Holinski et al. 2013) to transition the hind-limbs through the different phases (Dalrymple and Mushahwar 2017). Control of epidural stimulation of the spinal cord also utilized electroencephalography recordings from the motor cortex to deliver regional stimulation to the spinal cord to assist with flexion and extension movements in hemisected monkeys (Capogrosso et al. 2016) and people with incomplete SCI (Wagner et al. 2018).

The current study demonstrated that predictions can be learned to initiate transitions between the phases of the gait cycle using only two sensor signals: ground reaction force and angular velocity. These sensors can easily be integrated into a wearable system, as gyroscopes are small microchips and force sensitive resistors can be placed in the soles of shoes (Kirkwood et al. 1989; Kostov et al. 1992). Recent work has demonstrated that kinematic data can be used to identify the phases of the gait cycle during walking (Drnach et al. 2018). They used switched linear dynamical systems (SLDS) to model the joint angle kinematics in healthy people walking on a treadmill. The offline SLDS models were able to label the correct phase of the gait cycle with 84% precision. Future work may incorporate more portable sensors such as goniometers along with online models to build predictions of gait phases.

4.4.4 Experimental Limitations

A limitation of these experiments is that they were performed in anaesthetized cats with an intact spinal cord. This necessitated voluntary control of one hind-limb to be mimicked by a person moving the limb through the walking cycle. This was the first testing of these control strategies,

and the outcomes served as a proof-of-concept implementation. Further work may test these control strategies in chronically injured cats, either decerebrate or awake.
A hemisection SCI has more stereotypic functional deficits compared to other injuries such as bilateral contusion SCIs. Although these SCIs are rare, e.g., Brown-Sequard syndrome (Roth et al. 1991; Wirz et al. 2010), the control strategies may be extended to hemiplegia in general, which includes stroke and traumatic brain injury.

The thresholds for Pavlovian control did not require tuning for different people and cats, because the learned predictions acclimated to the changes. However, it may be beneficial to introduce adaptive thresholds in the future, especially if these strategies were to be employed in more variable injury models. Furthermore, the stimulation amplitudes and channels that produced the functional responses remained constant during a walking trial. Future work may introduce a learning strategy that aims to optimize and adapt the stimulation channels and amplitudes in addition to a strategy that controls the timing.

4.4.5 Conclusions

Pavlovian control of walking augmented function in a hemisection SCI model. Using predictions of sensor signals during walking, Pavlovian control was resilient to transitions between people walking the limb, between cat experiments, and recovered from mistakes made during walking. Pavlovian control of ISMS has the potential to enhance ambulation capacity greatly, generating alternating, over-ground walking with step periods ranging from 0.44 s to 2.82 s (average 1.32 s). This control strategy can also be extended to other injury models and other interventions such as peripheral FES, lower-limb prostheses, and exoskeletons.

Chapter 5: General Discussion

5.1 Summary and Significance

5.1.1 Thesis Summary and Significance

The work outlined in this thesis demonstrates the use of various machine learning approaches to real-life, neuroscience problems, including to characterize motor activity and restore function after neural injury. Specifically, this thesis aimed to characterize motor activity from the developing spinal cord, and to augment remaining function in a model of incomplete SCI using adaptive and predictive control strategies.

5.1.1.1 Classifying Spontaneous Activity

The goal of the work in chapter 2 was to develop a software tool for characterizing and classifying episodes of spontaneous activity. This work detailed the development and demonstration of a graphical user interface in Matlab that analyzed and classified episodes of DC-coupled spontaneous activity from the lumbar spinal cord using supervised machine learning. Spontaneous activity plays an important role in the development of neuronal networks in the central nervous system. Often, spontaneous activity is high-pass filtered for analysis, removing the fine details of the network activity that are present in DC-coupled recordings. Two multilayer perceptrons were trained to classify episodes as rhythmic or not, and multi-burst or not. Final classification also used the relative amplitude, resulting in 5 classes. The classification software was demonstrated in a preparation with increased KCl, which increased spinal excitability. The software revealed more episodes overall along with global and class-specific changes in feature values with the increase in excitability due to the addition of KCl. The machine learning-based classification provides a method of analysis of these detail-rich episodes of activity, allowing investigators to characterize these signals with a new perspective.

5.1.1.2 Speed-Adaptive Control

The goal of chapter 3 was to produce alternating, weight-bearing stepping in a hemisection model of spinal cord injury (SCI) using ISMS. This work is the first to demonstrate the use of ISMS for the restoration of walking in a model of incomplete SCI. Furthermore, it is the first use of machine learning to control spinal cord stimulation. Supervised machine learning was employed to first predict the step period of walking. Four different prediction methods were

compared. For slow walking, a simple IF-THEN algorithm transitioned the stimulation-controlled limb through the stepping cycle, opposite to the phase of the experimenter-moved limb. If the walking was predicted to be fast, then the predicted step period was used to modify the time spent in each phase of the step cycle in a feed-forward manner. Predictions were made on each step; hence, the control strategy was adapted on each step according to the predicted step period. Through the adaptive control strategies guided by supervised machine learning, weight-bearing was restored, and alternation and step symmetry were maintained at varying stepping speeds.

5.1.1.3 Pavlovian Control

The goal of chapter 4 project was to develop a predictive and versatile controller for using ISMS in a hemisection SCI model to produce alternating, over-ground walking. Versatility was achieved using Pavlovian control, which utilized reinforcement learning (RL) to learn predictions for walking-related signals. Using those predictions, transitions between the phases of the walking cycle were triggered using thresholds to produce over-ground walking in anaesthetized cats with an ISMS implant. Four people took turns to move one hind-limb through the walking cycle in 8 different cats to mimic various walking patterns in a model of hemisection SCI. The Pavlovian controller did not require any tuning of thresholds to achieve walking across the 4 people and 8 cats. Pavlovian control resumed walking after purposeful mistakes were made, continuing to have transitions between the phases of the gait cycle initiated by the learned predictions crossing the thresholds. This project combined the newest RL methods for Pavlovian control with a novel neuroprosthesis to produce a versatile and personalized approach to restoring alternating, over-ground walking after a hemisection SCI.

5.1.2 Limitations

5.1.2.1 Classifying Spontaneous Activity

Supervised machine learning was guided by the individuals classifying the data for the training set, and was limited to the class labels it trained on. Therefore, it is important to provide the algorithm with a training data set that includes many examples with variability and features representative of the full data of interest. The goal of a classifier is to generalize adequately on the training data set, as well as generalize to fresh, new data, to classify instances of data. In

order to train a classifier to generalize well, many examples of consistently labelled data need to be used for training. Several individuals should be involved in the initial labelling of data. Furthermore, the individuals should standardize their criteria and agree on the class labels. The individuals that classified the episodes of activity in chapter 2 had high agreement with each other. However, the individuals needed to revise their criteria for rhythmicity, stemming from the inability of any classifiers to generalize well, even after the addition of more episodes. Once a visual criterion was established, the new class labels were able to be generalized adequately with several classifiers. The classifying process should have been discussed further prior to initial training of classifiers. Future versions of the software may include many more episodes with more individuals responsible for manual classification for re-training. It is anticipated that this will increase accuracy further and reduce subjectivity by increasing the representation of each class, confirmed by more individuals.

5.1.2.2 Restoring Walking in a Hemisection Model

All experiments using ISMS to produce walking were done in anaesthetized cats with an intact spinal cord (chapters 3 and 4). This model was chosen to test the control strategies developed and provided a proof-of-concept for their implementation. To test the controllers further, experiments should be conducted in cats with a chronic hemisection SCI. These experiments would require a pre-mammillary decerebration to produce spontaneous walking in the intact limb free from extensor rigidity (Whelan 1996).

Alternating walking was the goal of the controllers used in chapters 3 and 4; therefore, a 4-phase breakdown of the gait cycle was used. The phases comprised F, E1, E2, and E3, corresponding to toe-off to early swing, late swing to paw-touch, paw-touch to mid-stance, and mid-stance to propulsion, respectively. To achieve alternation, the control strategies aimed for the limbs to be in the opposite phases (F opposite of E2, E1 opposite of E3). The methods by which the phase of the experimenter-moved limb was determined and the timing of when the phase transitions occurred varied between control strategies. However, more realistic walking is more complex and smoother than 4 phases. Furthermore, there is more overlap between the phases to ensure complete transfer of the body-weight during double-limb support (Holinski et al. 2011; Mazurek

et al. 2012). Nonetheless, alternating weight-bearing was achieved using the simplified 4-phase model of the step cycle.

5.1.2.3 Speed-Adaptive Control

Because the cat was suspended in a sling over the split-belt treadmill (chapter 3), it was unable to displace its position during propulsion. This resulted in in-place stepping as opposed to walking. During the propulsive phase, there was a large resistance between the stationary treadmill belt and the paw. Overcoming this resistance required large backward forces that resulted in kicking movements because the cat was physically prevented from moving forward. To avoid these abnormal movements, stimulation amplitudes for the channels producing propulsion were reduced, but were still sufficient for weight-bearing. This led to a decreased range of motion during extension. The subsequent study (chapter 4) avoided these issues by testing the control strategies in a cat moving over a walk-way.

5.1.2.4 Pavlovian Control

RL was used to predict cumulants using general value functions (GVFs). Using the GVFs, thresholds were used to transition the stimulation-controlled limb through the phases of the walking cycle. These thresholds were manually placed by using expert knowledge about walking and the sensor signals that were recorded. Once the best thresholds were found from earlier experiments, they did not require tuning between different people moving the experimenter-moved limb or between different cats. However, with more variable paralysis, some individual tuning may be required, especially with the initial setup of the thresholds and stimulation parameters. Because Pavlovian control utilized RL to learn the GVFs online, automatic adaptation to step-by-step and day-to-day variability is very likely.

5.1.3 Future Directions

5.1.3.1 Classifying Spontaneous Activity

Although the multilayer perceptrons (MLPs) from chapter 2 were trained on episodes of spontaneous activity recorded from the lumbar spinal cord of neonatal mice, they may be generalizable to other recordings from the nervous system, given that the data have similar features and are acquired using DC-coupling.

Recording from other ventral roots, such as from thoracic or sacral levels, may be used in combination with the lumbar recordings to investigate the propagation of activity through the spinal cord (Nakayama et al. 1999). This could reveal the origin of the activity and how recruitment of subsequent networks at other levels occurs. Additionally, a coincidence of particular classes of episodes between roots may occur, indicating root activity coordination. Further investigation may reveal a pattern of class order or particular class combinations between roots.

This study demonstrated the simplicity of characterizing changes in spontaneous activity after increasing the network excitability using KCl. Increasing concentrations of extracellular K^+ has previously been shown to excite spinal motor networks non-specifically (Sharples and Whelan 2017; Walton and Chesler 1988; Bracci et al. 1998). Manipulation of spinal cord excitability, such as with other neuromodulators, or through changes in temperature or pH, could further be used to study the development of spontaneous activity and tease out the role of spontaneous activity in the development of spinal locomotor networks (Hernandez et al. 1991; Nishimaru et al. 1996; Bonnot et al. 1998). Changes in spontaneous activity with genetic manipulations could also be used to investigate the development of locomotor networks and possibly locate the origin of spontaneous activity (Bonnot et al. 1998; Lapointe et al. 2009; Francius et al. 2013; Borgius et al. 2014; Myers et al. 2005; Sharples et al. 2015).

The current data were restricted to P0-P3; however, it may be interesting to track the changes in the distribution of classes and class composition throughout development, especially as the role of GABA changes and as innervation from descending and peripheral neural structures develop. Changes of spontaneous activity to pathological conditions, such as cerebral palsy, may provide clues to the changes that occur in the spinal cord after insult to the brain during development. Furthermore, removing regions such as the dorsal horn may provide understanding of the function of the networks producing the spontaneous activity. Removing regions while recording spontaneous activity could also help localize the origin of the activity, or allude to the distribution of the components of the network.

5.1.3.2 Adaptive Control

The speed-adaptive controller in chapter 3 used predictions from supervised machine learning to change the control strategy for faster steps. This concept of adaptive switching using supervised machine learning could be applied to other forms of locomotion. For example, it could be used to switch between control methods for walking, running, cycling, stand-to-sit transfers, stair climbing, slopes, etc. Adaptive switching using RL has been demonstrated previously in an upper-limb prosthesis (Edwards et al. 2013; Edwards et al. 2016). In those studies, RL was used to learn GVFs which represented the prediction of a subject's intention using electromyography (EMG) signals. The predictions were used to select the joint to control, rather than cycling through a set order. A similar prediction-driven switching method could be applied to the control of walking as well.

5.1.3.3 Machine Learning to Restore Walking in Other Injury Models

Both the speed-adaptable and Pavlovian controllers were tested in a model of hemisection SCI. Brown-Sequard syndrome is the human presentation of a hemisection SCI and does not occur frequently (Roth et al. 1991; Wirz et al. 2010). However, this model represents hemiparalysis, which also occurs after a stroke or traumatic brain injury. Therefore, ISMS controlled by either controller could also be used to restore walking after these conditions, with the Pavlovian controller providing further adaptability and universality. The concept of using information from an intact limb to control a paralyzed limb could also be extended to the control of lower limb prostheses or exoskeletons.

This work outlines the first use of machine learning to control an implanted neuroprosthesis. Further development using machine learning could also extend this work to restore walking after a bilateral injury, affecting both legs variably (e.g. contusion injury). Spasticity may interfere with the desired movements or create noisy and unreliable sensor recordings during walking. Other sensors such as EMG or accelerometers may be useful in addition to force sensors and gyroscopes to predict and adapt to spastic episodes during walking. RL is particularly well-suited for non-stationary environments. It may provide the solution of true adaptable control to restore walking in highly variable and changing levels of paresis. This study presents the first step towards that goal. However, care will have to be taken to ensure safe stepping at all times. For

RL, this means that the exploration of new states may have to be constricted to avoid unsafe leg positions, such as double limb unloading.

5.1.3.4 Machine Learning for More Predictions

The Pavlovian controller in chapter 4 learned predictions for ground reaction force and angular velocity signals; however, other sensor signals could also be used to provide more information about the environment. For example, muscle activity recorded using EMG, joint angles provided by goniometers, or visual information through cameras or infrared sensors could all be recorded and used to acquire more predictions. The addition of sensors (e.g. EMG, goniometers) could be useful to restore walking after variable injuries or to provide information regarding the walking terrain (visual, infrared) to adapt the control strategy. Additional sensors could also be used to provide stability information such as loss of balance, fatigue, and the reliance on the upper body for support. Additional control rules could be incorporated to predict and correct these safe situations. Furthermore, the addition of sensors is feasible if a state representation method such as selective Kanerva coding is used, as was the case in this work, because it is not affected by the increase in dimensions that plagues traditional tile coding (Travnik and Pilarski 2017).

Bibliography

Abbas, J. J., and R. J. Triolo. 1997. “Experimental Evaluation of an Adaptive Feedforward Controller for Use in Functional Neuromuscular Stimulation Systems.” *IEEE Transactions on Rehabilitation Engineering: A Publication of the IEEE Engineering in Medicine and Biology Society* 5 (1): 12–22.

Adams, M. M., and A. L. Hicks. 2005. “Spasticity after Spinal Cord Injury.” *Spinal Cord* 43 (10): 577–86. https://doi.org/10.1038/sj.sc.3101757.

Ahmad, Faiz U., Michael Y. Wang, and Allan D. Levi. 2014. “Hypothermia for Acute Spinal Cord Injury--a Review.” *World Neurosurgery* 82 (1–2): 207–14. https://doi.org/10.1016/j.wneu.2013.01.008.

Ajiboye, A. Bolu, Francis R. Willett, Daniel R. Young, William D. Memberg, Brian A. Murphy, Jonathan P. Miller, Benjamin L. Walter, et al. 2017. “Restoration of Reaching and Grasping Movements through Brain-Controlled Muscle Stimulation in a Person with Tetraplegia: A Proof-of-Concept Demonstration.” *Lancet (London, England)* 389 (10081): 1821–30. https://doi.org/10.1016/S0140-6736(17)30601-3.

Ajoudani, Arash, and Abbas Erfanian. 2007. “Neuro-Sliding Mode Control with Modular Models for Control of Knee-Joint Angle Using Quadriceps Electrical Stimulation.” *Conference Proceedings: ... Annual International Conference of the IEEE Engineering in Medicine and Biology Society. IEEE Engineering in Medicine and Biology Society. Annual Conference* 2007: 2424–27. https://doi.org/10.1109/IEMBS.2007.4352817.

Akazawa, K., J. W. Aldridge, J. D. Steeves, and R. B. Stein. 1982. “Modulation of Stretch Reflexes during Locomotion in the Mesencephalic Cat.” *The Journal of Physiology* 329 (August): 553–67.

Alcobendas-Maestro, Mónica, Ana Esclarín-Ruz, Rosa M. Casado-López, Alejandro Muñoz-González, Guillermo Pérez-Mateos, Esteban González-Valdizán, and José Luis R. Martín. 2012. “Lokomat Robotic-Assisted versus Overground Training within 3 to 6 Months of Incomplete Spinal Cord Lesion: Randomized Controlled Trial.” *Neurorehabilitation and Neural Repair* 26 (9): 1058–63. https://doi.org/10.1177/1545968312448232.

Altman, Joseph, and Shirley Ann Bayer. 2001. *Development of the Human Spinal Cord: An Interpretation Based on Experimental Studies in Animals*. Oxford University Press.

Amodei, Dario, Rishita Anubhai, Eric Battenberg, Carl Case, Jared Casper, Bryan Catanzaro, Jingdong Chen, et al. 2015. “Deep Speech 2: End-to-End Speech Recognition in English and Mandarin.” *ArXiv:1512.02595 [Cs]*, December. http://arxiv.org/abs/1512.02595.

Andersen, R. A., J. W. Burdick, S. Musallam, H. Scherberger, B. Pesaran, D. Meeker, B. D. Corneil, et al. 2004. “Recording Advances for Neural Prosthetics.” *Conference Proceedings: ... Annual International Conference of the IEEE Engineering in Medicine and Biology Society. IEEE Engineering in Medicine and Biology Society. Annual Conference* 7: 5352–55. https://doi.org/10.1109/IEMBS.2004.1404494.

Anderson, Kim D. 2004. “Targeting Recovery: Priorities of the Spinal Cord-Injured Population.” *Journal of Neurotrauma* 21 (10): 1371–83. https://doi.org/10.1089/neu.2004.21.1371.

Andrews, B. J., R. H. Baxendale, R. Barnett, G. F. Phillips, T. Yamazaki, J. P. Paul, and P. A. Freeman. 1988. “Hybrid FES Orthosis Incorporating Closed Loop Control and Sensory Feedback.” *Journal of Biomedical Engineering* 10 (2): 189–95.

Angeli, Claudia A., Maxwell Boakye, Rebekah A. Morton, Justin Vogt, Kristin Benton, Yangshen Chen, Christie K. Ferreira, and Susan J. Harkema. 2018. "Recovery of Over-Ground Walking after Chronic Motor Complete Spinal Cord Injury." *The New England Journal of Medicine* 379 (13): 1244–50. https://doi.org/10.1056/NEJMoa1803588.

Angeli, Claudia A., V. Reggie Edgerton, Yury P. Gerasimenko, and Susan J. Harkema. 2014. "Altering Spinal Cord Excitability Enables Voluntary Movements after Chronic Complete Paralysis in Humans." *Brain: A Journal of Neurology* 137 (Pt 5): 1394–1409. https://doi.org/10.1093/brain/awu038.

Antal, M., A. C. Berki, L. Horváth, and M. J. O'Donovan. 1994. "Developmental Changes in the Distribution of Gamma-Aminobutyric Acid-Immunoreactive Neurons in the Embryonic Chick Lumbosacral Spinal Cord." *The Journal of Comparative Neurology* 343 (2): 228–36. https://doi.org/10.1002/cne.903430204.

Arazpour, M., M. Samadian, K. Ebrahimzadeh, M. Ahmadi Bani, and S. W. Hutchins. 2016. "The Influence of Orthosis Options on Walking Parameters in Spinal Cord-Injured Patients: A Literature Review." *Spinal Cord* 54 (6): 412–22. https://doi.org/10.1038/sc.2015.238.

Armstrong, D. M. 1988. "The Supraspinal Control of Mammalian Locomotion." *The Journal of Physiology* 405 (November): 1–37.

Asadi, Alireza. 2014. "Inducing Stepping- Like Movement by Controlling Movement Primitive Blocks Using Intraspinal Microstimulation" 4 (2): 4.

Asadi, Ali-Reza, and Abbas Erfanian. 2012. "Adaptive Neuro-Fuzzy Sliding Mode Control of Multi-Joint Movement Using Intraspinal Microstimulation." *IEEE Transactions on Neural Systems and Rehabilitation Engineering: A Publication of the IEEE Engineering in Medicine and Biology Society* 20 (4): 499–509. https://doi.org/10.1109/TNSRE.2012.2197828.

Assinck, Peggy, Greg J. Duncan, Jason R. Plemel, Michael J. Lee, Jo A. Stratton, Sohrab B. Manesh, Jie Liu, et al. 2017. "Myelinogenic Plasticity of Oligodendrocyte Precursor Cells Following Spinal Cord Contusion Injury." *The Journal of Neuroscience: The Official Journal of the Society for Neuroscience* 37 (36): 8635–54. https://doi.org/10.1523/JNEUROSCI.2409-16.2017.

Awai, Lea, and Armin Curt. 2014. "Intralimb Coordination as a Sensitive Indicator of Motor-Control Impairment after Spinal Cord Injury." *Frontiers in Human Neuroscience* 8: 148. https://doi.org/10.3389/fnhum.2014.00148.

Bajd, T., B. J. Andrews, A. Kralj, and J. Katakis. 1985. "Restoration of Walking in Patients with Incomplete Spinal Cord Injuries by Use of Surface Electrical Stimulation--Preliminary Results." *Prosthetics and Orthotics International* 9 (2): 109–11. https://doi.org/10.3109/03093648509164716.

Bajd, Tadej, Alojz Kralj, Janez Šega, Rajko Turk, Helena Benko, and Primož Strojnik. 1981. "Use of a Two-Channel Functional Electrical Stimulator to Stand Paraplegic Patients." *Physical Therapy* 61 (4): 526–27.

Balasubramanian, Chitralakshmi K., Mark G. Bowden, Richard R. Neptune, and Steven A. Kautz. 2007. "Relationship between Step Length Asymmetry and Walking Performance in Subjects with Chronic Hemiparesis." *Archives of Physical Medicine and Rehabilitation* 88 (1): 43–49. https://doi.org/10.1016/j.apmr.2006.10.004.

Ballion, Bérangère, Pascal Branchereau, Jacqueline Chapron, and Denise Viala. 2002. "Ontogeny of Descending Serotonergic Innervation and Evidence for Intraspinal 5-HT

Neurons in the Mouse Spinal Cord." *Brain Research. Developmental Brain Research* 137 (1): 81–88.
Bamford, J. A., C. T. Putman, and V. K. Mushahwar. 2005. "Intraspinal Microstimulation Preferentially Recruits Fatigue-Resistant Muscle Fibres and Generates Gradual Force in Rat." *The Journal of Physiology* 569 (Pt 3): 873–84. https://doi.org/10.1113/jphysiol.2005.094516.
Bamford, J., R. Lebel, K. Parseyan, and V. Mushahwar. 2016. "The Fabrication, Implantation and Stability of Intraspinal Microwire Arrays in the Spinal Cord of Cat and Rat." *IEEE Transactions on Neural Systems and Rehabilitation Engineering* PP (99): 1–1. https://doi.org/10.1109/TNSRE.2016.2555959.
Bamford, Jeremy A., Charles T. Putman, and Vivian K. Mushahwar. 2011. "Muscle Plasticity in Rat Following Spinal Transection and Chronic Intraspinal Microstimulation." *IEEE Transactions on Neural Systems and Rehabilitation Engineering: A Publication of the IEEE Engineering in Medicine and Biology Society* 19 (1): 79–83. https://doi.org/10.1109/TNSRE.2010.2052832.
Barbeau, H., and S. Rossignol. 1987. "Recovery of Locomotion after Chronic Spinalization in the Adult Cat." *Brain Research* 412 (1): 84–95.
Barbeau, Hugues. 2003. "Locomotor Training in Neurorehabilitation: Emerging Rehabilitation Concepts." *Neurorehabilitation and Neural Repair* 17 (1): 3–11. https://doi.org/10.1177/0888439002250442.
Barolat, G., J. B. Myklebust, and W. Wenninger. 1986. "Enhancement of Voluntary Motor Function Following Spinal Cord Stimulation--Case Study." *Applied Neurophysiology* 49 (6): 307–14.
Barolat, G., J. B. Myklebust, and W. Wenninger. 1988. "Effects of Spinal Cord Stimulation on Spasticity and Spasms Secondary to Myelopathy." *Applied Neurophysiology* 51 (1): 29–44.
Behrman, Andrea L., Elizabeth Ardolino, Leslie R. Vanhiel, Marcie Kern, Darryn Atkinson, Douglas J. Lorenz, and Susan J. Harkema. 2012. "Assessment of Functional Improvement without Compensation Reduces Variability of Outcome Measures after Human Spinal Cord Injury." *Archives of Physical Medicine and Rehabilitation* 93 (9): 1518–29. https://doi.org/10.1016/j.apmr.2011.04.027.
Bélanger, M., T. Drew, J. Provencher, and S. Rossignol. 1996. "A Comparison of Treadmill Locomotion in Adult Cats before and after Spinal Transection." *Journal of Neurophysiology* 76 (1): 471–91. https://doi.org/10.1152/jn.1996.76.1.471.
Bélanger, M., R. B. Stein, G. D. Wheeler, T. Gordon, and B. Leduc. 2000. "Electrical Stimulation: Can It Increase Muscle Strength and Reverse Osteopenia in Spinal Cord Injured Individuals?" *Archives of Physical Medicine and Rehabilitation* 81 (8): 1090–98.
Bergquist, Austin J., Matheus J. Wiest, Yoshino Okuma, and David F. Collins. 2014. "H-Reflexes Reduce Fatigue of Evoked Contractions after Spinal Cord Injury." *Muscle & Nerve* 50 (2): 224–34. https://doi.org/10.1002/mus.24144.
Bhumbra, Gardave S., and Marco Beato. 2018. "Recurrent Excitation between Motoneurones Propagates across Segments and Is Purely Glutamatergic." *PLoS Biology* 16 (3): e2003586. https://doi.org/10.1371/journal.pbio.2003586.
Bickel, C. Scott, Chris M. Gregory, and Jesse C. Dean. 2011. "Motor Unit Recruitment during Neuromuscular Electrical Stimulation: A Critical Appraisal." *European Journal of Applied Physiology* 111 (10): 2399–2407. https://doi.org/10.1007/s00421-011-2128-4.

Biernaskie, Jeff, Joseph S. Sparling, Jie Liu, Casey P. Shannon, Jason R. Plemel, Yuanyun Xie, Freda D. Miller, and Wolfram Tetzlaff. 2007. "Skin-Derived Precursors Generate Myelinating Schwann Cells That Promote Remyelination and Functional Recovery after Contusion Spinal Cord Injury." *The Journal of Neuroscience: The Official Journal of the Society for Neuroscience* 27 (36): 9545–59. https://doi.org/10.1523/JNEUROSCI.1930-07.2007.

Bizzi, E., F. A. Mussa-Ivaldi, and S. Giszter. 1991. "Computations Underlying the Execution of Movement: A Biological Perspective." *Science (New York, N.Y.)* 253 (5017): 287–91.

Bojarski, Mariusz, Davide Del Testa, Daniel Dworakowski, Bernhard Firner, Beat Flepp, Prasoon Goyal, Lawrence D. Jackel, et al. 2016. "End to End Learning for Self-Driving Cars." *ArXiv:1604.07316 [Cs]*, April. http://arxiv.org/abs/1604.07316.

Bonnot, Agnès, Didier Morin, and Denise Viala. 1998. "Genesis of Spontaneous Rhythmic Motor Patterns in the Lumbosacral Spinal Cord of Neonate Mouse." *Developmental Brain Research* 108 (1): 89–99. https://doi.org/10.1016/S0165-3806(98)00033-9.

Boran, Burak O., Ahmet Colak, and Murat Kutlay. 2005. "Erythropoietin Enhances Neurological Recovery after Experimental Spinal Cord Injury." *Restorative Neurology and Neuroscience* 23 (5–6): 341–45.

Borgius, Lotta, Hiroshi Nishimaru, Vanessa Caldeira, Yuka Kunugise, Peter Löw, Ramon Reig, Shigeyoshi Itohara, Takuji Iwasato, and Ole Kiehn. 2014. "Spinal Glutamatergic Neurons Defined by EphA4 Signaling Are Essential Components of Normal Locomotor Circuits." *The Journal of Neuroscience: The Official Journal of the Society for Neuroscience* 34 (11): 3841–53. https://doi.org/10.1523/JNEUROSCI.4992-13.2014.

Bosch, Albert, E. Shannon Stauffer, and Vernon L. Nickel. 1971. "Incomplete Traumatic Quadriplegia: A Ten-Year Review." *JAMA* 216 (3): 473–78. https://doi.org/10.1001/jama.1971.03180290049006.

Bouyer, L. J. G., and S. Rossignol. 2003a. "Contribution of Cutaneous Inputs from the Hindpaw to the Control of Locomotion. I. Intact Cats." *Journal of Neurophysiology* 90 (6): 3625–39. https://doi.org/10.1152/jn.00496.2003.

Bouyer, L. J. G., and S. Rossignol. 2003b. "Contribution of Cutaneous Inputs from the Hindpaw to the Control of Locomotion. II. Spinal Cats." *Journal of Neurophysiology* 90 (6): 3640–53. https://doi.org/10.1152/jn.00497.2003.

Boyd, I. A. 1980. "The Isolated Mammalian Muscle Spindle." *Trends in Neurosciences* 3 (11): 258–65. https://doi.org/10.1016/0166-2236(80)90096-X.

Bracci, E., M. Beato, and A. Nistri. 1998. "Extracellular K+ Induces Locomotor-like Patterns in the Rat Spinal Cord in Vitro: Comparison with NMDA or 5-HT Induced Activity." *Journal of Neurophysiology* 79 (5): 2643–52. https://doi.org/10.1152/jn.1998.79.5.2643.

Bradbury, Elizabeth J., Lawrence D. F. Moon, Reena J. Popat, Von R. King, Gavin S. Bennett, Preena N. Patel, James W. Fawcett, and Stephen B. McMahon. 2002. "Chondroitinase ABC Promotes Functional Recovery after Spinal Cord Injury." *Nature* 416 (6881): 636–40. https://doi.org/10.1038/416636a.

Branchereau, Pascal, Jacqueline Chapron, and Pierre Meyrand. 2002. "Descending 5-Hydroxytryptamine Raphe Inputs Repress the Expression of Serotonergic Neurons and Slow the Maturation of Inhibitory Systems in Mouse Embryonic Spinal Cord." *The Journal of Neuroscience: The Official Journal of the Society for Neuroscience* 22 (7): 2598–2606. https://doi.org/20026199.

Brand, Rubia van den, Janine Heutschi, Quentin Barraud, Jack DiGiovanna, Kay Bartholdi, Michèle Huerlimann, Lucia Friedli, et al. 2012. "Restoring Voluntary Control of Locomotion after Paralyzing Spinal Cord Injury." *Science (New York, N.Y.)* 336 (6085): 1182–85. https://doi.org/10.1126/science.1217416.

Braun, Z., J. Mizrahi, T. Najenson, and D. Graupe. 1985. "Activation of Paraplegic Patients by Functional Electrical Stimulation: Training and Biomechanical Evaluation." *Scandinavian Journal of Rehabilitation Medicine. Supplement* 12: 93–101.

Braz, Gustavo P., Michael Russold, and Glen M. Davis. 2009. "Functional Electrical Stimulation Control of Standing and Stepping after Spinal Cord Injury: A Review of Technical Characteristics." *Neuromodulation: Journal of the International Neuromodulation Society* 12 (3): 180–90. https://doi.org/10.1111/j.1525-1403.2009.00213.x.

Bright, D., A. Nair, D. Salvekar, and S. Bhisikar. 2016. "EEG-Based Brain Controlled Prosthetic Arm." In *2016 Conference on Advances in Signal Processing (CASP)*, 479–83. https://doi.org/10.1109/CASP.2016.7746219.

Brindley, G. S. 1977. "An Implant to Empty the Bladder or Close the Urethra." *Journal of Neurology, Neurosurgery, and Psychiatry* 40 (4): 358–69.

Brown, T. G. 1914. "On the Nature of the Fundamental Activity of the Nervous Centres; Together with an Analysis of the Conditioning of Rhythmic Activity in Progression, and a Theory of the Evolution of Function in the Nervous System." *The Journal of Physiology* 48 (1): 18–46.

Brown, T. Graham. 1911. "The Intrinsic Factors in the Act of Progression in the Mammal." *Proceedings of the Royal Society of London B: Biological Sciences* 84 (572): 308–19. https://doi.org/10.1098/rspb.1911.0077.

Brown-Triolo, Denise L., Mary Joan Roach, Kristine Nelson, and Ronald J. Triolo. 2002. "Consumer Perspectives on Mobility: Implications for Neuroprosthesis Design." *Journal of Rehabilitation Research and Development* 39 (6): 659–69.

Burt, Jeremy R., Neslisah Torosdagli, Naji Khosravan, Harish RaviPrakash, Aliasghar Mortazi, Fiona Tissavirasingham, Sarfaraz Hussein, and Ulas Bagci. 2018. "Deep Learning beyond Cats and Dogs: Recent Advances in Diagnosing Breast Cancer with Deep Neural Networks." *The British Journal of Radiology*, April, 20170545. https://doi.org/10.1259/bjr.20170545.

Buss, Robert R., and Susan J. Shefchyk. 2003. "Sacral Dorsal Horn Neurone Activity during Micturition in the Cat." *The Journal of Physiology* 551 (Pt 1): 387–96. https://doi.org/10.1113/jphysiol.2003.041996.

Bussel, B., A. Roby-Brami, O. R. Néris, and A. Yakovleff. 1996. "Evidence for a Spinal Stepping Generator in Man. Electrophysiological Study." *Acta Neurobiologiae Experimentalis* 56 (1): 465–68.

Calancie, B., B. Needham-Shropshire, P. Jacobs, K. Willer, G. Zych, and B. A. Green. 1994. "Involuntary Stepping after Chronic Spinal Cord Injury. Evidence for a Central Rhythm Generator for Locomotion in Man." *Brain: A Journal of Neurology* 117 (Pt 5) (October): 1143–59.

Cang, Jianhua, René C. Rentería, Megumi Kaneko, Xiaorong Liu, David R. Copenhagen, and Michael P. Stryker. 2005. "Development of Precise Maps in Visual Cortex Requires Patterned Spontaneous Activity in the Retina." *Neuron* 48 (5): 797–809. https://doi.org/10.1016/j.neuron.2005.09.015.

Capaday, C., and R. B. Stein. 1986. “Amplitude Modulation of the Soleus H-Reflex in the Human during Walking and Standing.” *The Journal of Neuroscience: The Official Journal of the Society for Neuroscience* 6 (5): 1308–13.

Capogrosso, Marco, Tomislav Milekovic, David Borton, Fabien Wagner, Eduardo Martin Moraud, Jean-Baptiste Mignardot, Nicolas Buse, et al. 2016. “A Brain-Spine Interface Alleviating Gait Deficits after Spinal Cord Injury in Primates.” *Nature* 539 (7628): 284–88. https://doi.org/10.1038/nature20118.

Capogrosso, Marco, Nikolaus Wenger, Stanisa Raspopovic, Pavel Musienko, Janine Beauparlant, Lorenzo Bassi Luciani, Grégoire Courtine, and Silvestro Micera. 2013. “A Computational Model for Epidural Electrical Stimulation of Spinal Sensorimotor Circuits.” *The Journal of Neuroscience: The Official Journal of the Society for Neuroscience* 33 (49): 19326–40. https://doi.org/10.1523/JNEUROSCI.1688-13.2013.

Cardenas, D. D., J. Ditunno, V. Graziani, A. B. Jackson, D. Lammertse, P. Potter, M. Sipski, R. Cohen, and A. R. Blight. 2007. “Phase 2 Trial of Sustained-Release Fampridine in Chronic Spinal Cord Injury.” *Spinal Cord* 45 (2): 158–68. https://doi.org/10.1038/sj.sc.3101947.

Carhart, Michael R., Jiping He, Richard Herman, S. D’Luzansky, and Wayne T. Willis. 2004. “Epidural Spinal-Cord Stimulation Facilitates Recovery of Functional Walking Following Incomplete Spinal-Cord Injury.” *IEEE Transactions on Neural Systems and Rehabilitation Engineering: A Publication of the IEEE Engineering in Medicine and Biology Society* 12 (1): 32–42. https://doi.org/10.1109/TNSRE.2003.822763.

Carter, R. R., D. B. McCreery, B. J. Woodford, L. A. Bullara, and W. F. Agnew. 1995. “Micturition Control by Microstimulation of the Sacral Spinal Cord of the Cat: Acute Studies.” *IEEE Transactions on Rehabilitation Engineering* 3 (2): 206–14. https://doi.org/10.1109/86.392367.

Casha, Steven, David Zygun, M. Dan McGowan, Ish Bains, V. Wee Yong, and R. John Hurlbert. 2012. “Results of a Phase II Placebo-Controlled Randomized Trial of Minocycline in Acute Spinal Cord Injury.” *Brain: A Journal of Neurology* 135 (Pt 4): 1224–36. https://doi.org/10.1093/brain/aws072.

Cazalets, J. R., M. Gardette, and G. Hilaire. 2000. “Locomotor Network Maturation Is Transiently Delayed in the MAOA-Deficient Mouse.” *Journal of Neurophysiology* 83 (4): 2468–70. https://doi.org/10.1152/jn.2000.83.4.2468.

Chang, Sarah R., Rudi Kobetic, Musa L. Audu, Roger D. Quinn, and Ronald J. Triolo. 2015. “Powered Lower-Limb Exoskeletons to Restore Gait for Individuals with Paraplegia – a Review.” *Case Orthopaedic Journal* 12 (1): 75–80.

Chaplin, E. 1996. “Functional Neuromuscular Stimulation for Mobility in People with Spinal Cord Injuries. The Parastep I System.” *The Journal of Spinal Cord Medicine* 19 (2): 99–105.

Chávez, D., E. Rodríguez, I. Jiménez, and P. Rudomin. 2012. “Changes in Correlation between Spontaneous Activity of Dorsal Horn Neurones Lead to Differential Recruitment of Inhibitory Pathways in the Cat Spinal Cord.” *The Journal of Physiology* 590 (7): 1563–84. https://doi.org/10.1113/jphysiol.2011.223271.

Chen, Yu-Luen, Shih-Ching Chen, Weoi-Luen Chen, Chin-Chih Hsiao, Te-Son Kuo, and Jin-Shin Lai. 2004. “Neural Network and Fuzzy Control in FES-Assisted Locomotion for the Hemiplegic.” *Journal of Medical Engineering & Technology* 28 (1): 32–38. https://doi.org/10.1080/03091900310001211523.

Choi, Edward, Andy Schuetz, Walter F Stewart, and Jimeng Sun. 2017. "Using Recurrent Neural Network Models for Early Detection of Heart Failure Onset." *Journal of the American Medical Informatics Association : JAMIA* 24 (2): 361–70. https://doi.org/10.1093/jamia/ocw112.

Christian, Kimberly M., and Richard F. Thompson. 2003. "Neural Substrates of Eyeblink Conditioning: Acquisition and Retention." *Learning & Memory (Cold Spring Harbor, N.Y.)* 10 (6): 427–55. https://doi.org/10.1101/lm.59603.

Cinelli, Michael E., and Aftab E. Patla. 2008. "Locomotor Avoidance Behaviours during a Visually Guided Task Involving an Approaching Object." *Gait & Posture* 28 (4): 596–601. https://doi.org/10.1016/j.gaitpost.2008.04.006.

Clarac, F., L. Vinay, J. R. Cazalets, J. C. Fady, and M. Jamon. 1998. "Role of Gravity in the Development of Posture and Locomotion in the Neonatal Rat." *Brain Research. Brain Research Reviews* 28 (1–2): 35–43.

Clemens, Stefan, and Shawn Hochman. 2004. "Conversion of the Modulatory Actions of Dopamine on Spinal Reflexes from Depression to Facilitation in D3 Receptor Knock-out Mice." *The Journal of Neuroscience: The Official Journal of the Society for Neuroscience* 24 (50): 11337–45. https://doi.org/10.1523/JNEUROSCI.3698-04.2004.

Collinger, Jennifer L., Stephen Foldes, Tim M. Bruns, Brian Wodlinger, Robert Gaunt, and Douglas J. Weber. 2013. "Neuroprosthetic Technology for Individuals with Spinal Cord Injury." *The Journal of Spinal Cord Medicine* 36 (4): 258–72. https://doi.org/10.1179/2045772313Y.0000000128.

Conway, B. A., H. Hultborn, and O. Kiehn. 1987. "Proprioceptive Input Resets Central Locomotor Rhythm in the Spinal Cat." *Experimental Brain Research* 68 (3): 643–56.

Cormack, Gordon V. 2008. "Email Spam Filtering: A Systematic Review." *Foundations and Trends® in Information Retrieval* 1 (4): 335–455. https://doi.org/10.1561/1500000006.

Courtine, Grégoire, Yury Gerasimenko, Rubia van den Brand, Aileen Yew, Pavel Musienko, Hui Zhong, Bingbing Song, et al. 2009. "Transformation of Nonfunctional Spinal Circuits into Functional States after the Loss of Brain Input." *Nature Neuroscience* 12 (10): 1333–42. https://doi.org/10.1038/nn.2401.

Cowan, Helen. 2015. "Autonomic Dysreflexia in Spinal Cord Injury." *Nursing Times* 111 (44): 22–24.

Cowley, K. C., and B. J. Schmidt. 1997. "Regional Distribution of the Locomotor Pattern-Generating Network in the Neonatal Rat Spinal Cord." *Journal of Neurophysiology* 77 (1): 247–59. https://doi.org/10.1152/jn.1997.77.1.247.

Dalrymple, Ashley N., Dirk G. Everaert, David S. Hu, and Vivian K. Mushahwar. 2018. "A Speed-Adaptive Intraspinal Microstimulation Controller to Restore Weight-Bearing Stepping in a Spinal Cord Hemisection Model." *Journal of Neural Engineering* 15 (5): 056023. https://doi.org/10.1088/1741-2552/aad872.

Dalrymple, Ashley N., and Vivian K. Mushahwar. 2017. "Stimulation of the Spinal Cord for the Control of Walking." In *Neuroprosthetics*, Volume 8:811–49. Series on Bioengineering and Biomedical Engineering, Volume 8. World Scientific. https://doi.org/10.1142/9789813207158_0025.

D'Amico, Jessica M., Elizabeth G. Condliffe, Karen J. B. Martins, David J. Bennett, and Monica A. Gorassini. 2014. "Recovery of Neuronal and Network Excitability after Spinal Cord Injury and Implications for Spasticity." *Frontiers in Integrative Neuroscience* 8: 36. https://doi.org/10.3389/fnint.2014.00036.

Danner, Simon M., Ursula S. Hofstoetter, Brigitta Freundl, Heinrich Binder, Winfried Mayr, Frank Rattay, and Karen Minassian. 2015. "Human Spinal Locomotor Control Is Based on Flexibly Organized Burst Generators." *Brain: A Journal of Neurology* 138 (Pt 3): 577–88. https://doi.org/10.1093/brain/awu372.

Davies, S. J., M. T. Fitch, S. P. Memberg, A. K. Hall, G. Raisman, and J. Silver. 1997. "Regeneration of Adult Axons in White Matter Tracts of the Central Nervous System." *Nature* 390 (6661): 680–83. https://doi.org/10.1038/37776.

Davis, J. A., R. J. Triolo, J. Uhlir, C. Bieri, L. Rohde, D. Lissy, and S. Kukke. 2001. "Preliminary Performance of a Surgically Implanted Neuroprosthesis for Standing and Transfers--Where Do We Stand?" *Journal of Rehabilitation Research and Development* 38 (6): 609–17.

Davis, R., T. Houdayer, B. Andrews, and A. Barriskill. 1999. "Paraplegia: Prolonged Standing Using Closed-Loop Functional Electrical Stimulation and Andrews Ankle-Foot Orthosis." *Artificial Organs* 23 (5): 418–20.

DeJong, Gerben, Ching-Hui J. Hsieh, Patrick Brown, Randall J. Smout, Susan D. Horn, Pamela Ballard, and Tara Bouchard. 2014. "Factors Associated with Pressure Ulcer Risk in Spinal Cord Injury Rehabilitation." *American Journal of Physical Medicine & Rehabilitation* 93 (11): 971–86. https://doi.org/10.1097/PHM.0000000000000117.

Dekopov, Andrey V., Vladimir A. Shabalov, Aleksey A. Tomsky, Mariya V. Hit, and Ekaterina M. Salova. 2015. "Chronic Spinal Cord Stimulation in the Treatment of Cerebral and Spinal Spasticity." *Stereotactic and Functional Neurosurgery* 93 (2): 133–39. https://doi.org/10.1159/000368905.

Delpy, Alain, Anne-Emilie Allain, Pierre Meyrand, and Pascal Branchereau. 2008. "NKCC1 Cotransporter Inactivation Underlies Embryonic Development of Chloride-Mediated Inhibition in Mouse Spinal Motoneuron." *The Journal of Physiology* 586 (4): 1059–75. https://doi.org/10.1113/jphysiol.2007.146993.

Diambra, L. 2002. "Detecting Epileptic Spikes." *Epilepsia* 43 Suppl 5: 194–95.

Dididze, M., B. A. Green, W. Dalton Dietrich, S. Vanni, M. Y. Wang, and A. D. Levi. 2013. "Systemic Hypothermia in Acute Cervical Spinal Cord Injury: A Case-Controlled Study." *Spinal Cord* 51 (5): 395–400. https://doi.org/10.1038/sc.2012.161.

Dietz, V., G. Colombo, and L. Jensen. 1994. "Locomotor Activity in Spinal Man." *Lancet (London, England)* 344 (8932): 1260–63.

Dietz, V., G. Colombo, L. Jensen, and L. Baumgartner. 1995. "Locomotor Capacity of Spinal Cord in Paraplegic Patients." *Annals of Neurology* 37 (5): 574–82. https://doi.org/10.1002/ana.410370506.

Dimitrijevic, Milan R., Yuri Gerasimenko, and Michaela M. Pinter. 1998. "Evidence for a Spinal Central Pattern Generator in Humans." *Annals of the New York Academy of Sciences* 860 (1): 360–76. https://doi.org/10.1111/j.1749-6632.1998.tb09062.x.

Dolbow, D. R., A. S. Gorgey, J. A. Daniels, R. A. Adler, J. R. Moore, and D. R. Gater. 2011. "The Effects of Spinal Cord Injury and Exercise on Bone Mass: A Literature Review." *NeuroRehabilitation* 29 (3): 261–69. https://doi.org/10.3233/NRE-2011-0702.

Donelan, J. Maxwell, and Keir G. Pearson. 2004. "Contribution of Sensory Feedback to Ongoing Ankle Extensor Activity during the Stance Phase of Walking." *Canadian Journal of Physiology and Pharmacology* 82 (8–9): 589–98. https://doi.org/10.1139/y04-043.

Donnelly, Dustin J., and Phillip G. Popovich. 2008. "Inflammation and Its Role in Neuroprotection, Axonal Regeneration and Functional Recovery after Spinal Cord

Injury." *Experimental Neurology* 209 (2): 378–88. https://doi.org/10.1016/j.expneurol.2007.06.009.
Drew, T. 1988. "Motor Cortical Cell Discharge during Voluntary Gait Modification." *Brain Research* 457 (1): 181–87.
Drnach, Luke, Irfan Essa, and Lena H. Ting. 2018. "Identifying Gait Phases from Joint Kinematics during Walking with Switched Linear Dynamical Systems." *BioRxiv*, July, 378380. https://doi.org/10.1101/378380.
Dutta, Anirban, Rudi Kobetic, and Ronald J. Triolo. 2008. "Ambulation after Incomplete Spinal Cord Injury with EMG-Triggered Functional Electrical Stimulation." *IEEE Transactions on Bio-Medical Engineering* 55 (2 Pt 1): 791–94. https://doi.org/10.1109/TBME.2007.902225.
Duysens, J., and K. G. Pearson. 1980. "Inhibition of Flexor Burst Generation by Loading Ankle Extensor Muscles in Walking Cats." *Brain Research* 187 (2): 321–32.
Duysens, J., A. A. Tax, M. Trippel, and V. Dietz. 1992. "Phase-Dependent Reversal of Reflexly Induced Movements during Human Gait." *Experimental Brain Research* 90 (2): 404–14.
Dvorak, Marcel F., Vanessa K. Noonan, Nader Fallah, Charles G. Fisher, Joel Finkelstein, Brian K. Kwon, Carly S. Rivers, et al. 2015. "The Influence of Time from Injury to Surgery on Motor Recovery and Length of Hospital Stay in Acute Traumatic Spinal Cord Injury: An Observational Canadian Cohort Study." *Journal of Neurotrauma* 32 (9): 645–54. https://doi.org/10.1089/neu.2014.3632.
Edwards, AL, A Kearney, MR Dawson, RS Sutton, and PM Pilarski. 2013. "Temporal-Difference Learning to Assist Human Decision Making during the Control of an Artificial Limb." In . Princeton, NJ, USA.
Edwards, Ann L., Michael R. Dawson, Jacqueline S. Hebert, Craig Sherstan, Richard S. Sutton, K. Ming Chan, and Patrick M. Pilarski. 2016. "Application of Real-Time Machine Learning to Myoelectric Prosthesis Control: A Case Series in Adaptive Switching." *Prosthetics and Orthotics International* 40 (5): 573–81. https://doi.org/10.1177/0309364615605373.
Edwards, Ann L., Alexandra Kearney, Michael Rory Dawson, Richard S. Sutton, and Patrick M. Pilarski. 2013. "Temporal-Difference Learning to Assist Human Decision Making during the Control of an Artificial Limb." *ArXiv:1309.4714 [Cs]*, September. http://arxiv.org/abs/1309.4714.
Ekeberg, Orjan, and Keir Pearson. 2005. "Computer Simulation of Stepping in the Hind Legs of the Cat: An Examination of Mechanisms Regulating the Stance-to-Swing Transition." *Journal of Neurophysiology* 94 (6): 4256–68. https://doi.org/10.1152/jn.00065.2005.
Ekelem, Andrew, and Michael Goldfarb. 2018. "Supplemental Stimulation Improves Swing Phase Kinematics During Exoskeleton Assisted Gait of SCI Subjects With Severe Muscle Spasticity." *Frontiers in Neuroscience* 12: 374. https://doi.org/10.3389/fnins.2018.00374.
Endo, Gen, Jun Morimoto, Takamitsu Matsubara, Jun Nakanishi, and Gordon Cheng. 2008. "Learning CPG-Based Biped Locomotion with a Policy Gradient Method: Application to a Humanoid Robot." *The International Journal of Robotics Research* 27 (2): 213–28. https://doi.org/10.1177/0278364907084980.
Engberg, I., and A. Lundberg. 1969. "An Electromyographic Analysis of Muscular Activity in the Hindlimb of the Cat during Unrestrained Locomotion." *Acta Physiologica Scandinavica* 75 (4): 614–30. https://doi.org/10.1111/j.1748-1716.1969.tb04415.x.

Esteva, Andre, Brett Kuprel, Roberto A. Novoa, Justin Ko, Susan M. Swetter, Helen M. Blau, and Sebastian Thrun. 2017. "Dermatologist-Level Classification of Skin Cancer with Deep Neural Networks." *Nature* 542 (7639): 115–18. https://doi.org/10.1038/nature21056.

Everaert, Dirk G., Richard B. Stein, Gary M. Abrams, Alexander W. Dromerick, Gerard E. Francisco, Brian J. Hafner, Thy N. Huskey, Michael C. Munin, Karen J. Nolan, and Conrad V. Kufta. 2013. "Effect of a Foot-Drop Stimulator and Ankle-Foot Orthosis on Walking Performance after Stroke: A Multicenter Randomized Controlled Trial." *Neurorehabilitation and Neural Repair* 27 (7): 579–91. https://doi.org/10.1177/1545968313481278.

Fady, J. C., M. Jamon, and F. Clarac. 1998. "Early Olfactory-Induced Rhythmic Limb Activity in the Newborn Rat." *Brain Research. Developmental Brain Research* 108 (1–2): 111–23.

Farry, Angela. 2011. *The Incidence and Prevalence of Spinal Cord Injury in Canada: Overview and Estimates Based on Current Evidence*. Rick Hansen Institute.

Faulkner, Jill R., Julia E. Herrmann, Michael J. Woo, Keith E. Tansey, Ngan B. Doan, and Michael V. Sofroniew. 2004. "Reactive Astrocytes Protect Tissue and Preserve Function after Spinal Cord Injury." *The Journal of Neuroscience: The Official Journal of the Society for Neuroscience* 24 (9): 2143–55. https://doi.org/10.1523/JNEUROSCI.3547-03.2004.

Fehlings, M. G., C. H. Tator, and R. D. Linden. 1989. "The Effect of Nimodipine and Dextran on Axonal Function and Blood Flow Following Experimental Spinal Cord Injury." *Journal of Neurosurgery* 71 (3): 403–16. https://doi.org/10.3171/jns.1989.71.3.0403.

Feldblum, S., S. Arnaud, M. Simon, O. Rabin, and P. D'Arbigny. 2000. "Efficacy of a New Neuroprotective Agent, Gacyclidine, in a Model of Rat Spinal Cord Injury." *Journal of Neurotrauma* 17 (11): 1079–93. https://doi.org/10.1089/neu.2000.17.1079.

Fellippa-Marques, S., L. Vinay, and F. Clarac. 2000. "Spontaneous and Locomotor-Related GABAergic Input onto Primary Afferents in the Neonatal Rat." *The European Journal of Neuroscience* 12 (1): 155–64.

Fetz, E. E. 1999. "Real-Time Control of a Robotic Arm by Neuronal Ensembles." *Nature Neuroscience* 2 (7): 583–84. https://doi.org/10.1038/10131.

Field-Fote, Edelle C. 2001. "Combined Use of Body Weight Support, Functional Electric Stimulation, and Treadmill Training to Improve Walking Ability in Individuals with Chronic Incomplete Spinal Cord Injury." *Archives of Physical Medicine and Rehabilitation* 82 (6): 818–24. https://doi.org/10.1053/apmr.2001.23752.

Figueiredo, Joana, Paulo Felix, Luis Costa, Juan C. Moreno, and Cristina P. Santos. 2018. "Gait Event Detection in Controlled and Real-Life Situations: Repeated Measures From Healthy Subjects." *IEEE Transactions on Neural Systems and Rehabilitation Engineering: A Publication of the IEEE Engineering in Medicine and Biology Society* 26 (10): 1945–56. https://doi.org/10.1109/TNSRE.2018.2868094.

Finnerup, Nanna Brix. 2013. "Pain in Patients with Spinal Cord Injury." *Pain* 154 Suppl 1 (December): S71-76. https://doi.org/10.1016/j.pain.2012.12.007.

Fisekovic, N., and D. B. Popovic. 2001. "New Controller for Functional Electrical Stimulation Systems." *Medical Engineering & Physics* 23 (6): 391–99.

Forssberg, H. 1979. “Stumbling Corrective Reaction: A Phase-Dependent Compensatory Reaction during Locomotion.” *Journal of Neurophysiology* 42 (4): 936–53. https://doi.org/10.1152/jn.1979.42.4.936.

Forssberg, H. 1985. “Ontogeny of Human Locomotor Control. I. Infant Stepping, Supported Locomotion and Transition to Independent Locomotion.” *Experimental Brain Research* 57 (3): 480–93.

Fortun, Jenny, Raisa Puzis, Damien D. Pearse, Fred H. Gage, and Mary Bartlett Bunge. 2009. “Muscle Injection of AAV-NT3 Promotes Anatomical Reorganization of CST Axons and Improves Behavioral Outcome Following SCI.” *Journal of Neurotrauma* 26 (7): 941–53. https://doi.org/10.1089/neu.2008.0807.

Francius, Cédric, Audrey Harris, Vincent Rucchin, Timothy J. Hendricks, Floor J. Stam, Melissa Barber, Dorota Kurek, et al. 2013. “Identification of Multiple Subsets of Ventral Interneurons and Differential Distribution along the Rostrocaudal Axis of the Developing Spinal Cord.” *PloS One* 8 (8): e70325. https://doi.org/10.1371/journal.pone.0070325.

Frank, Eibe, Mark A. Hall, and Ian H. Witten. 2016. *WEKA* (version 3.8). Waikato Environment for Knowledge Analysis. New Zealand: Morgan Kaufmann.

Friedman, H., B. S. Nashold, and P. Senechal. 1972. “Spinal Cord Stimulation and Bladder Function in Normal and Paraplegic Animals.” *Journal of Neurosurgery* 36 (4): 430–37. https://doi.org/10.3171/jns.1972.36.4.0430.

Galli, L., and L. Maffei. 1988. “Spontaneous Impulse Activity of Rat Retinal Ganglion Cells in Prenatal Life.” *Science (New York, N.Y.)* 242 (4875): 90–91.

Gan, Liu Shi, Einat Ravid, Jan Andrzej Kowalczewski, Jaret Lawrence Olson, Michael Morhart, and Arthur Prochazka. 2012. “First Permanent Implant of Nerve Stimulation Leads Activated by Surface Electrodes, Enabling Hand Grasp and Release: The Stimulus Router Neuroprosthesis.” *Neurorehabilitation and Neural Repair* 26 (4): 335–43. https://doi.org/10.1177/1545968311420443.

Gao, Dayong, Michael Madden, Michael Schukat, Des Chambers, and Gerard Lyons. 2004. “Arrhythmia Identification from ECG Signals with a Neural Network Classifier Based on a Bayesian Framework,” 12.

Garaschuk, O., E. Hanse, and A. Konnerth. 1998. “Developmental Profile and Synaptic Origin of Early Network Oscillations in the CA1 Region of Rat Neonatal Hippocampus.” *The Journal of Physiology* 507 (Pt 1) (February): 219–36.

Garcia, John, Frank R. Ervin, and Robert A. Koelling. 1966. “Learning with Prolonged Delay of Reinforcement.” *Psychonomic Science* 5 (3): 121–22. https://doi.org/10.3758/BF03328311.

Garcia-Arguello, L. Y., J. C. O’Horo, A. Farrell, R. Blakney, M. R. Sohail, C. T. Evans, and N. Safdar. 2017. “Infections in the Spinal Cord-Injured Population: A Systematic Review.” *Spinal Cord* 55 (6): 526–34. https://doi.org/10.1038/sc.2016.173.

Gardner, M. B., M. K. Holden, J. M. Leikauskas, and R. L. Richard. 1998. “Partial Body Weight Support with Treadmill Locomotion to Improve Gait after Incomplete Spinal Cord Injury: A Single-Subject Experimental Design.” *Physical Therapy* 78 (4): 361–74.

Gater, David R., David Dolbow, Britney Tsui, and Ashraf S. Gorgey. 2011. “Functional Electrical Stimulation Therapies after Spinal Cord Injury.” *NeuroRehabilitation* 28 (3): 231–48. https://doi.org/10.3233/NRE-2011-0652.

Gaunt, R. A., A. Prochazka, V. K. Mushahwar, L. Guevremont, and P. H. Ellaway. 2006. “Intraspinal Microstimulation Excites Multisegmental Sensory Afferents at Lower

Stimulus Levels than Local Alpha-Motoneuron Responses." *Journal of Neurophysiology* 96 (6): 2995–3005. https://doi.org/10.1152/jn.00061.2006.
Gaunt, Robert A., and Arthur Prochazka. 2006. "Control of Urinary Bladder Function with Devices: Successes and Failures." *Progress in Brain Research* 152: 163–94. https://doi.org/10.1016/S0079-6123(05)52011-9.
Geisler, F. H., W. P. Coleman, G. Grieco, D. Poonian, and Sygen Study Group. 2001. "The Sygen Multicenter Acute Spinal Cord Injury Study." *Spine* 26 (24 Suppl): S87-98.
Gerasimenko, Yu P., V. D. Avelev, O. A. Nikitin, and I. A. Lavrov. 2003. "Initiation of Locomotor Activity in Spinal Cats by Epidural Stimulation of the Spinal Cord." *Neuroscience and Behavioral Physiology* 33 (3): 247–54.
Gerasimenko, Yu P., A. N. Makarovskii, and O. A. Nikitin. 2002. "Control of Locomotor Activity in Humans and Animals in the Absence of Supraspinal Influences." *Neuroscience and Behavioral Physiology* 32 (4): 417–23.
Gil-Agudo, Angel, Soraya Pérez-Nombela, Enrique Pérez-Rizo, Antonio del Ama-Espinosa, Beatriz Crespo-Ruiz, and José L. Pons. 2013. "Comparative Biomechanical Analysis of Gait in Patients with Central Cord and Brown-Séquard Syndrome." *Disability and Rehabilitation* 35 (22): 1869–76. https://doi.org/10.3109/09638288.2013.766268.
Gill, Megan L., Peter J. Grahn, Jonathan S. Calvert, Margaux B. Linde, Igor A. Lavrov, Jeffrey A. Strommen, Lisa A. Beck, et al. 2018. "Neuromodulation of Lumbosacral Spinal Networks Enables Independent Stepping after Complete Paraplegia." *Nature Medicine*, September. https://doi.org/10.1038/s41591-018-0175-7.
Giszter, S. F., F. A. Mussa-Ivaldi, and E. Bizzi. 1993. "Convergent Force Fields Organized in the Frog's Spinal Cord." *The Journal of Neuroscience* 13 (2): 467–91.
Giszter, Simon F. 2015. "Spinal Primitives and Intra-Spinal Micro-Stimulation (ISMS) Based Prostheses: A Neurobiological Perspective on the 'Known Unknowns' in ISMS and Future Prospects." *Frontiers in Neuroscience* 9: 72. https://doi.org/10.3389/fnins.2015.00072.
Glimcher, Paul W. 2011. "Understanding Dopamine and Reinforcement Learning: The Dopamine Reward Prediction Error Hypothesis." *Proceedings of the National Academy of Sciences of the United States of America* 108 Suppl 3 (September): 15647–54. https://doi.org/10.1073/pnas.1014269108.
Gordon, Ian T., Mary J. Dunbar, Kimberly J. Vanneste, and Patrick J. Whelan. 2008. "Interaction between Developing Spinal Locomotor Networks in the Neonatal Mouse." *Journal of Neurophysiology* 100 (1): 117–28. https://doi.org/10.1152/jn.00829.2007.
Gordon, Ian T., and Patrick J. Whelan. 2006. "Monoaminergic Control of Cauda-Equina-Evoked Locomotion in the Neonatal Mouse Spinal Cord." *Journal of Neurophysiology* 96 (6): 3122–29. https://doi.org/10.1152/jn.00606.2006.
Goslow, G. E., R. M. Reinking, and D. G. Stuart. 1973. "The Cat Step Cycle: Hind Limb Joint Angles and Muscle Lengths during Unrestrained Locomotion." *Journal of Morphology* 141 (1): 1–41. https://doi.org/10.1002/jmor.1051410102.
Grahn, Peter J., Kendall H. Lee, Aimen Kasasbeh, Grant W. Mallory, Jan T. Hachmann, John R. Dube, Christopher J. Kimble, et al. 2014. "Wireless Control of Intraspinal Microstimulation in a Rodent Model of Paralysis." *Journal of Neurosurgery*, 1–11. https://doi.org/10.3171/2014.10.JNS132370.

Granat, M. H., B. W. Heller, D. J. Nicol, R. H. Baxendale, and B. J. Andrews. 1993. "Improving Limb Flexion in FES Gait Using the Flexion Withdrawal Response for the Spinal Cord Injured Person." *Journal of Biomedical Engineering* 15 (1): 51–56.

Grasso, Renato, Yuri P. Ivanenko, Myrka Zago, Marco Molinari, Giorgio Scivoletto, Vincenzo Castellano, Velio Macellari, and Francesco Lacquaniti. 2004. "Distributed Plasticity of Locomotor Pattern Generators in Spinal Cord Injured Patients." *Brain: A Journal of Neurology* 127 (Pt 5): 1019–34. https://doi.org/10.1093/brain/awh115.

Graupe, D., and H. Kordylewski. 1995. "Artificial Neural Network Control of FES in Paraplegics for Patient Responsive Ambulation." *IEEE Transactions on Bio-Medical Engineering* 42 (7): 699–707. https://doi.org/10.1109/10.391169.

Graupe, Daniel, and Kate H Kohn. 1998. "Functional Neuromuscular Stimulator for Short-Distance Ambulation by Certain Thoracic-Level Spinal-Cord-Injured Paraplegics." *Surgical Neurology* 50 (3): 202–7. https://doi.org/10.1016/S0090-3019(98)00074-3.

Gregory, Chris M., and C. Scott Bickel. 2005. "Recruitment Patterns in Human Skeletal Muscle During Electrical Stimulation." *Physical Therapy* 85 (4): 358–64.

Grill, W. M., N. Bhadra, and B. Wang. 1999. "Bladder and Urethral Pressures Evoked by Microstimulation of the Sacral Spinal Cord in Cats." *Brain Research* 836 (1–2): 19–30.

Grillner, S., and S. Rossignol. 1978. "On the Initiation of the Swing Phase of Locomotion in Chronic Spinal Cats." *Brain Research* 146 (2): 269–77.

Grillner, S., and M. L. Shik. 1973. "On the Descending Control of the Lumbosacral Spinal Cord from the 'Mesencephalic Locomotor Region.'" *Acta Physiologica Scandinavica* 87 (3): 320–33. https://doi.org/10.1111/j.1748-1716.1973.tb05396.x.

Grillner, S, and P Wallen. 1985. "Central Pattern Generators for Locomotion, with Special Reference to Vertebrates." *Annual Review of Neuroscience* 8 (1): 233–61. https://doi.org/10.1146/annurev.ne.08.030185.001313.

Grillner, Sten. 1981. "Control of Locomotion in Bipeds, Tetrapods, and Fish." In *Comprehensive Physiology*, 1179–1236. American Cancer Society. https://doi.org/10.1002/cphy.cp010226.

Gross, R., F. Leboeuf, O. Rémy-Néris, and B. Perrouin-Verbe. 2012. "Unstable Gait Due to Spasticity of the Rectus Femoris: Gait Analysis and Motor Nerve Block." *Annals of Physical and Rehabilitation Medicine* 55 (9–10): 609–22. https://doi.org/10.1016/j.rehab.2012.08.013.

Guertin, P., M. J. Angel, M. C. Perreault, and D. A. McCrea. 1995. "Ankle Extensor Group I Afferents Excite Extensors throughout the Hindlimb during Fictive Locomotion in the Cat." *The Journal of Physiology* 487 (1): 197–209.

Guertin, Pierre A. 2009. "The Mammalian Central Pattern Generator for Locomotion." *Brain Research Reviews* 62 (1): 45–56. https://doi.org/10.1016/j.brainresrev.2009.08.002.

Guertin, Pierre A. 2012. "Central Pattern Generator for Locomotion: Anatomical, Physiological, and Pathophysiological Considerations." *Frontiers in Neurology* 3: 183. https://doi.org/10.3389/fneur.2012.00183.

Guevremont, Lisa, Jonathan A. Norton, and Vivian K. Mushahwar. 2007. "Physiologically Based Controller for Generating Overground Locomotion Using Functional Electrical Stimulation." *Journal of Neurophysiology* 97 (3): 2499–2510. https://doi.org/10.1152/jn.01177.2006.

Guevremont, Lisa, Costantino G. Renzi, Jonathan A. Norton, Jan Kowalczewski, Rajiv Saigal, and Vivian K. Mushahwar. 2006. "Locomotor-Related Networks in the Lumbosacral

Enlargement of the Adult Spinal Cat: Activation through Intraspinal Microstimulation." *IEEE Transactions on Neural Systems and Rehabilitation Engineering: A Publication of the IEEE Engineering in Medicine and Biology Society* 14 (3): 266–72. https://doi.org/10.1109/TNSRE.2006.881592.

Guiraud, David, Thomas Stieglitz, Klaus Peter Koch, Jean-Louis Divoux, and Pierre Rabischong. 2006. "An Implantable Neuroprosthesis for Standing and Walking in Paraplegia: 5-Year Patient Follow-Up." *Journal of Neural Engineering* 3 (4): 268–75. https://doi.org/10.1088/1741-2560/3/4/003.

Gustafsson, B., and E. Jankowska. 1976. "Direct and Indirect Activation of Nerve Cells by Electrical Pulses Applied Extracellularly." *The Journal of Physiology* 258 (1): 33–61.

Hagen, Ellen Merete, Tiina Rekand, Marit Grønning, and Svein Færestrand. 2012. "Cardiovascular Complications of Spinal Cord Injury." *Tidsskrift for Den Norske Laegeforening: Tidsskrift for Praktisk Medicin, Ny Raekke* 132 (9): 1115–20. https://doi.org/10.4045/tidsskr.11.0551.

Hägglund, Martin, Lotta Borgius, Kimberly J. Dougherty, and Ole Kiehn. 2010. "Activation of Groups of Excitatory Neurons in the Mammalian Spinal Cord or Hindbrain Evokes Locomotion." *Nature Neuroscience* 13 (2): 246–52. https://doi.org/10.1038/nn.2482.

Hansen, Morten, Morten K. Haugland, and Thomas Sinkjaer. 2004. "Evaluating Robustness of Gait Event Detection Based on Machine Learning and Natural Sensors." *IEEE Transactions on Neural Systems and Rehabilitation Engineering: A Publication of the IEEE Engineering in Medicine and Biology Society* 12 (1): 81–88. https://doi.org/10.1109/TNSRE.2003.819890.

Hanson, M. Gartz, and Lynn T. Landmesser. 2003. "Characterization of the Circuits That Generate Spontaneous Episodes of Activity in the Early Embryonic Mouse Spinal Cord." *The Journal of Neuroscience: The Official Journal of the Society for Neuroscience* 23 (2): 587–600.

Hanson, M. Gartz, and Lynn T. Landmesser. 2004. "Normal Patterns of Spontaneous Activity Are Required for Correct Motor Axon Guidance and the Expression of Specific Guidance Molecules." *Neuron* 43 (5): 687–701. https://doi.org/10.1016/j.neuron.2004.08.018.

Hardin, Elizabeth, Rudi Kobetic, Lori Murray, Michelle Corado-Ahmed, Gilles Pinault, Jonathan Sakai, Stephanie Nogan Bailey, Chester Ho, and Ronald J. Triolo. 2007. "Walking after Incomplete Spinal Cord Injury Using an Implanted FES System: A Case Report." *Journal of Rehabilitation Research and Development* 44 (3): 333–46.

Hargrove, LJ, K Englehart, and B Hudgins. 2007. "A Comparison of Surface and Intramuscular Myoelectric Signal Classification" 54 (5): 847–53.

Harkema, Susan, Andrea Behrman, and Hugues Barbeau. 2012. "Evidence-Based Therapy for Recovery of Function after Spinal Cord Injury." *Handbook of Clinical Neurology* 109: 259–74. https://doi.org/10.1016/B978-0-444-52137-8.00016-4.

Harkema, Susan, Yury Gerasimenko, Jonathan Hodes, Joel Burdick, Claudia Angeli, Yangsheng Chen, Christie Ferreira, et al. 2011. "Effect of Epidural Stimulation of the Lumbosacral Spinal Cord on Voluntary Movement, Standing, and Assisted Stepping after Motor Complete Paraplegia: A Case Study." *Lancet* 377 (9781): 1938–47. https://doi.org/10.1016/S0140-6736(11)60547-3.

Harkema, Susan J., Mary Schmidt-Read, Douglas J. Lorenz, V. Reggie Edgerton, and Andrea L. Behrman. 2012. "Balance and Ambulation Improvements in Individuals with Chronic Incomplete Spinal Cord Injury Using Locomotor Training-Based Rehabilitation."

Archives of Physical Medicine and Rehabilitation 93 (9): 1508–17. https://doi.org/10.1016/j.apmr.2011.01.024.

Harrison, Robert F., and R. Lee Kennedy. 2005. "Artificial Neural Network Models for Prediction of Acute Coronary Syndromes Using Clinical Data from the Time of Presentation." *Annals of Emergency Medicine* 46 (5): 431–39. https://doi.org/10.1016/j.annemergmed.2004.09.012.

Hayes, K. C., J. T. Hsieh, D. L. Wolfe, P. J. Potter, and G. A. Delaney. 2000. "Classifying Incomplete Spinal Cord Injury Syndromes: Algorithms Based on the International Standards for Neurological and Functional Classification of Spinal Cord Injury Patients." *Archives of Physical Medicine and Rehabilitation* 81 (5): 644–52.

Hebenstreit, Felix, Andreas Leibold, Sebastian Krinner, Götz Welsch, Matthias Lochmann, and Bjoern M. Eskofier. 2015. "Effect of Walking Speed on Gait Sub Phase Durations." *Human Movement Science* 43 (October): 118–24. https://doi.org/10.1016/j.humov.2015.07.009.

Heller, B. W., P. H. Veltink, N. J. Rijkhoff, W. L. Rutten, and B. J. Andrews. 1993. "Reconstructing Muscle Activation during Normal Walking: A Comparison of Symbolic and Connectionist Machine Learning Techniques." *Biological Cybernetics* 69 (4): 327–35.

Henneman, Elwood, George Somjen, and David O. Carpenter. 1965. "Functional Significance of Cell Size in Spinal Motoneurons." *Journal of Neurophysiology* 28 (3): 560–80.

Herman, R., J. He, S. D'Luzansky, W. Willis, and S. Dilli. 2002. "Spinal Cord Stimulation Facilitates Functional Walking in a Chronic, Incomplete Spinal Cord Injured." *Spinal Cord* 40 (2): 65–68. https://doi.org/10.1038/sj.sc.3101263.

Hernandez, P., K. Elbert, and M. H. Droge. 1991. "Spontaneous and NMDA Evoked Motor Rhythms in the Neonatal Mouse Spinal Cord: An in Vitro Study with Comparisons to in Situ Activity." *Experimental Brain Research* 85 (1): 66–74.

Herrmann, Julia E., Tetsuya Imura, Bingbing Song, Jingwei Qi, Yan Ao, Thu K. Nguyen, Rose A. Korsak, Kiyoshi Takeda, Shizuo Akira, and Michael V. Sofroniew. 2008. "STAT3 Is a Critical Regulator of Astrogliosis and Scar Formation after Spinal Cord Injury." *The Journal of Neuroscience: The Official Journal of the Society for Neuroscience* 28 (28): 7231–43. https://doi.org/10.1523/JNEUROSCI.1709-08.2008.

Hiebert, G. W., P. J. Whelan, A. Prochazka, and K. G. Pearson. 1995. "Suppression of the Corrective Response to Loss of Ground Support by Stimulation of Extensor Group I Afferents." *Journal of Neurophysiology* 73 (1): 416–20. https://doi.org/10.1152/jn.1995.73.1.416.

Hinton, G., L. Deng, D. Yu, G. E. Dahl, A. r Mohamed, N. Jaitly, A. Senior, et al. 2012. "Deep Neural Networks for Acoustic Modeling in Speech Recognition: The Shared Views of Four Research Groups." *IEEE Signal Processing Magazine* 29 (6): 82–97. https://doi.org/10.1109/MSP.2012.2205597.

Hiraiwa, A., N. Uchida, and K. Shimohara. 1992. "EMG Pattern Recognition by Neural Networks for Prosthetic Fingers Control." *Annual Review in Automatic Programming*, Artificial Intelligence in Real-time Control 1992, 17 (January): 73–79. https://doi.org/10.1016/S0066-4138(09)91014-X.

Hoffmann, Johann du, and Saleem M. Nicola. 2014. "Dopamine Invigorates Reward Seeking by Promoting Cue-Evoked Excitation in the Nucleus Accumbens." *The Journal of*

Neuroscience: The Official Journal of the Society for Neuroscience 34 (43): 14349–64. https://doi.org/10.1523/JNEUROSCI.3492-14.2014.

Hofstoetter, Ursula S., Brigitta Freundl, Heinrich Binder, and Karen Minassian. 2018. "Common Neural Structures Activated by Epidural and Transcutaneous Lumbar Spinal Cord Stimulation: Elicitation of Posterior Root-Muscle Reflexes." *PloS One* 13 (1): e0192013. https://doi.org/10.1371/journal.pone.0192013.

Hofstoetter, Ursula S., Matthias Krenn, Simon M. Danner, Christian Hofer, Helmut Kern, William B. McKay, Winfried Mayr, and Karen Minassian. 2015. "Augmentation of Voluntary Locomotor Activity by Transcutaneous Spinal Cord Stimulation in Motor-Incomplete Spinal Cord-Injured Individuals." *Artificial Organs* 39 (10): E176-186. https://doi.org/10.1111/aor.12615.

Holinski, B. J., D. G. Everaert, V. K. Mushahwar, and R. B. Stein. 2013. "Real-Time Control of Walking Using Recordings from Dorsal Root Ganglia." *Journal of Neural Engineering* 10 (5): 056008. https://doi.org/10.1088/1741-2560/10/5/056008.

Holinski, B. J., K. A. Mazurek, D. G. Everaert, A. Toossi, A. M. Lucas-Osma, P. Troyk, R. Etienne-Cummings, R. B. Stein, and V. K. Mushahwar. 2016. "Intraspinal Microstimulation Produces Over-Ground Walking in Anesthetized Cats." *Journal of Neural Engineering* 13 (5): 056016. https://doi.org/10.1088/1741-2560/13/5/056016.

Holinski, Bradley J., Kevin A. Mazurek, Dirk G. Everaert, Richard B. Stein, and Vivian K. Mushahwar. 2011. "Restoring Stepping after Spinal Cord Injury Using Intraspinal Microstimulation and Novel Control Strategies." *Conference Proceedings: ... Annual International Conference of the IEEE Engineering in Medicine and Biology Society. IEEE Engineering in Medicine and Biology Society. Annual Conference* 2011: 5798–5801. https://doi.org/10.1109/IEMBS.2011.6091435.

Holsheimer, J. 1998. "Computer Modelling of Spinal Cord Stimulation and Its Contribution to Therapeutic Efficacy." *Spinal Cord* 36 (8): 531–40.

Hotson, Guy, David P. McMullen, Matthew S. Fifer, Matthew S. Johannes, Kapil D. Katyal, Matthew P. Para, Robert Armiger, et al. 2016. "Individual Finger Control of a Modular Prosthetic Limb Using High-Density Electrocorticography in a Human Subject." *Journal of Neural Engineering* 13 (2): 026017. https://doi.org/10.1088/1741-2560/13/2/026017.

Huang, He, Jiping He, Richard Herman, and Michael R. Carhart. 2006. "Modulation Effects of Epidural Spinal Cord Stimulation on Muscle Activities during Walking." *IEEE Transactions on Neural Systems and Rehabilitation Engineering: A Publication of the IEEE Engineering in Medicine and Biology Society* 14 (1): 14–23. https://doi.org/10.1109/TNSRE.2005.862694.

Hulsebosch, C. E., B. C. Hains, K. Waldrep, and W. Young. 2000. "Bridging the Gap: From Discovery to Clinical Trials in Spinal Cord Injury." *Journal of Neurotrauma* 17 (12): 1117–28. https://doi.org/10.1089/neu.2000.17.1117.

Hunter, J., and P. Ashby. 1984. "Secondary Changes in Segmental Neurons below a Spinal Cord Lesion in Man." *Archives of Physical Medicine and Rehabilitation* 65 (11): 702–5.

Hurlbert, R. John, Mark N. Hadley, Beverly C. Walters, Bizhan Aarabi, Sanjay S. Dhall, Daniel E. Gelb, Curtis J. Rozzelle, Timothy C. Ryken, and Nicholas Theodore. 2015. "Pharmacological Therapy for Acute Spinal Cord Injury." *Neurosurgery* 76 Suppl 1 (March): S71-83. https://doi.org/10.1227/01.neu.0000462080.04196.f7.

Ichiyama, R. M., Yu P. Gerasimenko, H. Zhong, R. R. Roy, and V. R. Edgerton. 2005. "Hindlimb Stepping Movements in Complete Spinal Rats Induced by Epidural Spinal

Cord Stimulation." *Neuroscience Letters* 383 (3): 339–44. https://doi.org/10.1016/j.neulet.2005.04.049.
Inanici, Fatma, Soshi Samejima, Parag Gad, V. Reggie Edgerton, Christoph P. Hofstetter, and Chet T. Moritz. 2018. "Transcutaneous Electrical Spinal Stimulation Promotes Long-Term Recovery of Upper Extremity Function in Chronic Tetraplegia." *IEEE Transactions on Neural Systems and Rehabilitation Engineering: A Publication of the IEEE Engineering in Medicine and Biology Society* 26 (6): 1272–78. https://doi.org/10.1109/TNSRE.2018.2834339.
Iwahara, T., Y. Atsuta, E. Garcia-Rill, and R. D. Skinner. 1992. "Spinal Cord Stimulation-Induced Locomotion in the Adult Cat." *Brain Research Bulletin* 28 (1): 99–105.
Jamon, M., and F. Clarac. 1998. "Early Walking in the Neonatal Rat: A Kinematic Study." *Behavioral Neuroscience* 112 (5): 1218–28.
Jankowska, E., M. G. Jukes, S. Lund, and A. Lundberg. 1965. "Reciprocal Innervation through Interneuronal Inhibition." *Nature* 206 (980): 198–99.
Jankowska, E., M. G. Jukes, S. Lund, and A. Lundberg. 1967. "The Effect of DOPA on the Spinal Cord. 6. Half-Centre Organization of Interneurones Transmitting Effects from the Flexor Reflex Afferents." *Acta Physiologica Scandinavica* 70 (3): 389–402. https://doi.org/10.1111/j.1748-1716.1967.tb03637.x.
Jankowska, E., and W. J. Roberts. 1972. "An Electrophysiological Demonstration of the Axonal Projections of Single Spinal Interneurones in the Cat." *The Journal of Physiology* 222 (3): 597–622.
Jian, Rao, Yang Yixu, Lin Sheyu, Shen Jianhong, Yan Yaohua, Su Xing, Huang Qingfeng, et al. 2015. "Repair of Spinal Cord Injury by Chitosan Scaffold with Glioma ECM and SB216763 Implantation in Adult Rats." *Journal of Biomedical Materials Research. Part A* 103 (10): 3259–72. https://doi.org/10.1002/jbm.a.35466.
Jiang, Z., K. P. Carlin, and R. M. Brownstone. 1999. "An in Vitro Functionally Mature Mouse Spinal Cord Preparation for the Study of Spinal Motor Networks." *Brain Research* 816 (2): 493–99.
Jirenhed, Dan-Anders, and Germund Hesslow. 2011. "Learning Stimulus Intervals--Adaptive Timing of Conditioned Purkinje Cell Responses." *Cerebellum (London, England)* 10 (3): 523–35. https://doi.org/10.1007/s12311-011-0264-3.
Johnston, T. E., R. R. Betz, B. T. Smith, B. J. Benda, M. J. Mulcahey, R. Davis, T. P. Houdayer, M. A. Pontari, A. Barriskill, and G. H. Creasey. 2005. "Implantable FES System for Upright Mobility and Bladder and Bowel Function for Individuals with Spinal Cord Injury." *Spinal Cord* 43 (12): 713–23. https://doi.org/10.1038/sj.sc.3101797.
Jonić, S., T. Janković, V. Gajić, and D. Popović. 1999. "Three Machine Learning Techniques for Automatic Determination of Rules to Control Locomotion." *IEEE Transactions on Bio-Medical Engineering* 46 (3): 300–310.
Joseph Modayil, Adam White, and Richard S Sutton. 2014. "Multi-Timescale Nexting in a Reinforcement Learning Robot." *Adaptive Behavior* 22 (2): 146–60. https://doi.org/10.1177/1059712313511648.
Kandel, Eric R. 2013. *Principles of Neural Science, Fifth Edition*. McGraw Hill Professional.
Kanerva, Pentti. 1988. *Sparse Distributed Memory*. MIT Press.
Karlık, Bekir. 2014. "Machine Learning Algorithms for Characterization of EMG Signals." *International Journal of Information and Electronics Engineering* 4 (3). https://doi.org/10.7763/IJIEE.2014.V4.433.

Kasten, M. R., M. D. Sunshine, E. S. Secrist, P. J. Horner, and C. T. Moritz. 2013. "Therapeutic Intraspinal Microstimulation Improves Forelimb Function after Cervical Contusion Injury." *Journal of Neural Engineering* 10 (4): 044001. https://doi.org/10.1088/1741-2560/10/4/044001.

Kehoe, E. James, and Michaela Macrae. 2002. "Fundamental Behavioral Methods and Findings in Classical Conditioning." In *A Neuroscientist's Guide to Classical Conditioning*, edited by John W. Moore, 171–231. New York, NY: Springer New York. https://doi.org/10.1007/978-1-4419-8558-3_6.

Kelly, MF, PA Parker, and RN Scott. 1990. "The Application of Neural Networks to Myoelectric Signal Analysis: A Preliminary Study - IEEE Journals & Magazine" 37: 221–30.

Khazaee, A., and A. Ebrahimzadeh. 2010. "Classification of Electrocardiogram Signals with Support Vector Machines and Genetic Algorithms Using Power Spectral Features." *Biomedical Signal Processing and Control* 5 (4): 252–63. https://doi.org/10.1016/j.bspc.2010.07.006.

Khazaei, Mohammad, and Abbas Erfanian. 2016. "Adaptive Fuzzy Neuro Sliding Mode Control of the Hindlimb Movement Generated by Epidural Spinal Cord Stimulation in Cat." In , 4. La Grande Motte, France.

Kiehn, Ole. 2006. "Locomotor Circuits in the Mammalian Spinal Cord." *Annual Review of Neuroscience* 29: 279–306. https://doi.org/10.1146/annurev.neuro.29.051605.112910.

Kiehn, Ole. 2016. "Decoding the Organization of Spinal Circuits That Control Locomotion." *Nature Reviews. Neuroscience* 17 (4): 224–38. https://doi.org/10.1038/nrn.2016.9.

Kiehn, Ole, and Kimberly Dougherty. 2013. "Locomotion: Circuits and Physiology." In *Neuroscience in the 21st Century: From Basic to Clinical*, edited by Donald W. Pfaff, 1209–36. New York, NY: Springer New York. https://doi.org/10.1007/978-1-4614-1997-6_42.

Kilgore, Kevin L., P. Hunter Peckham, Michael W. Keith, Fred W. Montague, Ronald L. Hart, Martha M. Gazdik, Anne M. Bryden, Scott A. Snyder, and Thomas G. Stage. 2003. "Durability of Implanted Electrodes and Leads in an Upper-Limb Neuroprosthesis." *Journal of Rehabilitation Research and Development* 40 (6): 457–68.

Kim, Young-Hoon, Kee-Yong Ha, and Sang-Il Kim. 2017. "Spinal Cord Injury and Related Clinical Trials." *Clinics in Orthopedic Surgery* 9 (1): 1–9. https://doi.org/10.4055/cios.2017.9.1.1.

Kirkwood, C. A., and B. J. Andrews. 1989. "Finite State Control of FES Systems: Application of AI Inductive Learning Techniques." In *Images of the Twenty-First Century. Proceedings of the Annual International Engineering in Medicine and Biology Society,* 1020–21 vol.3. https://doi.org/10.1109/IEMBS.1989.96065.

Kirkwood, C. A., B. J. Andrews, and P. Mowforth. 1989. "Automatic Detection of Gait Events: A Case Study Using Inductive Learning Techniques." *Journal of Biomedical Engineering* 11 (6): 511–16.

Kirtley, C., M. W. Whittle, and R. J. Jefferson. 1985. "Influence of Walking Speed on Gait Parameters." *Journal of Biomedical Engineering* 7 (4): 282–88.

Klose, K. J., P. L. Jacobs, J. G. Broton, R. S. Guest, B. M. Needham-Shropshire, N. Lebwohl, M. S. Nash, and B. A. Green. 1997. "Evaluation of a Training Program for Persons with SCI Paraplegia Using the Parastep 1 Ambulation System: Part 1. Ambulation Performance and Anthropometric Measures." *Archives of Physical Medicine and Rehabilitation* 78 (8): 789–93.

Kobetic, R., R. J. Triolo, and E. B. Marsolais. 1997. “Muscle Selection and Walking Performance of Multichannel FES Systems for Ambulation in Paraplegia.” *IEEE Transactions on Rehabilitation Engineering: A Publication of the IEEE Engineering in Medicine and Biology Society* 5 (1): 23–29.

Kobetic, R., R. J. Triolo, J. P. Uhlir, C. Bieri, M. Wibowo, G. Polando, E. B. Marsolais, J. A. Davis, and K. A. Ferguson. 1999. “Implanted Functional Electrical Stimulation System for Mobility in Paraplegia: A Follow-up Case Report.” *IEEE Transactions on Rehabilitation Engineering: A Publication of the IEEE Engineering in Medicine and Biology Society* 7 (4): 390–98.

Kobravi, Hamid-Reza, and Abbas Erfanian. 2009. “Decentralized Adaptive Robust Control Based on Sliding Mode and Nonlinear Compensator for the Control of Ankle Movement Using Functional Electrical Stimulation of Agonist-Antagonist Muscles.” *Journal of Neural Engineering* 6 (4): 046007. https://doi.org/10.1088/1741-2560/6/4/046007.

Kobravi, Hamid-Reza, and Abbas Erfanian. 2012. “A Decentralized Adaptive Fuzzy Robust Strategy for Control of Upright Standing Posture in Paraplegia Using Functional Electrical Stimulation.” *Medical Engineering & Physics* 34 (1): 28–37. https://doi.org/10.1016/j.medengphy.2011.06.013.

Koshland, G. F., and J. L. Smith. 1989. “Mutable and Immutable Features of Paw-Shake Responses after Hindlimb Deafferentation in the Cat.” *Journal of Neurophysiology* 62 (1): 162–73. https://doi.org/10.1152/jn.1989.62.1.162.

Kostov, A., B. J. Andrews, D. B. Popović, R. B. Stein, and W. W. Armstrong. 1995. “Machine Learning in Control of Functional Electrical Stimulation Systems for Locomotion.” *IEEE Transactions on Bio-Medical Engineering* 42 (6): 541–51. https://doi.org/10.1109/10.387193.

Kostov, A., R. B. Stein, W. W. Armstrong, and M. Thomas. 1992. “Evaluation of Adaptive Logic Networks for Control of Walking in Paralyzed Patients.” In *1992 14th Annual International Conference of the IEEE Engineering in Medicine and Biology Society*, 4:1332–34. https://doi.org/10.1109/IEMBS.1992.5761816.

Kovacic, Zdenko, and Stjepan Bogdan. 2005. *Fuzzy Controller Design: Theory and Applications*. CRC Press.

Krawetz, P., and P. Nance. 1996. “Gait Analysis of Spinal Cord Injured Subjects: Effects of Injury Level and Spasticity.” *Archives of Physical Medicine and Rehabilitation* 77 (7): 635–38.

Kriellaars, D. J., R. M. Brownstone, B. R. Noga, and L. M. Jordan. 1994. “Mechanical Entrainment of Fictive Locomotion in the Decerebrate Cat.” *Journal of Neurophysiology* 71 (6): 2074–86. https://doi.org/10.1152/jn.1994.71.6.2074.

Kristan, W. B., and J. C. Weeks. 1983. “Neurons Controlling the Initiation, Generation and Modulation of Leech Swimming.” *Symposia of the Society for Experimental Biology* 37: 243–60.

Kudo, N., F. Furukawa, and N. Okado. 1993. “Development of Descending Fibers to the Rat Embryonic Spinal Cord.” *Neuroscience Research* 16 (2): 131–41.

Kudo, N., and T. Yamada. 1987. “Morphological and Physiological Studies of Development of the Monosynaptic Reflex Pathway in the Rat Lumbar Spinal Cord.” *The Journal of Physiology* 389 (August): 441–59.

Kunam, Vamsi K., Vinodkumar Velayudhan, Zeshan A. Chaudhry, Matthew Bobinski, Wendy R. K. Smoker, and Deborah L. Reede. 2018. “Incomplete Cord Syndromes: Clinical and

Imaging Review." *Radiographics: A Review Publication of the Radiological Society of North America, Inc* 38 (4): 1201–22. https://doi.org/10.1148/rg.2018170178.

Kurosawa, Kenji, Ryoko Futami, Takashi Watanabe, and Nozomu Hoshimiya. 2005. "Joint Angle Control by FES Using a Feedback Error Learning Controller." *IEEE Transactions on Neural Systems and Rehabilitation Engineering: A Publication of the IEEE Engineering in Medicine and Biology Society* 13 (3): 359–71. https://doi.org/10.1109/TNSRE.2005.847355.

Kwon, Brian K., Wolfram Tetzlaff, Jonathan N. Grauer, John Beiner, and Alexander R. Vaccaro. 2004. "Pathophysiology and Pharmacologic Treatment of Acute Spinal Cord Injury." *The Spine Journal: Official Journal of the North American Spine Society* 4 (4): 451–64. https://doi.org/10.1016/j.spinee.2003.07.007.

Lafreniere-Roula, Myriam, and David A. McCrea. 2005. "Deletions of Rhythmic Motoneuron Activity during Fictive Locomotion and Scratch Provide Clues to the Organization of the Mammalian Central Pattern Generator." *Journal of Neurophysiology* 94 (2): 1120–32. https://doi.org/10.1152/jn.00216.2005.

Lai, Yun-Ju, Cheng-Li Lin, Yen-Jung Chang, Ming-Chia Lin, Shih-Tan Lee, Fung-Chang Sung, Wen-Yuan Lee, and Chia-Hung Kao. 2014. "Spinal Cord Injury Increases the Risk of Type 2 Diabetes: A Population-Based Cohort Study." *The Spine Journal: Official Journal of the North American Spine Society* 14 (9): 1957–64. https://doi.org/10.1016/j.spinee.2013.12.011.

Lam, Tania, Katherine Pauhl, Amanda Ferguson, Raza N. Malik, BKin, Andrei Krassioukov, and Janice J. Eng. 2015. "Training with Robot-Applied Resistance in People with Motor-Incomplete Spinal Cord Injury: Pilot Study." *Journal of Rehabilitation Research and Development* 52 (1): 113–29. https://doi.org/10.1682/JRRD.2014.03.0090.

Landmesser, L. T., and M. J. O'Donovan. 1984. "Activation Patterns of Embryonic Chick Hind Limb Muscles Recorded in Ovo and in an Isolated Spinal Cord Preparation." *The Journal of Physiology* 347 (February): 189–204.

Lapointe, Nicolas P., Pascal Rouleau, Roth-Visal Ung, and Pierre A. Guertin. 2009. "Specific Role of Dopamine D1 Receptors in Spinal Network Activation and Rhythmic Movement Induction in Vertebrates." *The Journal of Physiology* 587 (Pt 7): 1499–1511. https://doi.org/10.1113/jphysiol.2008.166314.

Lau, Bernice, Lisa Guevremont, and Vivian K. Mushahwar. 2007. "Strategies for Generating Prolonged Functional Standing Using Intramuscular Stimulation or Intraspinal Microstimulation." *IEEE Transactions on Neural Systems and Rehabilitation Engineering: A Publication of the IEEE Engineering in Medicine and Biology Society* 15 (2): 273–85. https://doi.org/10.1109/TNSRE.2007.897030.

Laursen, Christian B., Jørgen F. Nielsen, Ole K. Andersen, and Erika G. Spaich. 2016. "Feasibility of Using Lokomat Combined with Functional Electrical Stimulation for the Rehabilitation of Foot Drop." *European Journal of Translational Myology* 26 (3): 6221. https://doi.org/10.4081/ejtm.2016.6221.

Lavrov, Igor, Yury P. Gerasimenko, Ronaldo M. Ichiyama, Gregoire Courtine, Hui Zhong, Roland R. Roy, and V. Reggie Edgerton. 2006. "Plasticity of Spinal Cord Reflexes after a Complete Transection in Adult Rats: Relationship to Stepping Ability." *Journal of Neurophysiology* 96 (4): 1699–1710. https://doi.org/10.1152/jn.00325.2006.

Lee, C. C. 1990. “Fuzzy Logic in Control Systems: Fuzzy Logic Controller. I.” *IEEE Transactions on Systems, Man, and Cybernetics* 20 (2): 404–18. https://doi.org/10.1109/21.52551.

Lepora, N. F., E. Mavritsaki, J. Porrill, C. H. Yeo, C. Evinger, and P. Dean. 2007. “Evidence from Retractor Bulbi EMG for Linearized Motor Control of Conditioned Nictitating Membrane Responses.” *Journal of Neurophysiology* 98 (4): 2074–88. https://doi.org/10.1152/jn.00210.2007.

Lewicki, Michael S. 1998. “A Review of Methods for Spike Sorting: The Detection and Classification of Neural Action Potentials” 9: 52–78.

Li, Cai, Robert Lowe, and Tom Ziemke. 2013. “Humanoids Learning to Walk: A Natural CPG-Actor-Critic Architecture.” *Frontiers in Neurorobotics* 7: 5. https://doi.org/10.3389/fnbot.2013.00005.

Li, Qiao, Cadathur Rajagopalan, and Gari D. Clifford. 2014. “Ventricular Fibrillation and Tachycardia Classification Using a Machine Learning Approach.” *IEEE Transactions on Bio-Medical Engineering* 61 (6): 1607–13. https://doi.org/10.1109/TBME.2013.2275000.

Li, S., and P. K. Stys. 2000. “Mechanisms of Ionotropic Glutamate Receptor-Mediated Excitotoxicity in Isolated Spinal Cord White Matter.” *The Journal of Neuroscience: The Official Journal of the Society for Neuroscience* 20 (3): 1190–98.

Li, T. S., Y. Su, S. Lai, and J. Hu. 2011. “Walking Motion Generation, Synthesis, and Control for Biped Robot by Using PGRL, LPI, and Fuzzy Logic.” *IEEE Transactions on Systems, Man, and Cybernetics, Part B (Cybernetics)* 41 (3): 736–48. https://doi.org/10.1109/TSMCB.2010.2089978.

Liberson, W. T., H. J. Holmquest, D. Scot, and M. Dow. 1961. “Functional Electrotherapy: Stimulation of the Peroneal Nerve Synchronized with the Swing Phase of the Gait of Hemiplegic Patients.” *Archives of Physical Medicine and Rehabilitation* 42 (February): 101–5.

Liu, Yancheng, Kun Lu, Songhua Yan, Ming Sun, D. Kevin Lester, and Kuan Zhang. 2014. “Gait Phase Varies over Velocities.” *Gait & Posture* 39 (2): 756–60. https://doi.org/10.1016/j.gaitpost.2013.10.009.

Ljungberg, T., P. Apicella, and W. Schultz. 1992. “Responses of Monkey Dopamine Neurons during Learning of Behavioral Reactions.” *Journal of Neurophysiology* 67 (1): 145–63. https://doi.org/10.1152/jn.1992.67.1.145.

Lou, Jenny W. H., Austin J. Bergquist, Abdulaziz Aldayel, Jennifer Czitron, and David F. Collins. 2017. “Interleaved Neuromuscular Electrical Stimulation Reduces Muscle Fatigue.” *Muscle & Nerve* 55 (2): 179–89. https://doi.org/10.1002/mus.25224.

Lovse, Lisa, Jacques Bobet, François D. Roy, Robert Rolf, Vivian K. Mushahwar, and Richard B. Stein. 2012. “External Sensors for Detecting the Activation and Deactivation Times of the Major Muscles Used in Walking.” *IEEE Transactions on Neural Systems and Rehabilitation Engineering: A Publication of the IEEE Engineering in Medicine and Biology Society* 20 (4): 488–98. https://doi.org/10.1109/TNSRE.2012.2203338.

Lu, Donghuan, Karteek Popuri, Gavin Weiguang Ding, Rakesh Balachandar, Mirza Faisal Beg, and Alzheimer’s Disease Neuroimaging Initiative. 2018. “Multimodal and Multiscale Deep Neural Networks for the Early Diagnosis of Alzheimer’s Disease Using Structural MR and FDG-PET Images.” *Scientific Reports* 8 (1): 5697. https://doi.org/10.1038/s41598-018-22871-z.

Lu, Paul, Armin Blesch, Lori Graham, Yaozhi Wang, Ramsey Samara, Karla Banos, Verena Haringer, et al. 2012. "Motor Axonal Regeneration after Partial and Complete Spinal Cord Transection." *The Journal of Neuroscience: The Official Journal of the Society for Neuroscience* 32 (24): 8208–18. https://doi.org/10.1523/JNEUROSCI.0308-12.2012.

Ludvig, Elliot A., Richard S. Sutton, and E. James Kehoe. 2008. "Stimulus Representation and the Timing of Reward-Prediction Errors in Models of the Dopamine System." *Neural Computation* 20 (12): 3034–54. https://doi.org/10.1162/neco.2008.11-07-654.

Ludvig, Elliot A., Richard S. Sutton, and E. James Kehoe. 2012. "Evaluating the TD Model of Classical Conditioning." *Learning & Behavior* 40 (3): 305–19. https://doi.org/10.3758/s13420-012-0082-6.

Lundberg, A. 1965. "[Interaction between the spinal reflex pathways]." *Actualites Neurophysiologiques* 6: 121–37.

Maffiuletti, Nicola A. 2010. "Physiological and Methodological Considerations for the Use of Neuromuscular Electrical Stimulation." *European Journal of Applied Physiology* 110 (2): 223–34. https://doi.org/10.1007/s00421-010-1502-y.

Marchal-Crespo, Laura, and David J. Reinkensmeyer. 2009. "Review of Control Strategies for Robotic Movement Training after Neurologic Injury." *Journal of Neuroengineering and Rehabilitation* 6 (June): 20. https://doi.org/10.1186/1743-0003-6-20.

Marigold, Daniel S. 2008. "Role of Peripheral Visual Cues in Online Visual Guidance of Locomotion." *Exercise and Sport Sciences Reviews* 36 (3): 145–51. https://doi.org/10.1097/JES.0b013e31817bff72.

Marigold, Daniel S., and Aftab E. Patla. 2005. "Adapting Locomotion to Different Surface Compliances: Neuromuscular Responses and Changes in Movement Dynamics." *Journal of Neurophysiology* 94 (3): 1733–50. https://doi.org/10.1152/jn.00019.2005.

Martin, Mario, Enrique Contreras-Hernández, Javier Béjar, Gennaro Esposito, Diógenes Chávez, Silvio Glusman, Ulises Cortés, and Pablo Rudomin. 2015. "A Machine Learning Methodology for the Selection and Classification of Spontaneous Spinal Cord Dorsum Potentials Allows Disclosure of Structured (Non-Random) Changes in Neuronal Connectivity Induced by Nociceptive Stimulation." *Frontiers in Neuroinformatics* 9: 21. https://doi.org/10.3389/fninf.2015.00021.

Mathews, Miranda A., Aaron J. Camp, and Andrew J. Murray. 2017. "Reviewing the Role of the Efferent Vestibular System in Motor and Vestibular Circuits." *Frontiers in Physiology* 8: 552. https://doi.org/10.3389/fphys.2017.00552.

Matjačić, Z., K. Hunt, H. Gollee, and T. Sinkjaer. 2003. "Control of Posture with FES Systems." *Medical Engineering & Physics* 25 (1): 51–62.

Mazurek, K. A., B. J. Holinski, D. G. Everaert, R. B. Stein, R. Etienne-Cummings, and V. K. Mushahwar. 2012. "Feed Forward and Feedback Control for Over-Ground Locomotion in Anaesthetized Cats." *Journal of Neural Engineering* 9 (2): 026003. https://doi.org/10.1088/1741-2560/9/2/026003.

Mazurek, K., B.J. Holinski, D.G. Everaert, R.B. Stein, V.K. Mushahwar, and R. Etienne-Cummings. 2010. "Locomotion Processing Unit." In *2010 IEEE Biomedical Circuits and Systems Conference (BioCAS)*, 286–89. https://doi.org/10.1109/BIOCAS.2010.5709627.

Mazurek, Kevin A., Bradley J. Holinski, Dirk G. Everaert, Vivian K. Mushahwar, and Ralph Etienne-Cummings. 2016. "A Mixed-Signal VLSI System for Producing Temporally Adapting Intraspinal Microstimulation Patterns for Locomotion." *IEEE Transactions on*

Biomedical Circuits and Systems 10 (4): 902–11. https://doi.org/10.1109/TBCAS.2015.2501419.
McCormick, D. A., and R. F. Thompson. 1984. "Cerebellum: Essential Involvement in the Classically Conditioned Eyelid Response." *Science (New York, N.Y.)* 223 (4633): 296–99.
McCrea, David A., and Ilya A. Rybak. 2007. "Modeling the Mammalian Locomotor CPG: Insights from Mistakes and Perturbations." *Progress in Brain Research* 165: 235–53. https://doi.org/10.1016/S0079-6123(06)65015-2.
McCrea, David A., and Ilya A. Rybak. 2008. "Organization of Mammalian Locomotor Rhythm and Pattern Generation." *Brain Research Reviews* 57 (1): 134–46. https://doi.org/10.1016/j.brainresrev.2007.08.006.
McGinty, Vincent B., Sylvie Lardeux, Sharif A. Taha, James J. Kim, and Saleem M. Nicola. 2013. "Invigoration of Reward Seeking by Cue and Proximity Encoding in the Nucleus Accumbens." *Neuron* 78 (5): 910–22. https://doi.org/10.1016/j.neuron.2013.04.010.
McVea, D. A., J. M. Donelan, A. Tachibana, and K. G. Pearson. 2005. "A Role for Hip Position in Initiating the Swing-to-Stance Transition in Walking Cats." *Journal of Neurophysiology* 94 (5): 3497–3508. https://doi.org/10.1152/jn.00511.2005.
McVea, D. A., and K. G. Pearson. 2007. "Long-Lasting, Context-Dependent Modification of Stepping in the Cat after Repeated Stumbling-Corrective Responses." *Journal of Neurophysiology* 97 (1): 659–69. https://doi.org/10.1152/jn.00921.2006.
Menendez de la Prida, L., S. Bolea, and J. V. Sanchez-Andres. 1996. "Analytical Characterization of Spontaneous Activity Evolution during Hippocampal Development in the Rabbit." *Neuroscience Letters* 218 (3): 185–87.
Mentis, George Z., Dvir Blivis, Wenfang Liu, Estelle Drobac, Melissa E. Crowder, Lingling Kong, Francisco J. Alvarez, Charlotte J. Sumner, and Michael J. O'Donovan. 2011. "Early Functional Impairment of Sensory-Motor Connectivity in a Mouse Model of Spinal Muscular Atrophy." *Neuron* 69 (3): 453–67. https://doi.org/10.1016/j.neuron.2010.12.032.
Mercier, L. M., E. J. Gonzalez-Rothi, K. A. Streeter, S. S. Posgai, A. S. Poirier, D. D. Fuller, P. J. Reier, and D. M. Baekey. 2017. "Intraspinal Microstimulation and Diaphragm Activation after Cervical Spinal Cord Injury." *Journal of Neurophysiology* 117 (2): 767–76. https://doi.org/10.1152/jn.00721.2016.
Merrill, Daniel R., Marom Bikson, and John G. R. Jefferys. 2005. "Electrical Stimulation of Excitable Tissue: Design of Efficacious and Safe Protocols." *Journal of Neuroscience Methods* 141 (2): 171–98. https://doi.org/10.1016/j.jneumeth.2004.10.020.
Messina, J. A., Alison St Paul, Sarah Hargis, Wengora E. Thompson, and Andrew D. McClellan. 2017. "Elimination of Left-Right Reciprocal Coupling in the Adult Lamprey Spinal Cord Abolishes the Generation of Locomotor Activity." *Frontiers in Neural Circuits* 11: 89. https://doi.org/10.3389/fncir.2017.00089.
Miller, Jason D., Mahyo Seyedali Beazer, and Michael E. Hahn. 2013. "Myoelectric Walking Mode Classification for Transtibial Amputees." *IEEE Transactions on Bio-Medical Engineering* 60 (10): 2745–50. https://doi.org/10.1109/TBME.2013.2264466.
Miller, S., and P. D. Scott. 1977. "The Spinal Locomotor Generator." *Experimental Brain Research* 30 (2–3): 387–403.
Minassian, K., I. Persy, F. Rattay, M. M. Pinter, H. Kern, and M. R. Dimitrijevic. 2007. "Human Lumbar Cord Circuitries Can Be Activated by Extrinsic Tonic Input to Generate

Locomotor-like Activity." *Human Movement Science* 26 (2): 275–95. https://doi.org/10.1016/j.humov.2007.01.005.
Minassian, Karen, Ursula S. Hofstoetter, Simon M. Danner, Winfried Mayr, Joy A. Bruce, W. Barry McKay, and Keith E. Tansey. 2016. "Spinal Rhythm Generation by Step-Induced Feedback and Transcutaneous Posterior Root Stimulation in Complete Spinal Cord-Injured Individuals." *Neurorehabilitation and Neural Repair* 30 (3): 233–43. https://doi.org/10.1177/1545968315591706.
Minsky, Marvin, Seymour A. Papert, and Léon Bottou. 2017. *Perceptrons: An Introduction to Computational Geometry*. MIT Press.
Mirbagheri, Mehdi M., Michel Ladouceur, Hugues Barbeau, and Robert E. Kearney. 2002. "The Effects of Long-Term FES-Assisted Walking on Intrinsic and Reflex Dynamic Stiffness in Spastic Spinal-Cord-Injured Subjects." *IEEE Transactions on Neural Systems and Rehabilitation Engineering: A Publication of the IEEE Engineering in Medicine and Biology Society* 10 (4): 280–89. https://doi.org/10.1109/TNSRE.2002.806838.
Modayil, Joseph, and Richard S. Sutton. 2014. "Prediction Driven Behavior: Learning Predictions That Drive Fixed Responses." 2014. https://www.aaai.org/ocs/index.php/WS/AAAIW14/paper/view/8740.
Modayil, Joseph, Adam White, Patrick M Pilarski, and Richard S Sutton. 2012. "Acquiring Diverse Predictive Knowledge in Real Time by Temporal-Difference Learning." In *IEEE International Conference on Systems, Man, and Cybernetics (SMC 2012)*, 1903–10. Seoul, Korea.
Mondello, Sarah E., Michael R. Kasten, Philip J. Horner, and Chet T. Moritz. 2014. "Therapeutic Intraspinal Stimulation to Generate Activity and Promote Long-Term Recovery." *Frontiers in Neuroscience* 8: 21. https://doi.org/10.3389/fnins.2014.00021.
Montague, P. R., P. Dayan, and T. J. Sejnowski. 1996. "A Framework for Mesencephalic Dopamine Systems Based on Predictive Hebbian Learning." *The Journal of Neuroscience: The Official Journal of the Society for Neuroscience* 16 (5): 1936–47.
Mooney, R., A. A. Penn, R. Gallego, and C. J. Shatz. 1996. "Thalamic Relay of Spontaneous Retinal Activity Prior to Vision." *Neuron* 17 (5): 863–74.
Moore, C. D., B. C. Craven, L. Thabane, A. C. Laing, A. W. Frank-Wilson, S. A. Kontulainen, A. Papaioannou, J. D. Adachi, and L. M. Giangregorio. 2015. "Lower-Extremity Muscle Atrophy and Fat Infiltration after Chronic Spinal Cord Injury." *Journal of Musculoskeletal & Neuronal Interactions* 15 (1): 32–41.
Mori, S., K. Matsuyama, J. Kohyama, Y. Kobayashi, and K. Takakusaki. 1992. "Neuronal Constituents of Postural and Locomotor Control Systems and Their Interactions in Cats." *Brain & Development* 14 Suppl (May): S109-120.
Mori, S., M. L. Shik, and A. S. Yagodnitsyn. 1977. "Role of Pontine Tegmentum for Locomotor Control in Mesencephalic Cat." *Journal of Neurophysiology* 40 (2): 284–95. https://doi.org/10.1152/jn.1977.40.2.284.
Morimoto, J., and C. G. Atkeson. 2007. "Learning Biped Locomotion." *IEEE Robotics Automation Magazine* 14 (2): 41–51. https://doi.org/10.1109/MRA.2007.380654.
Moritz, Chet T., Timothy H. Lucas, Steve I. Perlmutter, and Eberhard E. Fetz. 2007. "Forelimb Movements and Muscle Responses Evoked by Microstimulation of Cervical Spinal Cord in Sedated Monkeys." *Journal of Neurophysiology* 97 (1): 110–20. https://doi.org/10.1152/jn.00414.2006.

Morrison, Sarah A., Douglas Lorenz, Carol P. Eskay, Gail F. Forrest, and D. Michele Basso. 2018. "Longitudinal Recovery and Reduced Costs After 120 Sessions of Locomotor Training for Motor Incomplete Spinal Cord Injury." *Archives of Physical Medicine and Rehabilitation* 99 (3): 555–62. https://doi.org/10.1016/j.apmr.2017.10.003.

Morton, Susanne M., and Amy J. Bastian. 2006. "Cerebellar Contributions to Locomotor Adaptations during Splitbelt Treadmill Walking." *The Journal of Neuroscience: The Official Journal of the Society for Neuroscience* 26 (36): 9107–16. https://doi.org/10.1523/JNEUROSCI.2622-06.2006.

Mulder, A. J., H. B. Boom, H. J. Hermens, and G. Zilvold. 1990. "Artificial-Reflex Stimulation for FES-Induced Standing with Minimum Quadriceps Force." *Medical & Biological Engineering & Computing* 28 (5): 483–88.

Müller-Putz, Gernot R., Reinhold Scherer, Gert Pfurtscheller, and Christa Neuper. 2010. "Temporal Coding of Brain Patterns for Direct Limb Control in Humans." *Frontiers in Neuroscience* 4. https://doi.org/10.3389/fnins.2010.00034.

Murray, M., and I. Fischer. 2001. "Transplantation and Gene Therapy: Combined Approaches for Repair of Spinal Cord Injury." *The Neuroscientist: A Review Journal Bringing Neurobiology, Neurology and Psychiatry* 7 (1): 28–41. https://doi.org/10.1177/107385840100700107.

Murray, Spencer A., Kevin H. Ha, and Michael Goldfarb. 2014. "An Assistive Controller for a Lower-Limb Exoskeleton for Rehabilitation after Stroke, and Preliminary Assessment Thereof." *Conference Proceedings : ... Annual International Conference of the IEEE Engineering in Medicine and Biology Society. IEEE Engineering in Medicine and Biology Society. Annual Conference* 2014: 4083–86. https://doi.org/10.1109/EMBC.2014.6944521.

Mushahwar, and K. W. Horch. 1997. "INTERLEAVED DUAL-CHANNEL STIMULATION OF THE VENTRAL LUMBO-SACRAL SPINAL CORD REDUCES MUSCLE FATIGUE." 1997.

Mushahwar, V. K., D. F. Collins, and A. Prochazka. 2000. "Spinal Cord Microstimulation Generates Functional Limb Movements in Chronically Implanted Cats." *Experimental Neurology* 163 (2): 422–29. https://doi.org/10.1006/exnr.2000.7381.

Mushahwar, V. K., and K. W. Horch. 1998. "Selective Activation and Graded Recruitment of Functional Muscle Groups through Spinal Cord Stimulation." *Annals of the New York Academy of Sciences* 860 (November): 531–35.

Mushahwar, V. K., and K. W. Horch. 2000. "Selective Activation of Muscle Groups in the Feline Hindlimb through Electrical Microstimulation of the Ventral Lumbo-Sacral Spinal Cord." *IEEE Transactions on Rehabilitation Engineering: A Publication of the IEEE Engineering in Medicine and Biology Society* 8 (1): 11–21.

Mushahwar, V. K., A. Prochazka, P. H. Ellaway, L. Guevremont, and R. A. Gaunt. 2003. "Microstimulation in CNS Excites Axons before Neuronal Cell Bodies." 2003. https://www.sfn.org:443/annual-meeting/past-and-future-annual-meetings/abstract-archive/abstract-archive-search.

Mushahwar, Vivian K., Deborah M. Gillard, Michel J. A. Gauthier, and Arthur Prochazka. 2002. "Intraspinal Micro Stimulation Generates Locomotor-like and Feedback-Controlled Movements." *IEEE Transactions on Neural Systems and Rehabilitation Engineering: A Publication of the IEEE Engineering in Medicine and Biology Society* 10 (1): 68–81. https://doi.org/10.1109/TNSRE.2002.1021588.

Mushahwar, Vivian K., Lisa Guevremont, and Rajiv Saigal. 2006. "Could Cortical Signals Control Intraspinal Stimulators? A Theoretical Evaluation." *IEEE Transactions on Neural Systems and Rehabilitation Engineering: A Publication of the IEEE Engineering in Medicine and Biology Society* 14 (2): 198–201. https://doi.org/10.1109/TNSRE.2006.875532.

Musienko, P. E., I. N. Bogacheva, and Yu P. Gerasimenko. 2007. "Significance of Peripheral Feedback in the Generation of Stepping Movements during Epidural Stimulation of the Spinal Cord." *Neuroscience and Behavioral Physiology* 37 (2): 181–90. https://doi.org/10.1007/s11055-007-0166-5.

Musienko, Pavel, Gregoire Courtine, Jameson E. Tibbs, Vyacheslav Kilimnik, Alexandr Savochin, Alan Garfinkel, Roland R. Roy, V. Reggie Edgerton, and Yury Gerasimenko. 2012. "Somatosensory Control of Balance during Locomotion in Decerebrated Cat." *Journal of Neurophysiology* 107 (8): 2072–82. https://doi.org/10.1152/jn.00730.2011.

Musienko, Pavel, Janine Heutschi, Lucia Friedli, Rubia van den Brand, and Grégoire Courtine. 2012. "Multi-System Neurorehabilitative Strategies to Restore Motor Functions Following Severe Spinal Cord Injury." *Experimental Neurology* 235 (1): 100–109. https://doi.org/10.1016/j.expneurol.2011.08.025.

Musselman, Kristin E., Karim Fouad, John E. Misiaszek, and Jaynie F. Yang. 2009. "Training of Walking Skills Overground and on the Treadmill: Case Series on Individuals with Incomplete Spinal Cord Injury." *Physical Therapy* 89 (6): 601–11. https://doi.org/10.2522/ptj.20080257.

Myers, Christopher P., Joseph W. Lewcock, M. Gartz Hanson, Simon Gosgnach, James B. Aimone, Fred H. Gage, Kuo-Fen Lee, Lynn T. Landmesser, and Samuel L. Pfaff. 2005. "Cholinergic Input Is Required during Embryonic Development to Mediate Proper Assembly of Spinal Locomotor Circuits." *Neuron* 46 (1): 37–49. https://doi.org/10.1016/j.neuron.2005.02.022.

Nakayama, K., H. Nishimaru, M. Iizuka, S. Ozaki, and N. Kudo. 1999. "Rostrocaudal Progression in the Development of Periodic Spontaneous Activity in Fetal Rat Spinal Motor Circuits in Vitro." *Journal of Neurophysiology* 81 (5): 2592–95. https://doi.org/10.1152/jn.1999.81.5.2592.

Nashold, B. S., H. Friedman, and S. Boyarsky. 1971. "Electrical Activation of Micturition by Spinal Cord Stimulation." *The Journal of Surgical Research* 11 (3): 144–47.

Nashold, B. S., H. Friedman, J. F. Glenn, J. H. Grimes, W. F. Barry, and R. Avery. 1972. "Electromicturition in Paraplegia. Implantation of a Spinal Neuroprosthesis." *Archives of Surgery (Chicago, Ill.: 1960)* 104 (2): 195–202.

Nashold, B. S., H. Friedman, and J. Grimes. 1981. "Electrical Stimulation of the Conus Medullaris to Control the Bladder in the Paraplegic Patient. A 10-Year Review." *Applied Neurophysiology* 44 (4): 225–32.

Nekoukar, Vahab, and Abbas Erfanian. 2010. "Adaptive Terminal Sliding Mode Control of Ankle Movement Using Functional Electrical Stimulation of Agonist-Antagonist Muscles." *Conference Proceedings: ... Annual International Conference of the IEEE Engineering in Medicine and Biology Society. IEEE Engineering in Medicine and Biology Society. Annual Conference* 2010: 5448–51. https://doi.org/10.1109/IEMBS.2010.5626508.

Nekoukar, Vahab, and Abbas Erfanian. 2012. "A Decentralized Modular Control Framework for Robust Control of FES-Activated Walker-Assisted Paraplegic Walking Using Terminal

Sliding Mode and Fuzzy Logic Control." *IEEE Transactions on Bio-Medical Engineering* 59 (10): 2818–27. https://doi.org/10.1109/TBME.2012.2208963.
Ng, Andrew. 2012. "Coursera: Machine Learning, Linear Regression with One Variable." Stanford University.
Nicola, Saleem M., Irene A. Yun, Ken T. Wakabayashi, and Howard L. Fields. 2004. "Cue-Evoked Firing of Nucleus Accumbens Neurons Encodes Motivational Significance during a Discriminative Stimulus Task." *Journal of Neurophysiology* 91 (4): 1840–65. https://doi.org/10.1152/jn.00657.2003.
Nishimaru, H., M. Iizuka, S. Ozaki, and N. Kudo. 1996. "Spontaneous Motoneuronal Activity Mediated by Glycine and GABA in the Spinal Cord of Rat Fetuses in Vitro." *The Journal of Physiology* 497 (Pt 1) (November): 131–43.
Nistor, Gabriel I., Minodora O. Totoiu, Nadia Haque, Melissa K. Carpenter, and Hans S. Keirstead. 2005. "Human Embryonic Stem Cells Differentiate into Oligodendrocytes in High Purity and Myelinate after Spinal Cord Transplantation." *Glia* 49 (3): 385–96. https://doi.org/10.1002/glia.20127.
Noga, B. R., J. Kettler, and L. M. Jordan. 1988. "Locomotion Produced in Mesencephalic Cats by Injections of Putative Transmitter Substances and Antagonists into the Medial Reticular Formation and the Pontomedullary Locomotor Strip." *The Journal of Neuroscience: The Official Journal of the Society for Neuroscience* 8 (6): 2074–86.
Noonan, Vanessa K., Matthew Fingas, Angela Farry, David Baxter, Anoushka Singh, Michael G. Fehlings, and Marcel F. Dvorak. 2012. "Incidence and Prevalence of Spinal Cord Injury in Canada: A National Perspective." *Neuroepidemiology* 38 (4): 219–26. https://doi.org/10.1159/000336014.
Novikova, Liudmila N., Mallappa K. Kolar, Paul J. Kingham, Andreas Ullrich, Sven Oberhoffner, Monika Renardy, Michael Doser, Erhard Müller, Mikael Wiberg, and Lev N. Novikov. 2017. "Trimethylene Carbonate-Caprolactone Conduit with Poly-p-Dioxanone Microfilaments to Promote Regeneration after Spinal Cord Injury." *Acta Biomaterialia*, November. https://doi.org/10.1016/j.actbio.2017.11.028.
O'Dell, Michael W., Kari Dunning, Patricia Kluding, Samuel S. Wu, Jody Feld, Jivan Ginosian, and Keith McBride. 2014. "Response and Prediction of Improvement in Gait Speed from Functional Electrical Stimulation in Persons with Poststroke Drop Foot." *PM & R: The Journal of Injury, Function, and Rehabilitation* 6 (7): 587–601; quiz 601. https://doi.org/10.1016/j.pmrj.2014.01.001.
O'Donovan, M. J. 1987. "In Vitro Methods for the Analysis of Motor Function in the Developing Spinal Cord of the Chick Embryo." *Medicine and Science in Sports and Exercise* 19 (5 Suppl): S130-133.
O'Donovan, M. J. 1999. "The Origin of Spontaneous Activity in Developing Networks of the Vertebrate Nervous System." *Current Opinion in Neurobiology* 9 (1): 94–104.
O'Donovan, M. J., N. Chub, and P. Wenner. 1998. "Mechanisms of Spontaneous Activity in Developing Spinal Networks." *Journal of Neurobiology* 37 (1): 131–45.
O'Donovan, M. J., and L. Landmesser. 1987. "The Development of Hindlimb Motor Activity Studied in the Isolated Spinal Cord of the Chick Embryo." *The Journal of Neuroscience: The Official Journal of the Society for Neuroscience* 7 (10): 3256–64.
Ok, Ji-Hoon, Young-Hoon Kim, and Kee-Yong Ha. 2012. "Neuroprotective Effects of Hypothermia after Spinal Cord Injury in Rats: Comparative Study between Epidural

Hypothermia and Systemic Hypothermia." *Spine* 37 (25): E1551-1559. https://doi.org/10.1097/BRS.0b013e31826ff7f1.
Orlovskiĭ, G. N., F. V. Severin, and M. L. Shik. 1966. "[Locomotion induced by stimulation of the mesencephalon]." *Doklady Akademii nauk SSSR* 169 (5): 1223–26.
Orsal, D., J. M. Cabelguen, and C. Perret. 1990. "Interlimb Coordination during Fictive Locomotion in the Thalamic Cat." *Experimental Brain Research* 82 (3): 536–46.
Pang, M. Y., and J. F. Yang. 2000. "The Initiation of the Swing Phase in Human Infant Stepping: Importance of Hip Position and Leg Loading." *The Journal of Physiology* 528 Pt 2 (October): 389–404.
Pangratz-Fuehrer, Susanne, Werner Sieghart, Uwe Rudolph, Isabel Parada, and John R. Huguenard. 2016. "Early Postnatal Switch in GABAA Receptor α-Subunits in the Reticular Thalamic Nucleus." *Journal of Neurophysiology* 115 (3): 1183–95. https://doi.org/10.1152/jn.00905.2015.
Papadimitriou, S., S. Mavroudi, L. Vladutu, and A. Bezerianos. 2001. "Ischemia Detection with a Self-Organizing Map Supplemented by Supervised Learning." *IEEE Transactions on Neural Networks* 12 (3): 503–15. https://doi.org/10.1109/72.925554.
Papaloukas, C, DI Fotiadis, A Likas, and LK Michalis. 2003. "Automated Methods for Ischemia Detection in Long-Duration ECGs." *Medscape* 24: 313–19.
Park, Eugene, Alexander A. Velumian, and Michael G. Fehlings. 2004. "The Role of Excitotoxicity in Secondary Mechanisms of Spinal Cord Injury: A Review with an Emphasis on the Implications for White Matter Degeneration." *Journal of Neurotrauma* 21 (6): 754–74. https://doi.org/10.1089/0897715041269641.
Parkhi, Omkar M., Andrea Vedaldi, and Andrew Zisserman. 2015. "Deep Face Recognition." In *Procedings of the British Machine Vision Conference 2015*, 41.1-41.12. Swansea: British Machine Vision Association. https://doi.org/10.5244/C.29.41.
Pavlov, Ivan Petrovich. 1883. "The Work of the Digestive Glands." *Bristol Medico-Chirurgical Journal (1883)* 21 (80). https://www.ncbi.nlm.nih.gov/pmc/articles/PMC5046328/.
Pearson, K. G. 1995. "Proprioceptive Regulation of Locomotion." *Current Opinion in Neurobiology* 5 (6): 786–91.
Pearson, K. G., and D. F. Collins. 1993. "Reversal of the Influence of Group Ib Afferents from Plantaris on Activity in Medial Gastrocnemius Muscle during Locomotor Activity." *Journal of Neurophysiology* 70 (3): 1009–17. https://doi.org/10.1152/jn.1993.70.3.1009.
Pearson, K. G., and S. Rossignol. 1991. "Fictive Motor Patterns in Chronic Spinal Cats." *Journal of Neurophysiology* 66 (6): 1874–87. https://doi.org/10.1152/jn.1991.66.6.1874.
Peckham, P. Hunter, and Jayme S. Knutson. 2005. "Functional Electrical Stimulation for Neuromuscular Applications." *Annual Review of Biomedical Engineering* 7: 327–60. https://doi.org/10.1146/annurev.bioeng.6.040803.140103.
Pépin, A., K. E. Norman, and H. Barbeau. 2003. "Treadmill Walking in Incomplete Spinal-Cord-Injured Subjects: 1. Adaptation to Changes in Speed." *Spinal Cord* 41 (5): 257–70. https://doi.org/10.1038/sj.sc.3101452.
Pierrot-Deseilligny, E., and D. Mazevet. 2000. "The Monosynaptic Reflex: A Tool to Investigate Motor Control in Humans. Interest and Limits." *Neurophysiologie Clinique = Clinical Neurophysiology* 30 (2): 67–80.
Pilarski, P. M., M. R. Dawson, T. Degris, J. P. Carey, and R. S. Sutton. 2012. "Dynamic Switching and Real-Time Machine Learning for Improved Human Control of Assistive Biomedical Robots." In *2012 4th IEEE RAS EMBS International Conference on*

Biomedical Robotics and Biomechatronics (BioRob), 296–302. https://doi.org/10.1109/BioRob.2012.6290309.

Pilarski, Patrick M., Michael R. Dawson, Thomas Degris, Jason P. Carey, K. Ming Chan, Jacqueline S. Hebert, and Richard S. Sutton. 2013a. "Adaptive Artificial Limbs: A Real-Time Approach to Prediction and Anticipation." *IEEE Robotics Automation Magazine* 20 (1): 53–64.

Pilarski, Patrick M., Travis B. Dick, and Richard S. Sutton. 2013b. "Real-Time Prediction Learning for the Simultaneous Actuation of Multiple Prosthetic Joints." *IEEE ... International Conference on Rehabilitation Robotics: [Proceedings]* 2013 (June): 6650435. https://doi.org/10.1109/ICORR.2013.6650435.

Pineau, Isabelle, and Steve Lacroix. 2007. "Proinflammatory Cytokine Synthesis in the Injured Mouse Spinal Cord: Multiphasic Expression Pattern and Identification of the Cell Types Involved." *The Journal of Comparative Neurology* 500 (2): 267–85. https://doi.org/10.1002/cne.21149.

Pinter, M. M., F. Gerstenbrand, and M. R. Dimitrijevic. 2000. "Epidural Electrical Stimulation of Posterior Structures of the Human Lumbosacral Cord: 3. Control Of Spasticity." *Spinal Cord* 38 (9): 524–31.

Pisotta, Iolanda, and Marco Molinari. 2014. "Cerebellar Contribution to Feedforward Control of Locomotion." *Frontiers in Human Neuroscience* 8: 475. https://doi.org/10.3389/fnhum.2014.00475.

Popović, D. B. 1993. "Finite State Model of Locomotion for Functional Electrical Stimulation Systems." *Progress in Brain Research* 97: 397–407.

Popović, D., R. B. Stein, N. Oğuztöreli, M. Lebiedowska, and S. Jonić. 1999. "Optimal Control of Walking with Functional Electrical Stimulation: A Computer Simulation Study." *IEEE Transactions on Rehabilitation Engineering: A Publication of the IEEE Engineering in Medicine and Biology Society* 7 (1): 69–79.

Popović, Dejan, Milovan Radulović, Laszlo Schwirtlich, and Novak Jauković. 2003. "Automatic vs Hand-Controlled Walking of Paraplegics." *Medical Engineering & Physics* 25 (1): 63–73.

Prochazka, A. 1993. "Comparison of Natural and Artificial Control of Movement." *IEEE Transactions on Rehabilitation Engineering* 1 (1): 7–17. https://doi.org/10.1109/86.242403.

Prochazka, A., K. H. Sontag, and P. Wand. 1978. "Motor Reactions to Perturbations of Gait: Proprioceptive and Somesthetic Involvement." *Neuroscience Letters* 7 (1): 35–39.

Prochazka, Arthur. 1996. "Proprioceptive Feedback and Movement Regulation." In *Handbook of Physiology. Exercise: Regulation and Integration of Multiple Systems. Neural Control of Movement.*, 89–127. 12. Bethesda, MD: Am. Physiol. Soc. https://onlinelibrary-wiley-com.login.ezproxy.library.ualberta.ca/doi/full/10.1002/cphy.cp120103.

Prochazka, Arthur. 2011. "Proprioceptive Feedback and Movement Regulation." In *Comprehensive Physiology*, 89–127. American Cancer Society. https://doi.org/10.1002/cphy.cp120103.

Prochazka, Arthur, and Sergiy Yakovenko. 2007. "Predictive and Reactive Tuning of the Locomotor CPG." *Integrative and Comparative Biology* 47 (4): 474–81. https://doi.org/10.1093/icb/icm065.

Qi, H., D. J. Tyler, and D. M. Durand. 1999. "Neurofuzzy Adaptive Controlling of Selective Stimulation for FES: A Case Study." *IEEE Transactions on Rehabilitation Engineering: A Publication of the IEEE Engineering in Medicine and Biology Society* 7 (2): 183–92.
Quinlan, J R. 1992. "LEARNING WITH CONTINUOUS CLASSES," 6.
Quintern, J., R. Riener, and S. Rupprecht. 1997. "Comparison of Simulation and Experiments of Different Closed-Loop Strategies for Functional Electrical Stimulation: Experiments in Paraplegics." *Artificial Organs* 21 (3): 232–35.
Quintero, Hugo A., Ryan J. Farris, and Michael Goldfarb. 2012. "A Method for the Autonomous Control of Lower Limb Exo-Skeletons for Persons with Paraplegia." *Journal of Medical Devices* 6 (4). https://doi.org/10.1115/1.4007181.
Raisman, G. 2001. "Olfactory Ensheathing Cells - Another Miracle Cure for Spinal Cord Injury?" *Nature Reviews. Neuroscience* 2 (5): 369–75. https://doi.org/10.1038/35072576.
Ramer, Leanne M., Edmund Au, Miranda W. Richter, Jie Liu, Wolfram Tetzlaff, and A. Jane Roskams. 2004. "Peripheral Olfactory Ensheathing Cells Reduce Scar and Cavity Formation and Promote Regeneration after Spinal Cord Injury." *The Journal of Comparative Neurology* 473 (1): 1–15. https://doi.org/10.1002/cne.20049.
Rangappa, P, J Jeyadoss, A Flabouris, JM Clark, and R Marshall. 2010. "Cardiac Pacing in Patients with a Cervical Spinal Cord Injury." 2010. http://www.ncbi.nlm.nih.gov/pubmed/20498664.
Raslan, A. M., S. McCartney, and K. J. Burchiel. 2007. "Management of Chronic Severe Pain: Spinal Neuromodulatory and Neuroablative Approaches." *Acta Neurochirurgica. Supplement* 97 (Pt 1): 33–41.
Rehman, Ibraheem, and Chaudhry I. Rehman. 2018. "Classical Conditioning." In *StatPearls*. Treasure Island (FL): StatPearls Publishing. http://www.ncbi.nlm.nih.gov/books/NBK470326/.
Rejc, Enrico, Claudia Angeli, and Susan Harkema. 2015. "Effects of Lumbosacral Spinal Cord Epidural Stimulation for Standing after Chronic Complete Paralysis in Humans." *PLOS ONE* 10 (7): e0133998. https://doi.org/10.1371/journal.pone.0133998.
Rekand, Tiina, Ellen Merete Hagen, and Marit Grønning. 2012. "Spasticity Following Spinal Cord Injury." *Tidsskrift for Den Norske Laegeforening: Tidsskrift for Praktisk Medicin, Ny Raekke* 132 (8): 970–73. https://doi.org/10.4045/tidsskr.10.0872.
Ren, Jun, and John J. Greer. 2003. "Ontogeny of Rhythmic Motor Patterns Generated in the Embryonic Rat Spinal Cord." *Journal of Neurophysiology* 89 (3): 1187–95. https://doi.org/10.1152/jn.00539.2002.
Renaudo, Erwan, Benoît Girard, Raja Chatila, and Mehdi Khamassi. 2014. "Design of a Control Architecture for Habit Learning in Robots." In *Biomimetic and Biohybrid Systems*, edited by Armin Duff, Nathan F. Lepora, Anna Mura, Tony J. Prescott, and Paul F. M. J. Verschure, 8608:249–60. Cham: Springer International Publishing. https://doi.org/10.1007/978-3-319-09435-9_22.
Renshaw, Birdsey. 1940. "Activity in the Simplest Spinal Reflex Pathways." *Journal of Neurophysiology* 3 (5): 373–87. https://doi.org/10.1152/jn.1940.3.5.373.
Richardson, R. R., and D. G. McLone. 1978. "Percutaneous Epidural Neurostimulation for Paraplegic Spasticity." *Surgical Neurology* 9 (3): 153–55.
Roitman, Mitchell F., Robert A. Wheeler, and Regina M. Carelli. 2005. "Nucleus Accumbens Neurons Are Innately Tuned for Rewarding and Aversive Taste Stimuli, Encode Their

Predictors, and Are Linked to Motor Output." *Neuron* 45 (4): 587–97. https://doi.org/10.1016/j.neuron.2004.12.055.
Romero, M. I., N. Rangappa, L. Li, E. Lightfoot, M. G. Garry, and G. M. Smith. 2000. "Extensive Sprouting of Sensory Afferents and Hyperalgesia Induced by Conditional Expression of Nerve Growth Factor in the Adult Spinal Cord." *The Journal of Neuroscience: The Official Journal of the Society for Neuroscience* 20 (12): 4435–45.
Romo, R., and W. Schultz. 1987. "Neuronal Activity Preceding Self-Initiated or Externally Timed Arm Movements in Area 6 of Monkey Cortex." *Experimental Brain Research* 67 (3): 656–62.
Roshani, A., and Erfanian, A.. 2013a. "Fuzzy Logic Control of Ankle Movement Using Multi-Electrode Intraspinal Microstimulation." *Conference Proceedings: ... Annual International Conference of the IEEE Engineering in Medicine and Biology Society. IEEE Engineering in Medicine and Biology Society. Annual Conference* 2013: 5642–45. https://doi.org/10.1109/EMBC.2013.6610830.
Roshani, A., and Erfanian, A. 2013b. "Restoring Motor Functions in Paralyzed Limbs through Intraspinal Multielectrode Microstimulation Using Fuzzy Logic Control and Lag Compensator." *Basic and Clinical Neuroscience* 4 (3): 232–43.
Rossignol, S., C. Chau, E. Brustein, M. Bélanger, H. Barbeau, and T. Drew. 1996. "Locomotor Capacities after Complete and Partial Lesions of the Spinal Cord." *Acta Neurobiologiae Experimentalis* 56 (1): 449–63.
Roth, E. J., T. Park, T. Pang, G. M. Yarkony, and M. Y. Lee. 1991. "Traumatic Cervical Brown-Sequard and Brown-Sequard-plus Syndromes: The Spectrum of Presentations and Outcomes." *Paraplegia* 29 (9): 582–89. https://doi.org/10.1038/sc.1991.86.
Rouhani, E., and A. Erfanian. 2018. "Block-Based Robust Control of Stepping Using Intraspinal Microstimulation." *Journal of Neural Engineering* 15 (4): 046026–046026. https://doi.org/10.1088/1741-2552/aac4b8.
Rumelhart, David E., Geoffrey E. Hinton, and Ronald J. Williams. 1986. "Learning Representations by Back-Propagating Errors." *Nature* 323 (6088): 533–36. https://doi.org/10.1038/323533a0.
Rybak, Ilya A., Natalia A. Shevtsova, Myriam Lafreniere-Roula, and David A. McCrea. 2006a. "Modelling Spinal Circuitry Involved in Locomotor Pattern Generation: Insights from Deletions during Fictive Locomotion." *The Journal of Physiology* 577 (Pt 2): 617–39. https://doi.org/10.1113/jphysiol.2006.118703.
Rybak, Ilya A., Katinka Stecina, Natalia A. Shevtsova, and David A. McCrea. 2006b. "Modelling Spinal Circuitry Involved in Locomotor Pattern Generation: Insights from the Effects of Afferent Stimulation." *The Journal of Physiology* 577 (Pt 2): 641–58. https://doi.org/10.1113/jphysiol.2006.118711.
Ryczko, Dimitri, and Réjean Dubuc. 2013. "The Multifunctional Mesencephalic Locomotor Region." *Current Pharmaceutical Design* 19 (24): 4448–70.
Sabeti, M., M. H. Sadreddini, and J. T. Nezhad. 2007. "EEG Signal Classification Using an Association Rule-Based Classifier." In *2007 IEEE International Conference on Signal Processing and Communications*, 620–23. https://doi.org/10.1109/ICSPC.2007.4728395.
Saigal, R., C. Renzi, and V.K. Mushahwar. 2004. "Intraspinal Microstimulation Generates Functional Movements after Spinal-Cord Injury." *IEEE Transactions on Neural Systems and Rehabilitation Engineering* 12 (4): 430–40. https://doi.org/10.1109/TNSRE.2004.837754.

Salatian, A. W., Keon Young Yi, and Yuan F. Zheng. 1997. “Reinforcement Learning for a Biped Robot to Climb Sloping Surfaces.” *Journal of Robotic Systems* 14 (4): 283–96. https://doi.org/10.1002/(SICI)1097-4563(199704)14:4<283::AID-ROB5>3.0.CO;2-M.

Salm, Arjan van der, Anand V. Nene, Douglas J. Maxwell, Peter H. Veltink, Hermie J. Hermens, and Maarten J. IJzerman. 2005. “Gait Impairments in a Group of Patients with Incomplete Spinal Cord Injury and Their Relevance Regarding Therapeutic Approaches Using Functional Electrical Stimulation.” *Artificial Organs* 29 (1): 8–14. https://doi.org/10.1111/j.1525-1594.2004.29004.x.

Sasada, Syusaku, Kenji Kato, Suguru Kadowaki, Stefan J. Groiss, Yoshikazu Ugawa, Tomoyoshi Komiyama, and Yukio Nishimura. 2014. “Volitional Walking via Upper Limb Muscle-Controlled Stimulation of the Lumbar Locomotor Center in Man.” *The Journal of Neuroscience: The Official Journal of the Society for Neuroscience* 34 (33): 11131–42. https://doi.org/10.1523/JNEUROSCI.4674-13.2014.

Saulino, Michael. 2014. “Spinal Cord Injury Pain.” *Physical Medicine and Rehabilitation Clinics of North America* 25 (2): 397–410. https://doi.org/10.1016/j.pmr.2014.01.002.

Schafe, G. E., S. I. Sollars, and I. L. Bernstein. 1995. “The CS-US Interval and Taste Aversion Learning: A Brief Look.” *Behavioral Neuroscience* 109 (4): 799–802.

Schuitema, E., D. G. E. Hobbelen, P. P. Jonker, M. Wisse, and J. G. D. Karssen. 2005. “Using a Controller Based on Reinforcement Learning for a Passive Dynamic Walking Robot.” In *5th IEEE-RAS International Conference on Humanoid Robots, 2005.*, 232–37. https://doi.org/10.1109/ICHR.2005.1573573.

Schultz, W., P. Dayan, and P. R. Montague. 1997. “A Neural Substrate of Prediction and Reward.” *Science (New York, N.Y.)* 275 (5306): 1593–99.

Scivoletto, Giorgio, Angela Romanelli, Andrea Mariotti, Daniele Marinucci, Federica Tamburella, Alessia Mammone, Elena Cosentino, Silvia Sterzi, and Marco Molinari. 2008. “Clinical Factors That Affect Walking Level and Performance in Chronic Spinal Cord Lesion Patients.” *Spine* 33 (3): 259–64. https://doi.org/10.1097/BRS.0b013e3181626ab0.

Seijen, Harm H van, and Richard S Sutton. 2014. “True Online TD(Lambda).” In . Vol. 32. Beijing, China.

Seijen, Harm van, A. Rupam Mahmood, Patrick M. Pilarski, Marlos C. Machado, and Richard S. Sutton. 2015. “True Online Temporal-Difference Learning,” December. http://arxiv.org/abs/1512.04087.

Sepulveda, F., and A. Cliquet Júnior. 1995. “An Artificial Neural System for Closed Loop Control of Locomotion Produced via Neuromuscular Electrical Stimulation.” *Artificial Organs* 19 (3): 231–37.

Sepulveda, F., M. H. Granat, and A. Cliquet. 1997. “Two Artificial Neural Systems for Generation of Gait Swing by Means of Neuromuscular Electrical Stimulation.” *Medical Engineering & Physics* 19 (1): 21–28.

Shadmehr, Reza, Maurice A. Smith, and John W. Krakauer. 2010. “Error Correction, Sensory Prediction, and Adaptation in Motor Control.” *Annual Review of Neuroscience* 33: 89–108. https://doi.org/10.1146/annurev-neuro-060909-153135.

Shahdoost, S., S. Frost, G. Van Acker, S. DeJong, C. Dunham, S. Barbay, R. Nudo, and P. Mohseni. 2014. “Towards a Miniaturized Brain-Machine-Spinal Cord Interface (BMSI) for Restoration of Function after Spinal Cord Injury.” In *2014 36th Annual International*

Conference of the IEEE Engineering in Medicine and Biology Society, 486–89. https://doi.org/10.1109/EMBC.2014.6943634.

Sharples, Simon A., Jennifer M. Humphreys, A. Marley Jensen, Sunny Dhoopar, Nicole Delaloye, Stefan Clemens, and Patrick J. Whelan. 2015. "Dopaminergic Modulation of Locomotor Network Activity in the Neonatal Mouse Spinal Cord." *Journal of Neurophysiology* 113 (7): 2500–2510. https://doi.org/10.1152/jn.00849.2014.

Sharples, Simon A., and Patrick J. Whelan. 2017. "Modulation of Rhythmic Activity in Mammalian Spinal Networks Is Dependent on Excitability State." *ENeuro* 4 (1): ENEURO.0368-16.2017. https://doi.org/10.1523/ENEURO.0368-16.2017.

Shealy, C. N., J. T. Mortimer, and J. B. Reswick. 1967. "Electrical Inhibition of Pain by Stimulation of the Dorsal Columns: Preliminary Clinical Report." *Anesthesia and Analgesia* 46 (4): 489–91.

Sherrington, C. S. 1910. "Flexion-Reflex of the Limb, Crossed Extension-Reflex, and Reflex Stepping and Standing." *The Journal of Physiology* 40 (1–2): 28–121.

Sherstan, Craig, and Patrick Pilarski. 2014. "Multilayer General Value Functinos for Robotic Prediction and Control." In , 6. Chicago, IL,vUSA.

Shik, M. L., F. V. Severin, and G. N. Orlovskiĭ. 1966. "[Control of walking and running by means of electric stimulation of the midbrain]." *Biofizika* 11 (4): 659–66.

Shimada, Yoichi, Shigeru Ando, Toshiki Matsunaga, Akiko Misawa, Toshiaki Aizawa, Tsuyoshi Shirahata, and Eiji Itoi. 2005. "Clinical Application of Acceleration Sensor to Detect the Swing Phase of Stroke Gait in Functional Electrical Stimulation." *The Tohoku Journal of Experimental Medicine* 207 (3): 197–202.

Sipilä, Sampsa T., Sebastian Schuchmann, Juha Voipio, Junko Yamada, and Kai Kaila. 2006. "The Cation-Chloride Cotransporter NKCC1 Promotes Sharp Waves in the Neonatal Rat Hippocampus." *The Journal of Physiology* 573 (Pt 3): 765–73. https://doi.org/10.1113/jphysiol.2006.107086.

Skinner, BF. 1963. "Operant Behavior." *American Psychologist* 18 (8): 503–15.

Smith, J. C., and J. L. Feldman. 1987. "In Vitro Brainstem-Spinal Cord Preparations for Study of Motor Systems for Mammalian Respiration and Locomotion." *Journal of Neuroscience Methods* 21 (2–4): 321–33.

Smith, J. C., G. D. Funk, S. M. Johnson, X. W. Dong, J. Lai, S. Hsu, and J. L. Feldman. 1993. "Functional Networks for Locomotion in Spinal Cord of Neonatal Mice Lacking NMDA Receptors." In , 19:270.

Song, Yang, Yu-Dong Zhang, Xu Yan, Hui Liu, Minxiong Zhou, Bingwen Hu, and Guang Yang. 2018. "Computer-Aided Diagnosis of Prostate Cancer Using a Deep Convolutional Neural Network from Multiparametric MRI." *Journal of Magnetic Resonance Imaging: JMRI*, April. https://doi.org/10.1002/jmri.26047.

Spadone, R., G. Merati, E. Bertocchi, E. Mevio, A. Veicsteinas, A. Pedotti, and M. Ferrarin. 2003. "Energy Consumption of Locomotion with Orthosis versus Parastep-Assisted Gait: A Single Case Study." *Spinal Cord* 41 (2): 97–104. https://doi.org/10.1038/sj.sc.3101420.

"Spinal Cord Injury (SCI) 2017 Facts and Figures at a Glance." 2017. *The Journal of Spinal Cord Medicine* 40 (6): 872–73. https://doi.org/10.1080/10790268.2017.1379938.

Staddon, J. E. R., and D. T. Cerutti. 2003. "Operant Conditioning." *Annual Review of Psychology* 54: 115–44. https://doi.org/10.1146/annurev.psych.54.101601.145124.

Steeves, J. D., and L. M. Jordan. 1984. "Autoradiographic Demonstration of the Projections from the Mesencephalic Locomotor Region." *Brain Research* 307 (1–2): 263–76.

Stefanovska, A., N. Gros, L. Vodovnik, S. Rebersek, and R. Acimović-Janezic. 1988. “Chronic Electrical Stimulation for the Modification of Spasticity in Hemiplegic Patients.” *Scandinavian Journal of Rehabilitation Medicine. Supplement* 17: 115–21.

Stefanovska, A., L. Vodovnik, N. Gros, S. Rebersek, and R. Acimović-Janezic. 1989. “FES and Spasticity.” *IEEE Transactions on Bio-Medical Engineering* 36 (7): 738–45. https://doi.org/10.1109/10.32106.

Stein, P. S. 1971. “Intersegmental Coordination of Swimmeret Motoneuron Activity in Crayfish.” *Journal of Neurophysiology* 34 (2): 310–18. https://doi.org/10.1152/jn.1971.34.2.310.

Stelzner, DJ, ED Weber, and WF BryGornia. 1986. *Sparing of Function in Developing Spinal Cord: Anatomical Substrate*. Development and Plasticity of the Mammalian Spinal Cord. Springer, New York.

Stephens, M. J., and J. F. Yang. 1996. “Short Latency, Non-Reciprocal Group I Inhibition Is Reduced during the Stance Phase of Walking in Humans.” *Brain Research* 743 (1–2): 24–31.

Strojnik, P., R. Acimovic, E. Vavken, V. Simic, and U. Stanic. 1987. “Treatment of Drop Foot Using an Implantable Peroneal Underknee Stimulator.” *Scandinavian Journal of Rehabilitation Medicine* 19 (1): 37–43.

Subasi, A, and M Ismail Gursoy. 2010. “EEG Signal Classification Using PCA, ICA, LDA and Support Vector Machines - Semantic Scholar” 37: 8659–8666.

Sullivan, Jennifer L., Nikunj A. Bhagat, Nuray Yozbatiran, Ruta Paranjape, Colin G. Losey, Robert G. Grossman, Jose L. Contreras-Vidal, Gerard E. Francisco, and Marcia K. O’Malley. 2017. “Improving Robotic Stroke Rehabilitation by Incorporating Neural Intent Detection: Preliminary Results from a Clinical Trial.” *IEEE ... International Conference on Rehabilitation Robotics: [Proceedings]* 2017 (July): 122–27. https://doi.org/10.1109/ICORR.2017.8009233.

Sun, Yi, Ding Liang, Xiaogang Wang, and Xiaoou Tang. 2015. “DeepID3: Face Recognition with Very Deep Neural Networks.” *ArXiv:1502.00873 [Cs]*, February. http://arxiv.org/abs/1502.00873.

Sunshine, Michael D., Frances S. Cho, Danielle R. Lockwood, Amber S. Fechko, Michael R. Kasten, and Chet T. Moritz. 2013. “Cervical Intraspinal Microstimulation Evokes Robust Forelimb Movements before and after Injury.” *Journal of Neural Engineering* 10 (3): 036001. https://doi.org/10.1088/1741-2560/10/3/036001.

Sunshine, Michael D., Comron N. Ganji, Paul J. Reier, David D. Fuller, and Chet T. Moritz. 2018. “Intraspinal Microstimulation for Respiratory Muscle Activation.” *Experimental Neurology* 302 (April): 93–103. https://doi.org/10.1016/j.expneurol.2017.12.014.

Supynuk, A.G., and W.W. Armstrong. 1992. “Adaptive Logic Networks and Robot Control.” In , 181–86. Vancouver, BC, Canada.

Sutton, Richard S. 1988. “Learning to Predict by the Methods of Temporal Differences.” *Machine Learning* 3 (1): 9–44. https://doi.org/10.1007/BF00115009.

Sutton, Richard S, and Andrew G Barto. 2018. *Reinforcement Learning: An Introduction*. 2nd ed. Adaptive Computation and Machine Learning Series. Cambridge, MA: MIT Press.

Sutton, Richard S, Joseph Modayil, Michael Delp, Thomas Degris, Patrick M Pilarski, Adam White, and Doina Precup. 2011. “Horde: A Scalable Real-Time Architecture for Learning Knowledge from Unsupervised Sensorimotor Interaction,” 8.

Sweeney, P. C., G. M. Lyons, and P. H. Veltink. 2000. “Finite State Control of Functional Electrical Stimulation for the Rehabilitation of Gait.” *Medical & Biological Engineering & Computing* 38 (2): 121–26.

Takakusaki, Kaoru. 2013. “Neurophysiology of Gait: From the Spinal Cord to the Frontal Lobe.” *Movement Disorders: Official Journal of the Movement Disorder Society* 28 (11): 1483–91. https://doi.org/10.1002/mds.25669.

Takakusaki, Kaoru, Nozomi Tomita, and Masafumi Yano. 2008. “Substrates for Normal Gait and Pathophysiology of Gait Disturbances with Respect to the Basal Ganglia Dysfunction.” *Journal of Neurology* 255 Suppl 4 (August): 19–29. https://doi.org/10.1007/s00415-008-4004-7.

Talonen, P., J. Malmivuo, G. Baer, H. Markkula, and V. Häkkinen. 1983. “Transcutaneous, Dual Channel Phrenic Nerve Stimulator for Diaphragm Pacing.” *Medical & Biological Engineering & Computing* 21 (1): 21–30.

Talpalar, Adolfo E., Julien Bouvier, Lotta Borgius, Gilles Fortin, Alessandra Pierani, and Ole Kiehn. 2013. “Dual-Mode Operation of Neuronal Networks Involved in Left-Right Alternation.” *Nature* 500 (7460): 85–88. https://doi.org/10.1038/nature12286.

Tanagho, E. A., R. A. Schmidt, and B. R. Orvis. 1989. “Neural Stimulation for Control of Voiding Dysfunction: A Preliminary Report in 22 Patients with Serious Neuropathic Voiding Disorders.” *The Journal of Urology* 142 (2 Pt 1): 340–45.

Tator, C. H., and M. G. Fehlings. 1991. “Review of the Secondary Injury Theory of Acute Spinal Cord Trauma with Emphasis on Vascular Mechanisms.” *Journal of Neurosurgery* 75 (1): 15–26. https://doi.org/10.3171/jns.1991.75.1.0015.

Tator, Charles H., Karen Minassian, and Vivian K. Mushahwar. 2012. “Spinal Cord Stimulation: Therapeutic Benefits and Movement Generation after Spinal Cord Injury.” *Handbook of Clinical Neurology* 109: 283–96. https://doi.org/10.1016/B978-0-444-52137-8.00018-8.

Thompson, R. F., and J. E. Steinmetz. 2009. “The Role of the Cerebellum in Classical Conditioning of Discrete Behavioral Responses.” *Neuroscience* 162 (3): 732–55. https://doi.org/10.1016/j.neuroscience.2009.01.041.

Thrasher, T. A., H. M. Flett, and M. R. Popovic. 2006. “Gait Training Regimen for Incomplete Spinal Cord Injury Using Functional Electrical Stimulation.” *Spinal Cord* 44 (6): 357–61. https://doi.org/10.1038/sj.sc.3101864.

Thrasher, T. A., and M. R. Popovic. 2008. “Functional Electrical Stimulation of Walking: Function, Exercise and Rehabilitation.” *Annales De Réadaptation Et De Médecine Physique: Revue Scientifique De La Société Française De Rééducation Fonctionnelle De Réadaptation Et De Médecine Physique* 51 (6): 452–60. https://doi.org/10.1016/j.annrmp.2008.05.006.

Tohidi, Mina, Tiffany Lung, and David Yen. 2018. “Routine Perioperative Practices and Postoperative Outcomes for Elective Lumbar Laminectomies.” *Journal of Spine Surgery (Hong Kong)* 4 (3): 588–93. https://doi.org/10.21037/jss.2018.09.01.

Tong, K. Y., and M. H. Granat. 1999. “Gait Control System for Functional Electrical Stimulation Using Neural Networks.” *Medical & Biological Engineering & Computing* 37 (1): 35–41.

Toossi, Amirali, Dirk G. Everaert, Austin Azar, Christopher R. Dennison, and Vivian K. Mushahwar. 2017. “Mechanically Stable Intraspinal Microstimulation Implants for Human Translation.” *Annals of Biomedical Engineering* 45 (3): 681–94. https://doi.org/10.1007/s10439-016-1709-0.

Torborg, Christine L., and Marla B. Feller. 2005. “Spontaneous Patterned Retinal Activity and the Refinement of Retinal Projections.” *Progress in Neurobiology* 76 (4): 213–35. https://doi.org/10.1016/j.pneurobio.2005.09.002.

Totoiu, Minodora O., and Hans S. Keirstead. 2005. “Spinal Cord Injury Is Accompanied by Chronic Progressive Demyelination.” *The Journal of Comparative Neurology* 486 (4): 373–83. https://doi.org/10.1002/cne.20517.

Travnik, Jaden B., and Patrick M. Pilarski. 2017. “Representing High-Dimensional Data to Intelligent Prostheses and Other Wearable Assistive Robots: A First Comparison of Tile Coding and Selective Kanerva Coding.” *IEEE ... International Conference on Rehabilitation Robotics: [Proceedings]* 2017: 1443–50. https://doi.org/10.1109/ICORR.2017.8009451.

Triolo, Ronald J., Stephanie Nogan Bailey, Michael E. Miller, Loretta M. Rohde, James S. Anderson, John A. Davis, James J. Abbas, et al. 2012. “Longitudinal Performance of a Surgically Implanted Neuroprosthesis for Lower-Extremity Exercise, Standing, and Transfers after Spinal Cord Injury.” *Archives of Physical Medicine and Rehabilitation* 93 (5): 896–904. https://doi.org/10.1016/j.apmr.2012.01.001.

Troyk, Philip R., Vivian K. Mushahwar, Richard B. Stein, Sungjae Suh, Dirk Everaert, Brad Holinski, Zhe Hu, Glenn DeMichele, Douglas Kerns, and Kevin Kayvani. 2012. “An Implantable Neural Stimulator for Intraspinal Microstimulation.” *Conference Proceedings: ... Annual International Conference of the IEEE Engineering in Medicine and Biology Society. IEEE Engineering in Medicine and Biology Society. Annual Conference* 2012: 900–903. https://doi.org/10.1109/EMBC.2012.6346077.

Utkin, Vadim. 2009. “Sliding Mode Control.” In *CONTROL SYSTEMS, ROBOTICS AND AUTOMATION - System Analysis and Control: Classical Approaches-II*, 13th ed., 2:130–52. EOLSS Publications. http://www.eolss.net/outlinecomponents/Control-Systems-Robotics-Automation.aspx.

Van Wezel, B. M., F. A. Ottenhoff, and J. Duysens. 1997. “Dynamic Control of Location-Specific Information in Tactile Cutaneous Reflexes from the Foot during Human Walking.” *The Journal of Neuroscience: The Official Journal of the Society for Neuroscience* 17 (10): 3804–14.

Vanderhorst, V. G., and G. Holstege. 1997. “Organization of Lumbosacral Motoneuronal Cell Groups Innervating Hindlimb, Pelvic Floor, and Axial Muscles in the Cat.” *The Journal of Comparative Neurology* 382 (1): 46–76.

Vasudevan, Erin V., Susan K. Patrick, and Jaynie F. Yang. 2016. “Gait Transitions in Human Infants: Coping with Extremes of Treadmill Speed.” *PloS One* 11 (2): e0148124. https://doi.org/10.1371/journal.pone.0148124.

Vavrek, R., J. Girgis, W. Tetzlaff, G. W. Hiebert, and K. Fouad. 2006. “BDNF Promotes Connections of Corticospinal Neurons onto Spared Descending Interneurons in Spinal Cord Injured Rats.” *Brain: A Journal of Neurology* 129 (Pt 6): 1534–45. https://doi.org/10.1093/brain/awl087.

Vecchio, Claudio. 2008. “Sliding Mode Control: Theoretical Developments and Applications to Uncertain Mechanical Systems.” Pavia, Italy: Universita Degli Studi di Pavia. https://www.tesionline.it/tesi/35561/Sliding_Mode_Control%3A_theoretical_developments_and_applications_to_uncertain_mechanical_systems.

Vette, Albert H., Kei Masani, Joon-Young Kim, and Milos R. Popovic. 2009. “Closed-Loop Control of Functional Electrical Stimulation-Assisted Arm-Free Standing in Individuals

with Spinal Cord Injury: A Feasibility Study." *Neuromodulation: Journal of the International Neuromodulation Society* 12 (1): 22–32. https://doi.org/10.1111/j.1525-1403.2009.00184.x.

Vogelstein, R. J., F. Tenore, L. Guevremont, R. Etienne-Cummings, and V. K. Mushahwar. 2008. "A Silicon Central Pattern Generator Controls Locomotion in Vivo." *IEEE Transactions on Biomedical Circuits and Systems* 2 (3): 212–22. https://doi.org/10.1109/TBCAS.2008.2001867.

Wagner, Fabien B., Jean-Baptiste Mignardot, Camille G. Le Goff-Mignardot, Robin Demesmaeker, Salif Komi, Marco Capogrosso, Andreas Rowald, et al. 2018. "Targeted Neurotechnology Restores Walking in Humans with Spinal Cord Injury." *Nature* 563 (7729): 65–71. https://doi.org/10.1038/s41586-018-0649-2.

Wallén, P., and T. L. Williams. 1984. "Fictive Locomotion in the Lamprey Spinal Cord in Vitro Compared with Swimming in the Intact and Spinal Animal." *The Journal of Physiology* 347 (February): 225–39.

Walton, K. D., and M. Chesler. 1988. "Activity-Related Extracellular Potassium Transients in the Neonatal Rat Spinal Cord: An in Vitro Study." *Neuroscience* 25 (3): 983–95.

Wand, P., A. Prochazka, and K. H. Sontag. 1980. "Neuromuscular Responses to Gait Perturbations in Freely Moving Cats." *Experimental Brain Research* 38 (1): 109–14.

Wang, Wei, Jennifer L. Collinger, Alan D. Degenhart, Elizabeth C. Tyler-Kabara, Andrew B. Schwartz, Daniel W. Moran, Douglas J. Weber, et al. 2013. "An Electrocorticographic Brain Interface in an Individual with Tetraplegia." *PloS One* 8 (2): e55344. https://doi.org/10.1371/journal.pone.0055344.

Watt, Alanna J., Hermann Cuntz, Masahiro Mori, Zoltan Nusser, P. Jesper Sjöström, and Michael Häusser. 2009. "Traveling Waves in Developing Cerebellar Cortex Mediated by Asymmetrical Purkinje Cell Connectivity." *Nature Neuroscience* 12 (4): 463–73. https://doi.org/10.1038/nn.2285.

Weber, D. J., R. B. Stein, D. G. Everaert, and A. Prochazka. 2007. "Limb-State Feedback from Ensembles of Simultaneously Recorded Dorsal Root Ganglion Neurons." *Journal of Neural Engineering* 4 (3): S168-180. https://doi.org/10.1088/1741-2560/4/3/S04.

Wessels, Monique, Cees Lucas, Inge Eriks, and Sonja de Groot. 2010. "Body Weight-Supported Gait Training for Restoration of Walking in People with an Incomplete Spinal Cord Injury: A Systematic Review." *Journal of Rehabilitation Medicine* 42 (6): 513–19. https://doi.org/10.2340/16501977-0525.

Westerga, J., and A. Gramsbergen. 1990. "The Development of Locomotion in the Rat." *Brain Research. Developmental Brain Research* 57 (2): 163–74.

Whelan, P., A. Bonnot, and M. J. O'Donovan. 2000. "Properties of Rhythmic Activity Generated by the Isolated Spinal Cord of the Neonatal Mouse." *Journal of Neurophysiology* 84 (6): 2821–33. https://doi.org/10.1152/jn.2000.84.6.2821.

Whelan, P. J. 1996. "Control of Locomotion in the Decerebrate Cat." *Progress in Neurobiology* 49 (5): 481–515.

Whelan, P. J., G. W. Hiebert, and K. G. Pearson. 1995. "Stimulation of the Group I Extensor Afferents Prolongs the Stance Phase in Walking Cats." *Experimental Brain Research* 103 (1): 20–30.

Whelan, P. J., and K. G. Pearson. 1997. "Comparison of the Effects of Stimulating Extensor Group I Afferents on Cycle Period during Walking in Conscious and Decerebrate Cats." *Experimental Brain Research* 117 (3): 444–52.

Whelan, Patrick J. 2003. “Developmental Aspects of Spinal Locomotor Function: Insights from Using the in Vitro Mouse Spinal Cord Preparation.” *The Journal of Physiology* 553 (Pt 3): 695–706. https://doi.org/10.1113/jphysiol.2003.046219.

White, Adam. 2015. “Developing a Predictive Approach to Knowledge.” Edmonton, AB, Canada: University of Alberta.

Williamson, R., and B. J. Andrews. 2000. “Gait Event Detection for FES Using Accelerometers and Supervised Machine Learning.” *IEEE Transactions on Rehabilitation Engineering: A Publication of the IEEE Engineering in Medicine and Biology Society* 8 (3): 312–19.

Wirz, M., B. Zörner, R. Rupp, and V. Dietz. 2010. “Outcome after Incomplete Spinal Cord Injury: Central Cord versus Brown-Sequard Syndrome.” *Spinal Cord* 48 (5): 407–14. https://doi.org/10.1038/sc.2009.149.

Witten, Ian H., Eibe Frank, Mark A. Hall, and Christopher J. Pal. 2016. *Data Mining: Practical Machine Learning Tools and Techniques*. Morgan Kaufmann.

Wrathall, J. R., Y. D. Teng, and R. Marriott. 1997. “Delayed Antagonism of AMPA/Kainate Receptors Reduces Long-Term Functional Deficits Resulting from Spinal Cord Trauma.” *Experimental Neurology* 145 (2 Pt 1): 565–73. https://doi.org/10.1006/exnr.1997.6506.

Xu, Duo, Tao Liu, James Ashe, and Khalafalla O. Bushara. 2006. “Role of the Olivo-Cerebellar System in Timing.” *The Journal of Neuroscience: The Official Journal of the Society for Neuroscience* 26 (22): 5990–95. https://doi.org/10.1523/JNEUROSCI.0038-06.2006.

Yang, Jaynie F., Tania Lam, Marco Y. C. Pang, Erin Lamont, Kristin Musselman, and Elizabeth Seinen. 2004. “Infant Stepping: A Window to the Behaviour of the Human Pattern Generator for Walking.” *Canadian Journal of Physiology and Pharmacology* 82 (8–9): 662–74. https://doi.org/10.1139/y04-070.

Yang, Jaynie F., Kristin E. Musselman, Donna Livingstone, Kelly Brunton, Gregory Hendricks, Denise Hill, and Monica Gorassini. 2014. “Repetitive Mass Practice or Focused Precise Practice for Retraining Walking after Incomplete Spinal Cord Injury? A Pilot Randomized Clinical Trial.” *Neurorehabilitation and Neural Repair* 28 (4): 314–24. https://doi.org/10.1177/1545968313508473.

Ying, Z., R. R. Roy, H. Zhong, S. Zdunowski, V. R. Edgerton, and F. Gomez-Pinilla. 2008. “BDNF-Exercise Interactions in the Recovery of Symmetrical Stepping after a Cervical Hemisection in Rats.” *Neuroscience* 155 (4): 1070–78. https://doi.org/10.1016/j.neuroscience.2008.06.057.

Yu, C. Ron, Jennifer Power, Gilad Barnea, Sean O’Donnell, Hannah E. V. Brown, Joseph Osborne, Richard Axel, and Joseph A. Gogos. 2004. “Spontaneous Neural Activity Is Required for the Establishment and Maintenance of the Olfactory Sensory Map.” *Neuron* 42 (4): 553–66.

Yvert, Blaise, Pascal Branchereau, and Pierre Meyrand. 2004. “Multiple Spontaneous Rhythmic Activity Patterns Generated by the Embryonic Mouse Spinal Cord Occur within a Specific Developmental Time Window.” *Journal of Neurophysiology* 91 (5): 2101–9. https://doi.org/10.1152/jn.01095.2003.

Zehr, E. P., T. Komiyama, and R. B. Stein. 1997. “Cutaneous Reflexes during Human Gait: Electromyographic and Kinematic Responses to Electrical Stimulation.” *Journal of Neurophysiology* 77 (6): 3311–25. https://doi.org/10.1152/jn.1997.77.6.3311.

Zehr, E. P., and R. B. Stein. 1999. “What Functions Do Reflexes Serve during Human Locomotion?” *Progress in Neurobiology* 58 (2): 185–205.

Zehr, E. P., R. B. Stein, and T. Komiyama. 1998. “Function of Sural Nerve Reflexes during Human Walking.” *The Journal of Physiology* 507 (Pt 1) (February): 305–14.
Zeng, Wei, Fenglin Liu, Qinghui Wang, Ying Wang, Limin Ma, and Yu Zhang. 2016. “Parkinson’s Disease Classification Using Gait Analysis via Deterministic Learning.” *Neuroscience Letters* 633: 268–78. https://doi.org/10.1016/j.neulet.2016.09.043.
Zentall, Thomas R., Edward A. Wasserman, and Peter J. Urcuioli. 2014. “Associative Concept Learning in Animals.” *Journal of the Experimental Analysis of Behavior* 101 (1): 130–51. https://doi.org/10.1002/jeab.55.
Zheng, Yang, and Xiaogang Hu. 2018. “Reduced Muscle Fatigue Using Kilohertz-Frequency Subthreshold Stimulation of the Proximal Nerve.” *Journal of Neural Engineering* 15 (6): 066010. https://doi.org/10.1088/1741-2552/aadecc.
Zimmermann, Jonas B., and Andrew Jackson. 2014. “Closed-Loop Control of Spinal Cord Stimulation to Restore Hand Function after Paralysis.” *Frontiers in Neuroscience* 8: 87. https://doi.org/10.3389/fnins.2014.00087.
Zimmermann, Jonas B., Kazuhiko Seki, and Andrew Jackson. 2011. “Reanimating the Arm and Hand with Intraspinal Microstimulation.” *Journal of Neural Engineering* 8 (5): 054001. https://doi.org/10.1088/1741-2560/8/5/054001.
Zörner, Björn, and Martin E. Schwab. 2010. “Anti-Nogo on the Go: From Animal Models to a Clinical Trial.” *Annals of the New York Academy of Sciences* 1198 Suppl 1 (June): E22-34. https://doi.org/10.1111/j.1749-6632.2010.05566.x.